

AE 639232

REPORT NUMBER 166

MARCH 1966

HASE I - FLIGHT TEST RESULTS

VOLUME II



CLEARINGHOUSE
FOR FEDERAL SCIENTIFIC AND
TECHNICAL INFORMATION

Hardcopy

Microfiche

\$6.00

\$1.25

215pp as

/ ARCHIVE COPY

F

DDC AVAILABILITY NOTICES

1. Distribution of this document is unlimited.
2. This document is subject to special report controls and each transmittal to foreign governments or foreign nationals may be made only with prior approval of US Army Aviation Materiel Laboratories, Fort Eustis, Virginia 23604.
3. In addition to security requirements which must be met, this document is subject to special export controls and each transmittal to foreign governments or foreign nationals may be made only with prior approval of USAAVLABS, Fort Eustis, Virginia 23604.
4. Each transmittal of this document outside the agencies of the US Government must have prior approval of US Army Aviation Materiel Laboratories, Fort Eustis, Virginia 23604.
5. In addition to security requirements which apply to this document and must be met, each transmittal outside the agencies of the US Government must have prior approval of US Army Aviation Materiel Laboratories, Fort Eustis, Virginia.
6. Each transmittal of this document outside the Department of Defense must have prior approval of US Army Aviation Materiel Laboratories, Fort Eustis, Va.
7. In addition to security requirements which apply to this document and must be met, each transmittal outside the Department of Defense must have prior approval of US Army Aviation Materiel Laboratories, Fort Eustis, Virginia 23604.
8. This document may be further distributed by any holder only with specific prior approval of US Army Aviation Materiel Laboratories, Fort Eustis, Va. 23604.
9. In addition to security requirements which apply to this document and must be met, it may be further distributed by the holder only with specific prior approval of US Army Aviation Materiel Laboratories, Fort Eustis, Virginia 23604.

DISCLAIMER

10. The findings in this report are not to be construed as an official Department of the Army position unless so designated by other authorized documents.
11. When Government drawings, specifications, or other data are used for any purpose other than in connection with a definitely related Government procurement operation, the United States Government thereby incurs no responsibility nor any obligation whatsoever; and the fact that the Government may have formulated, furnished, or in any way supplied the said drawings, specifications, or other data is not to be regarded by implication or otherwise as in any manner licensing the holder or any other person or corporation, or conveying any rights or permission, to manufacture, use, or sell any patented invention that may in any way be related thereto.
12. Trade names cited in this report do not constitute an official endorsement or approval of the use of such commercial hardware or software.

DISPOSITION INSTRUCTIONS

13. Destroy this report when no longer needed. Do not return it to originator.

14. When this report is no longer needed, Department of the Army organizations will destroy it in accordance with the procedures given in AR 380-5. Navy and Air Force elements will destroy it in accordance with applicable directions. Department of Defense contractors will destroy the report according to the requirement of Section 14 of the Industrial Security Manual for Safeguarding Classified Information. All others will return the report to US Army Aviation Materiel Laboratories, Fort Eustis, Virginia 23604.

VR

Report Number 166

PHASE I FLIGHT TEST RESULTS

VOLUME II

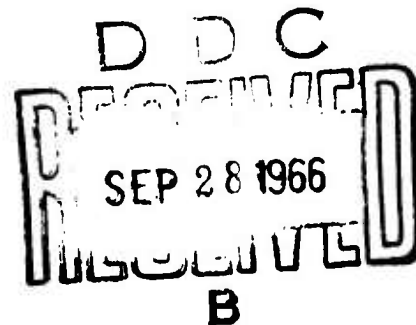
ACCESSION NO.	
CPSTI	WHITE SECTION <input checked="" type="checkbox"/>
DDC	BUFF SECTION <input type="checkbox"/>
UNANNOUNCED	<input type="checkbox"/>
CLASSIFICATION	
DISTRIBUTION/AVAILABILITY CODES	
Dist.	AVAIL. and/or SPECIAL
1	

XV-5A Lift Fan

Flight Research Aircraft

Contract DA 44-177-TC-715

March, 1966



ADVANCED ENGINE & TECHNOLOGY DEPARTMENT
GENERAL ELECTRIC COMPANY
CINCINNATI, OHIO 45215



FOREWORD

For the convenience of the reader, this report is divided into three volumes - Volumes I, II and III.

Volume I contains Sections 1.0 through 6.2.

Volume II contains Sections 6.3 through 11.0.

Volume III contains Section 12.0, which consists of parameter illustrations only.

Volume I includes a complete Table of Contents for all three Volumes. A partial Table of Contents is included in the other Volumes.

CONTENTS - VOLUME II

SECTION	PAGE
6.3 Thermodynamics	195
7.0 CONVENTIONAL FLIGHT TEST RESULTS	269
7.1 Performance	269
7.2 Stability and Control	273
7.3 Thermodynamics	327
8.0 AIRCRAFT SYSTEMS	335
8.1 Hydraulic	335
8.2 Electrical	337
8.3 Propulsion System History	343
8.4 XV-5A Landing Gear	349
8.5 Airspeed System	351
9.0 STRUCTURES AND LOADS	375
10.0 REFERENCES	385
11.0 CONCLUSIONS	395

BLANK PAGE

LIST OF ILLUSTRATIONS VOLUME II

FIGURE		PAGE
6.91	Estimated Allowable Fan Mode Flight Time vs Ambient Temperature for Flight Speeds from 30 to 95 knots	205
6.92	Estimated Allowable Fan Mode Hover Time vs Ambient Temperature - Effective for Flight Speeds from 0 to 30 Knots, $h/D = 2.0$, Aircraft Weight 10,000 Pounds	206
6.93	Estimated Allowable Fan Mode Hover Time vs Ambient Temperature - Effective for Flight Speeds from 0 to 30 Knots, $h/D = 2.0$, Aircraft Weight 10,500 Pounds	207
6.94	Estimated Allowable Fan Mode Hover Time vs Ambient Temperature - Effective for Flight Speeds from 0 to 30 Knots, $h/D = 1.0$, Aircraft Weight 10,000 Pounds	208
6.95	Estimated Allowable Fan Mode Hover Time vs Ambient Temperature - Effective for Flight Speeds from 0 to 30 Knots, $h/D = 1.0$, Aircraft Weight 10,500 Pounds	209
6.96	Available XV-5A Aircraft Temperature Instrumentation	210
6.97	Comparison of Selected XV-5A Structural Temperature Time Profiles for Hover Flight In and Out of Ground Effect	211
6.98	Effect of Velocity on Front Spar Temperatures for Fan Mode Operation	212
6.99	Effect of Velocity on Selected Wing Panel Temperatures for Fan Mode Operation	213
6.100	Effect of Velocity on Space Frame Temperature for Fan Mode Operation	214
6.101	Effect of Velocity on Some Pitch Fan and Main Landing Gear Components for Fan Mode Operation	215
6.102	Effect of Velocity on Rear Spar Temperatures for Fan Mode Operation	216
6.103	Front Spar Temperature - Time Profiles for Fan Mode Transitions from Lift Off or Prior to Touchdown	217
6.104	Effect of Aircraft Control Settings on Structural and Air Temperatures During Ground Operation in Fan Mode	218

LIST OF ILLUSTRATIONS (Continued)
VOLUME II

FIGURE		PAGE
6.105	Structural Temperatures Experienced During Short Takeoff and Landing Maneuvers for Fan Mode Operation	219
6.106	Some Wing Temperatures Experienced During a Short Takeoff and Landing Maneuver for Fan Mode Operation	220
6.107	Wing Panel Temperatures During Fan Mode Operation in Ground Effect	221
6.108	Main Wheel Well Air Temperatures for Fan Mode Operation During Vertical Takeoff and Landing with Wheel Well Open and Gear Extended	222
6.109	Various Main Wheel Well and Landing Gear Structural Temperatures for Fan Mode Operation During Vertical Takeoff and Landing with Wheel Well Open and Gear Extended	223
6.110	Main Wheel Well Enclosure Door Temperatures for Fan Mode Operation During Vertical Takeoff and Landing with Wheel Well Open and Gear Extended	224
6.111	Main Wheel Well Door Temperature During Vertical Takeoff and Transition - Wheel Well Open and Gear Extended	225
6.112	Main Wheel Well Door Linkage and Landing Gear Temperature During Vertical Takeoff and Transition	226
6.113	Main Wheel Well Door Temperature During Fan Mode Transition - Wheel Well Enclosed	227
6.114	Wheel Well Component Temperatures During Maximum Fan Mode Thrust, Wheel Well Open Dash to Conversion	228
6.115	Aircraft Component Temperatures During Maximum Mode Thrust, Wheel Well Open Dash to Conversion	229
6.116	Wheel Well Component Temperatures During Maximum Fan Mode Thrust, Wheel Well Open Dash to Conversion	230
6.117	Estimated Maximum Landing Gear Temperature During Fan Mode, Wheel Well Open Dash Conversion	231

LIST OF ILLUSTRATIONS (Continued)
VOLUME II

FIGURE		PAGE
6.118	Effect of Fan Stream Vector Angle and Pitch Control Setting on the Generator Ingestion for Fan Mode Operation in Ground Effect	232
6.119	Effect of Aircraft Control Inputs on Gas Generator Ingestion for Fan Mode Operation in Ground Effect - Zero Fan Stream Vector Angle - Winds to 15 Knots	233
6.120	Effect of Aircraft Control Inputs on Gas Generator Ingestion for Fan Mode Operation in Ground Effect - Zero Fan Stream Vector Angle - Winds 18 to 27 Knots	234
6.121	Effect of Collective Stick Position on Gas Generator Ingestion	235
6.122	Effect of Aircraft Control Inputs on Gas Generator Ingestion for Fan Mode Operation in Ground Effect, -70 Fan Stream Vector Angle - Winds Light	236
6.123	Cooling System Hot Gas Ingestion	237
6.124	Comparison of Ingestion by L/H and R/H Gas Generators	238
6.125	Circumferential Comparison of Inlet Temperature Distribution During R/H Engine Stall	239
6.126	Immersion Comparison of Inlet Temperature Distribution During R/H Engine Stall	240
6.127	Immersion Comparison of Inlet Temperature Distribution During L/H Engine Stall	241
6.128	Circumferential Comparison of Inlet Temperature Distribution During L/H Engine Stall	242
6.129	Typical Inlet Temperature Distribution for R/H Gas Generator During Fan Mode Operation in Ground Effects	243
6.130	Hot Gas Ingestion Experienced During Several Vertical Lift Off and Hover Maneuvers	244
6.131	Hot Gas Ingestion Experienced During Several Vertical Lift Off and Hover Maneuvers	245
6.132	Hot Gas Ingestion and Some Aircraft Control Positions During Vertical Lift Off and Hovering	246
6.133	Gas Ingestion Experienced During Short Takeoff and Landing Maneuvers During Fan Mode Operation	247
6.134	Inlet Temperature Distribution During Slow Speed Short Landing Maneuvers During Fan Mode Operation	248

LIST OF ILLUSTRATIONS (Continued)
VOLUME II

FIGURE		PAGE
6.135	Representative Cockpit Air Temperatures - Fan Mode Operation in Ground Effect	249
6.136	Electronic Compartment Inlet Air Temperature	250
6.137	Representative Temperature Difference Across Hydraulic Oil Cooler (HOC)	251
6.138	Cooling Air Temperature Rise from Ambient to Compressor and Engine Compartment Conditions	252
6.139	Engine Compartment Air Temperatures During Several Hover Maneuvers	253
6.140	Engine Compartment Air Temperature During Fan Mode Flight	254
6.141	Engine Compartment Air Temperature During Fan Mode Flight	255
6.142	Engine Compartment Air Temperature During Fan Mode Flight	256
6.143	Effect of Aircraft Speed on Cooling Air Temperatures at Engine Compartment and Tailpipe Ejector Outlets	257
6.144	Miscellaneous Air and Structural Temperature During Fan Mode Operation in Ground Effect	258
6.145	Main Wheel Well and Landing Gear Components Temperature Fan Mode Operation in Ground Effect, Wheel Well Enclosed, Gear Fixed	259
6.146	Engine Oil and Miscellaneous Air Temperatures During Hover	260
6.147	Comparison of R/H Engine Oil Temperatures for Several Flights	261
6.148	Wing Fan Ejector Cooling Air Temperature Following Conversion from Jet to Fan Mode	262
6.149	Wing Fan Ejector Cooling Air Temperature During Fan Mode Flight	263
6.150	Wing Fan Ejector Cooling Air Static Pressure During Fan Mode Flight	264
6.151	Wing Fan Ejector Cooling Air Static Pressures During Short Takeoff Maneuver in Fan Mode	265
6.152	Typical Cooling System Temperature Differences for a Series of Short Takeoff Maneuvers in Fan Mode	266
6.153	Typical Cooling System Temperature Differences for a Series of Vertical Takeoff, Transition and Landing Maneuvers	267
6.154	Representative Structural Temperatures for Fan Mode Operation in Ground Effect	268

LIST OF ILLUSTRATIONS (Continued)
VOLUME II

FIGURE		PAGE
7.1	Estimated Stall Speeds for Power-on and Power-off	285
7.2	Altitude vs Maximum Rate of Climb	286
7.3	Altitude vs Velocity for Maximum Rate of Climb	286
7.4	Flight Experience Envelope and Predicted Speed-Altitude Envelope	287
7.5	As-Flown Flight Envelope	288
7.6	" " "	289
7.7	Time History - Stall Approach and Stall	290
7.8	Static Longitudinal Stability - Configuration CR	291
7.9	Photograph of Tufted XV-5A	292
7.10	" " " "	292
7.11	Tail Buffet Problem	293
7.12	Static Longitudinal Stability - Configuration PA	294
7.13	" " " - Preconversion Configuration	295
7.14	Static Lateral-Directional Stability	296
7.15	" " " "	297
7.16	" " " "	298
7.17	" " " "	299
7.18	Longitudinal Dynamic Stability - Short Period Characteristics	300
7.19	T-Section Installation on Rudder and Trim Tab Trailing Edge	301
7.20	Lateral-Directional Dynamic Stability	302
7.21	" " " "	303
7.22	Time History of Sideslip with Rudder Release - Configuration L	304
7.23	Time History of Sideslip with Rudder Release - Configuration L	305
7.24	Time History of Sideslip with Rudder Release - Configuration L	306
7.25	Time History of Sideslip with Rudder Release - Configuration L	307
7.26	Time History of Sideslip with Rudder Release - Configuration PA	308
7.27	Time History of Sideslip with Rudder Release - Configuration PA	309

LIST OF ILLUSTRATIONS (Continued)
VOLUME II

FIGURE		PAGE
7.28	Time History of Roll Maneuvers - Configuration PA	310
7.29	" " " " " "	311
7.30	" " " " " "	312
7.31	" " " " " "	313
7.32	" " " " " "	314
7.33	" " " " " "	315
7.34	" " " " " "	316
7.35	" " " " " "	317
7.36	Dynamic Lateral-Directional Stability - Precon- version Configuration	318
7.37	Dynamic Lateral-Directional Stability - Precon- version Configuration	319
7.38	Dynamic Lateral-Directional Stability - Precon- version Configuration	320
7.39	Dynamic Lateral-Directional Stability - Precon- version Configuration	321
7.40	Bank-to-Bank Rolls - Preconversion Mode	322
7.41	" " " " " "	323
7.42	Elevator and Stabilizer Required to Trim	324
7.43	Rudder Effectiveness - Clean Configuration	325
7.44	" " " "	326
7.45	Engine Thrust Performance Summary	329
7.46	Fuel Flow vs Engine RPM	330
7.47	Thrust Loss due to Stall Free Operation Modifications	331
7.48	Pitch Fan Temperatures for Conventional Flight	332
7.49	Temperature Study - Turbojet Mode	333
8.1	Airspeed Measurement System History	355
8.2	" " " "	356
8.3	" " " "	357
8.4	" " " "	358
8.5	" " " "	359
8.6	" " " "	360
8.7	" " " "	361
8.8	" " " "	362
8.9	" " " "	363
8.10	" " " "	364
8.11	" " " "	365
8.12	" " " "	366
8.13	" " " "	367
8.14	" " " "	368

LIST OF ILLUSTRATIONS (Continued)
VOLUME II

FIGURE		PAGE
8.15	Comparison of Nose and Wing Pitot Static Readouts	369
8.16	Effect of Airspeed System Leakage	370
8.17	" " " "	371
8.18	Airspeed Position Error Correction-wing Boom System	372
8.19	Airspeed Position Error Correction-nose Boom System	373
8.20	Airspeed Position Error Correction-nose Boom System	374
9.1	Maneuvering Envelope - Gust Diagram for Altitudes Below 10,000 Feet	384

BLANK PAGE

6.3 THERMODYNAMICS

6.3.1 Engine and Fan Performance

Installed gas generator performance after modifications to provide stall-free operation is equal to, or slightly better than the specification engine of Reference 6.4 at the increased allowable maximum speed of 102% as shown in Figures 7.45 and 7.46. Installed wing fan performance also is virtually equal to that of Reference 6.4 as shown by data of Figure 6.1. Installed pitch fan performance was assumed to be that presented by E.G. Smith in Section 7.2 of Reference 6.1 since the assumption is valid within the accuracy of experimental data. Very careful screening and evaluation of all flight test data might validate slight deviation from Smith's data but otherwise would not invalidate conclusions reached above.

Ingestion effects are considered in Paragraph 6.3.3. However, flight test data generally validate Ames ramp test data and the general trends expected in Reference 6.11. Results show gas generator inlet air temperatures can be as much as 150° F above ambient conditions for various combinations of aircraft control settings while in ground effect. For a normal fan mode lift off, data show a typical hot gas ingestion pattern with the following average engine inlet air temperature increments: nose-up maneuver 55° F, lift off 30° F, out of ground effect 15° F. Modifications to provide stall-free operation appear to have been successful, but this conclusion is based more on the absence of stall experience since modification, than on any clearly defined or assured increase in stall margin.

6.3.2 Structural Heating

It may be concluded from the Phase I Flight Test Program that the XV-5A aircraft can be operated in fan mode without undue restriction. In those areas where restrictions were evident, means were developed which eliminated or minimized their effects. The allowable operating time restrictions on record and in effect for the Phase I Program are summarized in Table 6.5 and Figures 6.91 through 6.95. From a practical viewpoint, however, their existence is more a matter of conservative procedure than proven necessity. The restrictions were sufficiently liberal so that the test program could be effectively developed, and no real need arose to validate or extend them.

Throughout the Flight Test Program, temperature data from a number of thermocouples summarized in Figure 6.96 were recorded and monitored

to provide substantiating evidence as to the airworthiness and integrity of the aircraft structure. These data also provided useful information regarding general temperature levels, heating rates, and critical heating conditions over much of the aircraft operating envelope. Representative data are shown in Figure 6.97 through 6.117.

As shown in Table 6.6, two structural temperature limits were considered. These were normal load or permanent loss of strength limits and design load limits. It is important, therefore, that results be understood and interpreted in terms of whether or not design loads can be applied during a given mission. If so, either according to plan or inadvertently, then aircraft operation must be restricted according to the design load temperature limit (e.g. 250°F for aluminum). If not, then the design load limits may be relaxed in favor of the higher values. In all cases checked, permanent loss of strength temperature limits (e.g. 325°F for aluminum) occurred before normal loads exceeded allowable loads at operating temperature levels.

Based on flight test results, critical design heating conditions can occur for the XV-5A aircraft during prolonged hovering in proximity to the ground and during the prolonged flight at the high speed end of fan mode transitions. During the former, component heating is aggravated by the relatively high temperature environment induced around the aircraft, particularly on the lower surfaces; and by the cooling system hot gas ingestion. With the fixed landing gear and the insulated wheel well enclosure, hovering flight limits in ground effect were established by electronic compartment inlet air temperatures. With the retractable landing gear-wheel wells open configuration, wheel well temperature levels limit the operation.

During high speed fan flight, wheel well temperatures limited the operation for the retractable landing gear-wheel well open condition, but with the landing gear retracted and landing gear doors closed, the door temperatures instead limited the operation. On the other hand, with fixed landing gear and the insulated wheel well enclosure, the only limits experienced were wing rib and spar temperatures which occasionally showed a tendency to run high and to limit operation. Although the reasons are not entirely clear, it is suspected this tendency is due to hot gas leakage into the wing area via the fan-wing finger seals and/or the fuselage-canoe junction, or to reduced effectiveness of the wing fan cooling air ejectors, or to a combination of these. It is believed, however, that most of these critical conditions can be eliminated from future and even the present designs by determined effort.

Representative temperature time histories for various conditions of fan mode operation are discussed below for the aircraft in the fixed landing gear wheel well enclosed configuration. Figure 6.97 compares various structural temperatures for hovering in and out of ground effect. The general conclusion to be drawn is that heating is somewhat more severe when in than out of ground effect, although there appear to be exceptions.

Figure 6.98 shows comparative data for a series of fan mode flights at varying speed which were followed by conversion to turbojet mode and conventional landing. At flight speeds below 50 knots, the front spar temperatures stabilized at relatively low values near 150 F. Above 50 knots, they stabilized at values near 250°F. The characteristic jump in temperatures prior to conversion (at end of curve) is representative of maximum power and thrust settings for fan mode flight.

Similar trends are to be noted for the wing panels and ribs as shown in Figure 6.99. Figure 6.100 is of interest for two reasons: (1) temperatures of the maraging steel space frame located in the crossover duct compartment are relatively insensitive to aircraft velocity; and (2) comparison of (b) and (g) shows the effect of hot gas leakage from the diverter valve. In this particular case, no limit (700°F) was exceeded. However, had design loads been planned, data of plate (g) for TS 501 show the temperature limit of 400°F (Table 6.6) would have been exceeded. Figure 6.101 shows representative pitch fan area temperatures which are relatively independent of flight speed.

Wing spar temperature levels as presented in Figure 6.102 are particularly encouraging since the aft wing fan cooling air ejectors lose pumping capacity at the higher fan mode flight speeds as a result of a pressure build-up on the rear fan segments. The relatively low stabilized temperature below 60 knots is characteristic. At speeds higher than 60 knots, stabilized levels are not so certain because of the hot gas leakage problems referred to earlier. This leakage is believed to be highlighted in Figure 6.103 by the sharp cooling rates following conversion from fan to turbojet mode and the sharp heating rates following conversion from turbojet to fan mode. Further support to the leakage concept is given by Figure 6.104, particularly by the correlation between the stagger angle β_s of plate (b) and the aft wing fan cooling air ejector air temperature TG 27-OAT of plate (a).

Figures 6.105 and 6.106 show several temperature-time profiles for a series of short take-off (STOL) fan mode flights. The main difference between these data and those for VTOL flights is the relatively high initial heating rate experienced during STOL operations (compare Figure 6.105

with Figure 6.98, plate (g). Various wing temperature levels are established in the 5 minute flight of Figure 6.106 which show the wing panel or ribs to be heated to near maximum limits of 325°F. Other values are normally well below the design limit of 250°F except for the forward spar cap (TS 617) which, at the risk of being repetitive, is probably due to hot gas leakage through the wing-fan finger seals at the high β_v .

One recorded instance of an overheat condition which occurred during ground test is presented in Figure 6.107 which shows the R/H upper forward wing panel briefly exceeded the allowable limit of 325°F by approximately 15°F. Test was temporarily terminated due to activation of the structural overheat warning system, and aircraft controls and power settings were returned to more favorable conditions for cooling.

Figure 6.108 through 6.116 summarize results from two fan mode flights with the aircraft in the retractable landing gear configuration with wheel wells open and closed. Figures 6.108 through 6.112 show temperature-time data gathered during the XV-5A demonstration flight 143-2-80F covering a vertical lift-off and vertical landing. For this flight, landing gear was retracted and wheel wells enclosed at indicated aircraft speeds above 60 knots. Wheel well heating is strongly affected in ground effect as shown by TS 811 of Figure 6.108. As the aircraft moves out of ground effect, a pronounced reversal takes place and a cooling rate of 1.6°F/sec is evident. The main landing gear door heating rate of 1.3°F at the right occurs with the wheel well door closed and protected by a 1/8 inch thickness of high performance insulation. Results agree with design estimates. Current design is limiting for high speed fan mode flights to 4.0 minutes for this configuration. However, redesign easily could permit any desired practical duration. Considering Flight 143-2-80F to represent typical fan mode lift-off and landings, the recorded temperatures show the landing to be surprisingly less severe than the lift-off (compare data of Figures 6.109 and 6.110). In ground effect, the forward regions of the main wheel well are somewhat more strongly heated than the aft regions, as can be seen by comparing data of 6.112. Figure 6.111 shows that the main wheel well doors are not heated severely during a normal take-off.

Figures 6.113 and 6.114 summarize temperature data for Flight 142-2-79F which included evaluation of main landing gear door insulation performance and evaluation of main wheel well open heating at flight speeds of 40 and 60 knots, and during a dash acceleration to conversion from fan to turbojet mode.

Figure 6.113 shows main landing gear door heating (1.33°F/sec) to

occur only at high flight speeds approaching 90 knots ($\beta_v = 45^\circ$). These data also show that below flight speeds of 80 knots, fan turbine exhaust gases do not scrub the doors severely. Comparison of TG812 and TG817 of Figure 6.114 shows the aft main wheel well regions to be heated much more at the higher forward flight speeds (60 knots) than the forward regions.

Figures 6.114 through 6.116 show rather sharp increases in heating rates with increased flight speeds. Figure 6.116 is of special interest because it presents results occurring during the dash acceleration from 60 knots to conversion and shows a rather sharp increase in the heating rate of the aluminum drag strut fold joint (TS703). While the rate is quite high, the data suggest a leveling out of temperature may be near. This is encouraging, because it is a general characteristic of the XV-5A aircraft that temperatures approach their maximum values at very rapid rates, only to abruptly level off. Figure 6.117 provides an estimate of the drag strut fold joint for various louver angles based on the aft wheel well air temperature TG817. Combining this with flight speed and louver angle data for fan mode flight, it is possible to estimate drag strut fold joint temperatures at various flight speeds.

Only representative temperature data have been presented in this section. Many data are available and their thorough analysis would reveal much interesting and worthwhile information. It is believed, however, that essential areas of the fan mode flight envelope have been covered and that the general claims at the beginning of this section have been substantiated.

6.3.3 Reingestion

Fan mode operation, as has been pointed out previously (Paragraph 6.1.1.1 and Reference 6.1), is influenced by the induced environment - particularly temperature increases due to hot gas ingestion by the engines and/or fans. Figures 6.118 through 6.134 present typical inlet air temperatures for a variety of XV-5A operating conditions in and out of ground effect and during various fan mode lift-off and touchdown conditions. The maximum temperature increase due to hot gas ingestion recorded to date is approximately 150°F and was experienced by the gas generators.

Figure 6.118 presents one of the most extreme examples of hot gas ingestion by the engine. Interpreted as in Reference 6.11, with full up collective, forward or neutral longitudinal stick, and large collective vector (30°) the interaction zones beneath the aircraft are weak and no ingestion was experienced. As full pitch up moment (aft longitudinal stick)

is called for, the stagnation point moves back under the wing causing some but relatively little ingestion. However, as the vector (β_v) is symmetrically decreased from 30° to 20° , a sharp rise in engine air ingestion occurs. The highest peak of Figure 6.118 suggests even greater ingestion temperature increases might be experienced with finer vector control increments.

The effect of rudder pedal and lateral stick positions on ingestion for minimum and mid collective stick positions are presented in Figures 6.119 and 6.120, respectively. With all controls neutral, collective position does not have a significant effect on ingestion (see Figure 6.121). Maximum ingestion by the R/H engine for minimum collective and a full forward stick occurs for a right lateral stick and a left rudder pedal. (See Figures 6.119 and 6.122.)

In general, ingestion conditions measured at one inlet for a given set of asymmetrical control settings will be experienced in the other inlet for the opposite control settings. This is illustrated to some degree by the engine T_2 sensor data of Figure 6.124. Conditions at the cooling system air inlet closely parallel those at the engine inlet, (compare Figures 6.123 and 6.124). Representative engine inlet air temperature distribution patterns obtained during engine stall investigation are presented in Figures 6.125 through 6.129, however, they offer no rational clue to the cause of the stall. Spread in the levels of temperature with respect to radial position does not appear significant. However, as shown in Figure 6.129, the maximum engine inlet air temperature appears to develop at the 10 o'clock position rather than the 2 and 4 o'clock positions, contrary to expectations.

Representative engine, wing fan and pitch fan inlet air temperatures experienced during typical vertical lift-off and touchdown maneuvers are presented in Figure 6.130. The large engine inlet air temperature rise prior to lift-off is typical of the nose up maneuver but it is largely eliminated by the time lift-off is initiated. As shown in Figure 6.131, a small spike frequently appears shortly after the nose up maneuver is completed, as the collective stick is increased. Little ingestion occurs, for out of ground effect hover (Figure 6.131) as compared to the in ground effect hover of Figure 6.130. Wing and pitch fan inlet air temperatures do not appear to be influenced significantly by the lift-off conditions. Touchdown ingestion conditions are similar to lift-off conditions and effects of relatively slow right and left lateral translations are shown in Figure 6.132.

Representative engine inlet air temperatures for rolling (STOL) lift-off and touchdowns, as distinguished from the vertical maneuvers, are presented in Figures 6.133 and 6.134, for a range of aircraft speeds varying from 75 to 30 knots. Significant hot gas ingestion was noted only at the lowest touchdown speed of 30 knots. It is expected that varying degrees of hot gas ingestion will be experienced at these low forward speeds and the amount would be dependent on relatively precise combinations of aircraft operating conditions, control settings, and proximity to the ground, (as suggested by Figure 6.118). The maximum engine inlet air temperature rise expected due to hot gas ingestion probably will not exceed 150°F.

6.3.4 Compartment Cooling

In the study of compartment cooling, no attempt has been made to correlate data with hot gas ingestion. It is obvious, however, that they are influenced by such ingestion, particularly in ground effect. As mentioned in Paragraph 6.3.3, cooling system hot gas ingestion closely parallels that of the inlet and can result in cooling system inlet air temperatures 100°F or more above ambient air temperatures. Representative compartment temperatures are presented in Figures 6.135 through 6.154.

Figure 6.135 presents typical cockpit air temperatures for a ground run. Cockpit air temperatures are dependent upon time of day, ambient temperature, degree of sunshine, and hot gas ingestion. For prolonged ground runs such as required for compressor stall investigations, relief from heating was obtained by using opaque paper on the inside of the canopy. Early in the test program, pilot's complaints of hot gas leakage led to sealing of holes in aft bulkhead and floor of the cockpit. Complaints of cockpit heating stopped until hot weather and prolonged ground running began. The temperature fluctuations of Figure 6.135 are due to hot gas ingestion.

Following the pilot, the electronic compartment environment is most sensitive to hot gas ingestion. The data of Figure 6.136 shows the effect of ingestion and ambient temperature on inlet air temperature to the electronic compartment. This air is a blend of cockpit, cooling fan compartment, and generator cooling air which has passed through the small cooling air blower and the hydraulic oil cooler.

The average temperature rise across the hydraulic oil cooler varied about 20°F for flight 143-2-79F, (Figure 6.137), and 40°F for Flight 143-2-60F, (Figure 6.146). This difference is due to the difference in control power required in hovering, as compared to translational flight.

An interesting fact is that the temperatures between the electronic compartment inlet air temperature, and outside ambient air temperature, are remarkably uniform, being about 60-65°F for ground runs (Figure 6.136), for STO operations including climb, (Figure 6.152), for hover flights (Figure 6.146) and for VTOL translational flights (Figure 6.153).

During the correction for compressor stall, an ejector was installed to purge the compressor compartment. Comparing TG-21 for ground runs 12.11 and 12.12 before and after ejector installation, Figure 6.138 shows that little if any improvement was realized. Comparing TG 23, it is evident that engine bay compartment cooling was adversely affected by an increase in temperature of at least 100°F.

Figures 6.139 through 6.143 show that the high engine bay temperatures continue for a variety of fan mode hover and translational flights.

Figure 6.143 shows the increase of shroud air temperature along the tailpipe.

Figures 6.144 and 6.145 show representative main landing gear wheel well temperatures during tie down ground testing for the fixed landing gear wheel well enclosed with the insulated heat shield. The high gas temperatures (TG 812) show the necessity for care, during installation, that cracks are closed so that small electrical and hydraulic components are not overheated. Data of Figure 6.144 show the nose wheel well (not enclosed, TS725) is heated close to its limit. Figure 6.145 shows that the more massive main landing gear V-brace and mode change cylinder components (TS 705 and TS 707) were not heated severely.

Figure 6.146 shows engine oil (TL1 and TL2) and wing fan aft ejector temperatures (TG27) for a relatively long hover flight. The engine oil temperatures are running close to the limit and show uniformity from run to run, (Figure 6.147). For a series of 30 different flights, the maximum engine oil temperature recorded averaged 361°, $\pm 10^\circ\text{F}$.

Wing fan temperatures are indicated by ejector cooling air temperatures TG 27 and TG 29 as presented in Figures 6.148 and 6.149. A noticeable difference exists between the aft ejector cooling air temperatures (TG 27). Flight 143-2-79F data as presented in Figure 6.148 is for fan mode flight following conversion from turbojet to fan mode, whereas flight 143-2-29F was a STO fan mode flight. It is possible hot gas leakage could account for the high temperatures of Figure 6.149.

A check of left-hand wing structural temperatures around B.L. 61.0

showed them to be normal so that, if valid, the high temperature could be due only to localized scroll leakage. Figures 6.150 and 6.151 show similar results in that the left wing fan aft air ejector loses pumping capacity in forward fan flight.

Figures 6.152 and 6.153 summarize cooling system air temperature relative to ambient air for a series of STO operations involving climb and VTOL flights respectively. Generally the flight temperatures associated with the STO operations appear to run somewhat higher than those for the VTOL flights. The main wheel well air temperature ran quite high for the STO operations (TG 812, plate A, Figure 6.152). Otherwise, the data were normal.

Figure 6.154 summarizes some results of a rather extensive fan mode ground run consisting of a series of high power settings. Perhaps the most interesting results were the front spar temperatures (TS 617 and TS 618) and the main axle temperature (TS709) during the first few minutes when the louver angle was at 45°. The value of 280°F is the highest known temperature for the main axles. It is indicative of an extreme exposure to which the XV-5A aircraft may be subjected, although such exposure is unrealistic operationally. The spar temperatures are believed to reflect hot gas leakage through the fan-wing finger seals as a result of forward spillage from the highly vectored forward louver. Other temperatures were more representative of operational conditions.

Only representative compartment air temperature data have been presented in this section. Many data are available and their thorough analysis would reveal interesting and worthwhile information, but it is believed that essential areas of fan mode operation have been discussed, and that satisfactory cooling system performance has been demonstrated. Additional information is available in Paragraphs 6.3.3 and 7.3.

TABLE 6.5

**XV-5A FAN MODE OPERATING RESTRICTIONS WITH RETRACTABLE
LANDING GEAR CONFIGURATION**

1. Flights above 60 KIAS with landing gear up and wheel wells closed are limited to 4.0 minutes.
2. Fan Mode Ground Operation at 70% engine RPM with wheel wells open and landing down is limited to 6.0 minutes.
3. Fan Mode operation in ground effect at or near lift-off power with wheel well open and landing gear down is limited to 2.0 minutes (hot day operation may require further restrictions).
4. Fan Mode operation out of ground effect at speeds to 60 KIAS and $\beta_v < 30^\circ$ is not restricted by landing gear down and wheel well open condition; however, the restrictions of Figures 6.92 through 6.95 still hold until modified by test data.
5. Fan Mode dash accelerations from 60 KIAS to conversion with landing gear down and wheel wells open must be accomplished within 15 seconds.

TABLE 6.6

XV-5A AIRCRAFT - STRUCTURAL TEMPERATURE LIMITS

	<u>Design</u>	<u>Normal Load</u>
Aluminum Alloys	250°F	325°F
Titanium -99 T _C	550°F	1000°F
6A1AV	700°F	1100°F
Magnesium AZ318H24	250°F	400°F
Steel Marage	300°F	700°F
Fiberglas Laminate - Silicone	700°F	700°F
Rubber - Silicone	450°F	450°F

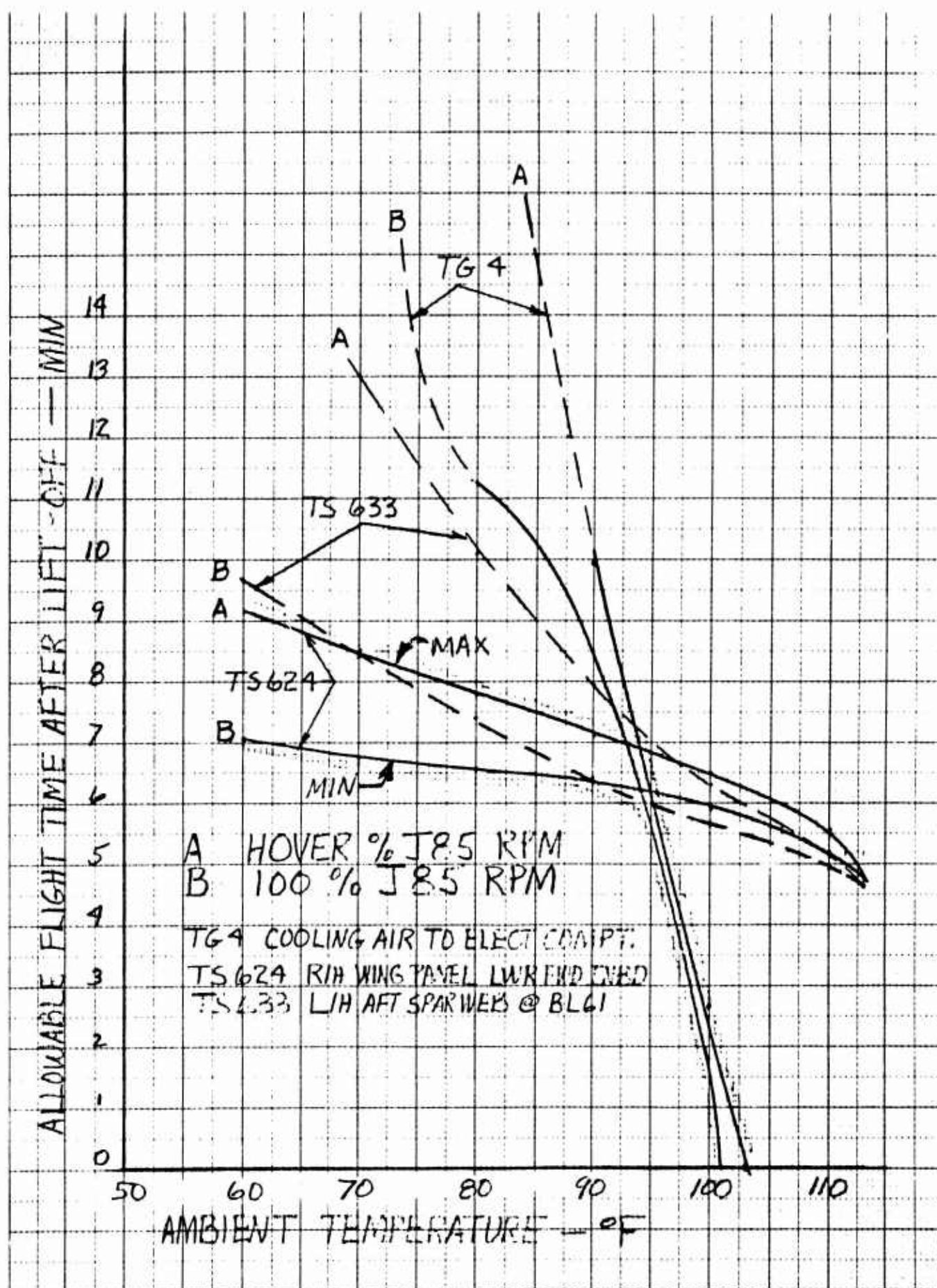


Figure 6.91 Estimated Allowable Fan Mode Flight Time vs Ambient Temperature for Flight Speeds from 30 to 95 Knots

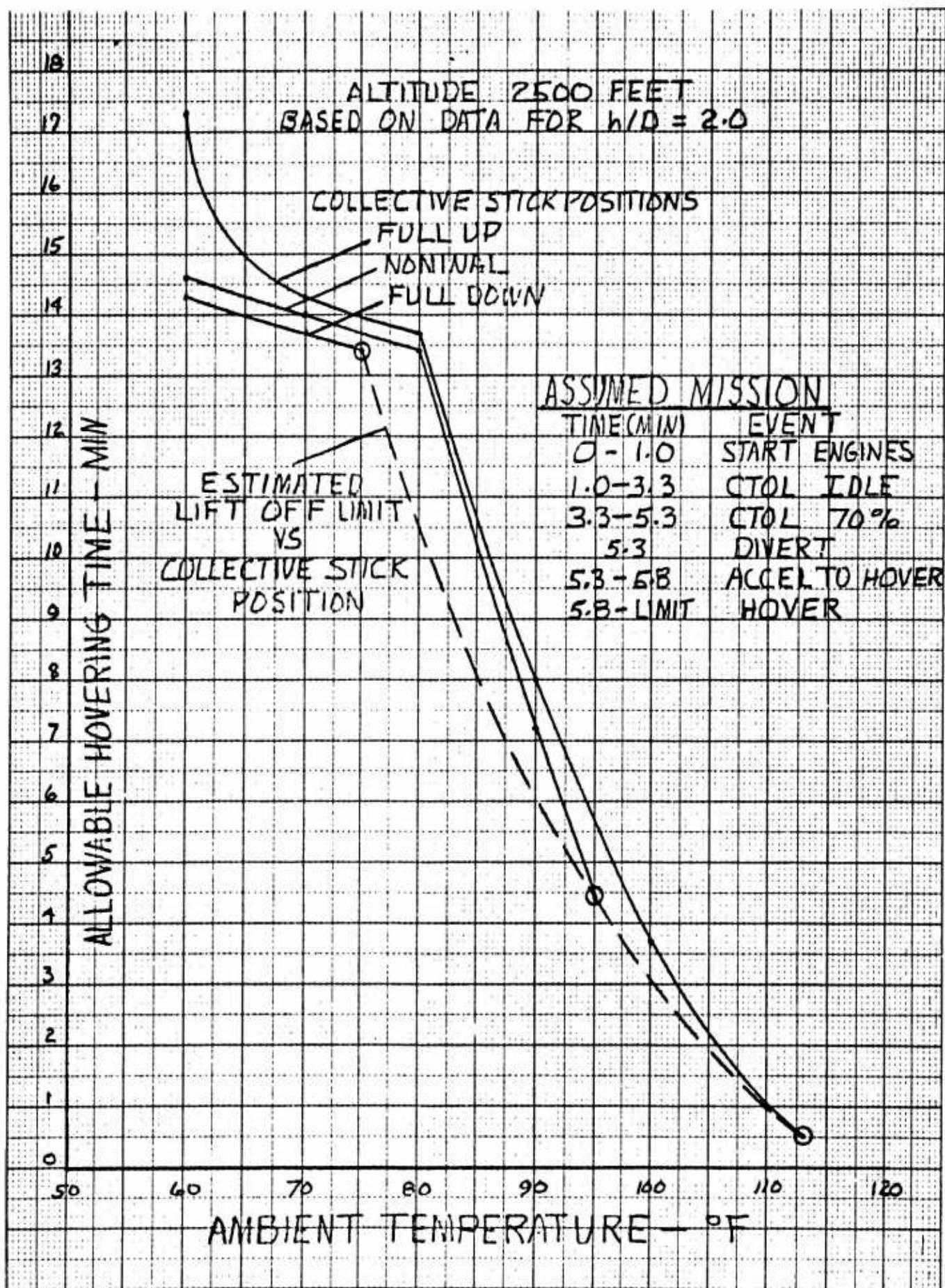


Figure 6.92 Estimated Allowable Fan Mode Hover Time vs Ambient Temperature - Effective for Flight Speeds from 0 to 30 Knots, $h/D = 2.0$, Aircraft Weight 10,000 Pounds

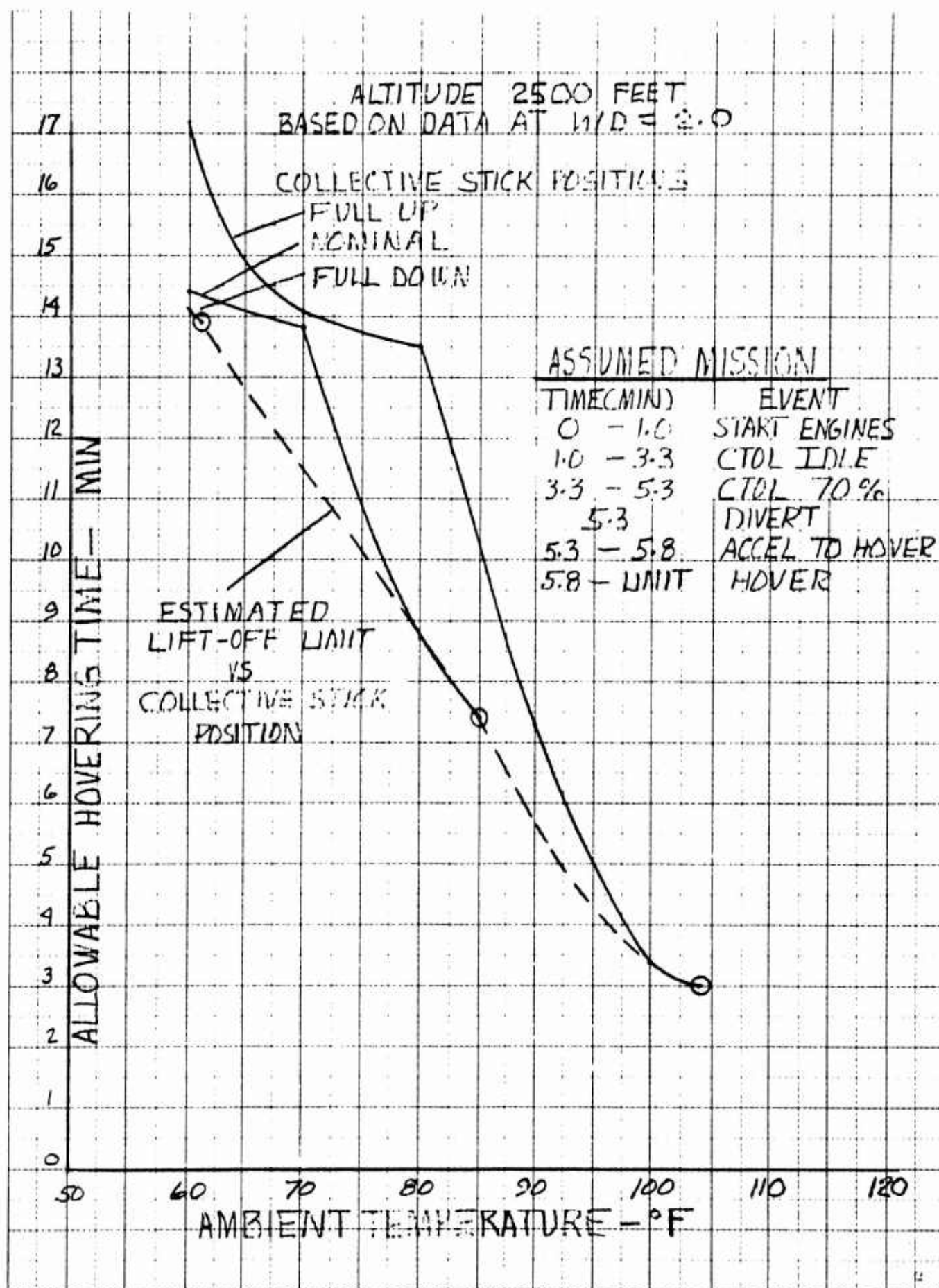


Figure 6.93 Estimated Allowable Fan Mode Hover Time vs Ambient Temperature - Effective for Flight Speeds from 0 to 30 Knots, $h/D = 2.0$, Aircraft Weight 10,500 Pounds

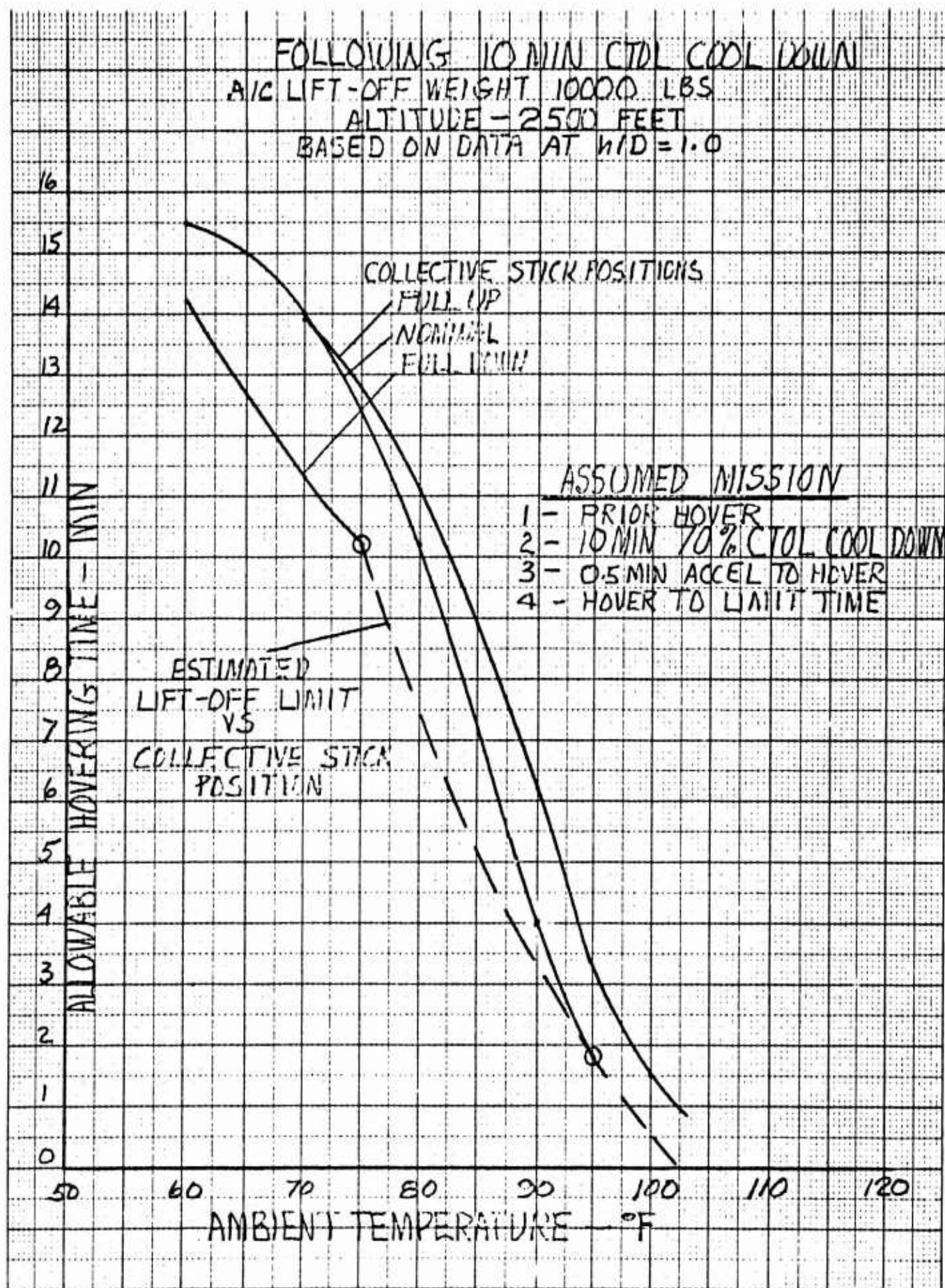


Figure 6.94 Estimated Allowable Fan Mode Hover Time vs Ambient Temperature - Effective for Flight Speeds from 0 to 30 Knots, $h/D = 1.0$, Aircraft Weight 10,000 Pounds

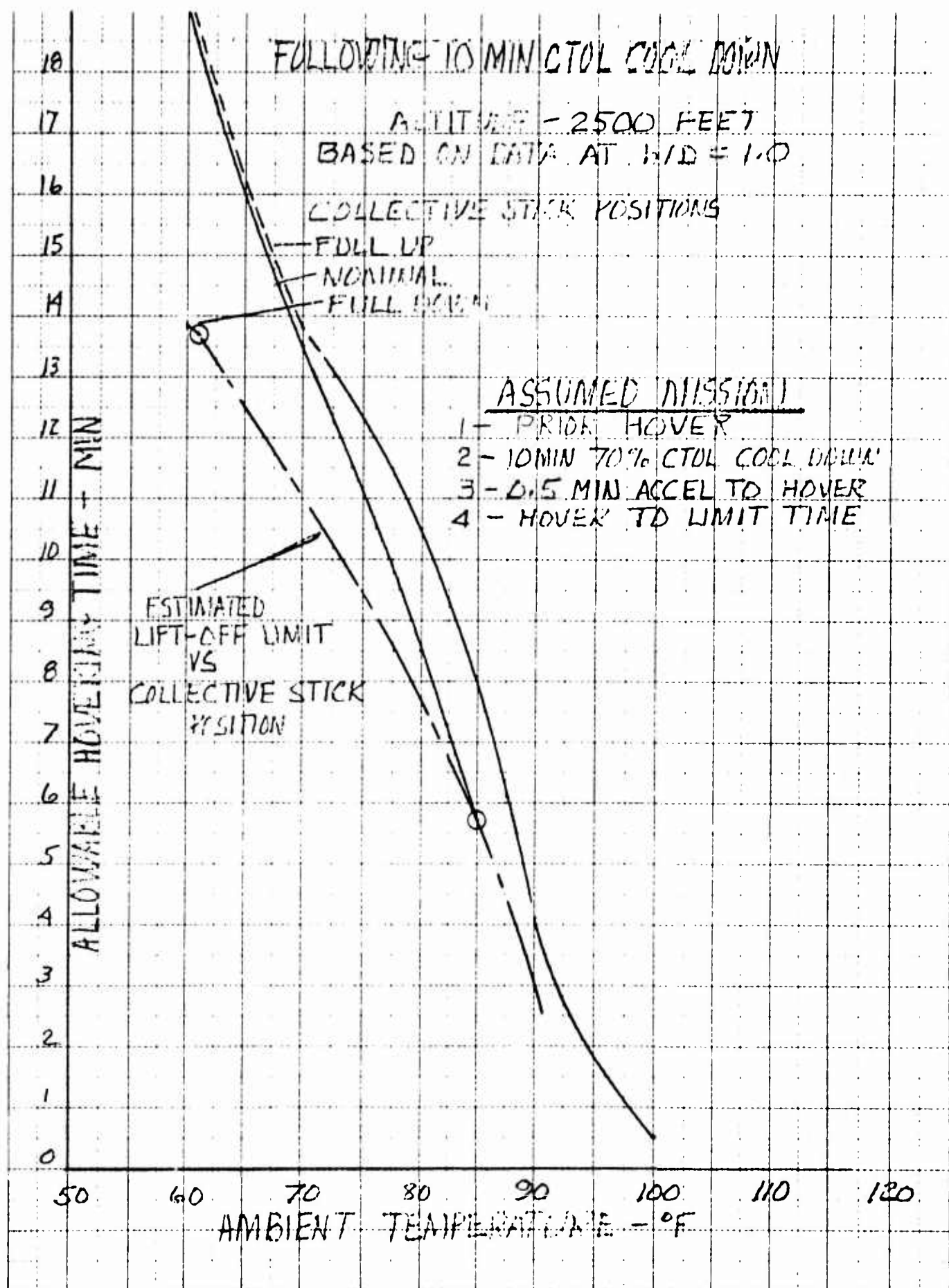


Figure 6.95 Estimated Allowable Fan Mode Hover Time vs Ambient Temperature - Effective for Flight Speeds from 0 to 30 Knots, $h/D = 1.0$, Aircraft Weight 10,500 Pounds

SURFACE TEMPERATURE IDENT. & LOC. CHART.

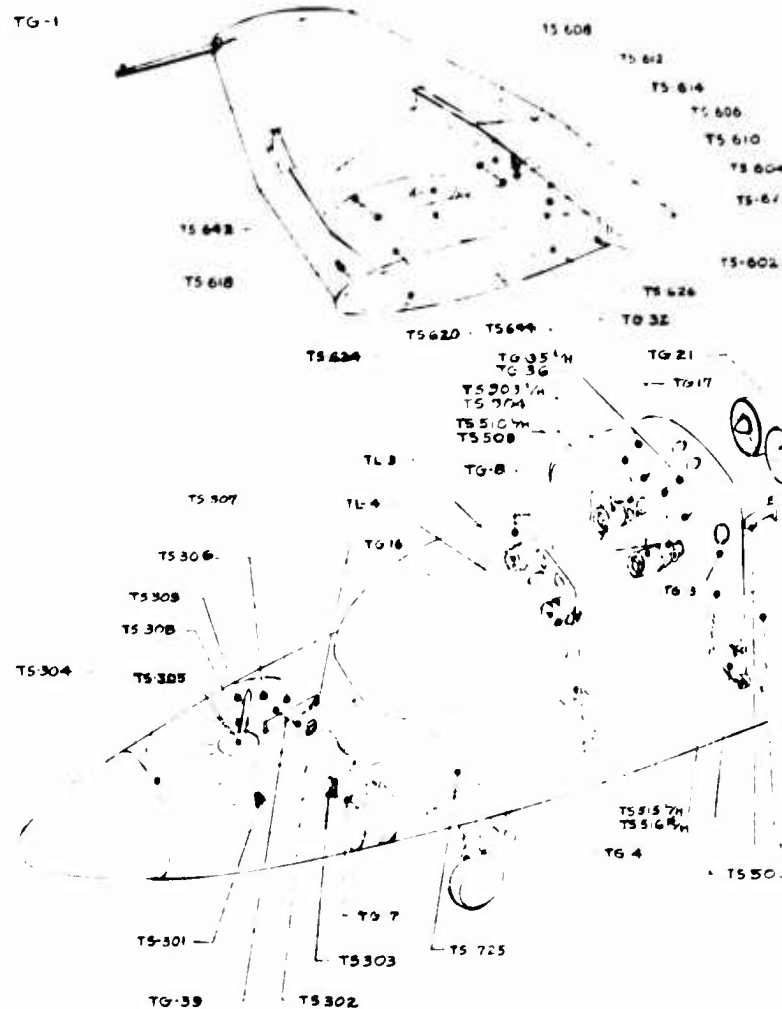
ITEM NO	MEASURE	INSTR	STA.	B.L.	N.L.	GAGE TYPE	MATERIAL	PRINT	SHT	ZONE	FLY TEST
TS-601	WIND - REAR SPAR L/H CAP	L/H X	286.	24.		FE/CN	143W003	5/1			*
TS-602	" " " " " "	R/H X		24.							*
TS-603	" " " " " "	L/H X		44.							*
TS-604	" " " " " "	R/H X		44.							*
TS-605	" " " " " "	L/H X		61.							*
TS-606	" " " " " "	R/H X		61.							*
TS-607	" " " " " "	L/H X		71.					06		*
TS-608	" " " " " "	R/H X		71.					06		*
TS-609	UPPER CAP L/H X	L/H X		44.							*
TS-610	" " " " " "	R/H X		44.							*
TS-611	" " " " " "	L/H X		61.							*
TS-612	" " " " " "	R/H X		61.							*
TS-613	WING FAN REARMT. SUPPORT STRUCT	L/H X	285.7	61.	102	280, 280	143W016	5/3			*
TS-614	" " " " " "	R/H X	285.7	61.	102	280, 280	"	"			*
TS-615	WIND - REAR SPAR LWR CAP	L/H X	215.	30.			143W002	5/1	D-5		*
TS-617	" " " " " "	L/H X	215.5	61.					D-9		*
TS-618	" " " " " "	R/H X	215.5	61.							*
TS-619	WIND - REAR SPAR LWR CAP	L/H X	240.				143W028	5/1			*
TS-620	" " " " " "	R/H X	240.							C-8	*
TS-621	" " " " " "	L/H X	272.								*
TS-622	" " " " " "	R/H X	272.								*
TS-623	" " " " " "	L/H X	240.								*
TS-624	" " " " " "	R/H X	240.								*
TS-625	" " " " " "	L/H X	272.								*
TS-626	" " " " " "	R/H X	272.								*
TS-627	WING FLAP FAIRING INDO.	L/H X		30.	100.		143W085	5/1	A-2		*
TS-629	" " " " " "	L/H X		56.	100.		"	"			*
TS-511	INVERTER	L/H X	450.	4.	105.		143E023	5/2			*
TS-512	" " " " " "	R/H X	450.	4.	105.		"	"			*
TS-509	GENERATOR	L/H X	185.		140.		2710755				*
TS-510	" " " " " "	R/H X	185.		140.		"				*
TS-630	WING FLAP FAIRING INDO.	L/H X	286.				143W025				*
TS-651	FLAP - INDO. FITTING	L/H X	307	86.	97.5		43W010	5/1	A-4		*
TS-661	" " " " " "	L/H X	310	61.			143W010	5/1			*
TS-721	LOG GEAR - TOP OF OLEO STRUT	L/H X					143L006				*
TS-701	LANDING GEAR - MAIN TOWER STRUCTURE	L/H X			835		143L006	5/1			*
TS-703	" " " " " "	L/H X					143L006				*
TS-705	" " " " " "	L/H X			87		143L006				*
TS-707	" " " " " "	L/H X					143L010	5/1			*
TS-709	" " " " " "	L/H X					143L006	5/1			*
TS-711	" " " " " "	L/H X					143L006	5/1			*
TS-713	LOG GEAR - TOP OF OLEO STRUT	L/H X	284.				143L008	5/1	B-9		*
TS-715	" " " " " "	L/H X	314.						B-11		*
TS-717	" " " " " "	L/H X	283.						C-9		*
TS-719	" " " " " "	L/H X	314.						D-11		*
TS-725	NOSE LANDING GEAR - WHEEL WELL	L/H X	106.	61.	79						*
TS-501	FRAME - 23 INCH 3-8	L/H X	256	22.	32		143F009	5/1	B-9		*
TS-502	" " " " " "	L/H X	251.	3.	32		"		B-11		*
TS-503	" " " " " "	L/H X	272.	22	132				C-9		*
TS-504	" " " " " "	L/H X	257.	22.	127.						*
TS-505	" " " " " "	L/H X	245.	22.	955				A-9		*
TS-301	PITCH LEVER - 100 INCH 3-8	L/H X	59.				143F010	5/1	A-5		*
TS-302	" " " " " "	L/H X	78				143F010	5/1	C-4		*
TS-303	" " " " " "	L/H X	85.	75	855		143F011	5/1	B-5		*
TS-304	" " " " " "	L/H X					143F011				*
TS-305	" " " " " "	L/H X					143F011				*
TS-306	" " " " " "	L/H X					143F011				*
TS-307	" " " " " "	L/H X					143F011				*
TS-308	" " " " " "	L/H X					143F011				*
TS-309	" " " " " "	L/H X					143F011				*
TS-506	FRAME - 23 INCH 3-8	L/H X	214	40	95		143F010	5/1	A-5		*
TS-507	" " " " " "	L/H X	256	24	945		143F010	5/1			*
TS-508	" " " " " "	L/H X	310.	23.5	935		143F010	5/1	B-10		*
TS-513	" " " " " "	L/H X	305				143F010				*
TS-514	" " " " " "	L/H X					143F010				*
TS-641	" " " " " "	L/H X	256.	61.			143F010				*
TS-642	" " " " " "	R/H X	256.	61.							*
TS-643	" " " " " "	L/H X	256.	61.							*
TS-644	" " " " " "	R/H X	256.	61.							*
TS-430	APT FUSELAGE	L/H X	287			FE/CN	143F016				*
TS-432	" " " " " "	L/H X	983.				143F016				*
TS-460	" " " " " "	L/H X	253.		143		143F016				*
TS-461	" " " " " "	R/H X	253.		143		143F016				*
TS-462	" " " " " "	L/H X					143F016				*
TS-451	" " " " " "	L/H X	400.	19.	94.	CR/AL	143F012	5/1	A-4		*
TS-453	" " " " " "	L/H X	400.	21.	94	CR/AL	143F012	5/1			*
TS-454	" " " " " "	L/H X	400		94	CR/AL					*
TS-455	" " " " " "	L/H X				FE/CN	143F016	5/1	A-3		*
TS-457	" " " " " "	L/H X		6.							*
TS-458	" " " " " "	L/H X	285.7	0.0			143F016				*

A

GAS & LIQUID TEMP. GAUGE IDENT. & LOC.

ITEM NO.	MEASURE	INST. TEST	STA.	B.L.	W.L.	PROBE TYPE	REF. PRINT NO.	FLT. TEST
TL-1	ENG. OIL TEMP. (BRAV)	L/H X	220		30.	G.E.	4012028-441	* *
TL-2	"	R/H X	"		"	G.E.	"	* *
TL-3	HYD RES. OIL TEMP.	L/H X	170.		30.	FE/CN	143P006	* *
TL-4	"	R/H X	170.		30.	"	"	* *
TG-1	OUTSIDE AIR TEMP.	R/H X	270	171.		ROSEMOUNT PROBE 110-2	143D021	* *
TG-2	ENG EXHAUST GAS TEMP. (EFT)	L/H X	240			G.E.	4012028-441	* *
TG-3	"	R/H X	240			G.E.	"	* *
TG-4	ELECTRONIC BR. 2 COMP. COOL AIR INLET	L/H X				FE/CN	143P004	* *
TG-5	WING FAN SCROLL COMP. TEMP.	L/H X				"	4012001-942	* *
TG-6	"	R/H X				"	"	* *
TG-7	PITCH FAN COMP COOL AIR INLET	L/H X				"	143P008	* *
TG-8	COOPIT COMP. AIR TEMP.						143P004	* *
TG-11	CROSS DUCT COMP. TEMP.					FE/CN	143P050	* *
TG-13	COOLING FAN COMP AIR INLET						143P051	* *
TG-15	"						"	* *
TG-16	PITCH FAN COMP COOL AIR EJECTOR INLET	X	77	O.			143P010	* *
TG-17	COOLING FAN (FWD) EXHAUST TEMP.	L/H X					143P051	* *
TG-19	AFT COOLING FAN EXHAUST TEMP.	L/H X					"	* *
TG-21	ENG COMPRESSOR SECTION	L/H X		2			143D057	* *
TG-23	ENG TURBINE SECT T	L/H X					"	* *
TG-25	ENG EXHAUST TAILOR EJECTOR TEMP.	L/H X	400	O			143P088	* *
TG-27	WING FAN COOLING AIR EJECTOR (LEFT)	L/H X	285.	61.			143W041	* *
TG-29	" (FWD)	R/H X	227.	61.			143W057	* *
TG-31	WING FAN INLET AIR TEMP.	R/H X					4012001-942	* *
TG-32	WING FAN INLET AIR TEMP.	L/H X				CR/AL	4012001-941	* *
TG-33	CROSSOVER DUCT INSIDE SHROUD	L/H X				CR/AL	143P013	* *
TG-34	CROSSOVER DUCT INSIDE SHROUD	R/H X				FE/CN	"	* *
TG-35	ENGINE INLET AIR TEMP.	L/H X					143P006	* *
TG-36	ENGINE INLET AIR TEMP.	R/H X					143P006	* *
TG-37	FLAP ACTUATOR SLOT IN FUSELAGE	L/H X					143F016	* *
TG-38	FLAP ACTUATOR SLOT IN FUSELAGE	R/H X					"	* *
TG-39	"						143P010	* *
TG-812	MLO WHEEL WELL AIR TEMP. (W. C)				CO		143L006	* *
TG-817	MLO WHEEL WELL AIR TEMP. (AFT)						"	* *

TG-1



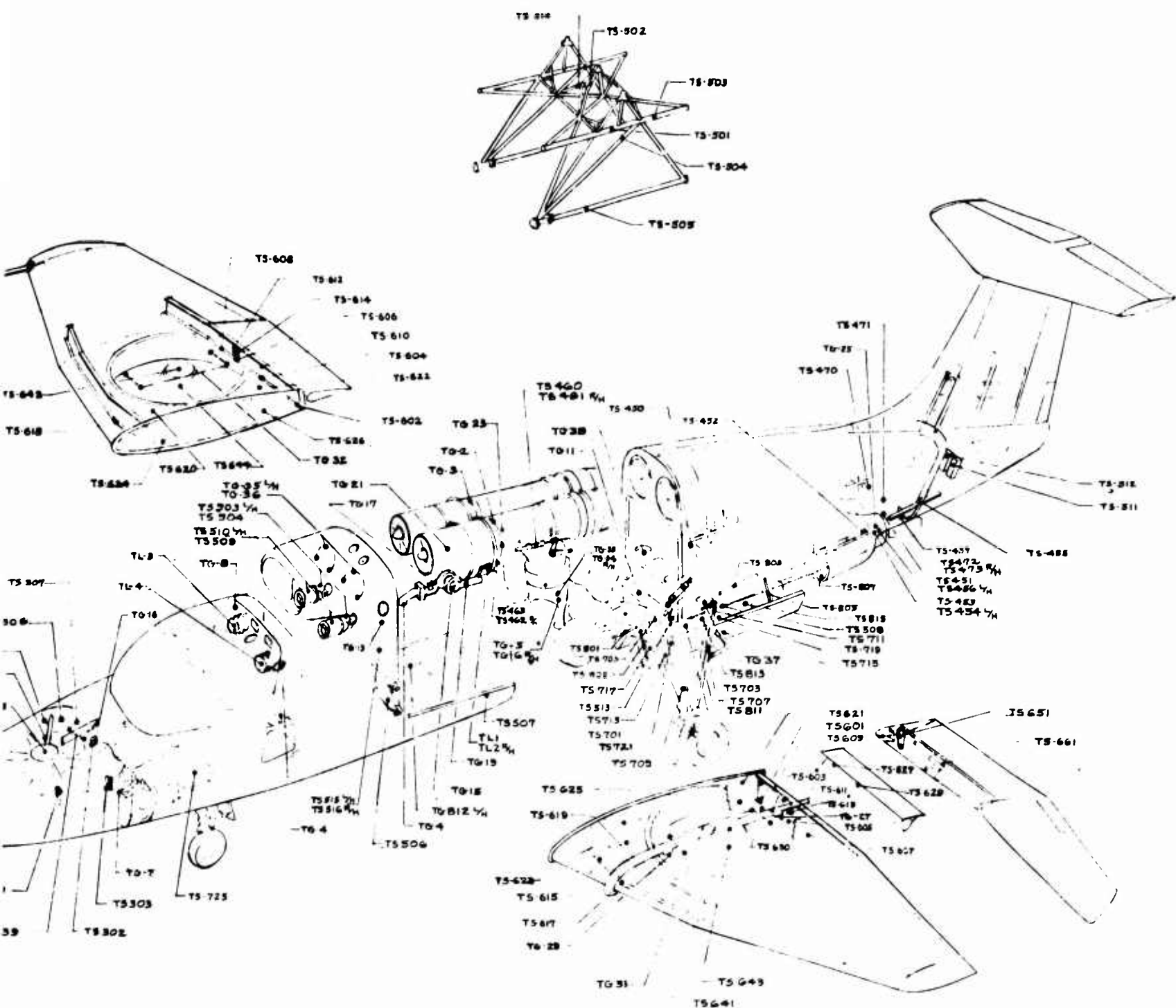
ADDITIONAL SURFACE TEMP. GAUGE LOG.

ITEM NO.	MEASURE	INST. TEST	STA.	B.L.	W.L.	PROBE TYPE	REF. PRINT NO.	FLT. TEST
TS-801	FWD LG. GEAR DOOR/DOOR-95	L/H X				FE/CN	143L007	
TS-802	FWD LG. GEAR DOOR/DOOR-95	X				"	"	5/2
TS-803	AFT LG. GEAR DOOR/DOOR-95	X				"	"	5/2
TS-805	AFT LG. GEAR SUPPORT ROD	L/H X					143L006	
TS-807	AFT A. LESS PANEL	L/H X					143F033	
TS-811	MLO WHEEL WELL HEAT	X	232.				143L060	*
TS-813	"	X	309.				"	*
TS-814	"	X	333.				"	*
TS-456	AFT FUSELAGE CANAL DUCT	L/H X	400	9	94.	CR/AL	143P012	
TS-463	FWD FUSELAGE TURNING SECTION	R/H X				CR/AL	4012018-441	* *
TS-464	ENGINE FUEL CONTROL VALVE	L/H X				FE/CN	"	
TS-465	ENGINE IGNITION BOARD	X					"	
TS-466	ENGINE OIL COOLER	X					"	
TS-470	AFT FUSELAGE PAINTED BLIND	L/H X	3897	6.			143F038	
TS-471	"	L/H X	3897	6.			"	
TS-472	"	L/H X	400				143F016	*
TS-473	"	L/H X	400				"	*
TS-515	FIRE BOTTLE	L/H X					143P004	
TS-516	FIRE BOTTLE	R/H X					143P004	
TS-903	GENERATOR DRIVE OIL COOLER (FWD)	L/H X				FE/CN	"	
TS-904	"	R/H X				FE/CN	"	

THERMO
FOR WIRE ROUT
FOR WIRING CONN
FOR WIRING CONN
FOR EXACT LOCAT

Figure 6.96 A

B



THERMOCOUPLE LOCATIONS
 FOR WIRE ROUTING SEE 143 D020
 FOR WIRING CONN. RIC#1 SEE 143 D053 5/8, 5/16, 1/4
 FOR WIRING CONN. RIC#2 SEE 143 D054 5/8, 5/16, 1/4
 FOR EXACT LOCATIONS REFER TO MARKED PRINTS INDICATED

C

Figure 6.96 Available XV-5A Aircraft Temperature Instrumentation

A/C No. 624506

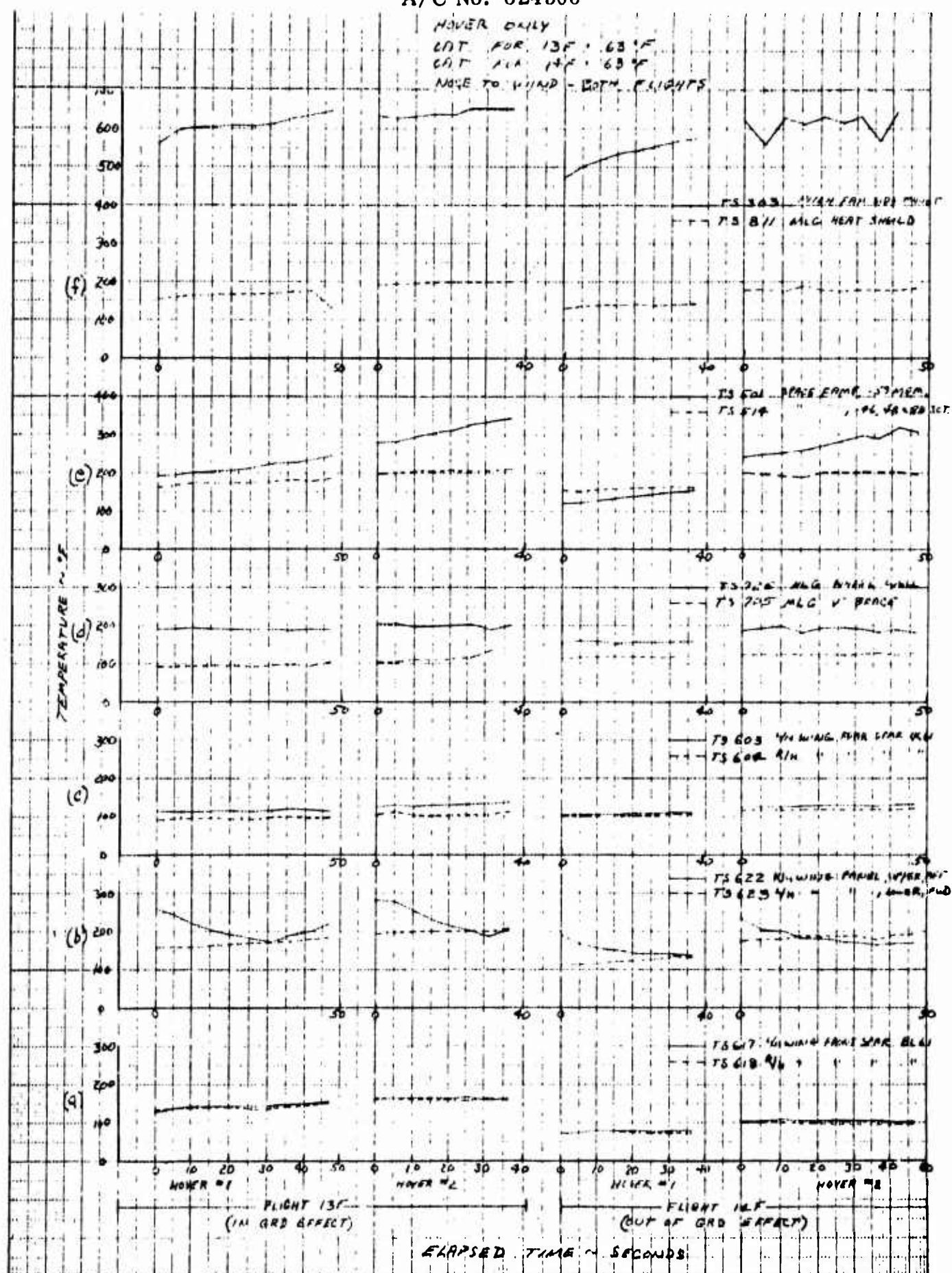


Figure 6.97 Comparison of Selected XV-5A Structural Temperature Time Profiles for Hover Flight in and out of Ground Effect

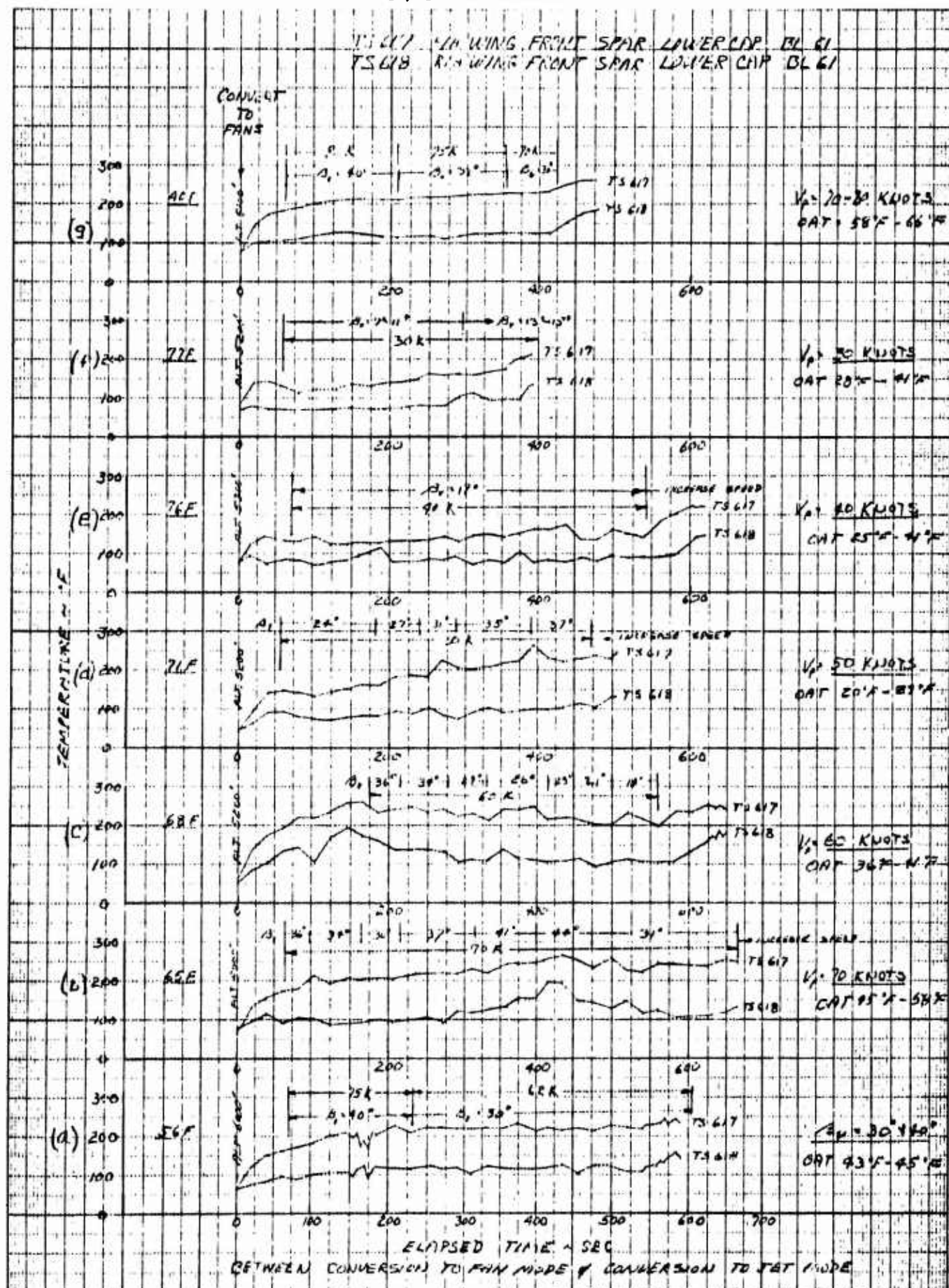


Figure 6.98 Effect of Velocity on Front Spar Temperatures for Fan Mode Operation

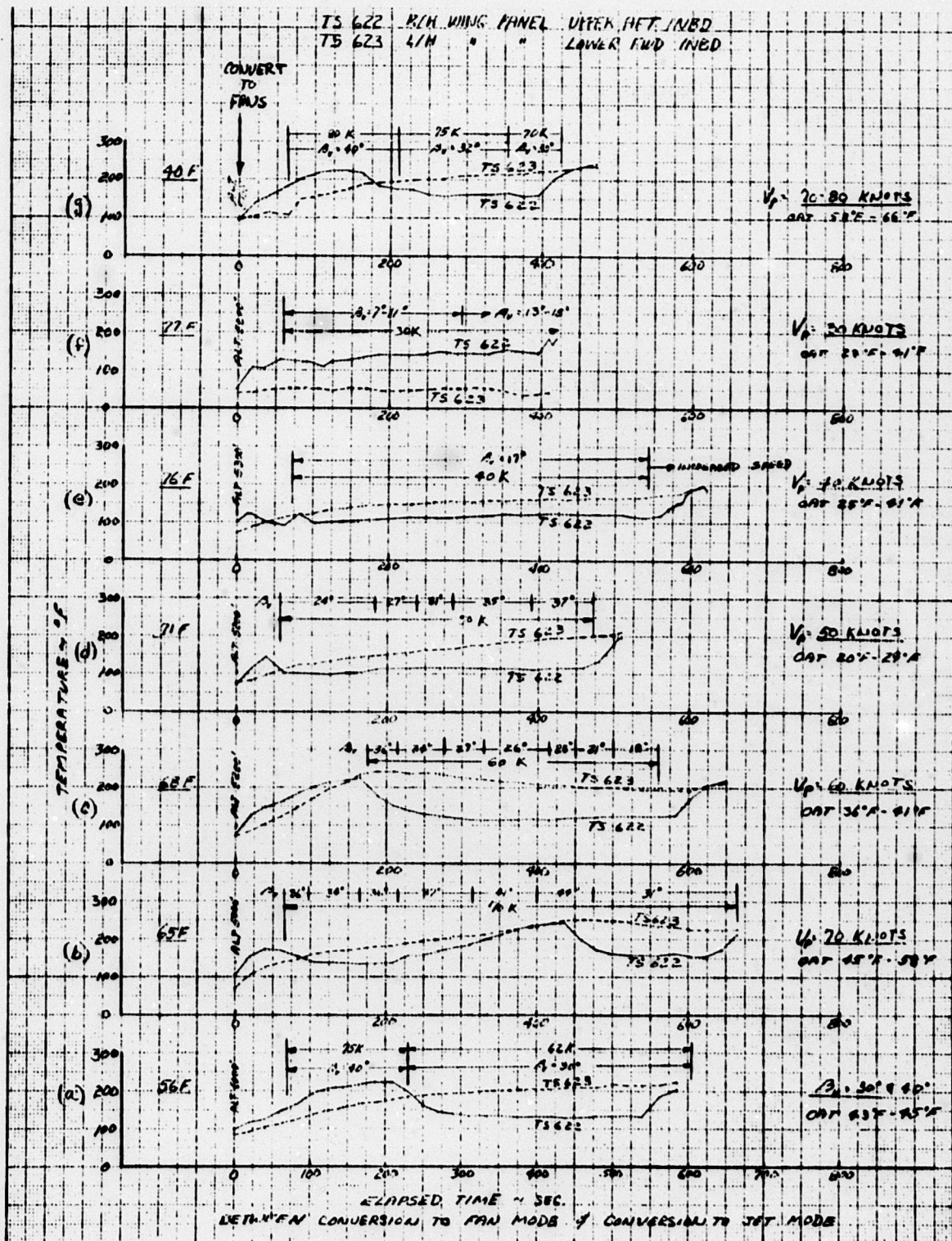


Figure 6.99 Effect of Velocity on Selected Wing Panel Temperatures for Fan Mode Operation

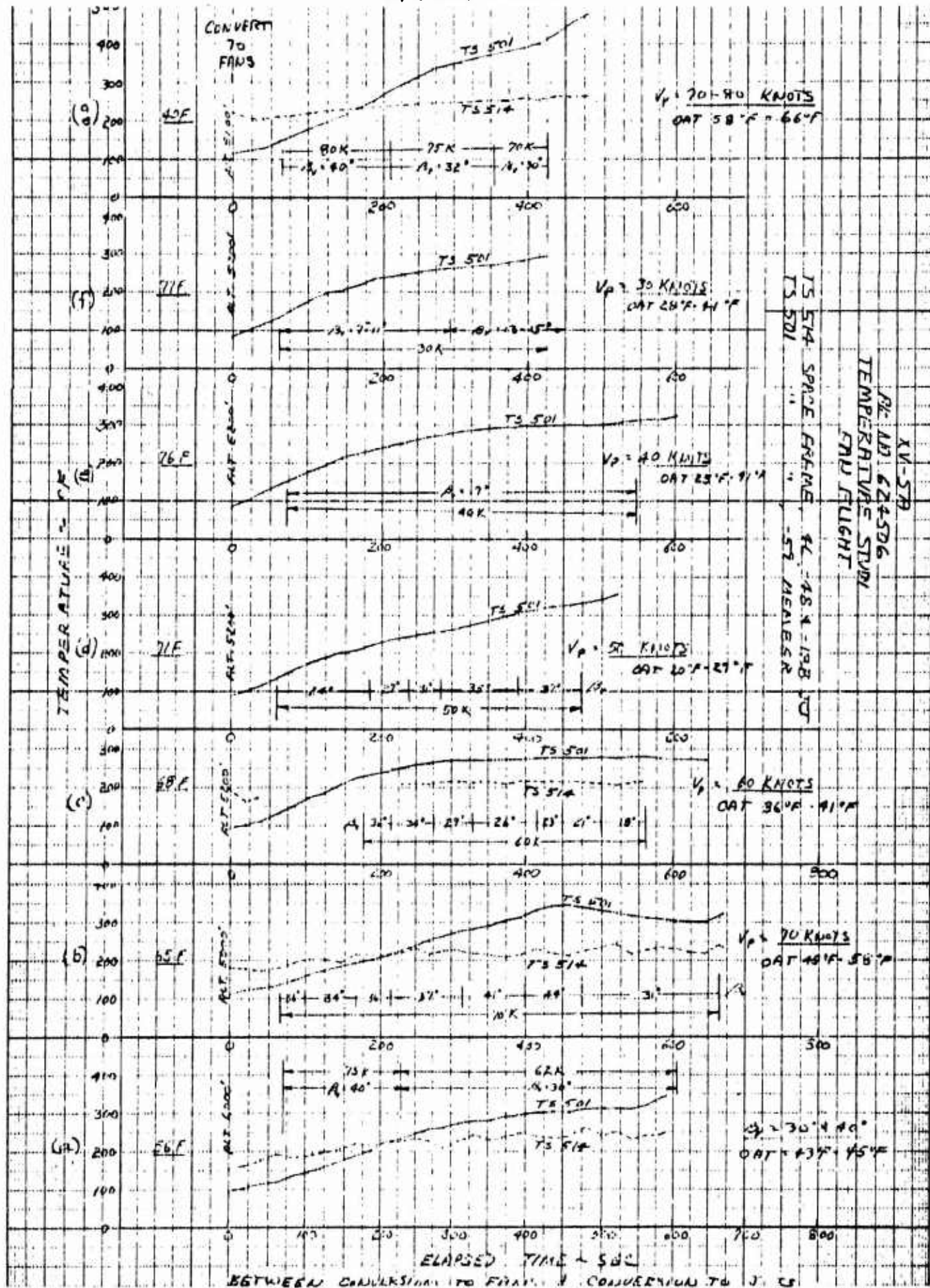


Figure 6.100 Effect of Velocity on Space Frame Temperature for Fan Mode Operation

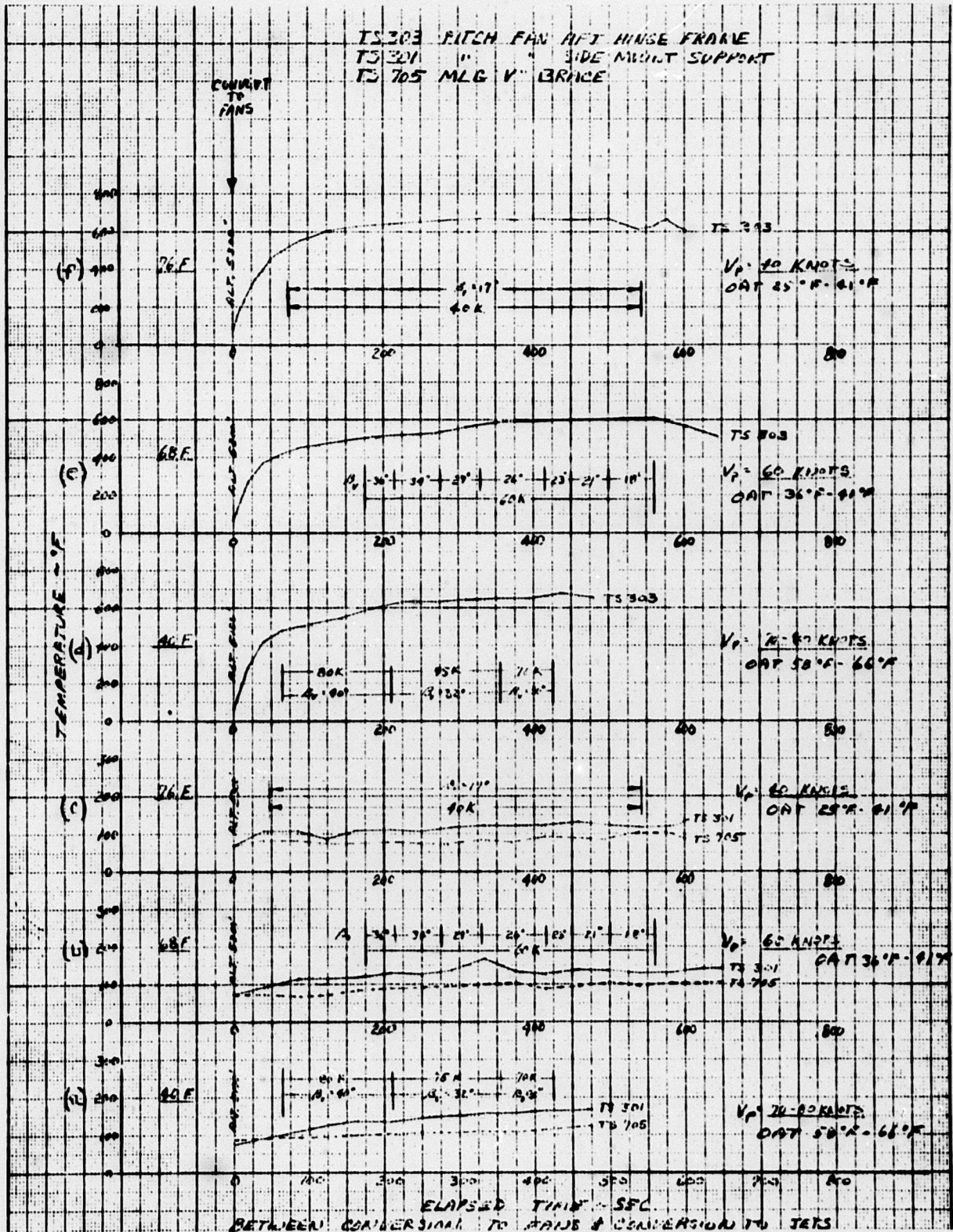


Figure 6.101 Effect of Velocity on Some Pitch Fan and Main Landing Gear Components for Fan Mode Operation

A/C No. 624506

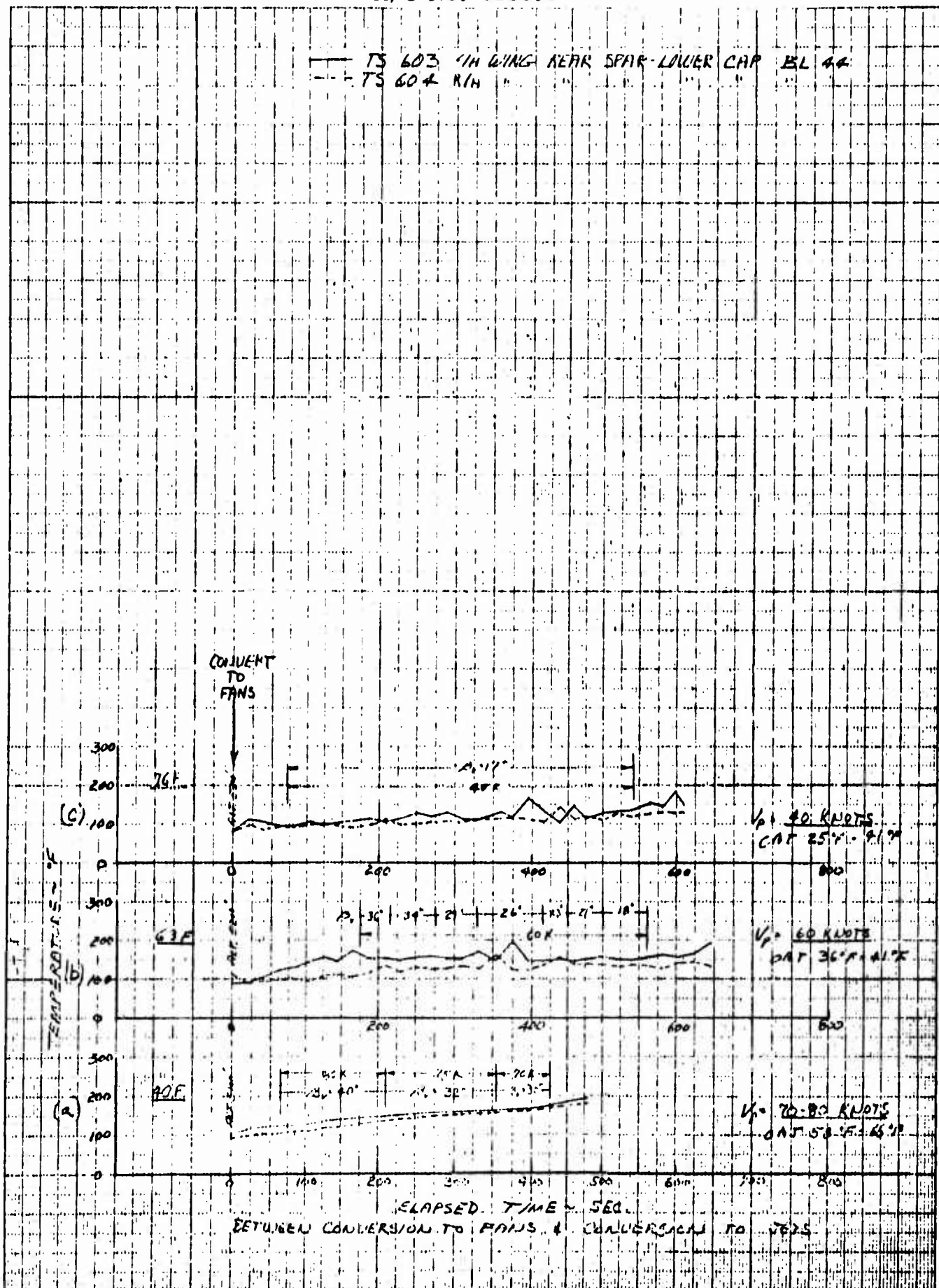


Figure 6.102 Effect of Velocity on Rear Spar Temperatures for Fan Mode Operation

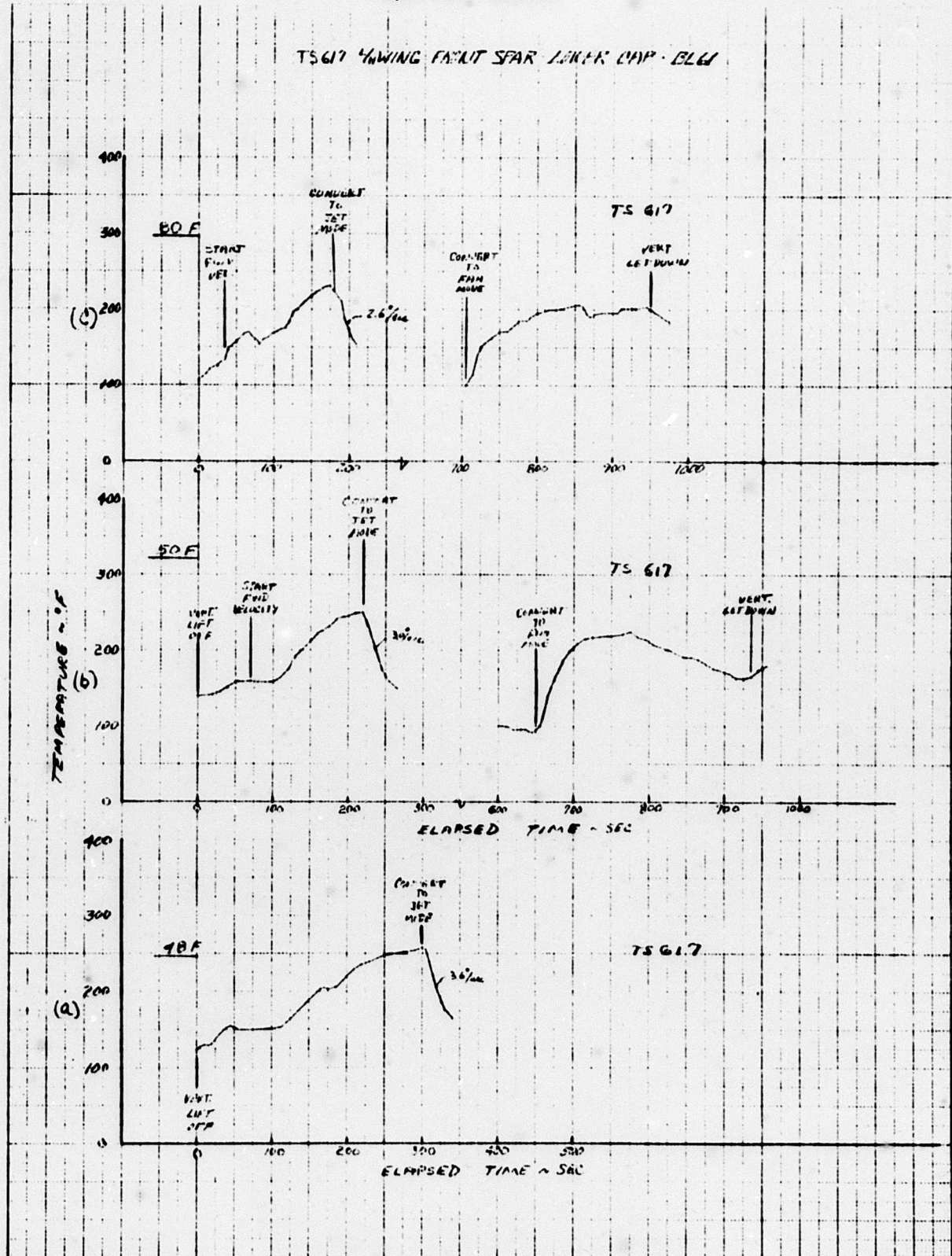


Figure 6.103 Front Spar Temperature - Time Profiles for Fan Mode Transitions from Lift Off or Prior to Touchdown

A/C No. 624506

12.04G T/H03
OAT: 90 °F
WIND 1.2 KNOTS

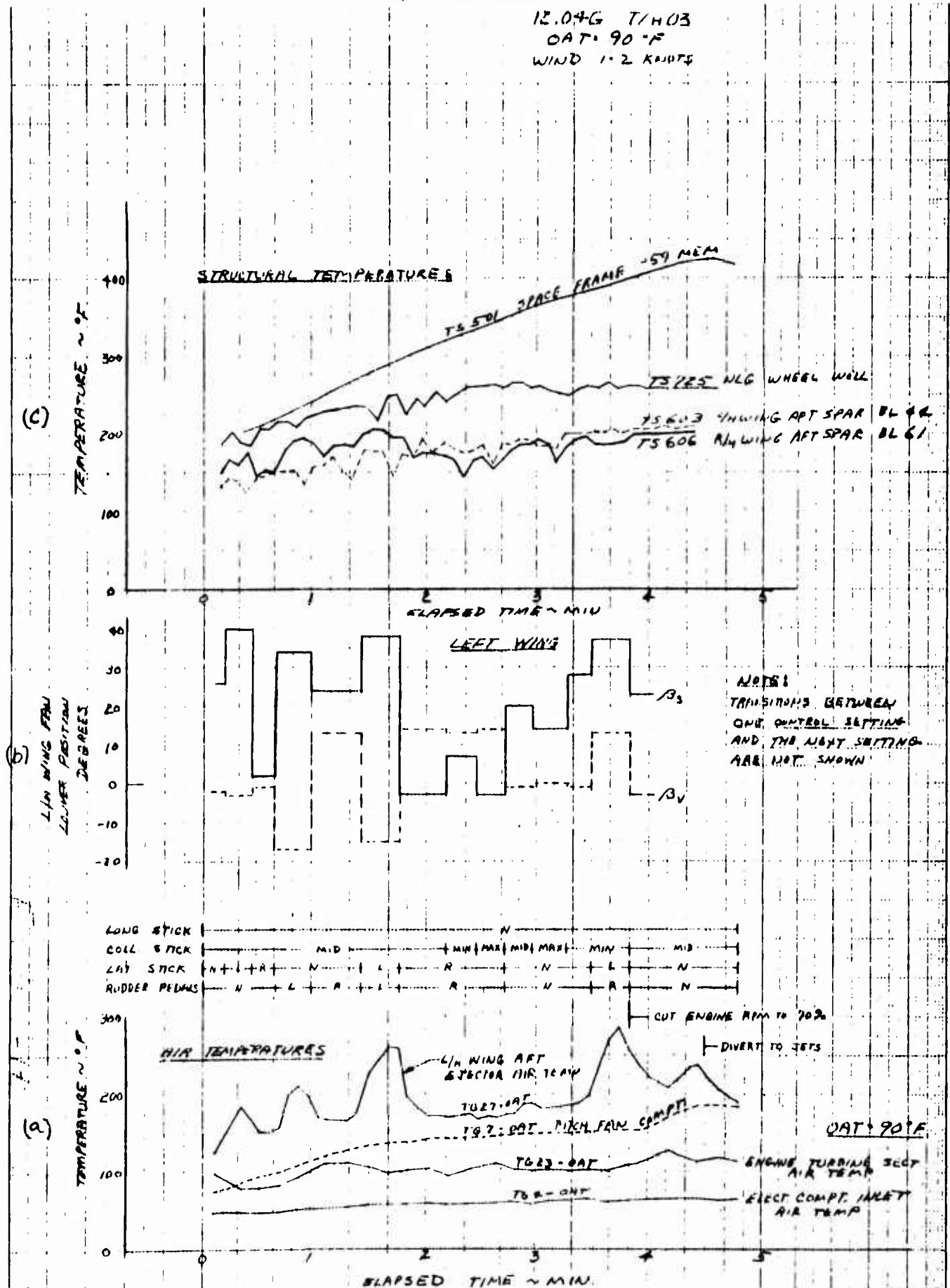


Figure 6.104 Effect of Aircraft Control Settings on Structural and Air Temperatures During Ground Operation in Fan Mode

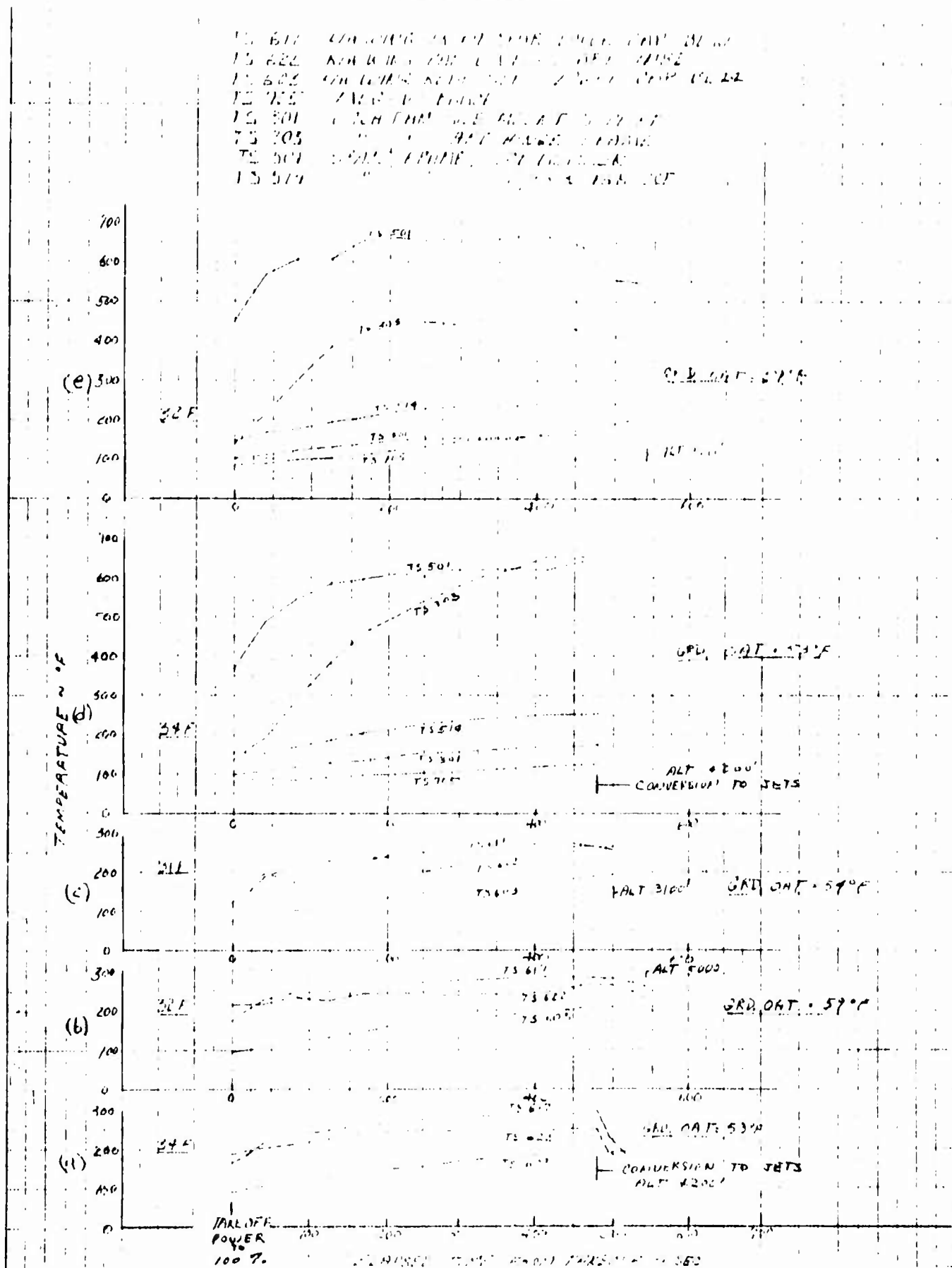


Figure 6.105 Structural Temperatures Experienced During Short Takeoff and Landing Manuevers for Fan Mode Operation

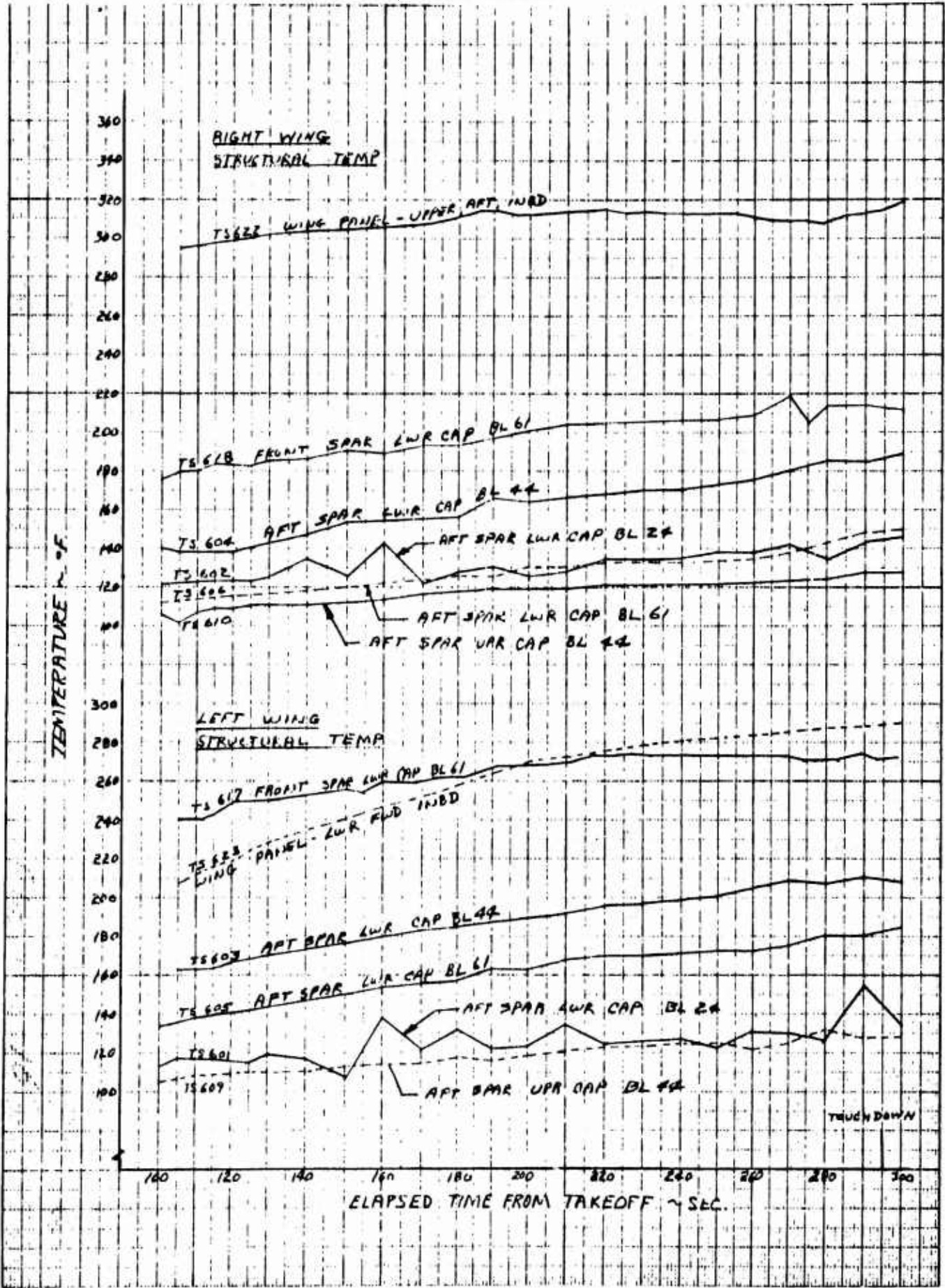


Figure 6.106 Some Wing Temperatures Experienced During a Short Takeoff and Landing Maneuver for Fan Mode Operation

XV-5A A/C NO 624506 GROUND RUN 12.11 G

TS-622 R/H WING PANEL UPPER FWD INBD
 TS-623 L/H WING PANEL LOWER FWD INBD

OAT = 100 °F

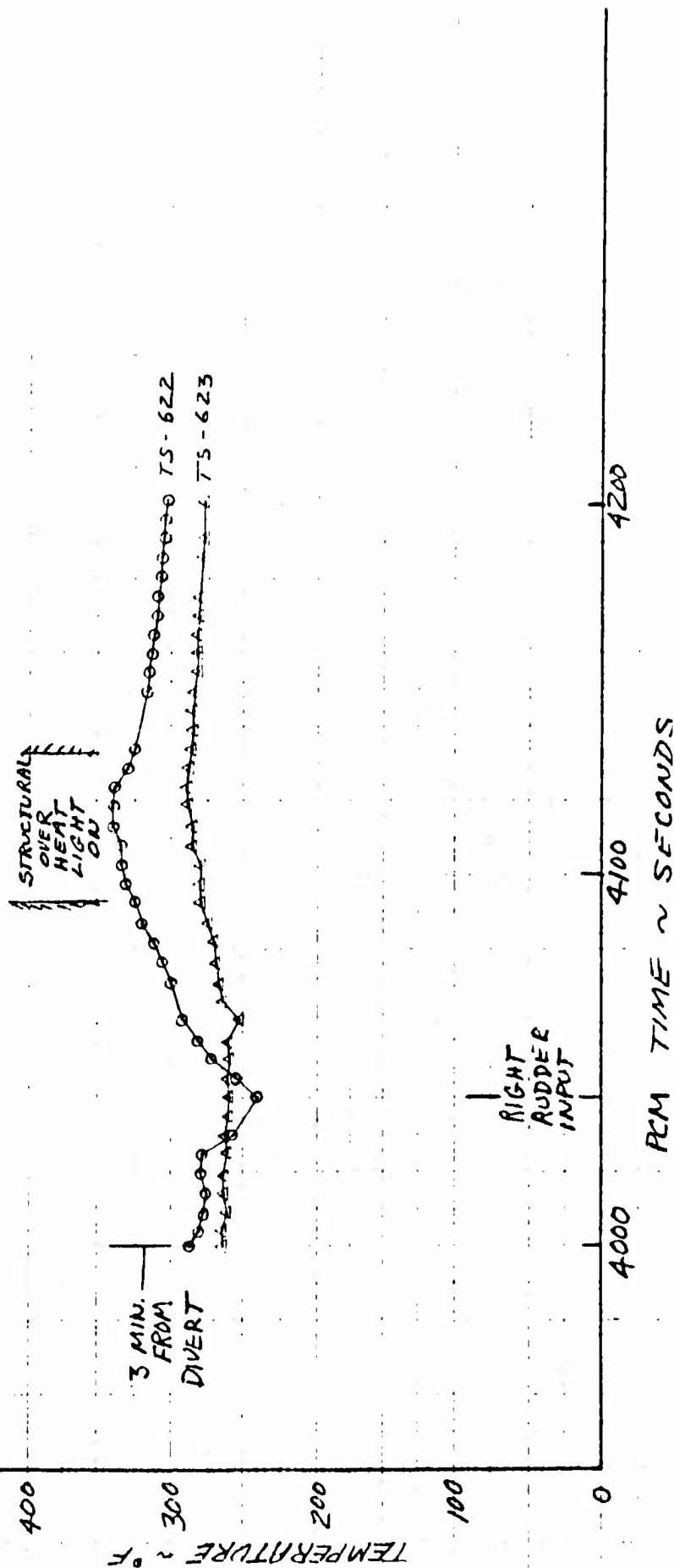


Figure 6.107 Wing Panel Temperatures During Fan Mode Operation in Ground Effect

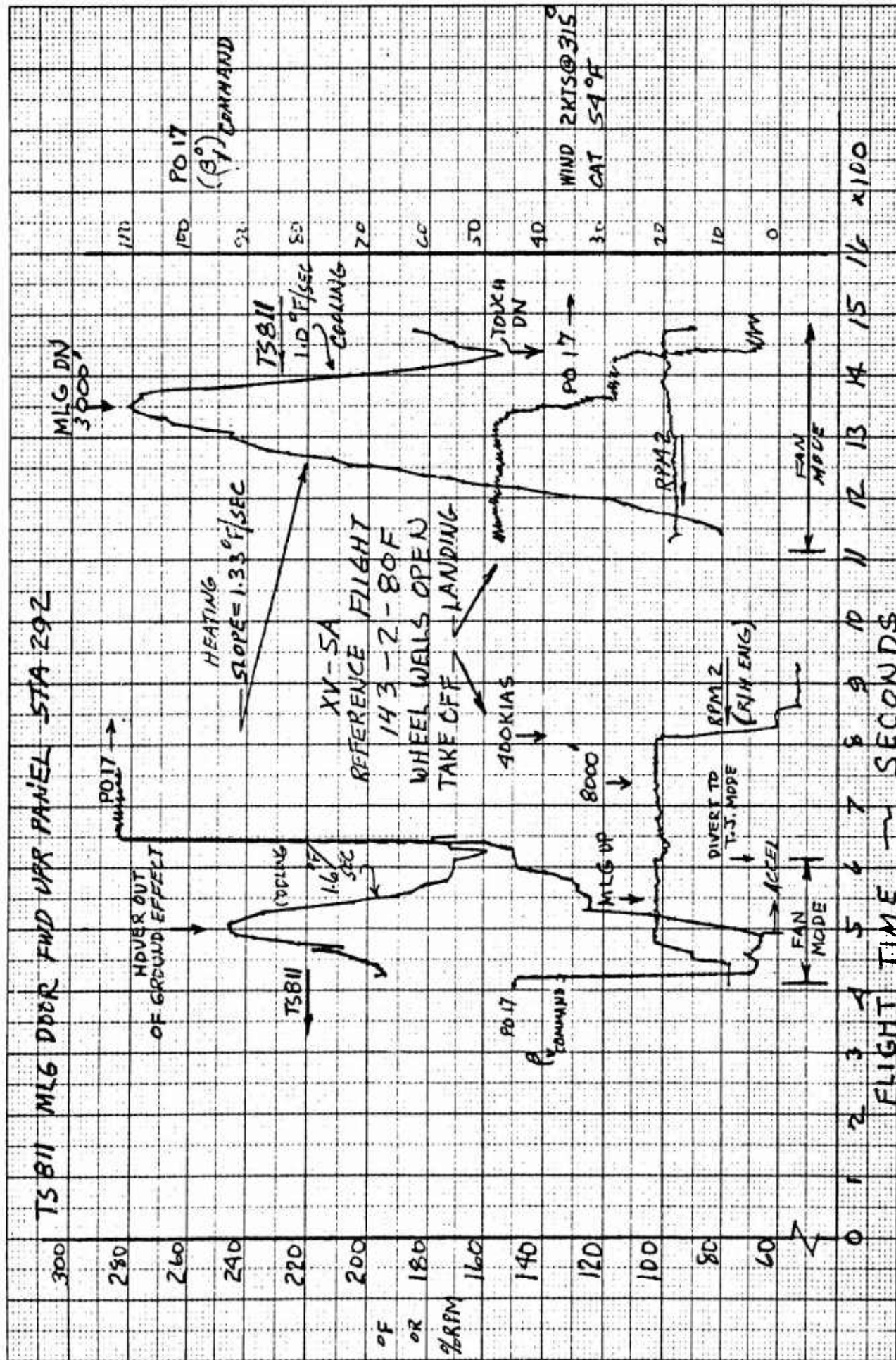


Figure 6.108 Main Wheel Well Air Temperatures for Fan Mode Operation During Vertical Takeoff and Landing with Wheel Well Open and Gear Extended

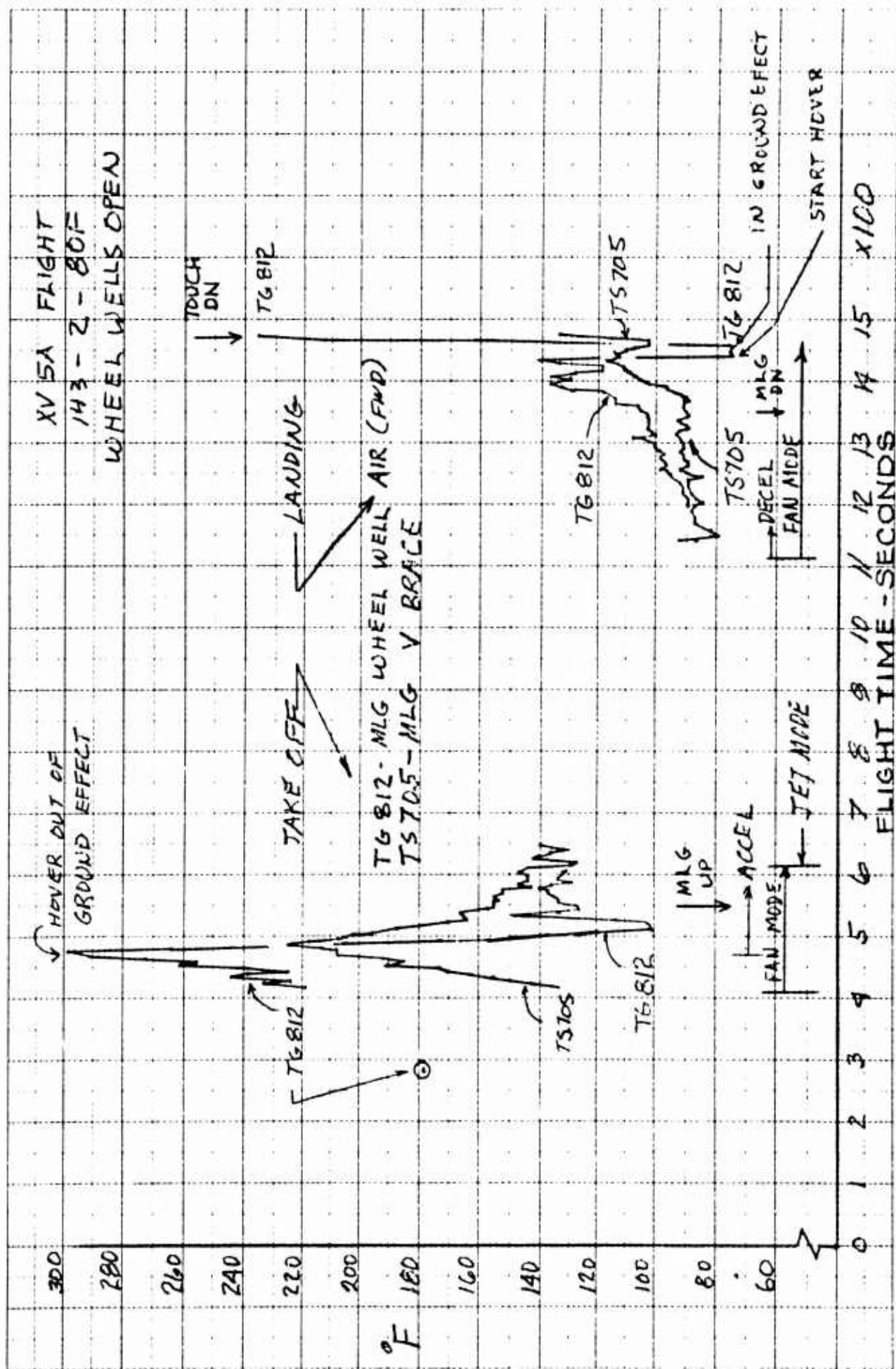


Figure 6.109 Various Main Wheel Well and Landing Gear Structural Temperatures for Fan Mode Operation During Vertical Takeoff and Landing with Wheel Well Open and Gear Extended

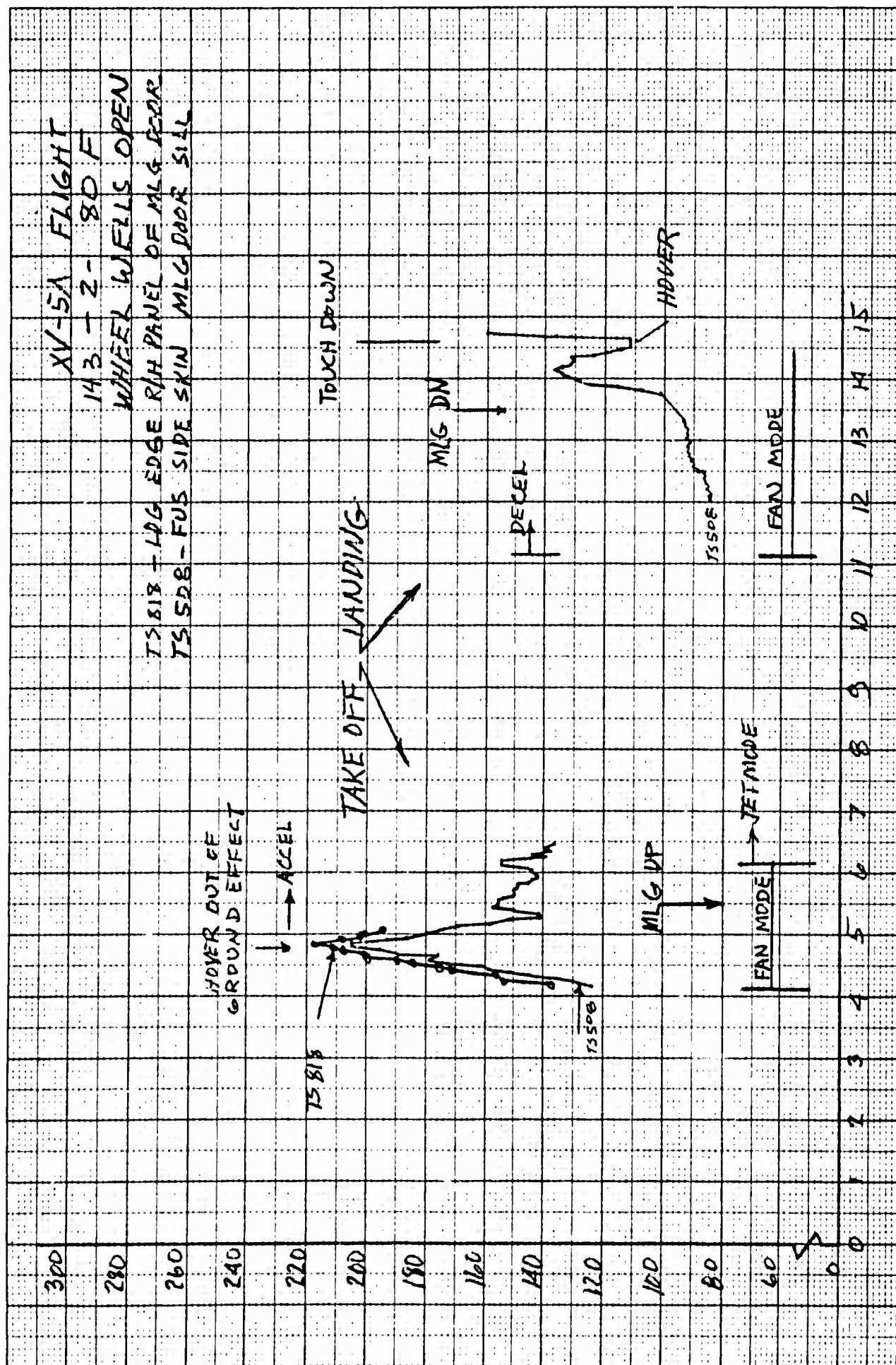


Figure 6.110 Main Wheel Well Enclosure Door Temperatures for Fan Mode Operation During Vertical Takeoff and Landing with Wheel Well Open and Gear Extended

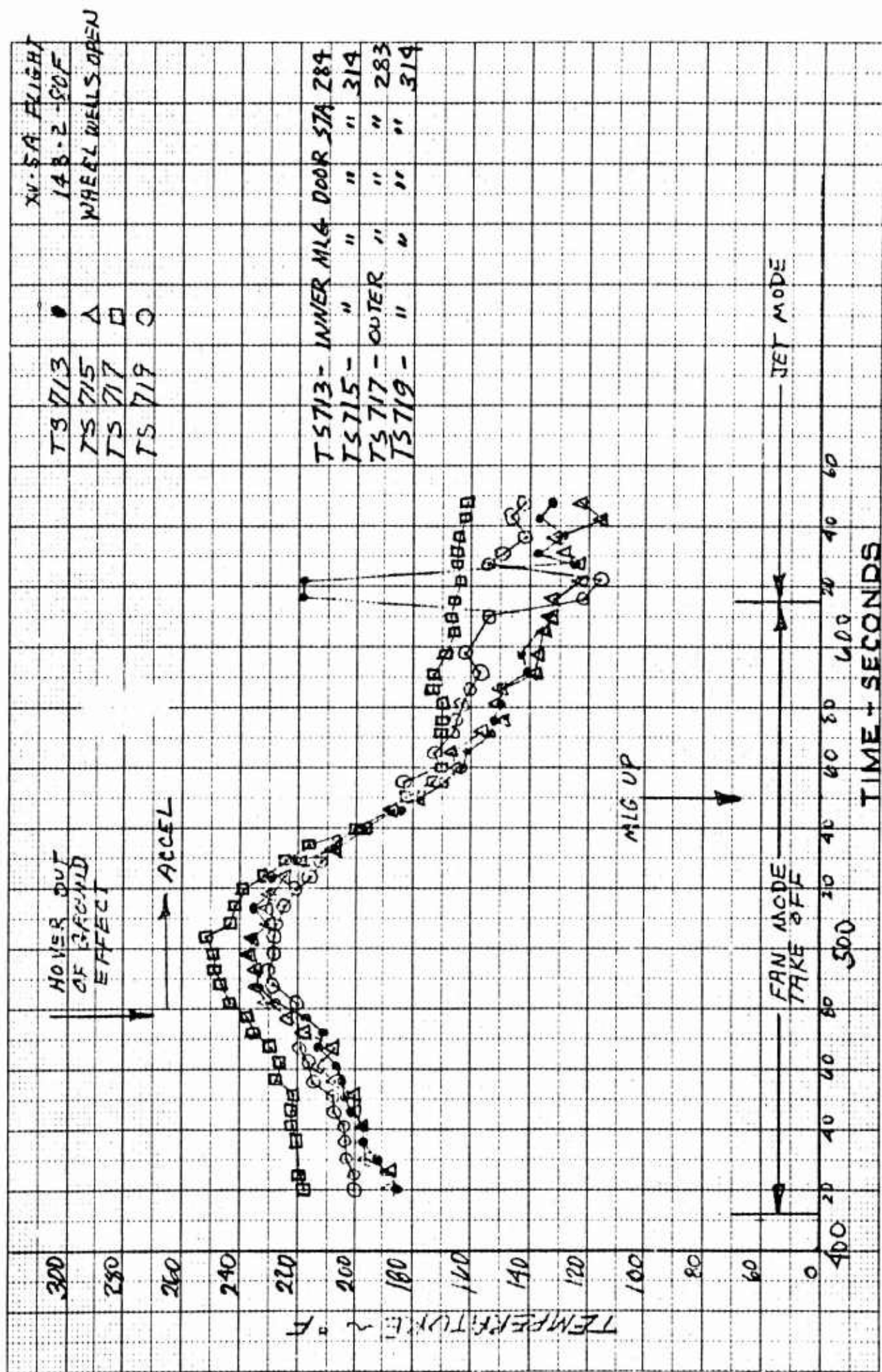


Figure 6.111 Main Wheel Well Door Temperature During Vertical Takeoff and Transition - Wheel Well Open Gear Extended

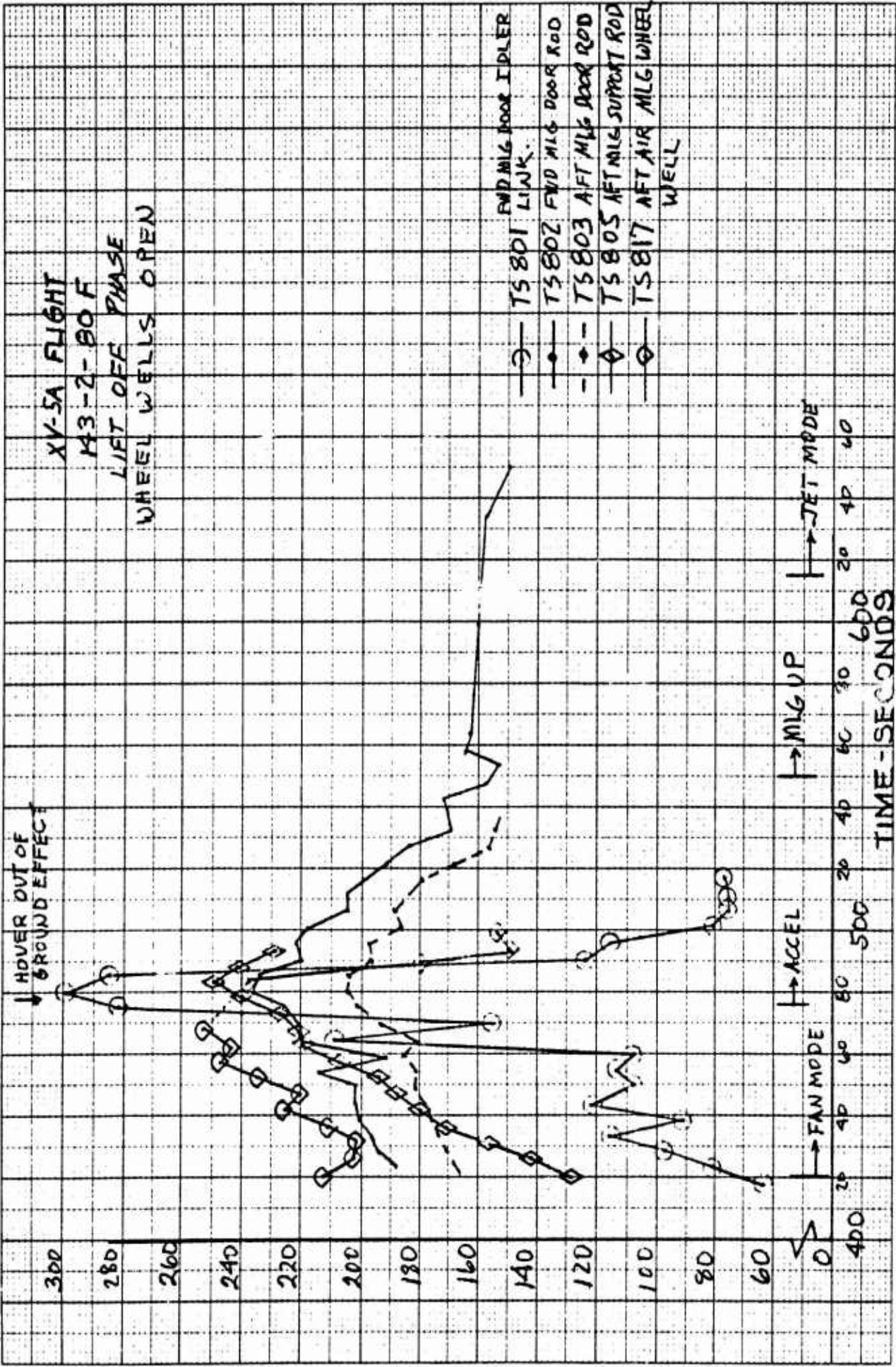


Figure 6.112 Main Wheel Well Door Linkage and Landing Gear Temperature During Vertical Takeoff and Transition

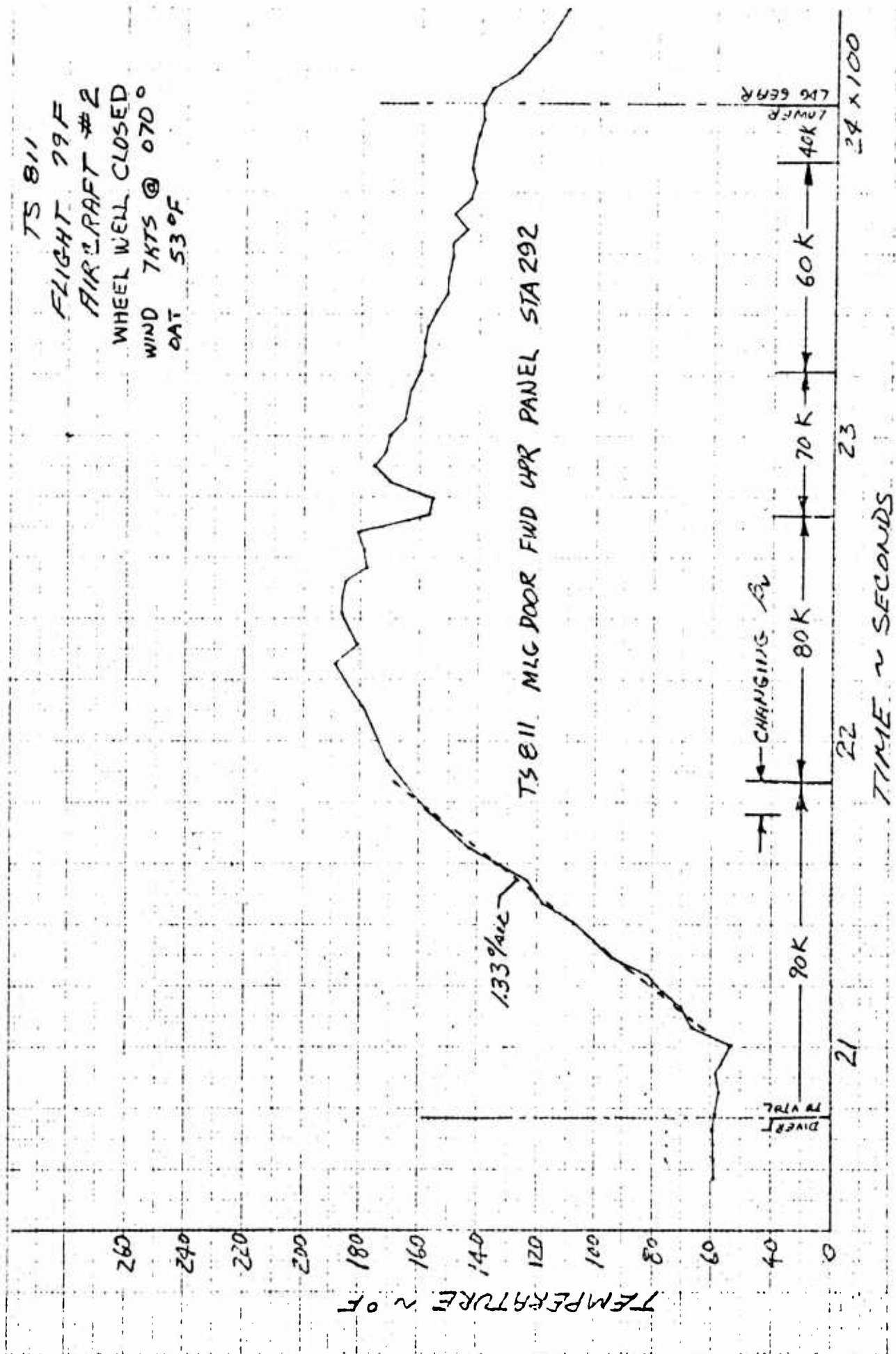


Figure 6.113 Main Wheel Well Door Temperature During Fan Mode Transition - Wheel Well Enclosed

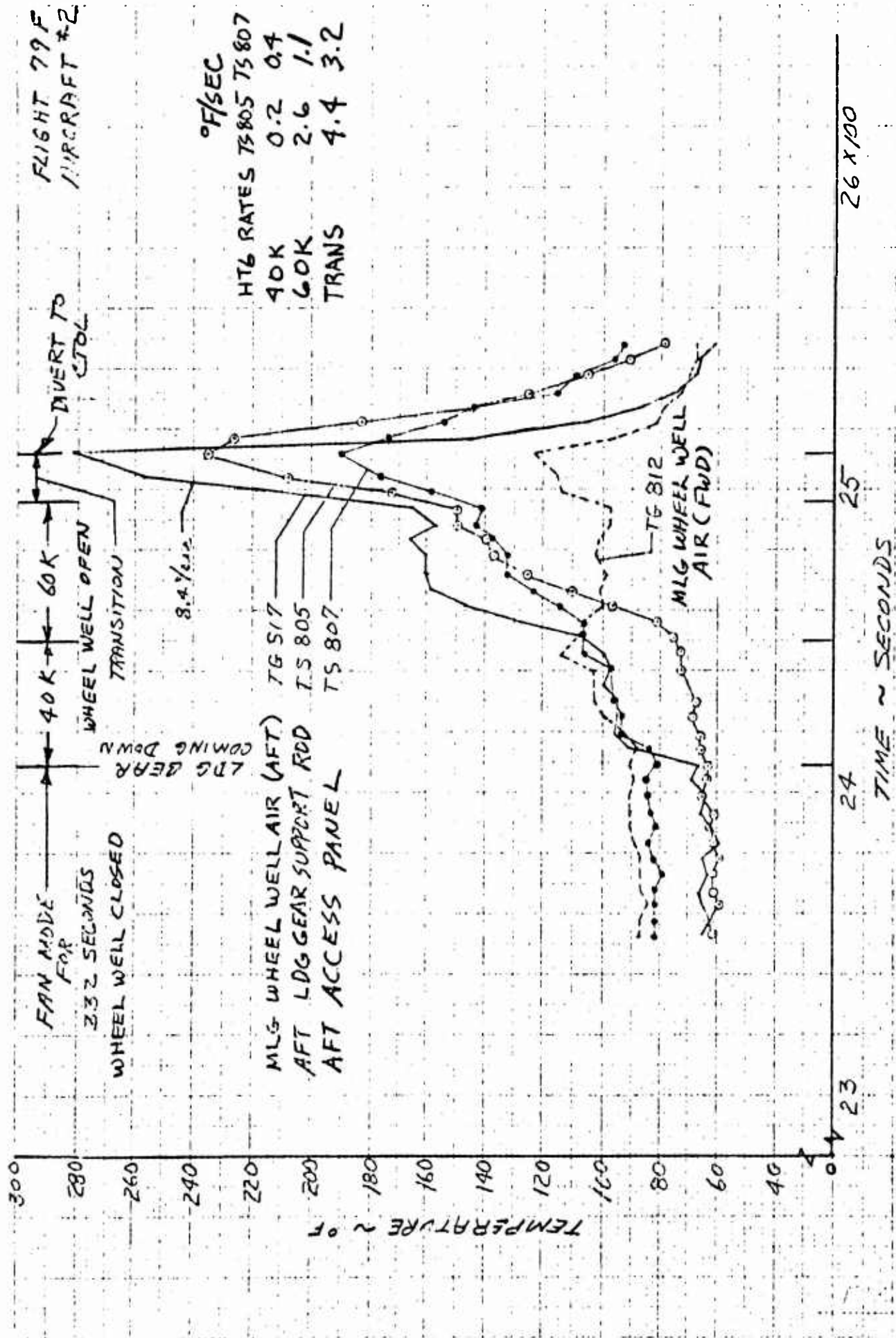


Figure 6.114 Wheel Well Component Temperatures During Maximum Fan Mode Thrust, Wheel Well Open Dash to Conversion

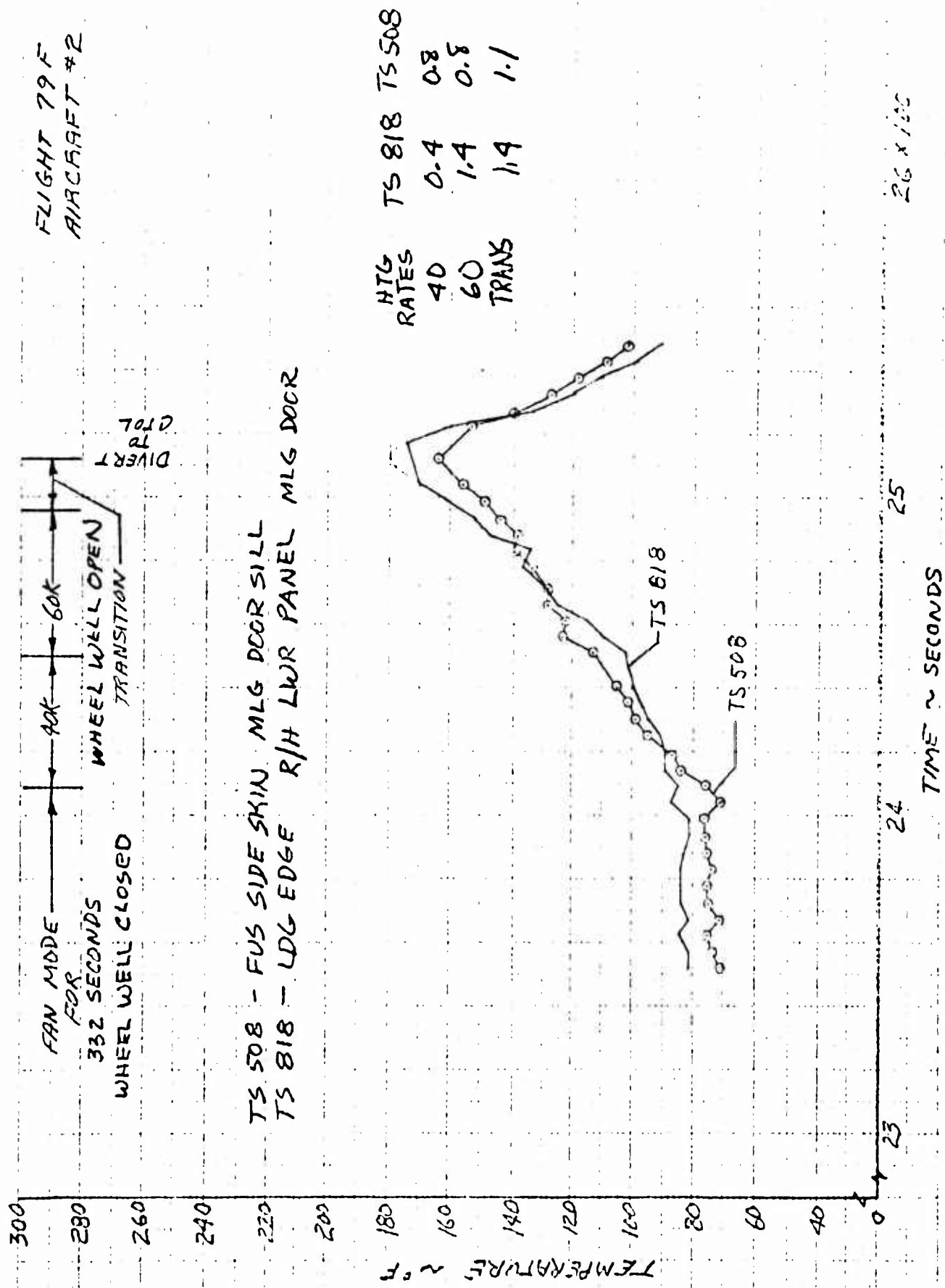


Figure 6.115 Aircraft Component Temperatures During Maximum Fan Mode Thrust, Wheel Well Open Dash to Conversion

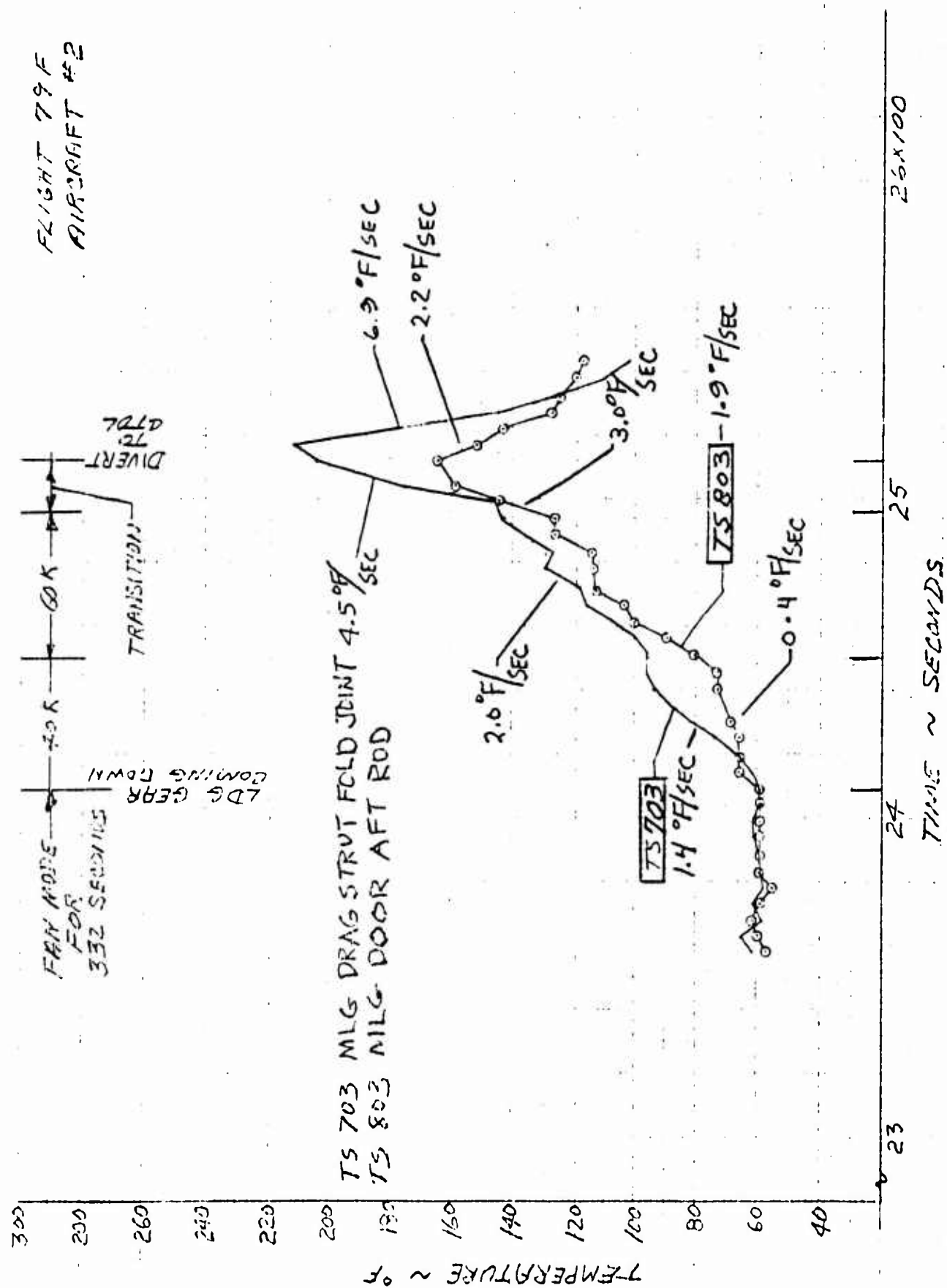


Figure 6.116 Wheel Well Component Temperatures During Maximum Fan Mode Thrust, Wheel Well Open Dash to Conversion

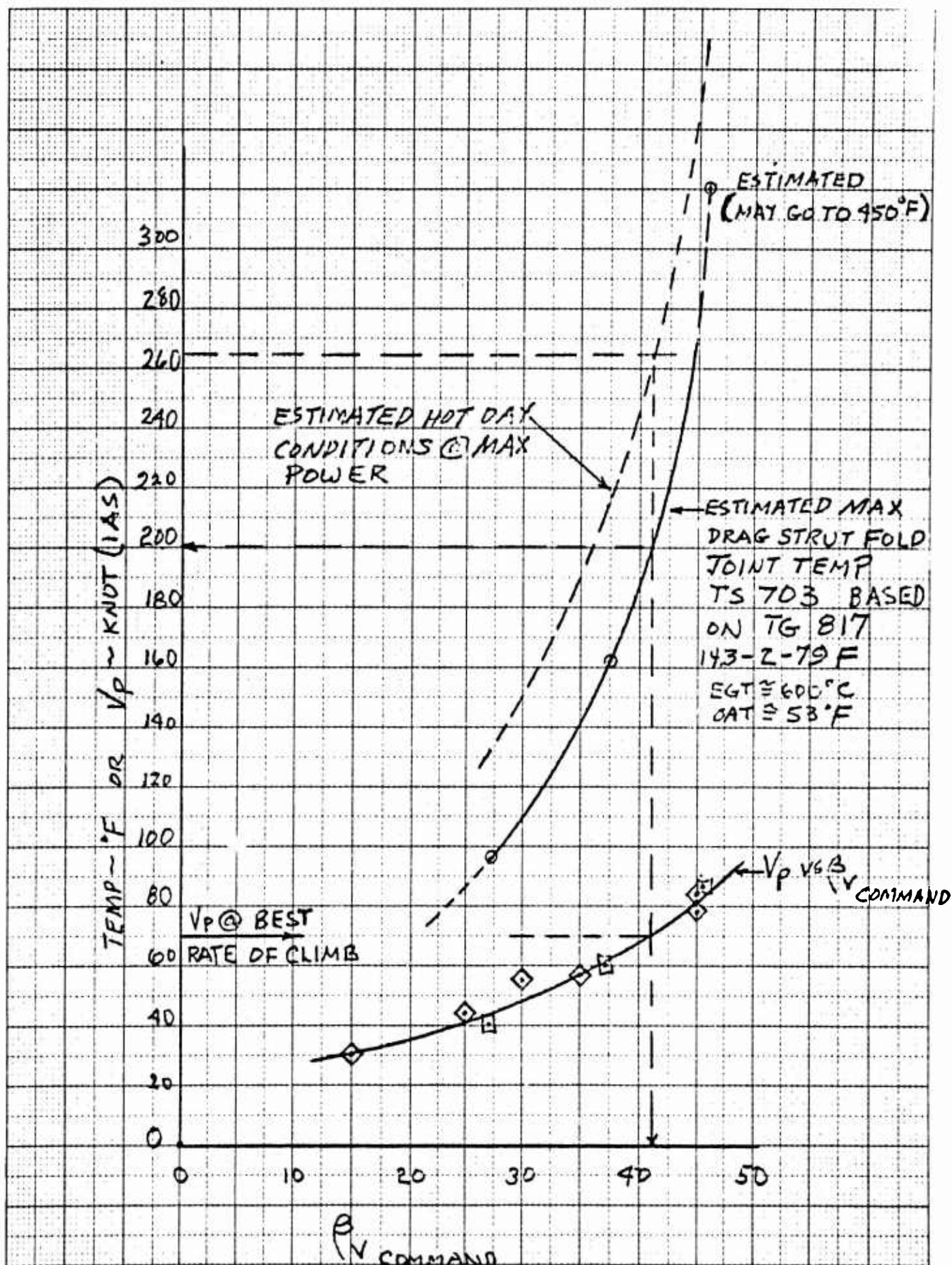


Figure 6.117 Estimated Maximum Landing Gear Temperature During Fan Mode, Wheel Well Open Dash Conversion

A/C NO 624506
 REINGESTION STUDY
 GROUND RUN 12.08G
 WIND 6 KNOTS - 85° LEFT OF THE NOSE
 EFFECT OF LONGITUDINAL STICK POS
 AND LOUVER VECTOR ANGLE

R/H ENGINE INLET TEMPERATURE
 AVERAGE OF 14 THERMOCOUPLES
 TQ 52 THRU TG 65

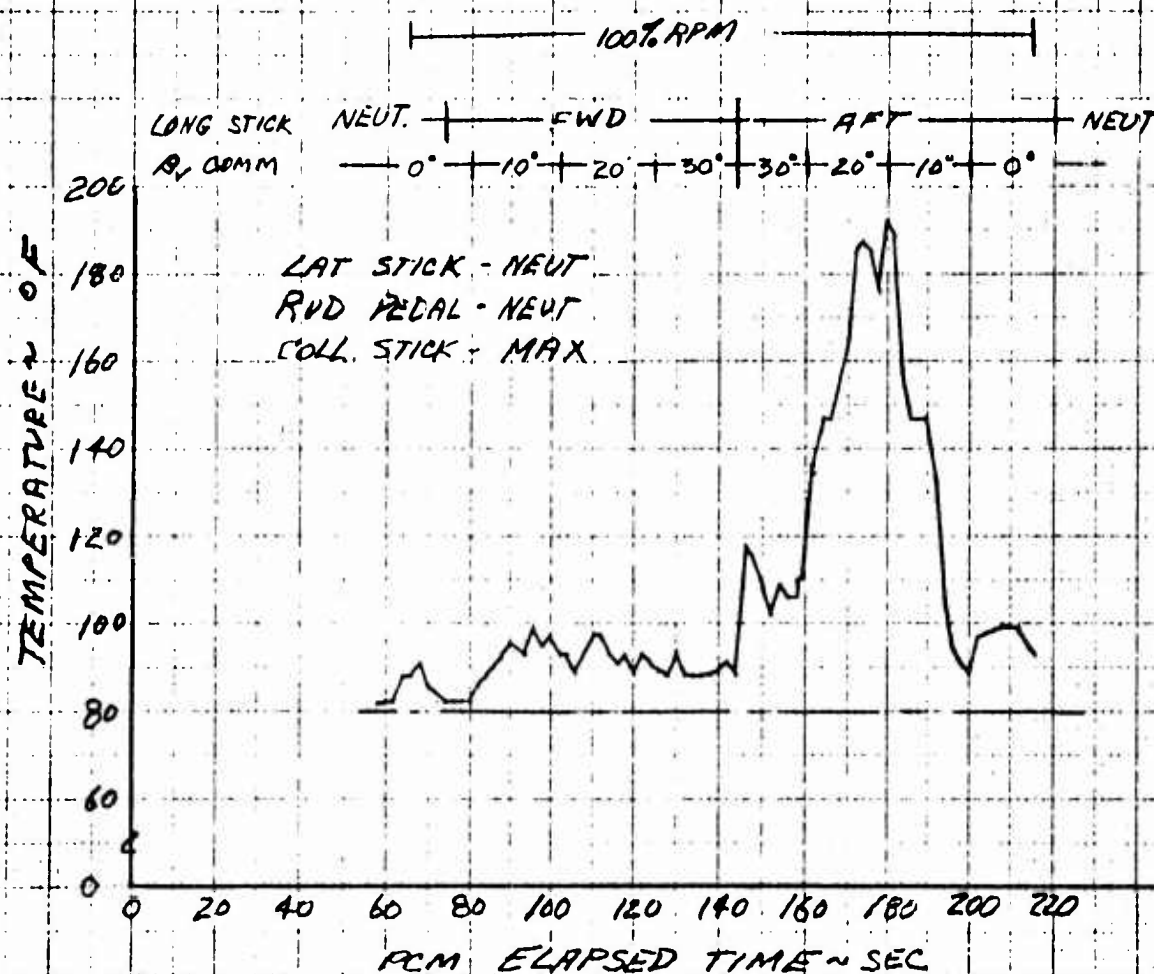


Figure 6.118 Effect of Fan Stream Vector Angle and Pitch Control Setting on the Generator Ingestion for Fan Mode Operation in Ground Effect

AIC NO 624506
 REINGESTION STUDY
 GROUND RUN 12.06 G
 WIND 15 KNOTS ~105° LEFT OF THE NOSE

EFFECT OF RUDDER PEDAL AND
 LATERAL STICK POSITION

RIH ENGINE INLET TEMPERATURE
 AVERAGE OF 17 THERMOCOUPLES
 TG 52 THRU TG 65

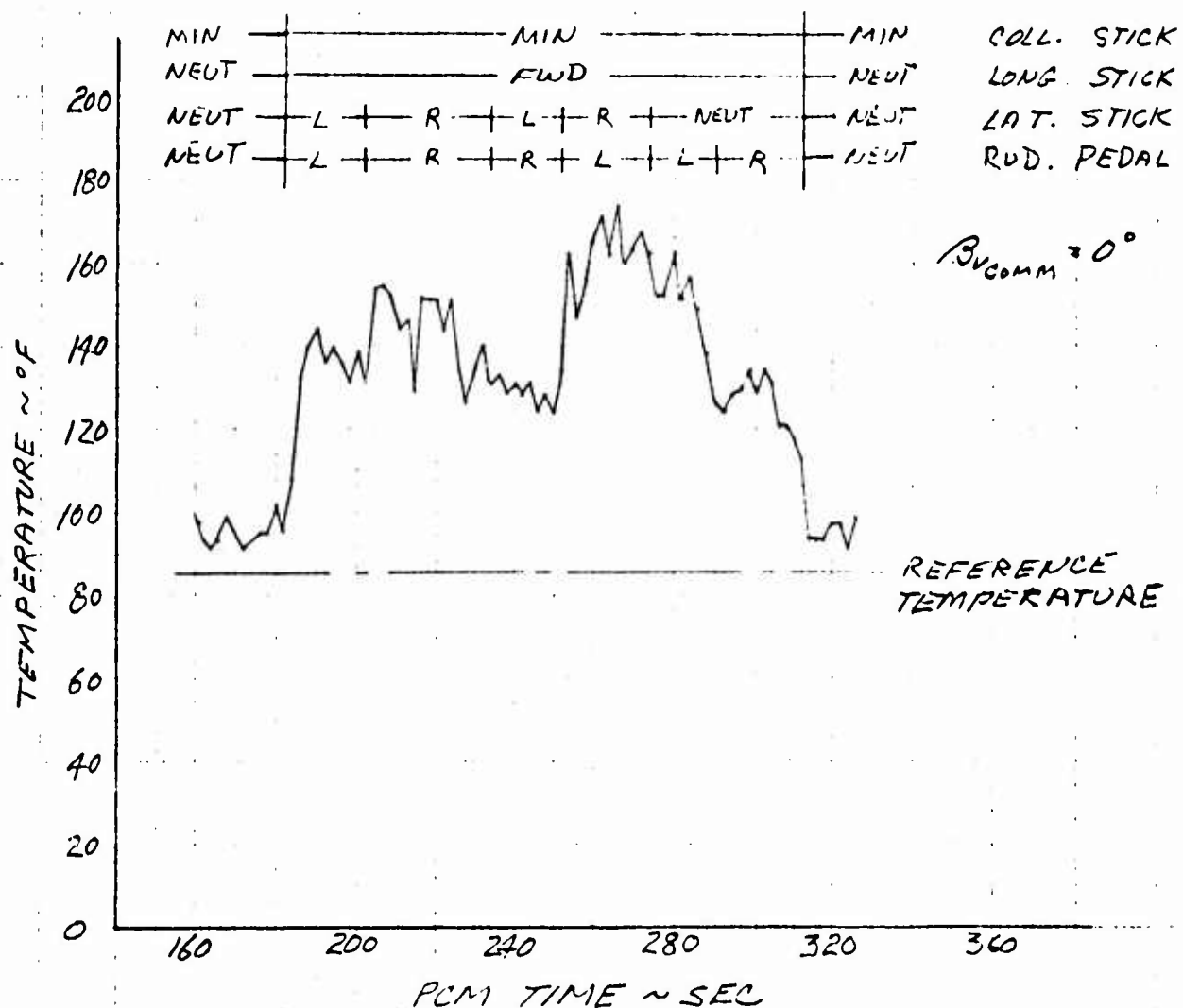


Figure 6.119 Effect of Aircraft Control Inputs on Gas Generator Ingestion for Fan Mode Operation in Ground Effect - Zero Fan Stream Vector Angle - Winds to 15 Knots

AIC NO 624506
 REINGESTION STUDY
 GROUND RUN 12.05G
 WIND 18-27 KNOTS - 60° LEFT OF NOSE

EFFECT OF RUDDER PEDAL AND
 LATERAL STICK POSITION

R/H ENGINE
 INLET TEMPERATURE
 AVERAGE OF 14 THERMOCOUPLES
 TG 52 THRU TG 65

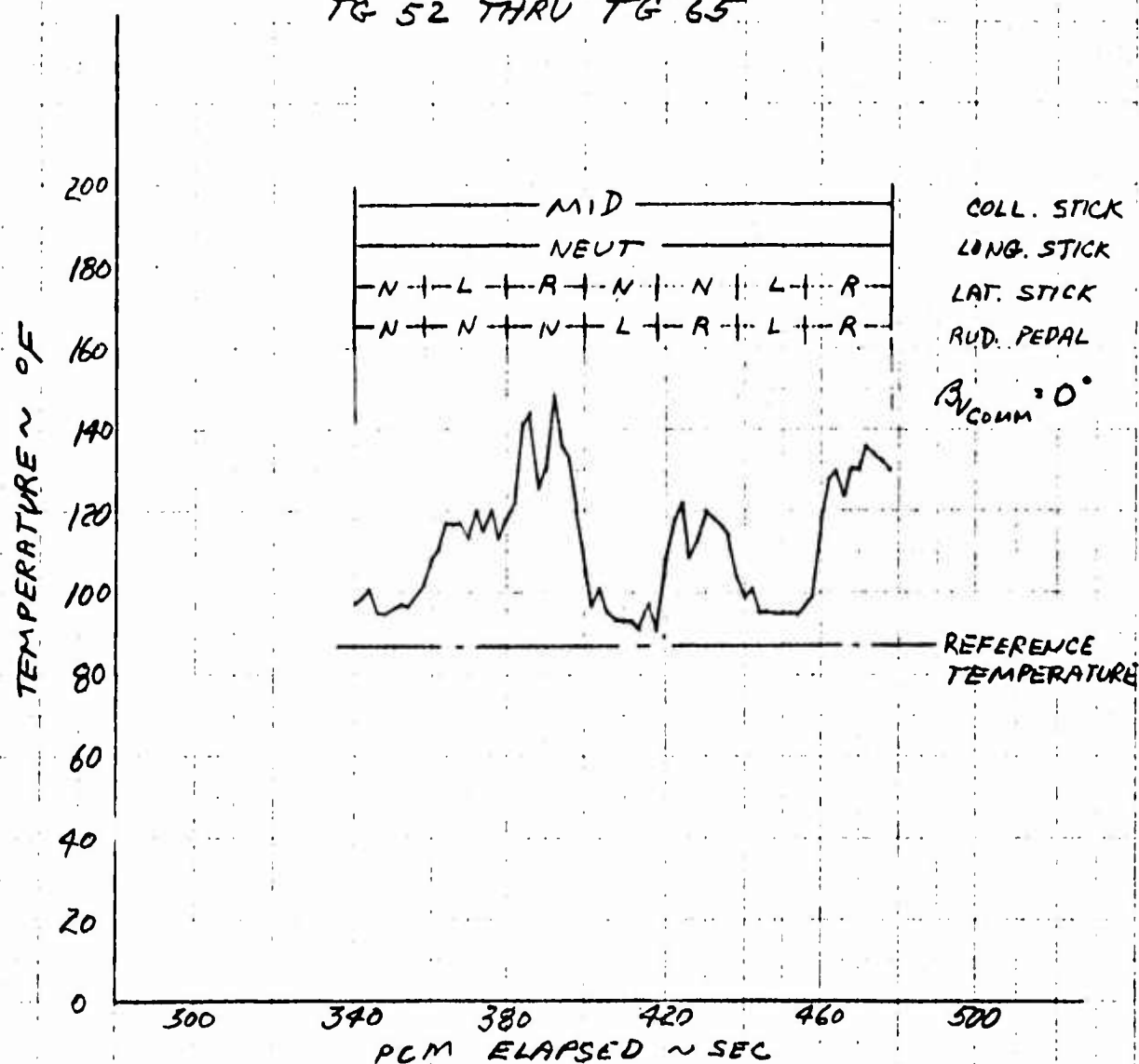


Figure 6.120 Effect of Aircraft Control Inputs on Gas Generator Ingestion for Fan Mode Operation in Ground Effect - Zero Fan Stream Vector Angle - Winds 18 to 27 Knots

AIC NO 624506
REINGESTION STUDY
GROUND RUN 12.07 G

EFFECT OF COLLECTIVE STICK POSITION

RM ENGINE INLET TEMPERATURE
AVERAGE OF 14 THERMOCOUPLES
TG 52 THRU TG 65

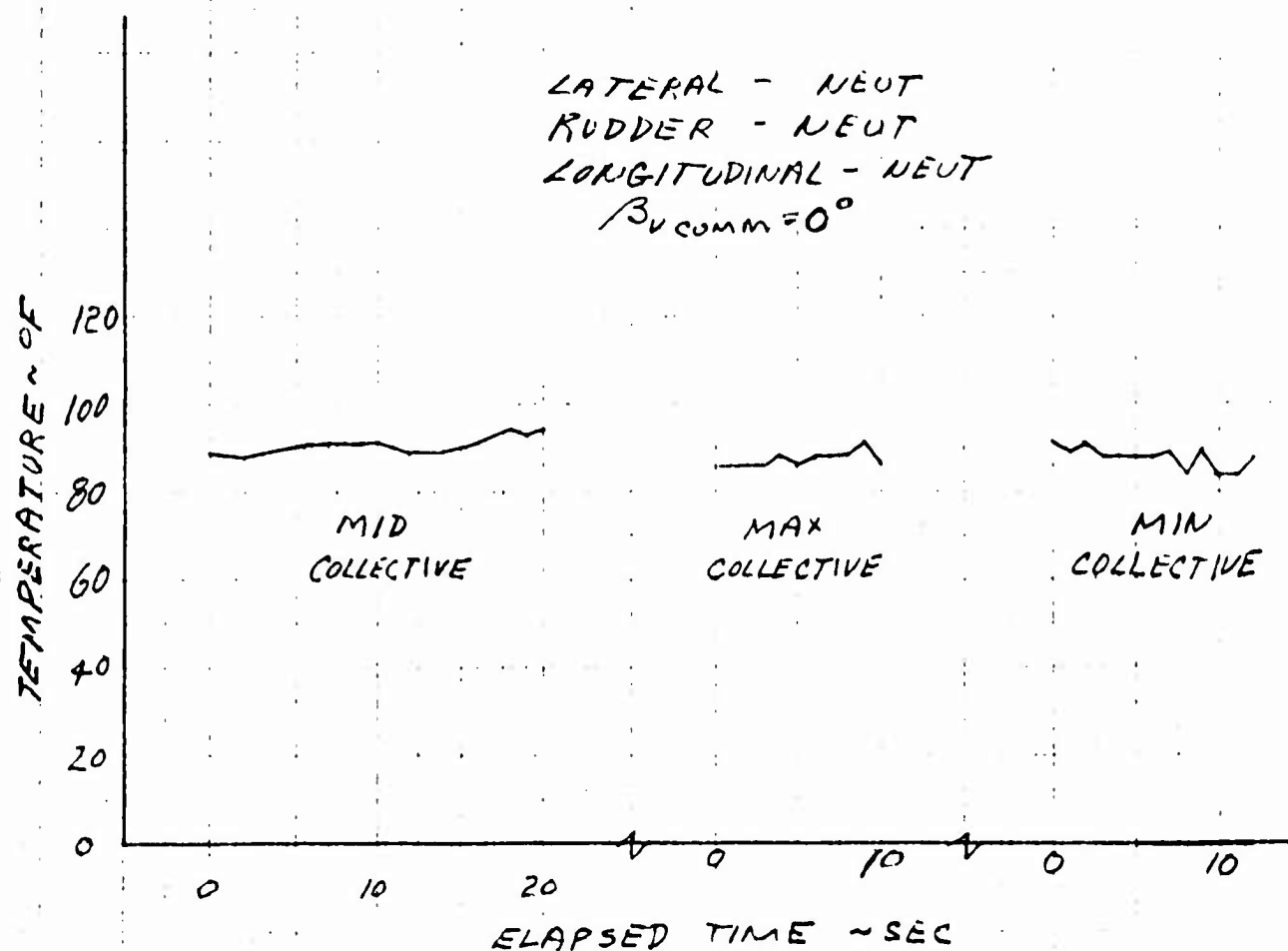


Figure 6.121 Effect of Collective Stick Position on Gas Generator Ingestion

XV-5A A/C NO 624506
 REINGESTION STUDY
 GROUND RUN 12.09 G
 LIGHT WIND

R/H ENGINE INLET AVERAGE OF 14 THERMOCOUPLES - T&S2 THRU T&65

B_Vconn = -7°

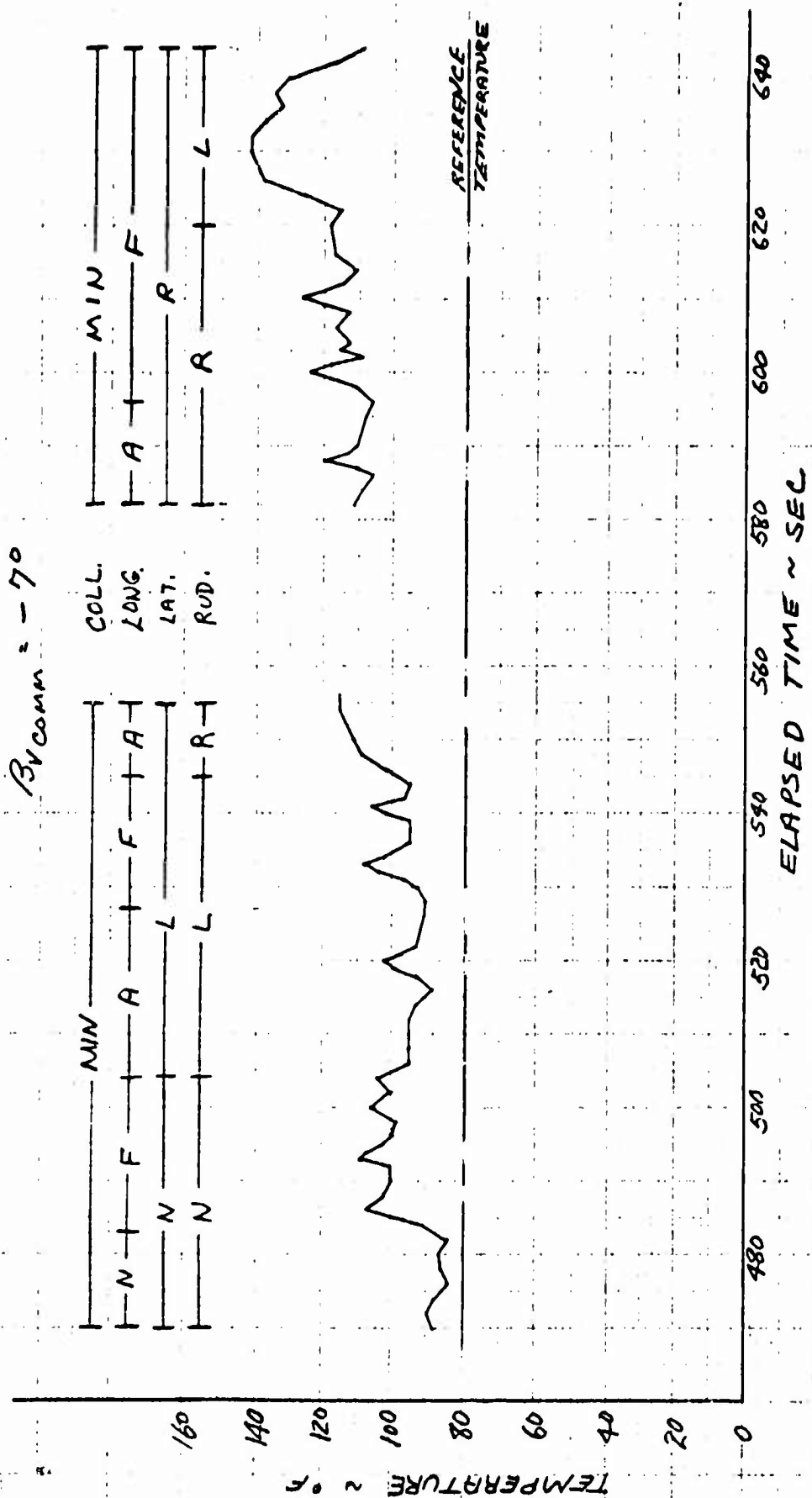


Figure 6.122 Effect of Aircraft Control Inputs on Gas Generator Ingestion for Fan Mode Operation in Ground Effect, -7° Fan Stream Vector Angle - Winds Light

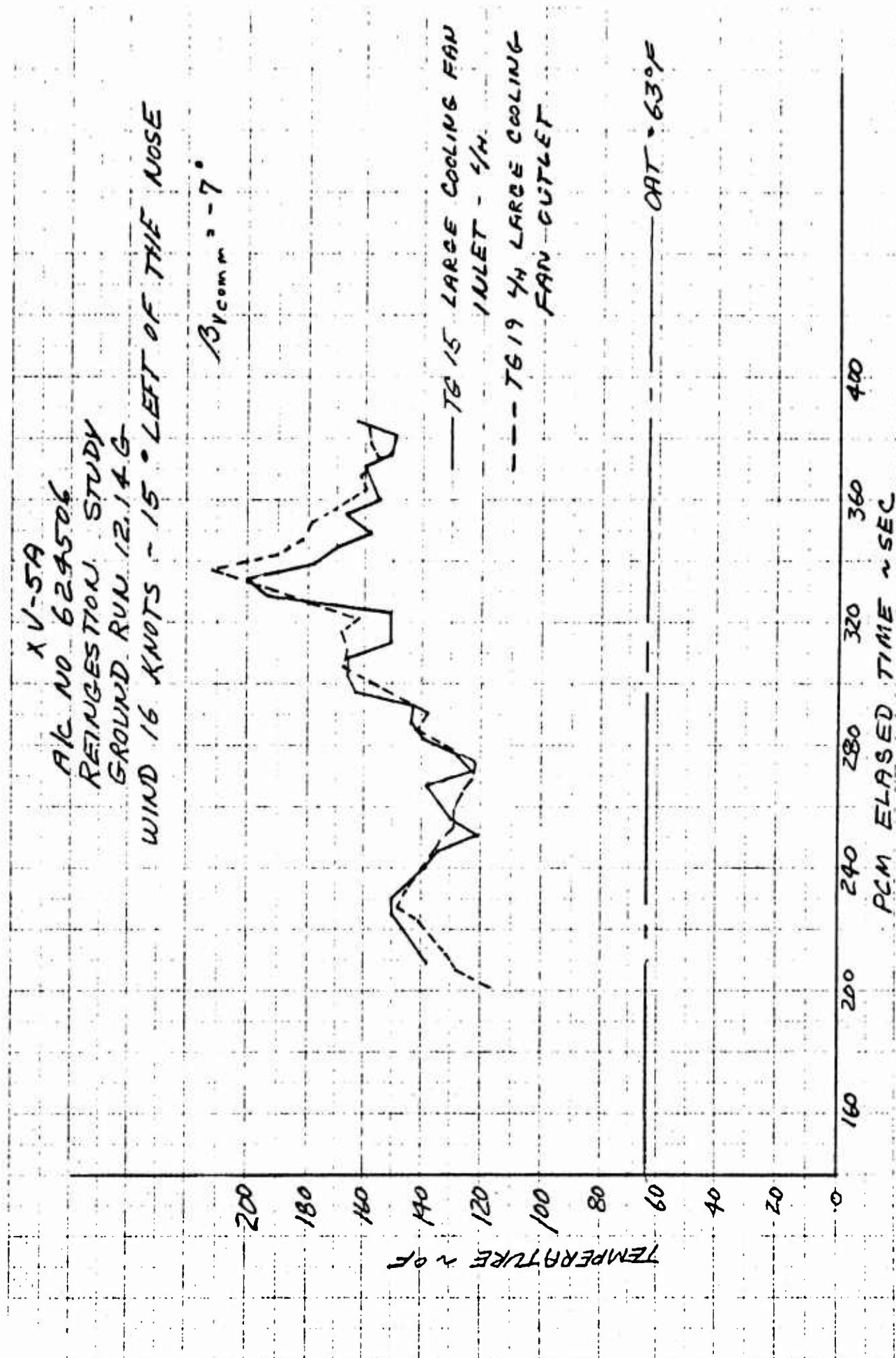


Figure 6.123 Cooling System Hot Gas Ingestion

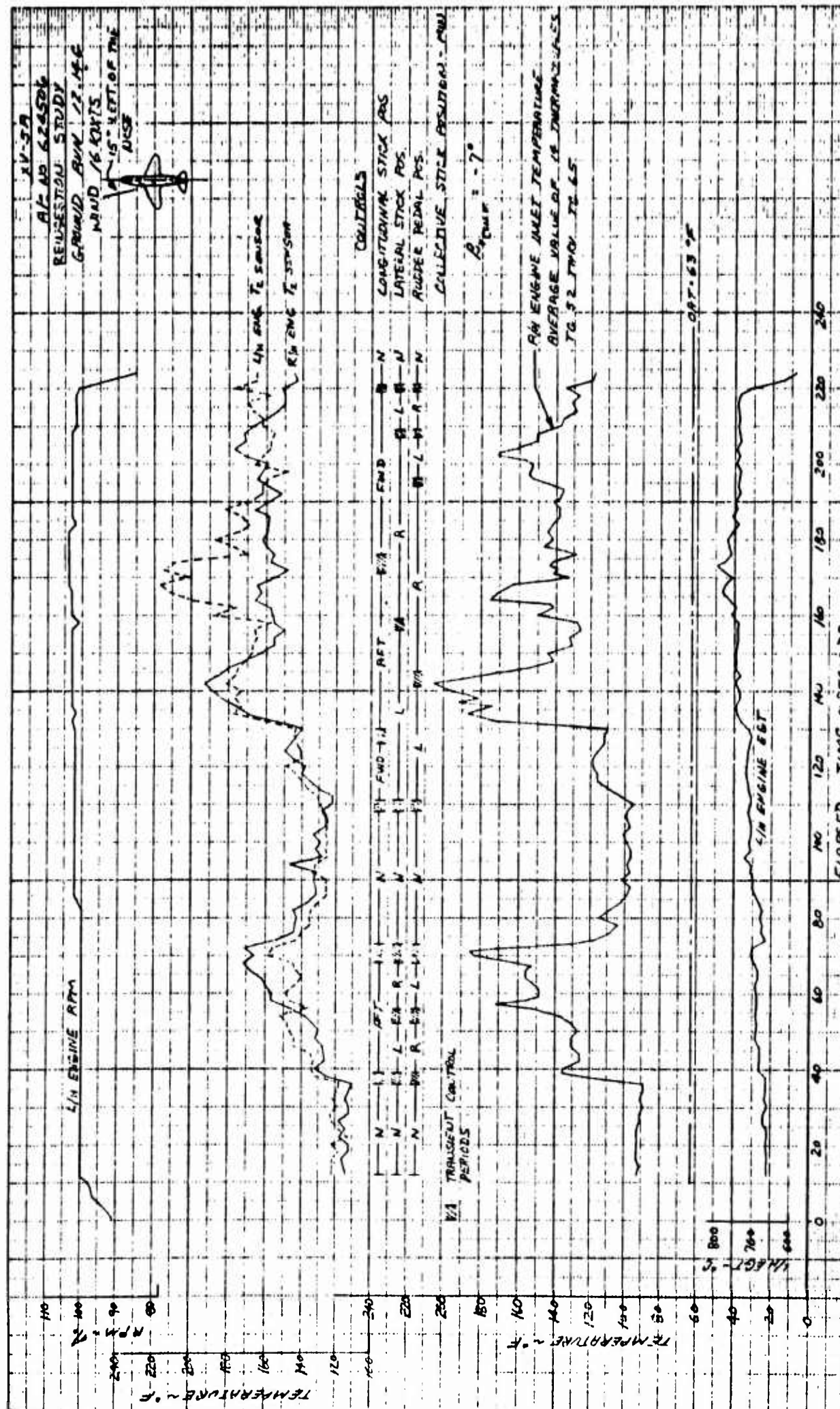


Figure 6.124 Comparison of Ingestion by L/H and R/H Gas Generators

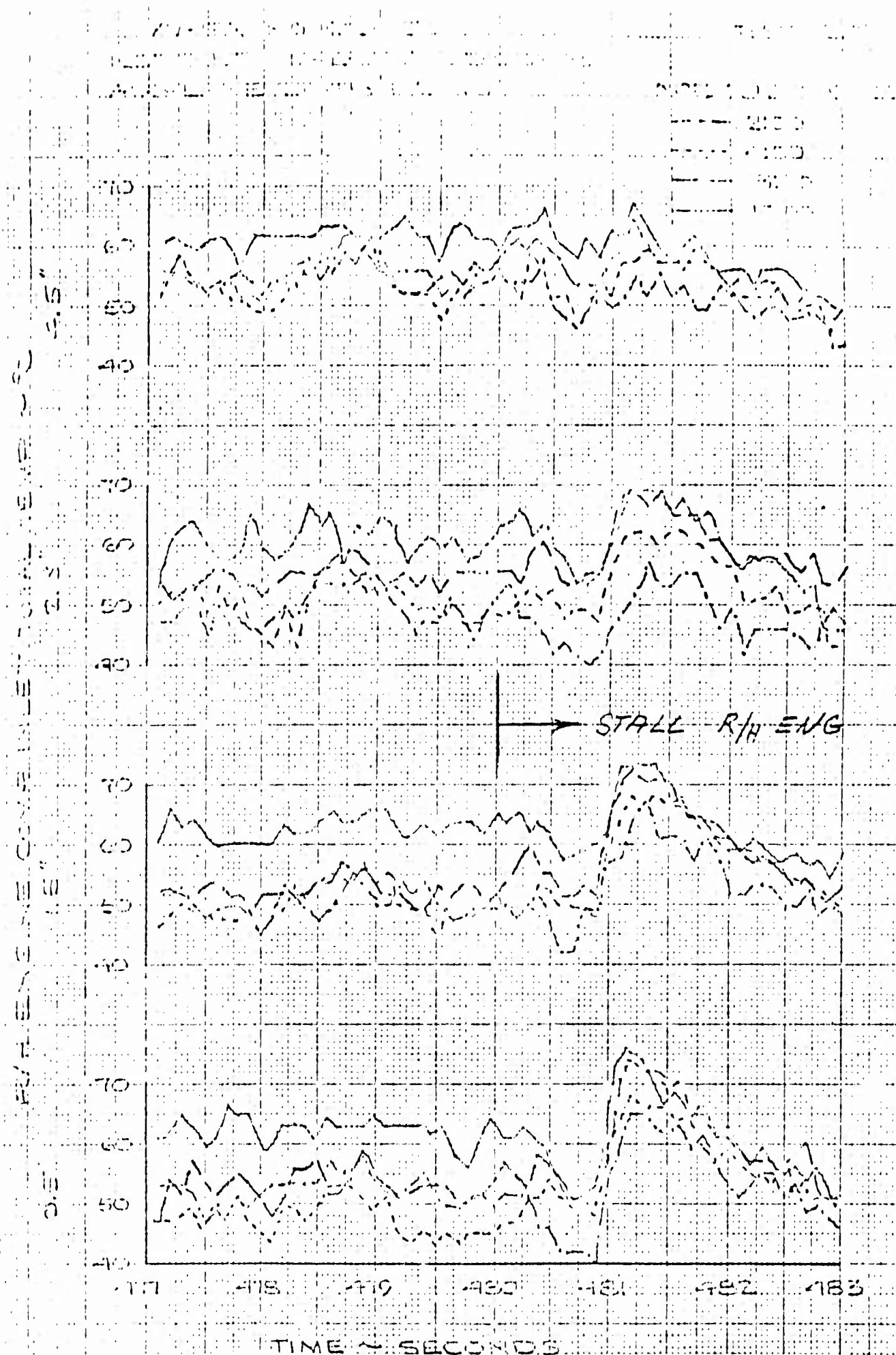


Figure 6.125 Circumferential Comparison of Inlet Temperature Distribution During R/H Engine Stall

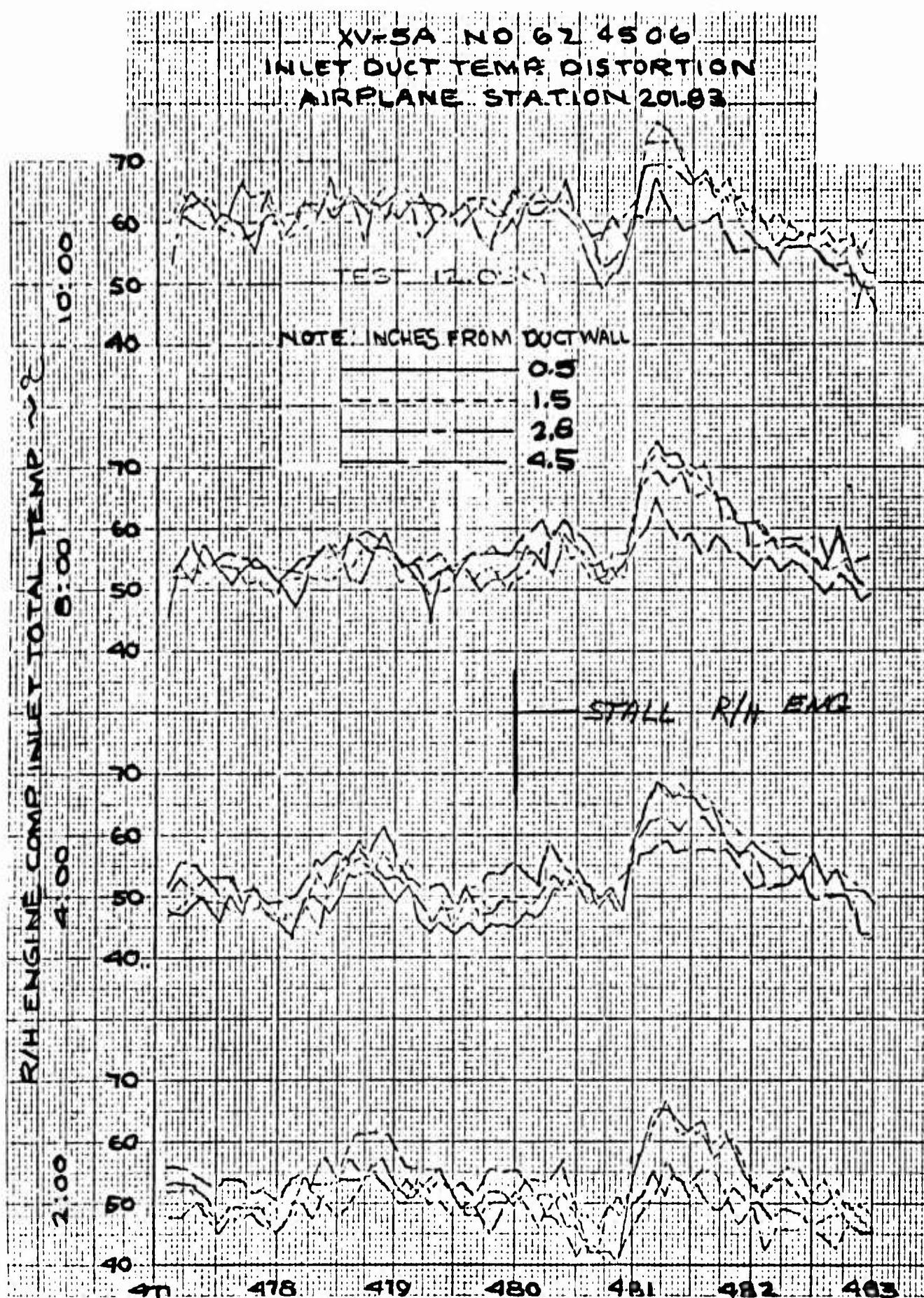


Figure 6.126 Immersion Comparison of Inlet Temperature Distribution During R/H Engine Stall

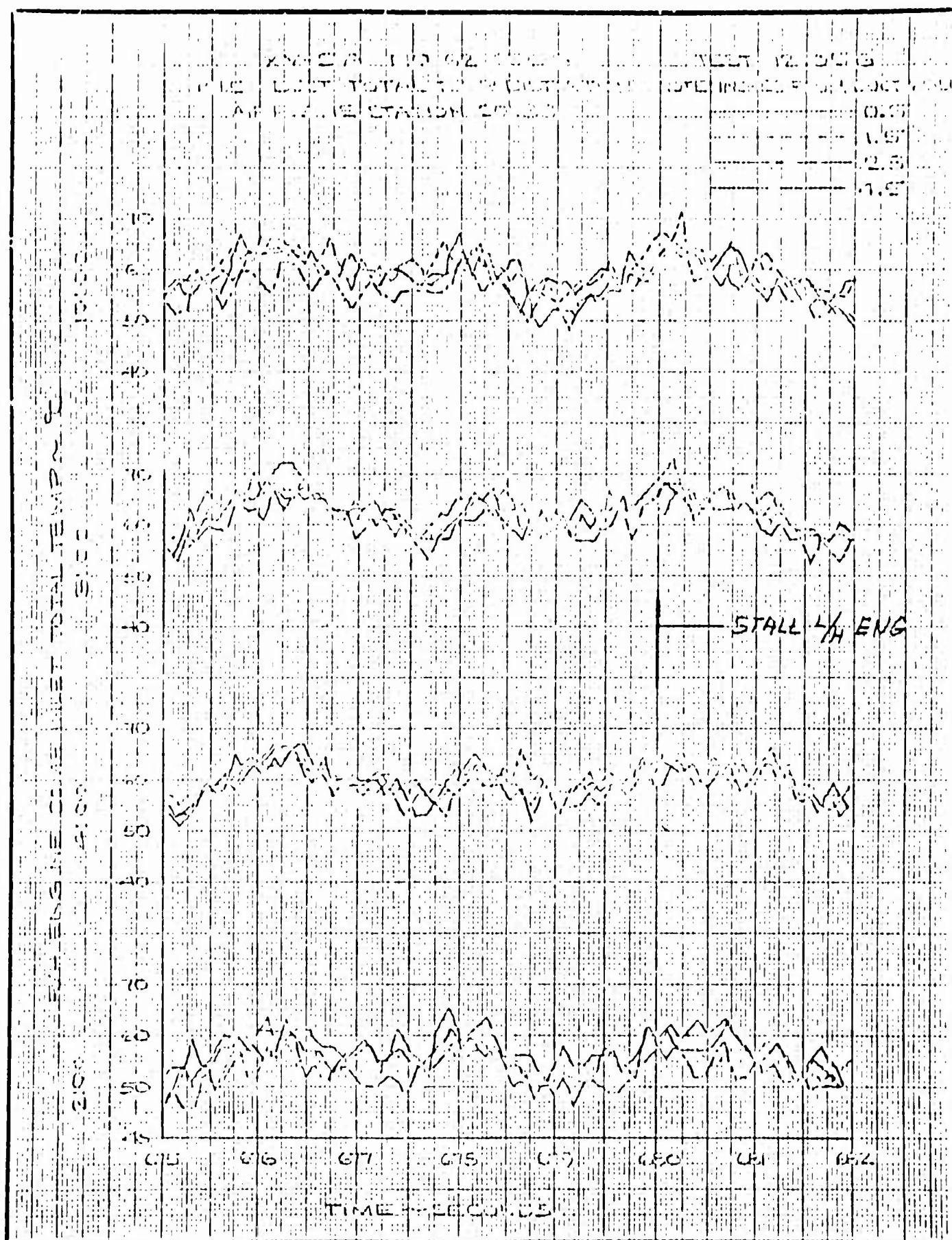


Figure 6.127 Immersion Comparison of Inlet Temperature Distribution During L/H Engine Stall

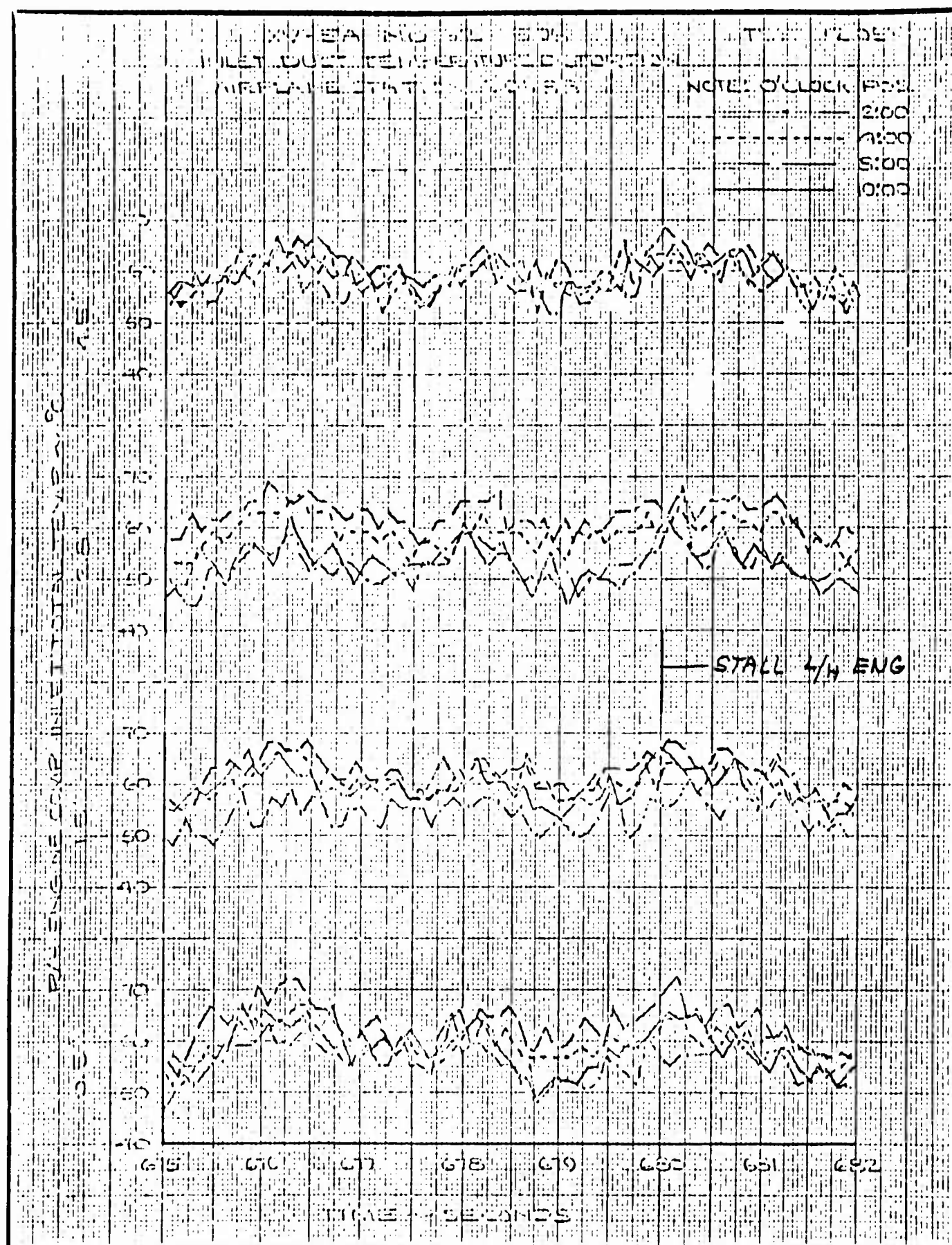


Figure 6.128 Circumferential Comparison of Inlet Temperature Distribution During L/H Engine Stall

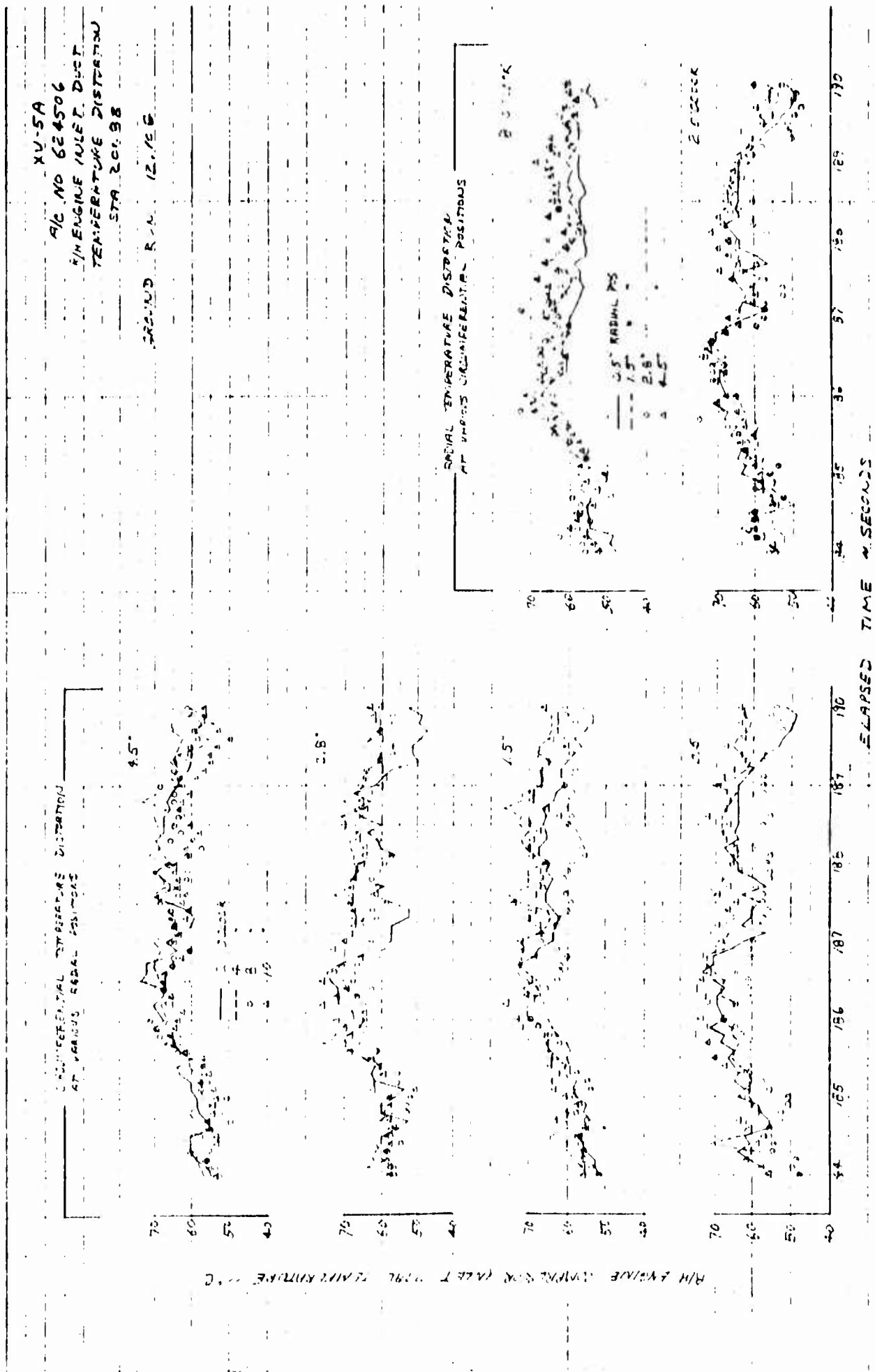


Figure 6.129 Typical Inlet Temperature Distribution for R/H Gas Generator During Fan Mode Operation in Ground Effects



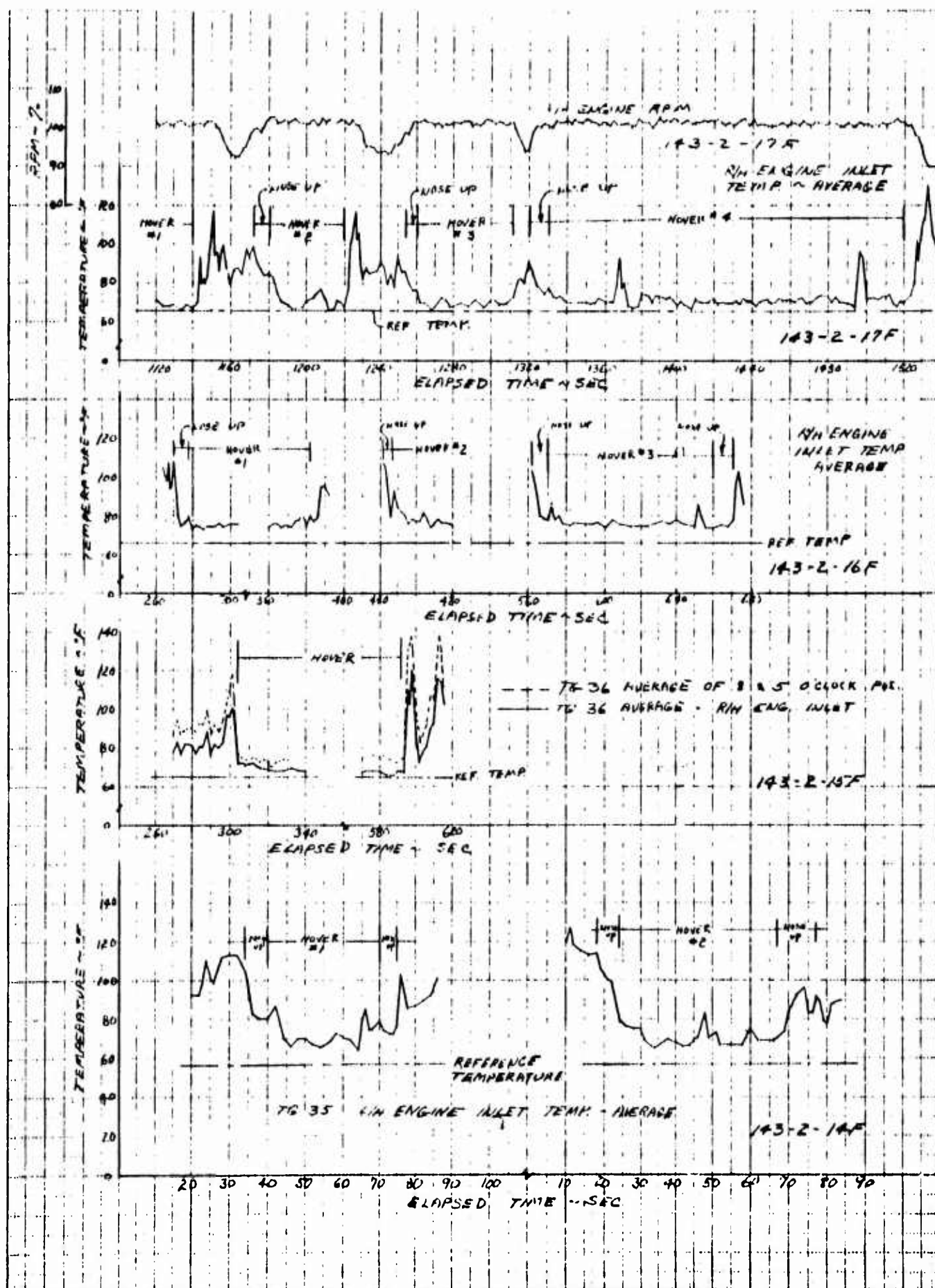


Figure 6.131 Hot Gas Ingestion Experienced During Several Vertical Lift Off and Hover Maneuvers

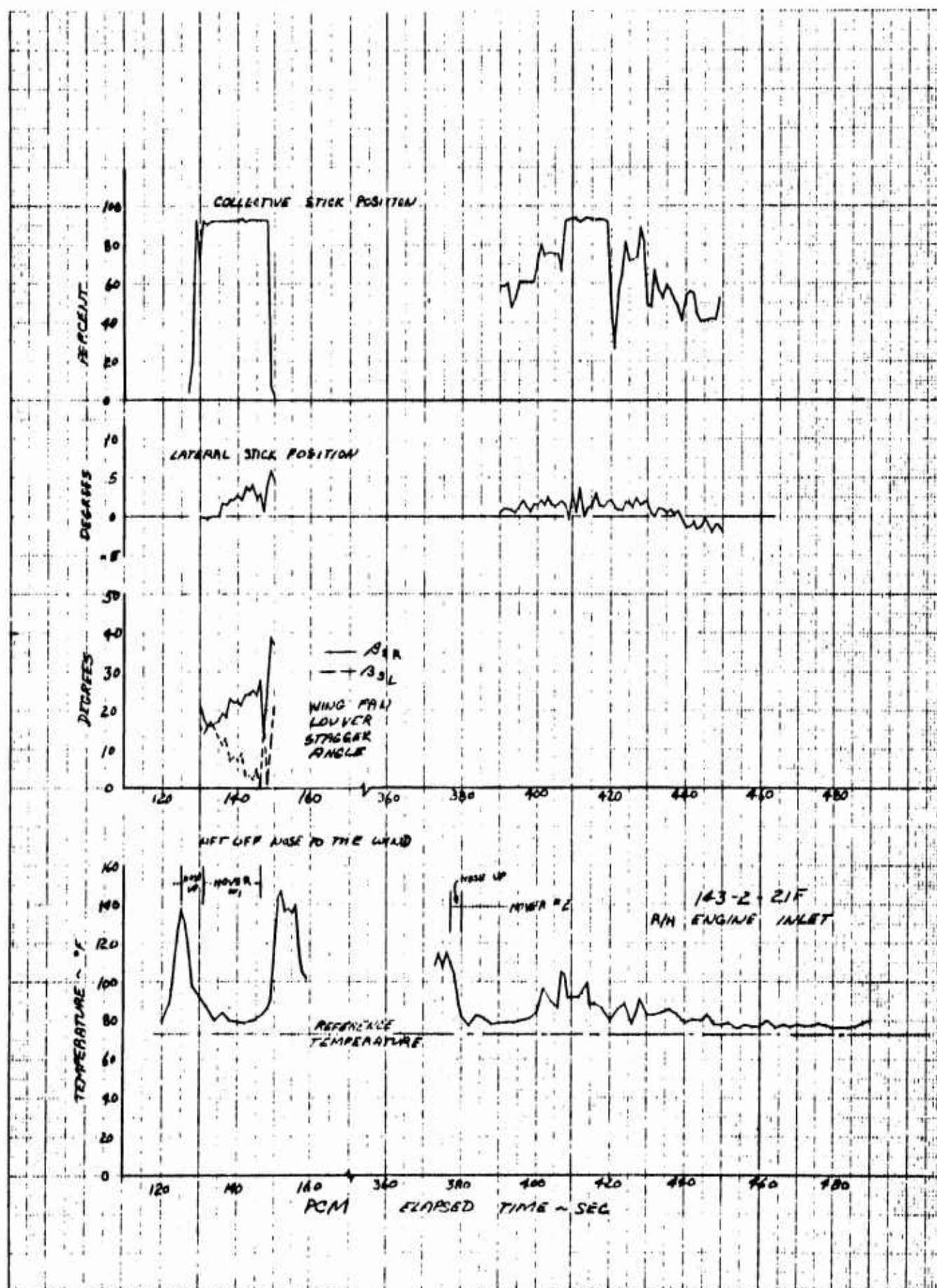


Figure 6.132 Hot Gas Ingestion and Some Aircraft Control Positions During Vertical Lift Off and Hovering

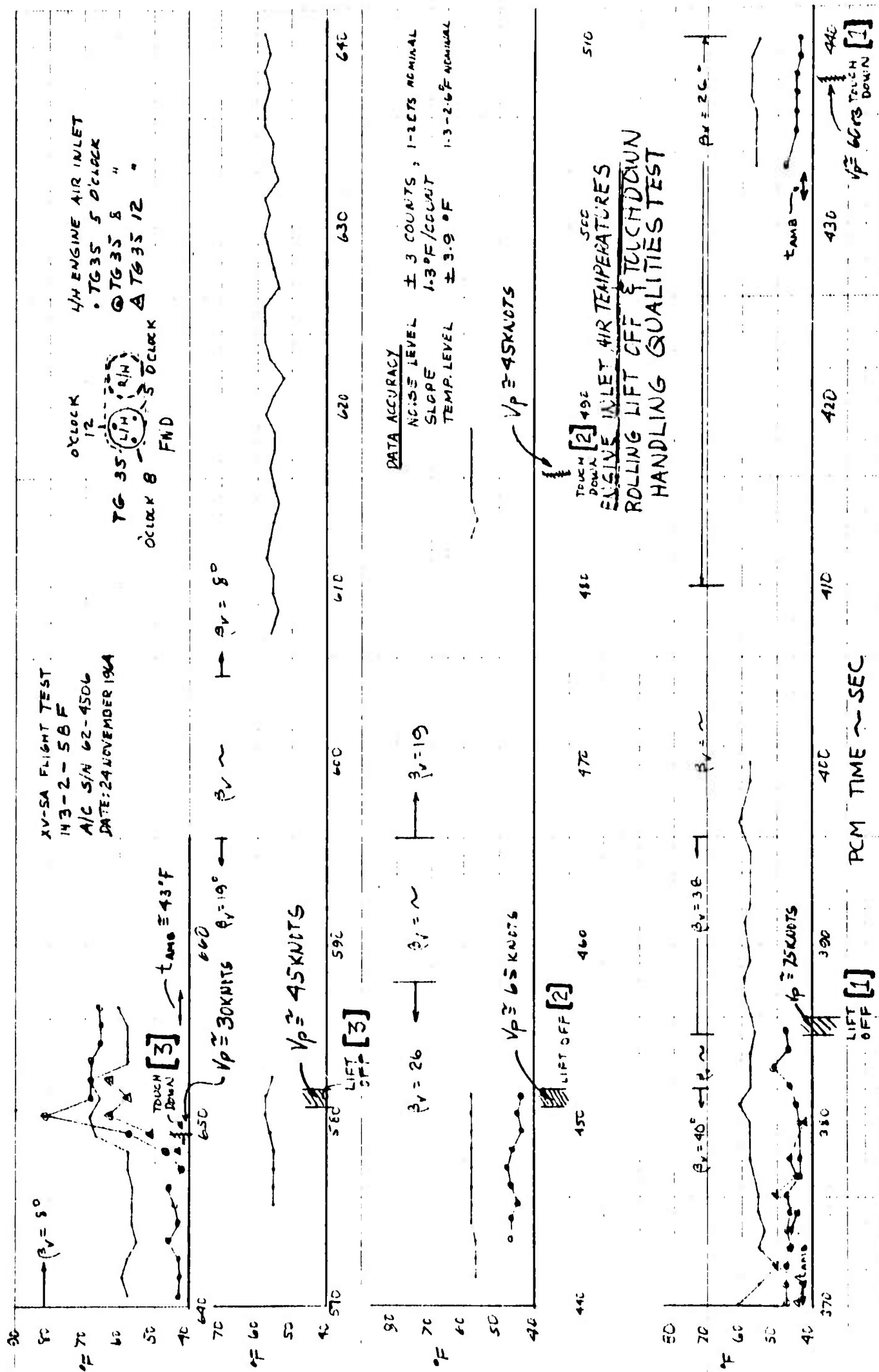


Figure 6.133 Gas Ingestion Experienced During Short Takeoff and Landing Maneuvers During Fan Mode Operation

ENGINE INLET AIR TEMPERATURES

XV-5A FLIGHT TEST
143-2-58F
A/C #N 62-4506
DATE: 24 NOVEMBER 1965

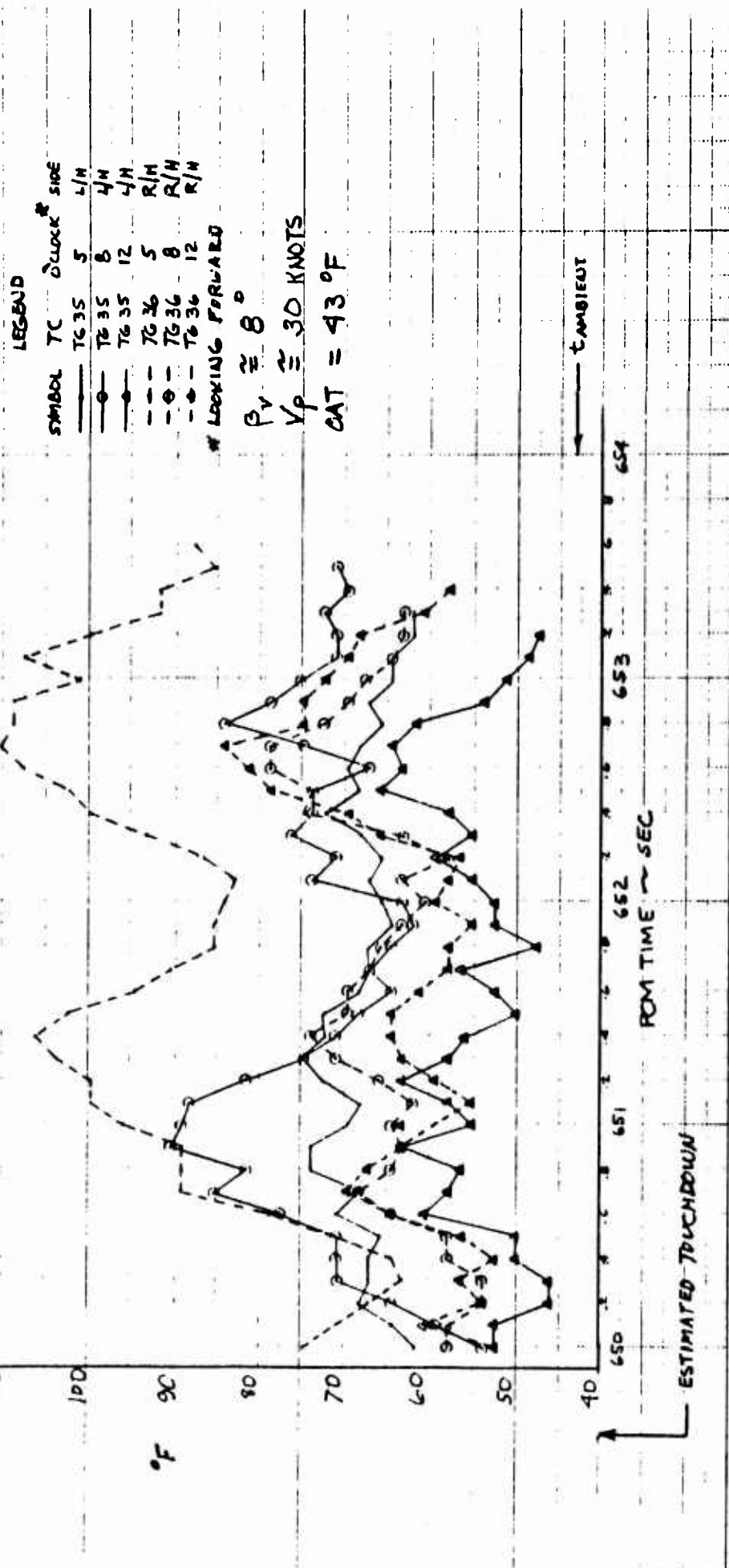


Figure 6.134 Inlet Temperature Distribution During Slow Speed Short Landing Maneuvers During Fan Mode Operation

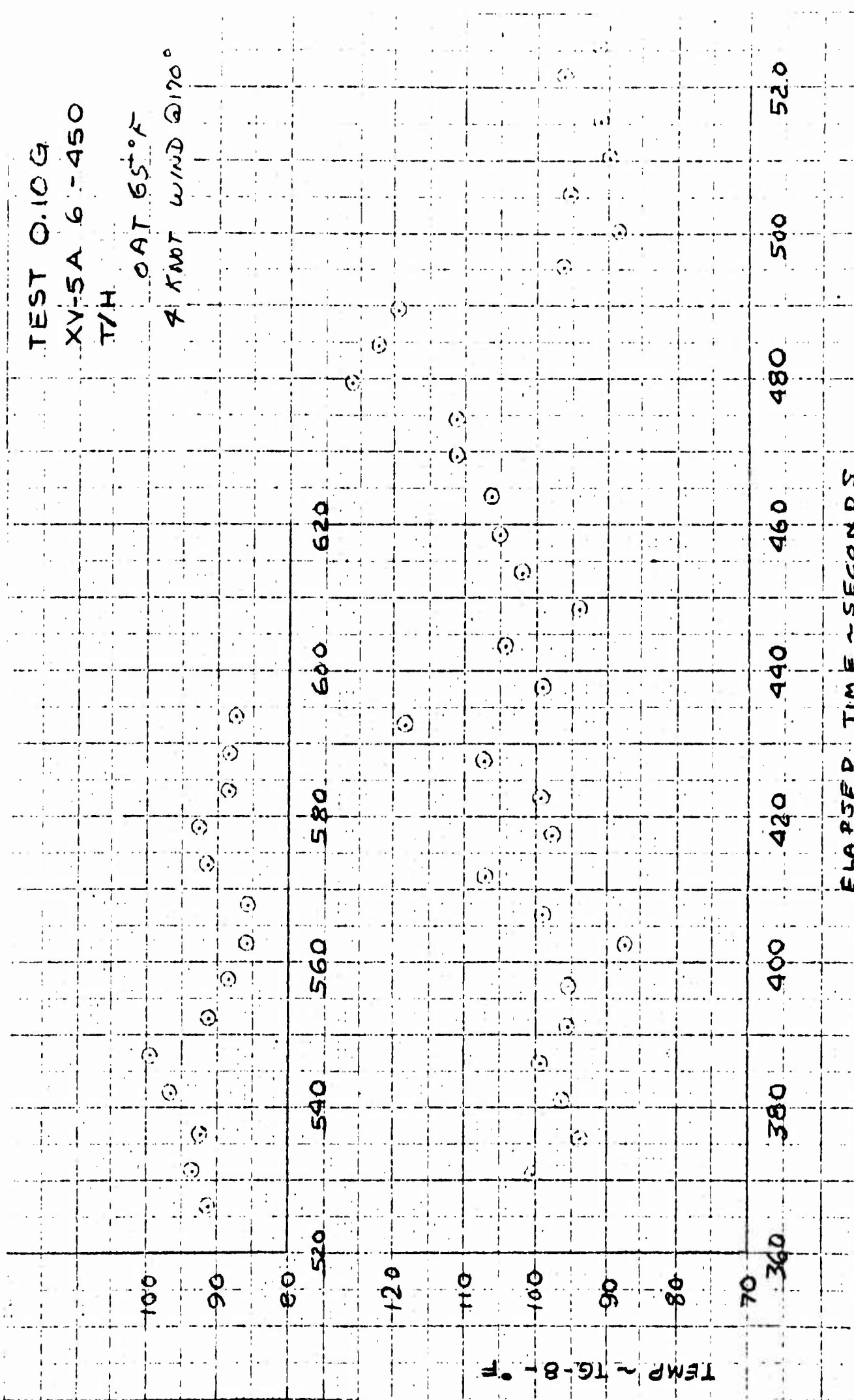


Figure 6.135 Representative Cockpit Air Temperatures - Fan Mode Operation in Ground Effect

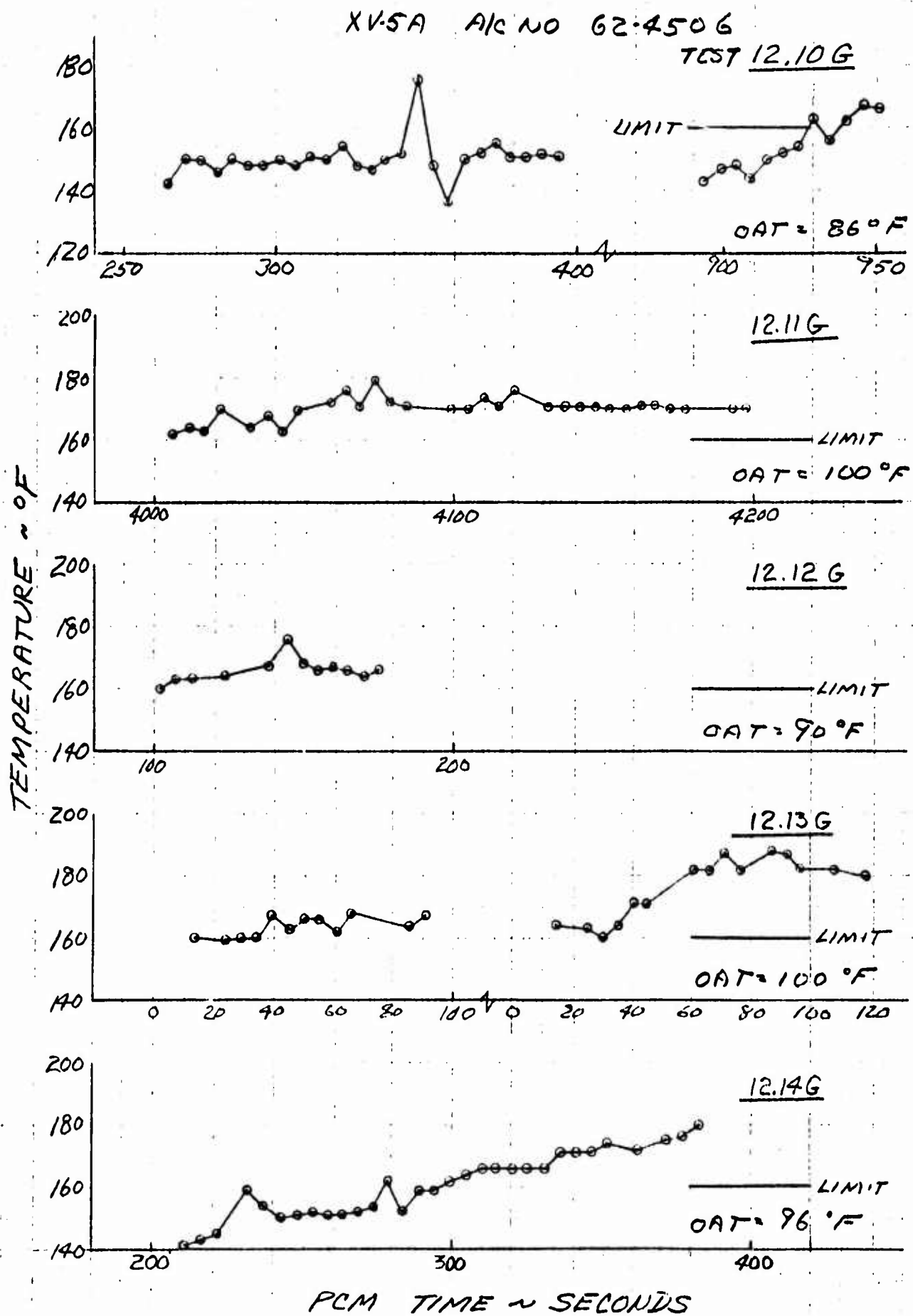


Figure 6.136 Electronic Compartment Inlet Air Temperature TG-4

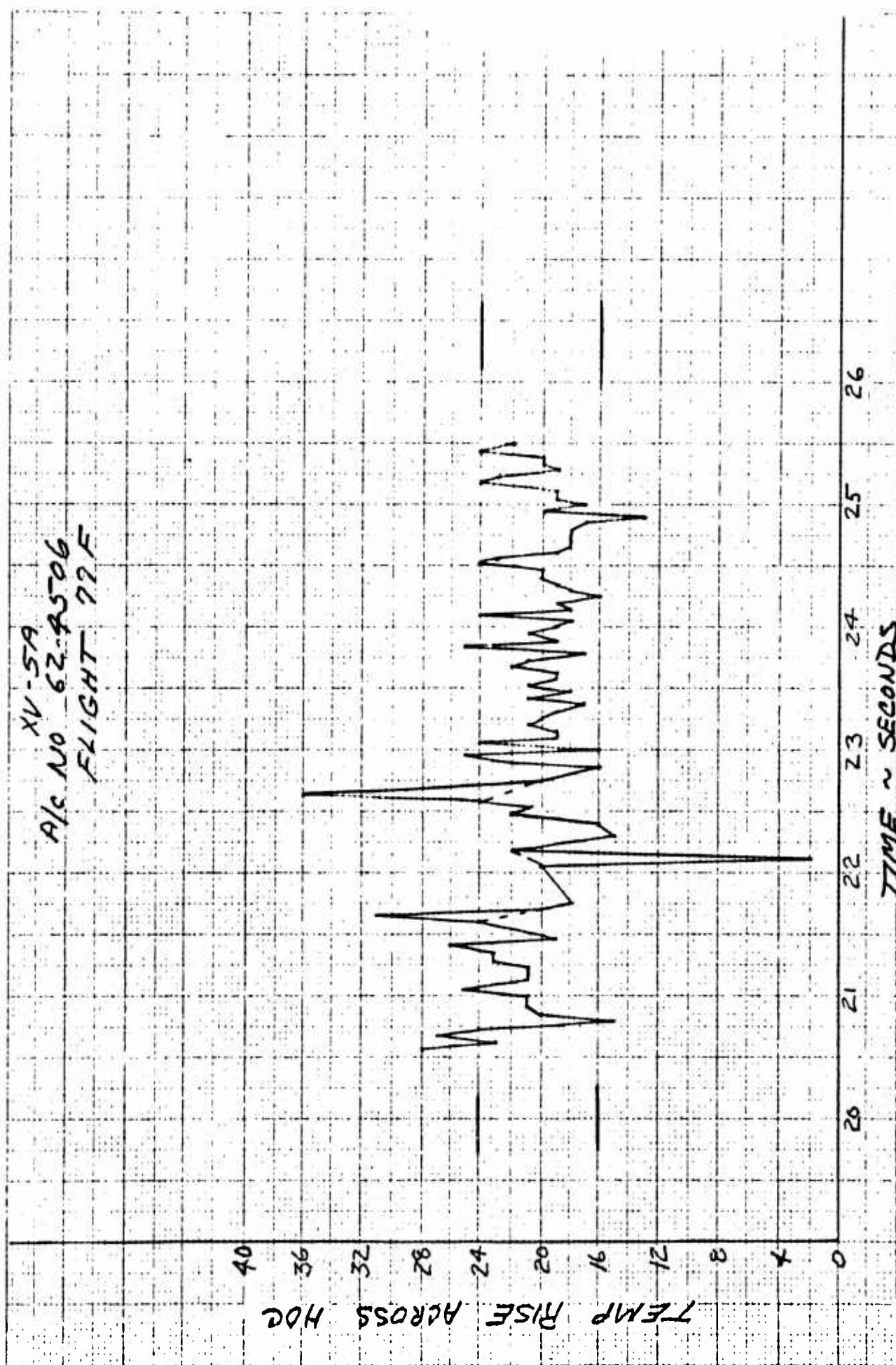


Figure 6.137 Representative Temperature Difference Across Hydraulic Oil Cooler (HOC)

XV-5A
A/C NO 624506
TEMPERATURE STUDY
GROUND RUNS

TG 21 COMPRESSOR COMPT. AIR TEMP.
 TG 23 ENGINE TURBINE COMPT AIR TEMP

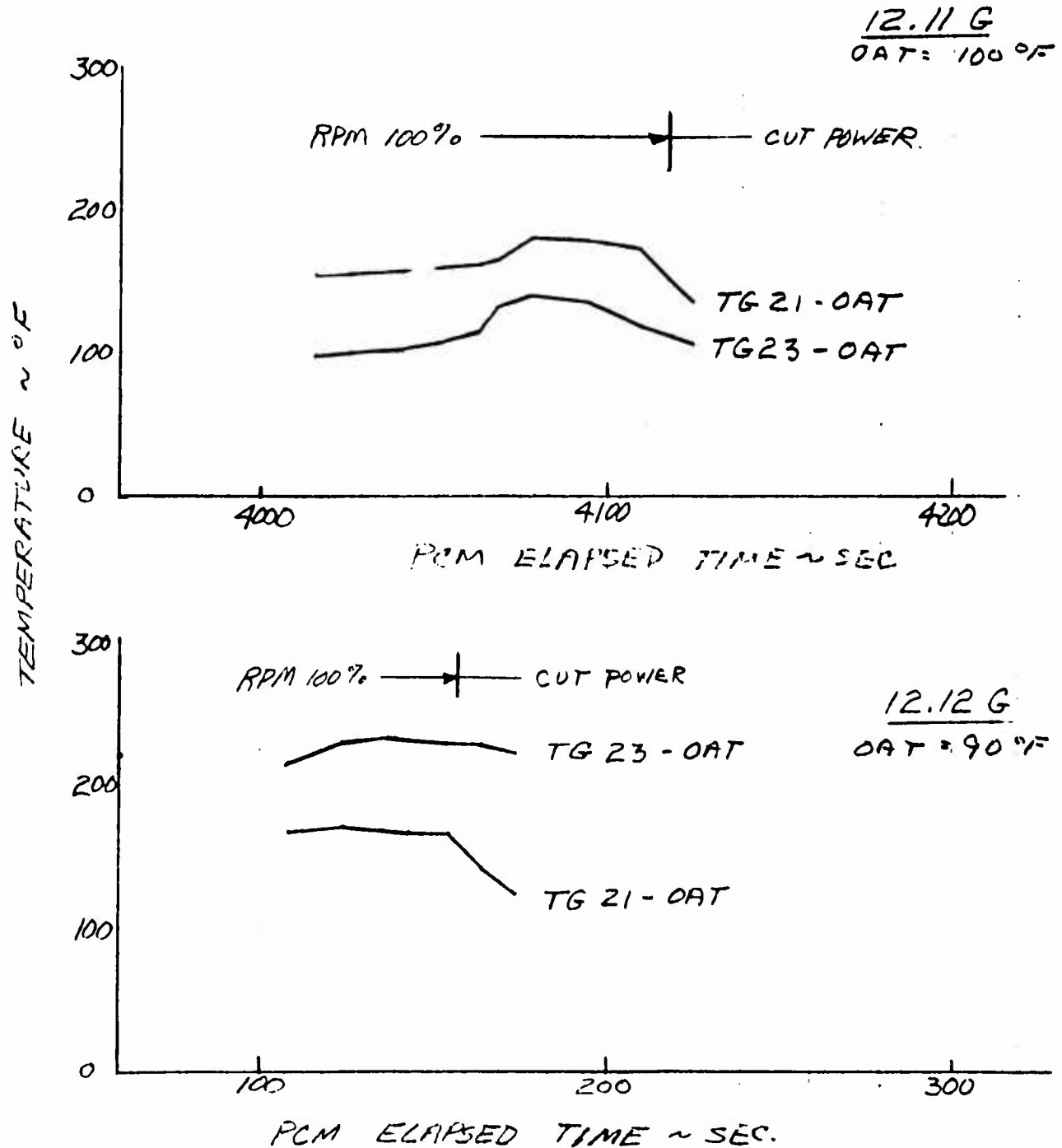


Figure 6.138 Cooling Air Temperature Rise from Ambient to Compressor and Engine Compartment Conditions

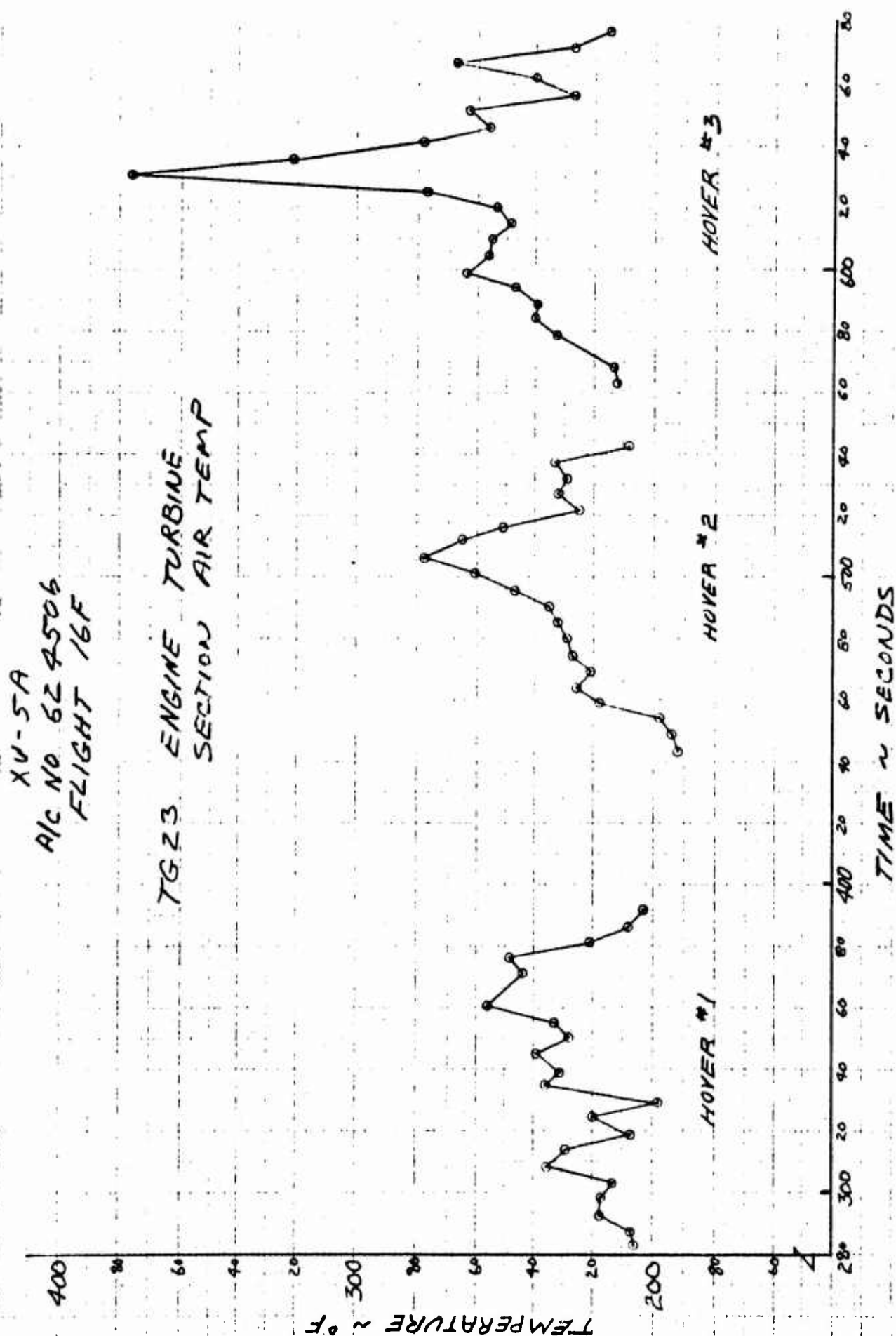


Figure 6.139 Engine Compartment Air Temperatures During Several Hover Maneuvers

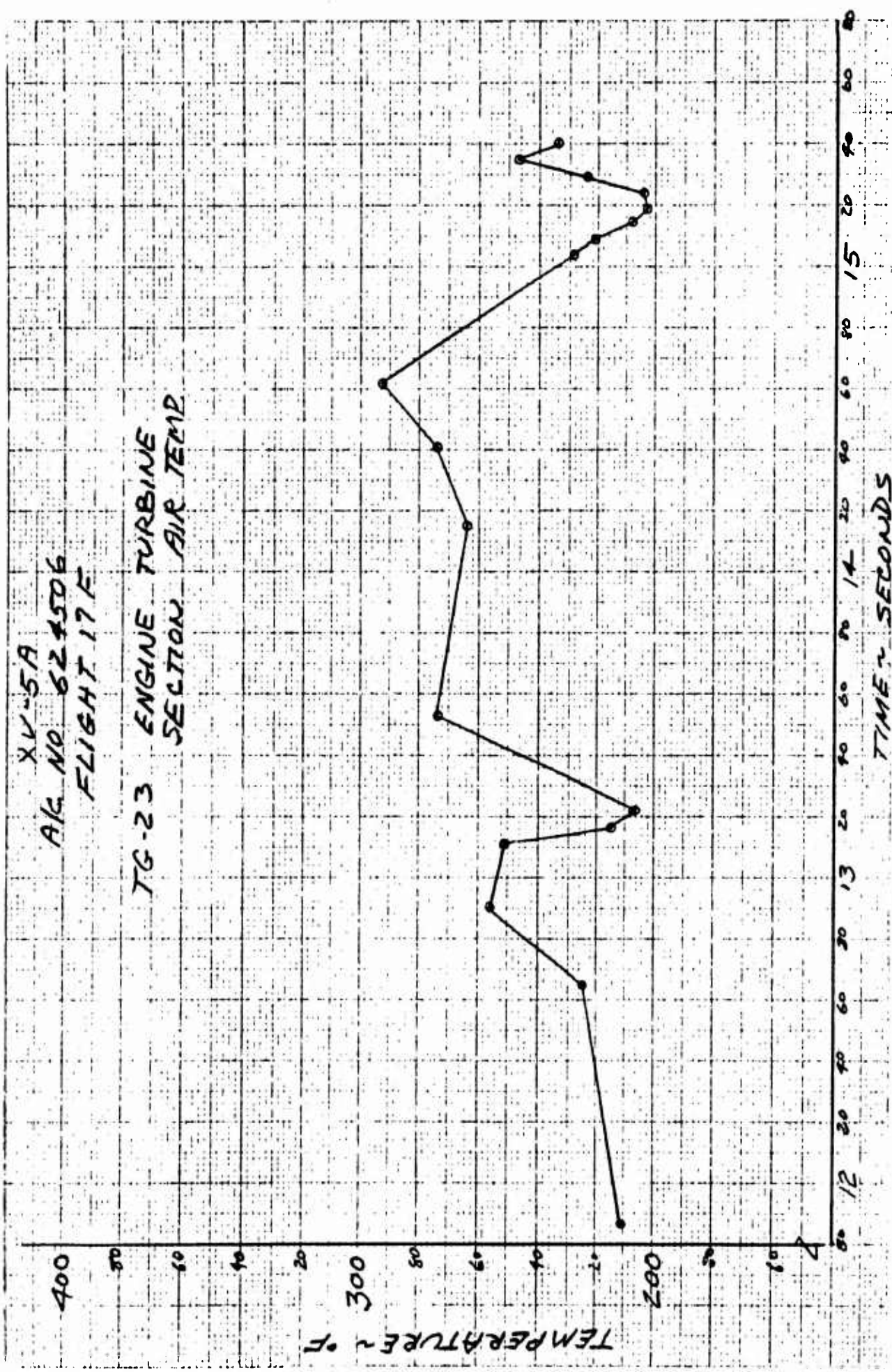


Figure 6.140 Engine Compartment Air Temperatures During Fan Mode Flight

XV-5A
A/C NO 624506
FLIGHT 18 F

TG 23 ENGINE TURBINE
SECTION AIR TEMP.

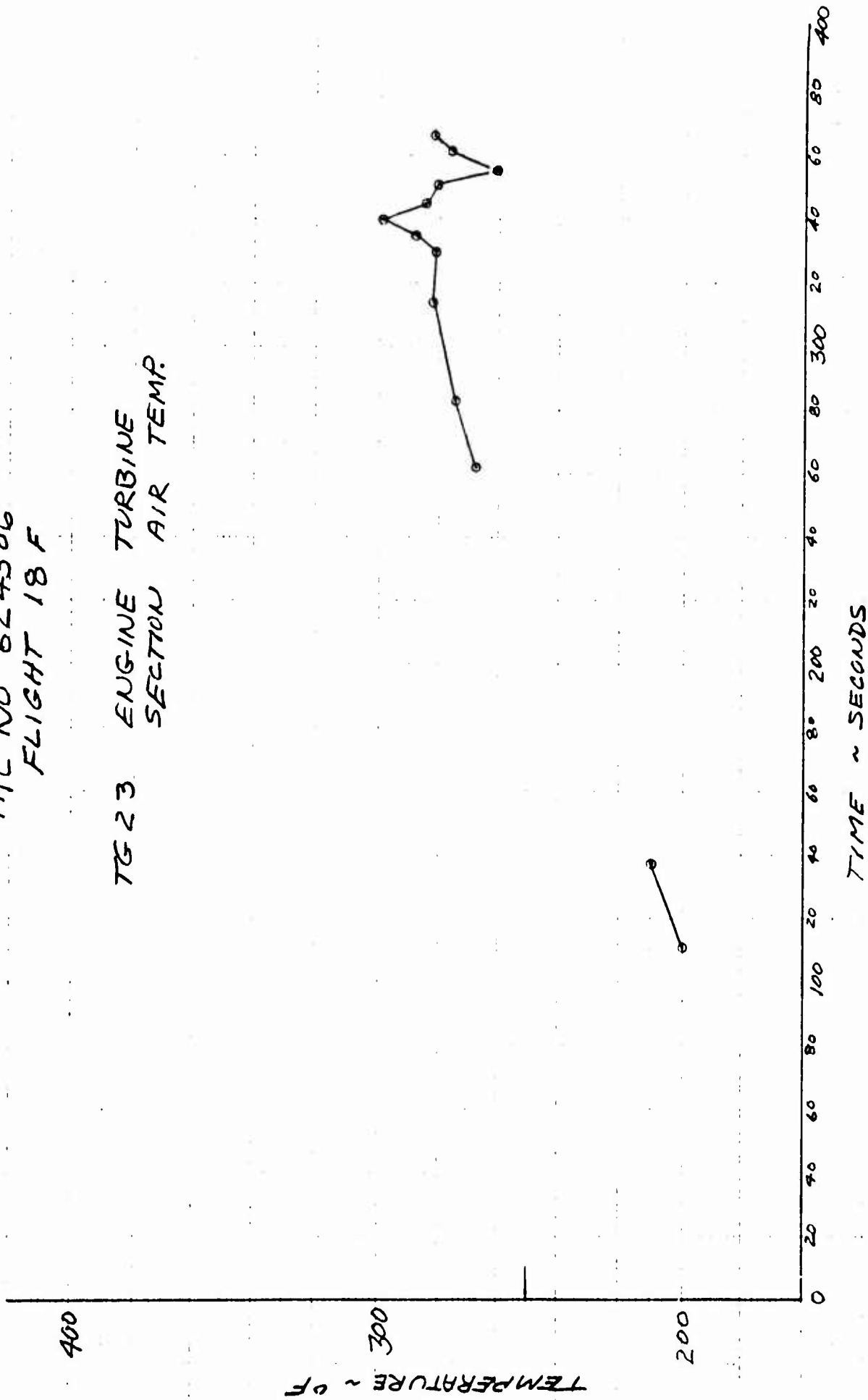


Figure 6.141 Engine Compartment Air Temperature During Fan Mode Flight

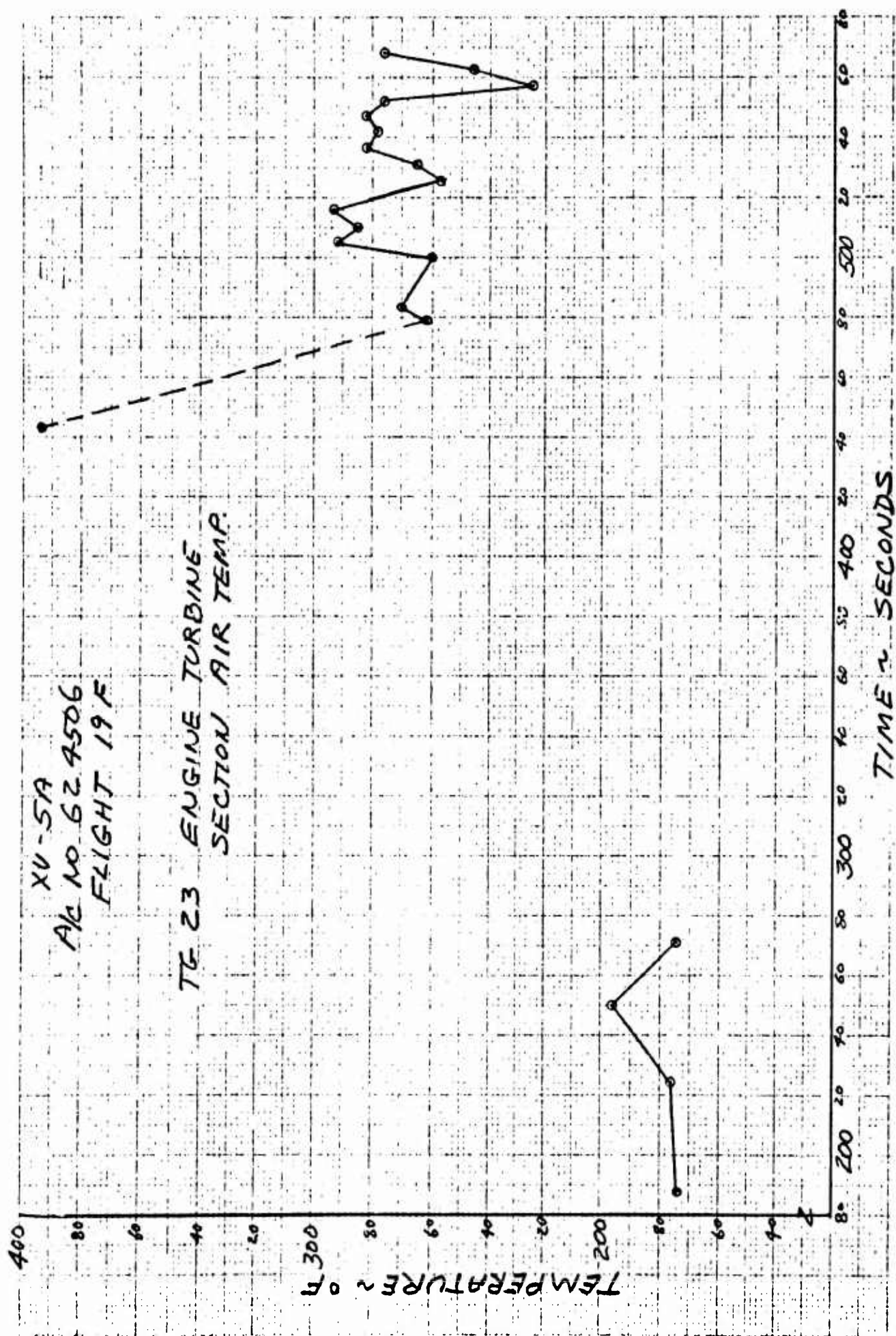


Figure 6.142 Engine Compartment Air Temperature During Fan Mode Flight

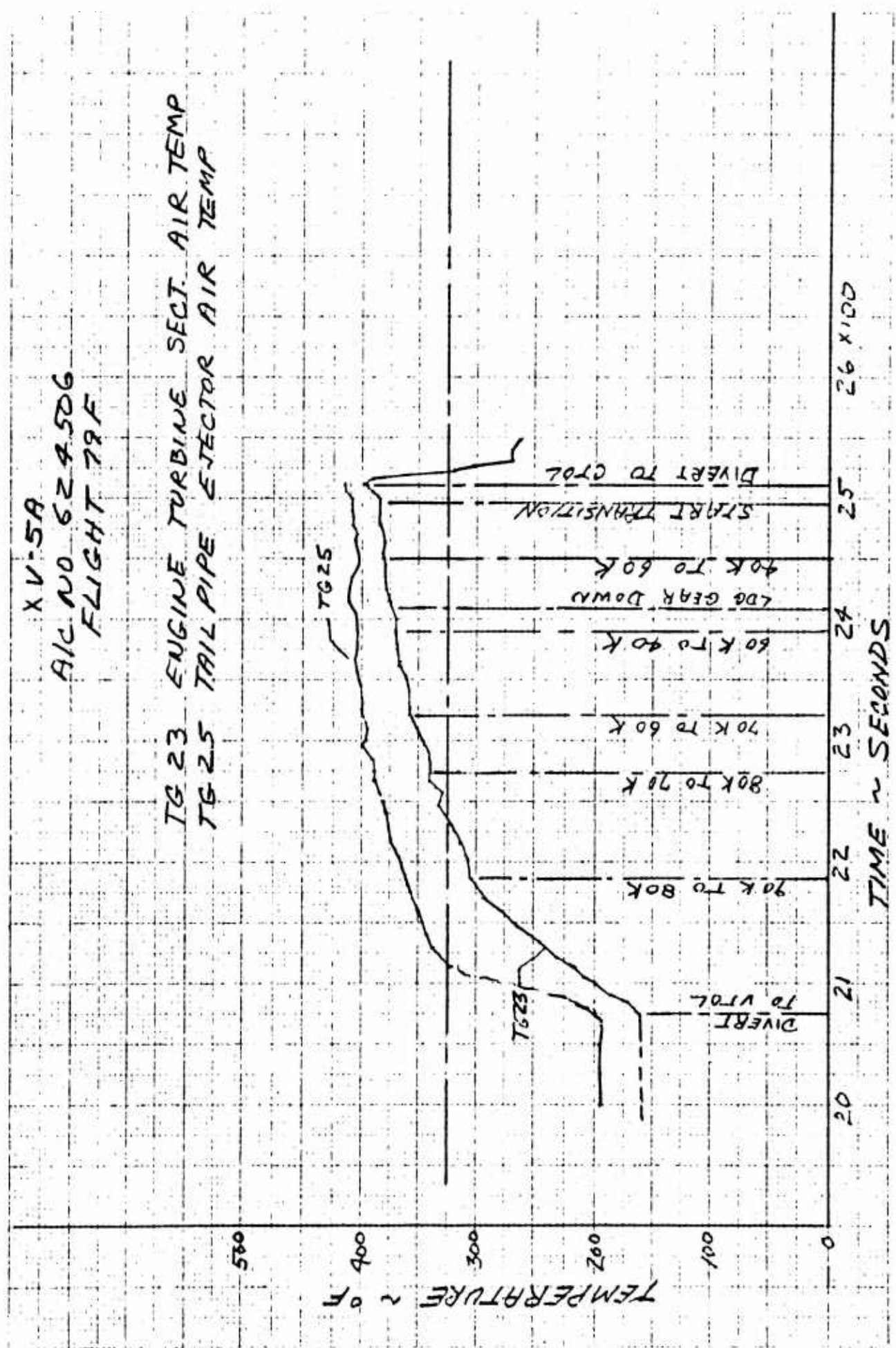


Figure 6.143 Effect of Aircraft Speed on Cooling Air Temperatures at Engine Compartment and Tailpipe Ejector Outlets

○ TS-725
 △ TG-39
 □ TS-622
 ◇ TG-812



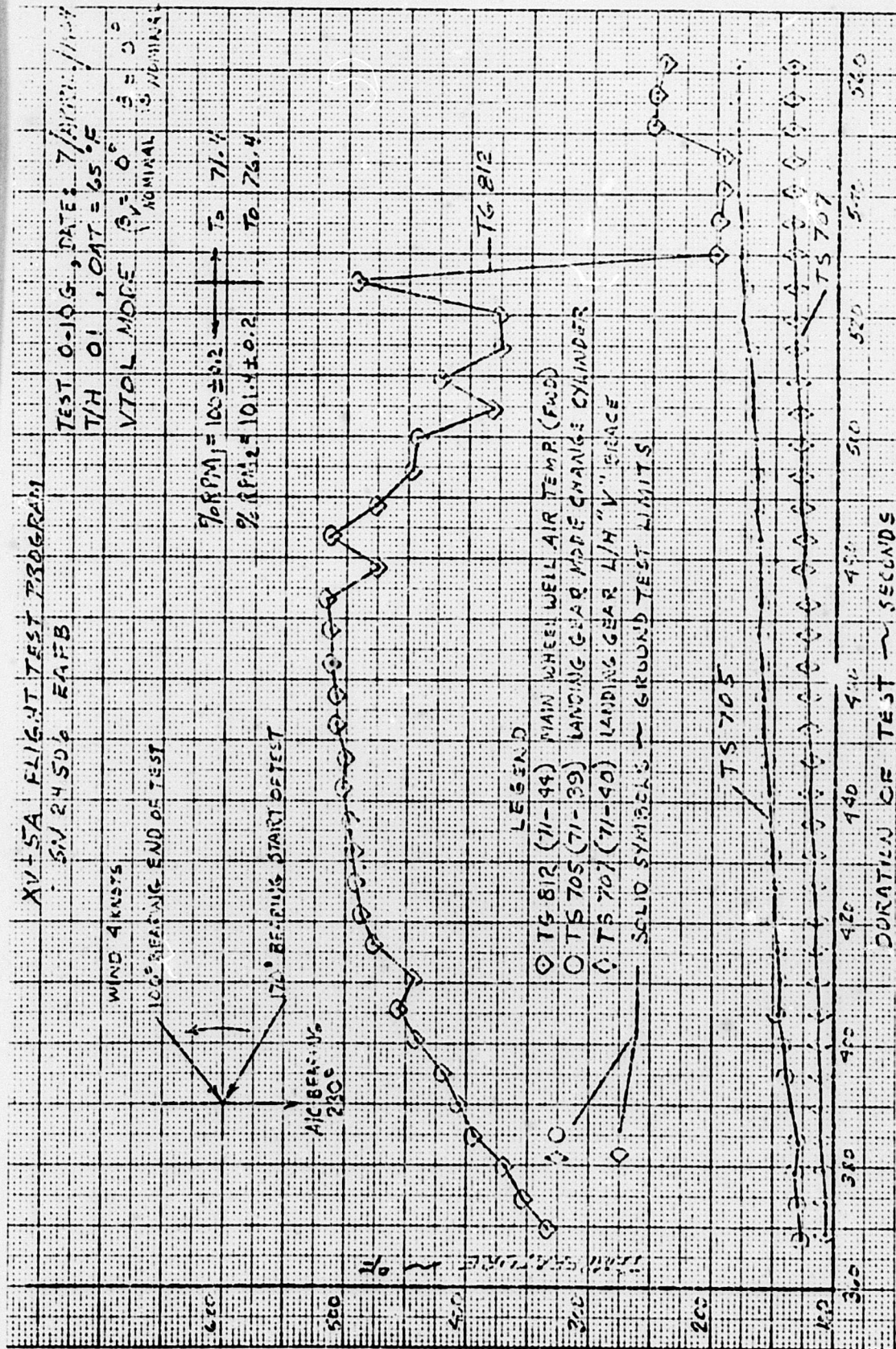


Figure 6.145 Main Wheel Well and Landing Gear Components Temperature Fan Mode Operation in Ground Effect, Wheel Well Enclosed, Gear Fixed

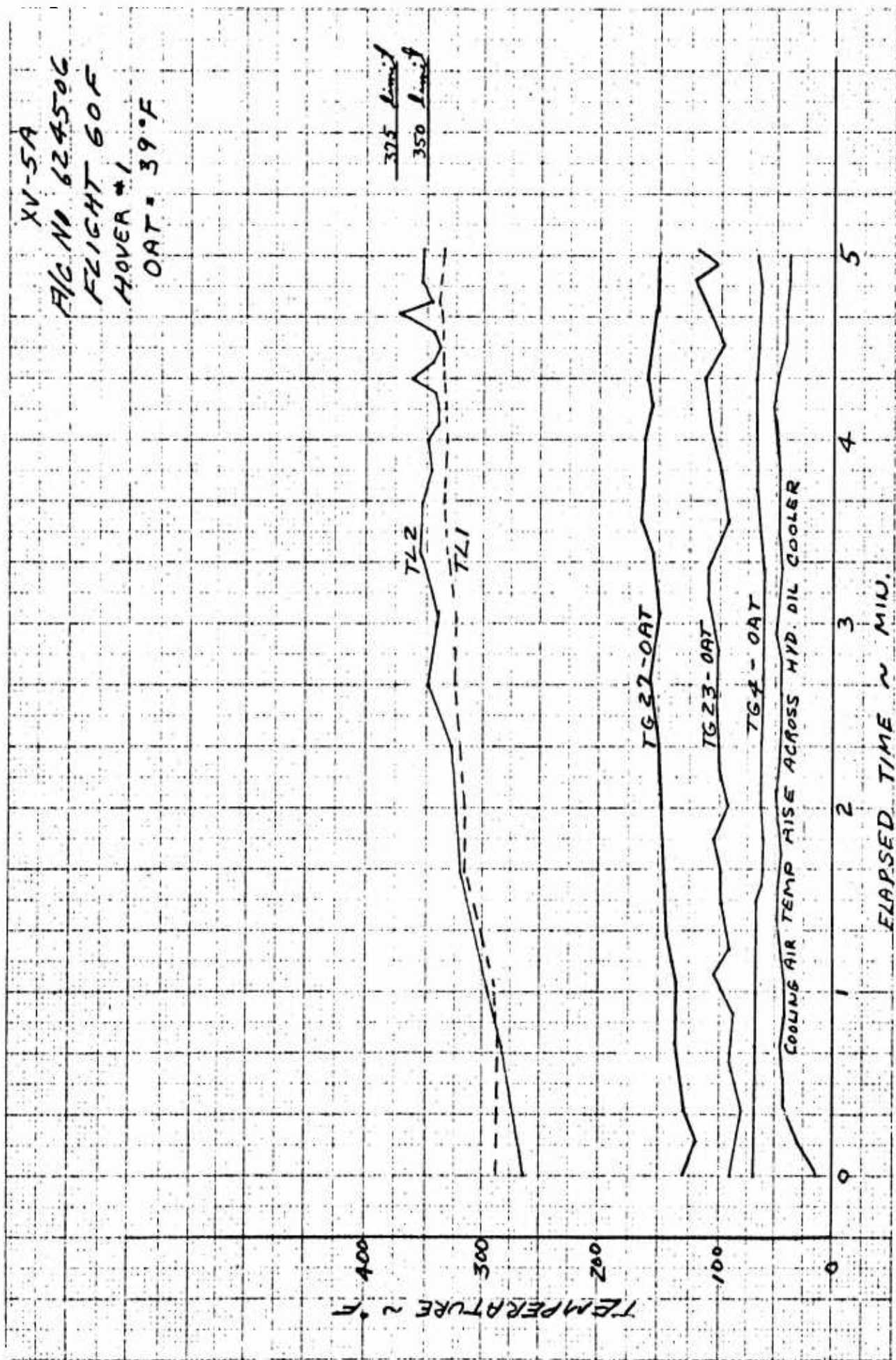


Figure 6.146 Engine Oil and Miscellaneous Air Temperatures During Hover

XV-5A A/C NO 624506

R/H ENGINE OIL TEMPERATURE

STOL FLIGHTS

29 F

30 F

31 F

32 F

34 F

36 F

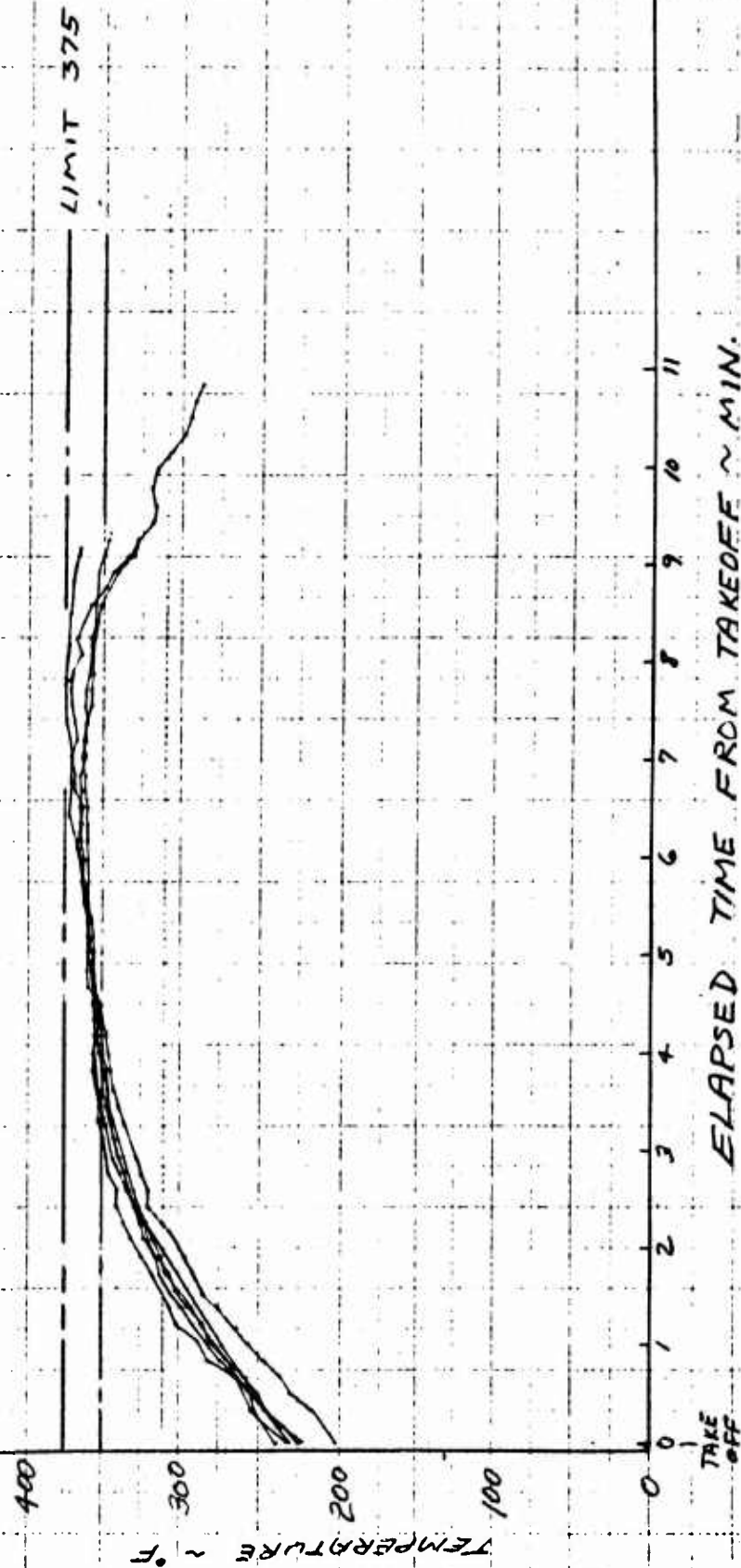


Figure 6.147 Comparison of R/H Engine Oil Temperatures for Several Flights

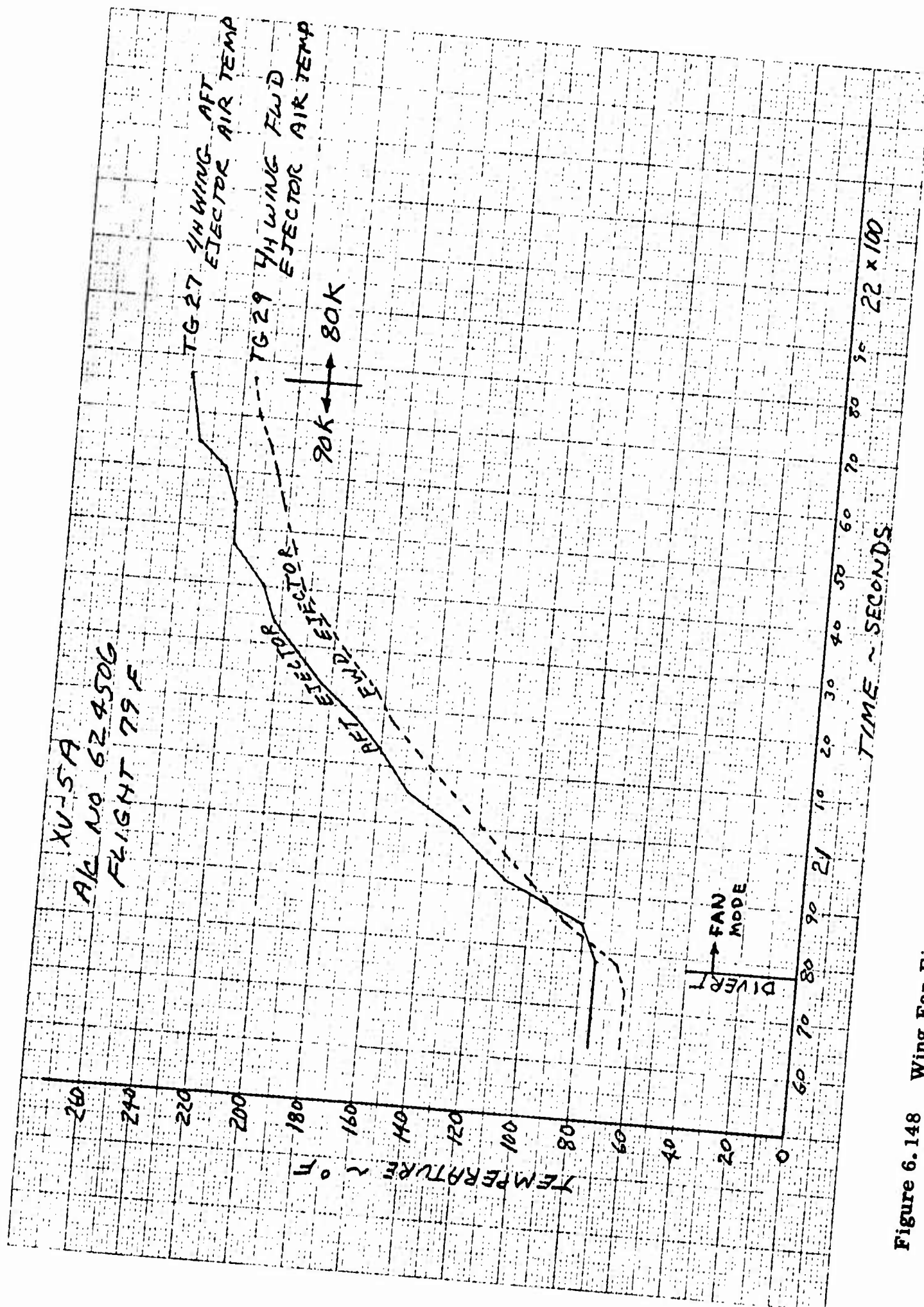


Figure 6.148 Wing Fan Ejector Cooling Air Temperature Following Conversion from Jet to Fan Mode

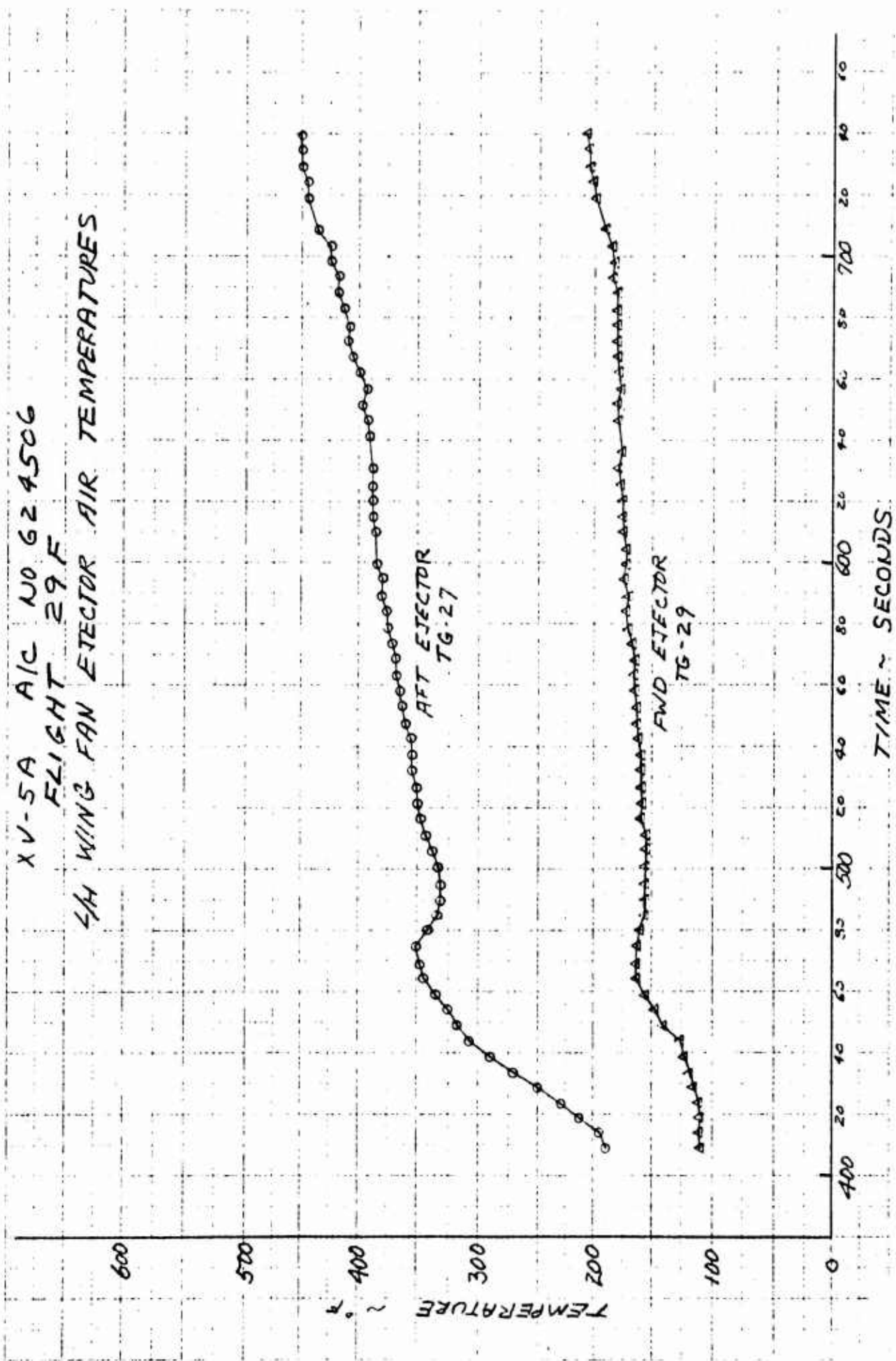


Figure 6.149 Wing Fan Ejector Cooling Air Temperature During Fan Mode Flight

XV-5A A/C NO 624506
 FLIGHT 49 F
4th WING FAN EJECTOR AIR
PRESSURE

CONVERSION FROM TURBOJET
 MODE TO FAN MODE

(SIMILAR TO 143-2-79 F)

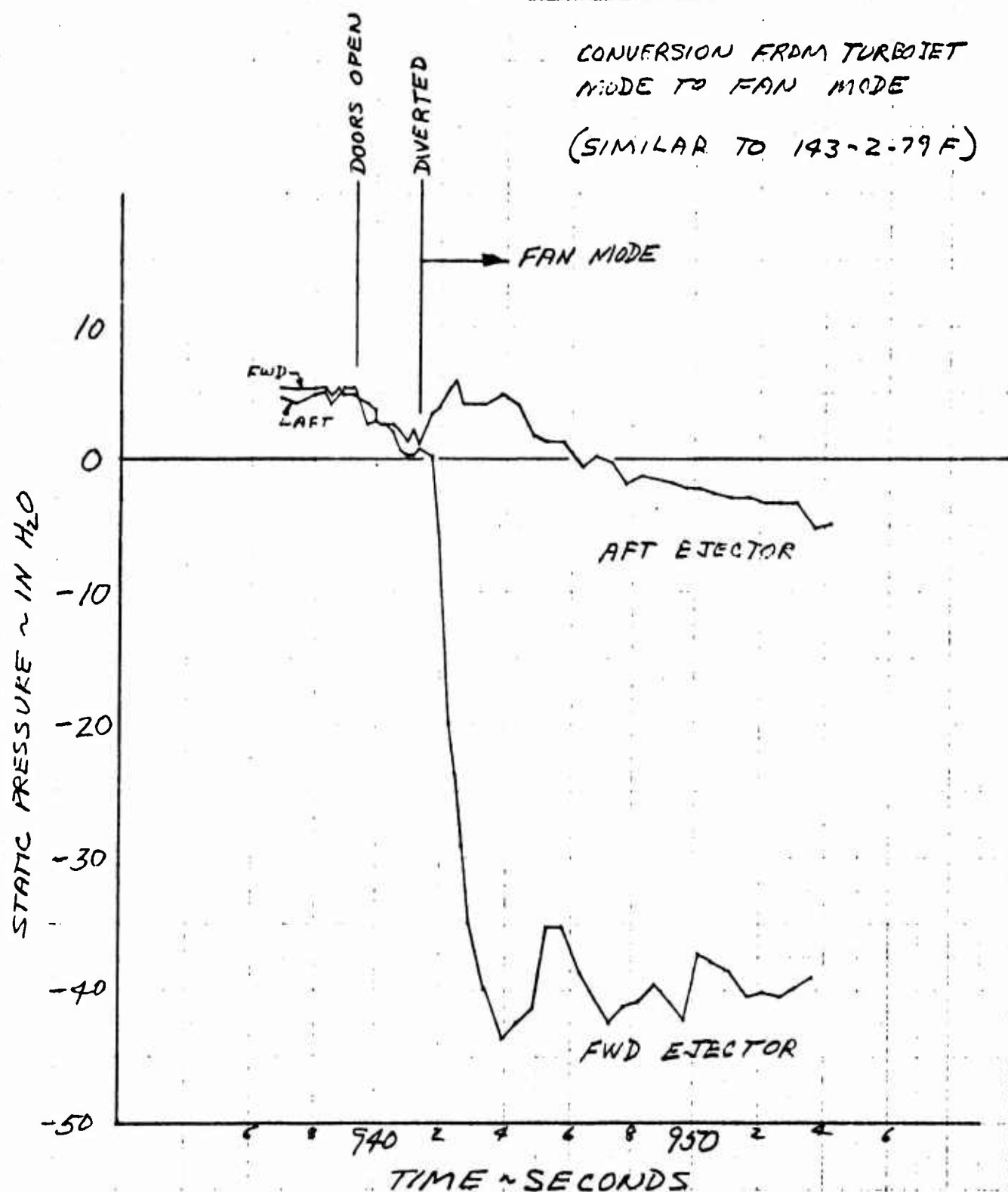


Figure 6.150 Wing Fan Ejector Cooling Air Static Pressure During Fan Mode Flight

XV-5A A/C NO 624506
 FLIGHT 29 F
 1/4 WING FAN EJECTOR PRESSURE
 STOL TAKE OFF

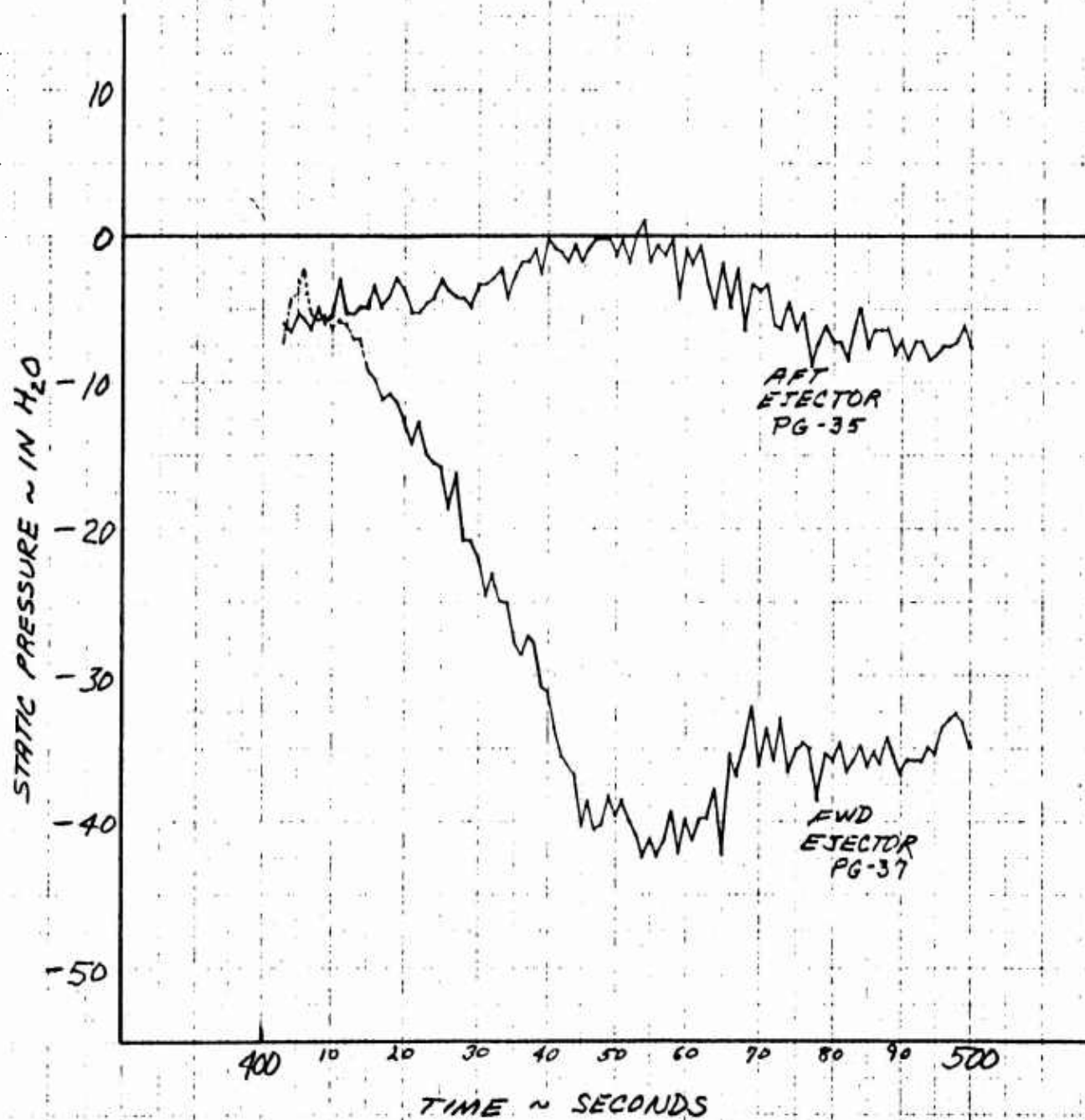


Figure 6.151 Wing Fan Ejector Cooling Air Static Pressures During Short Take Off Maneuver in Fan Mode

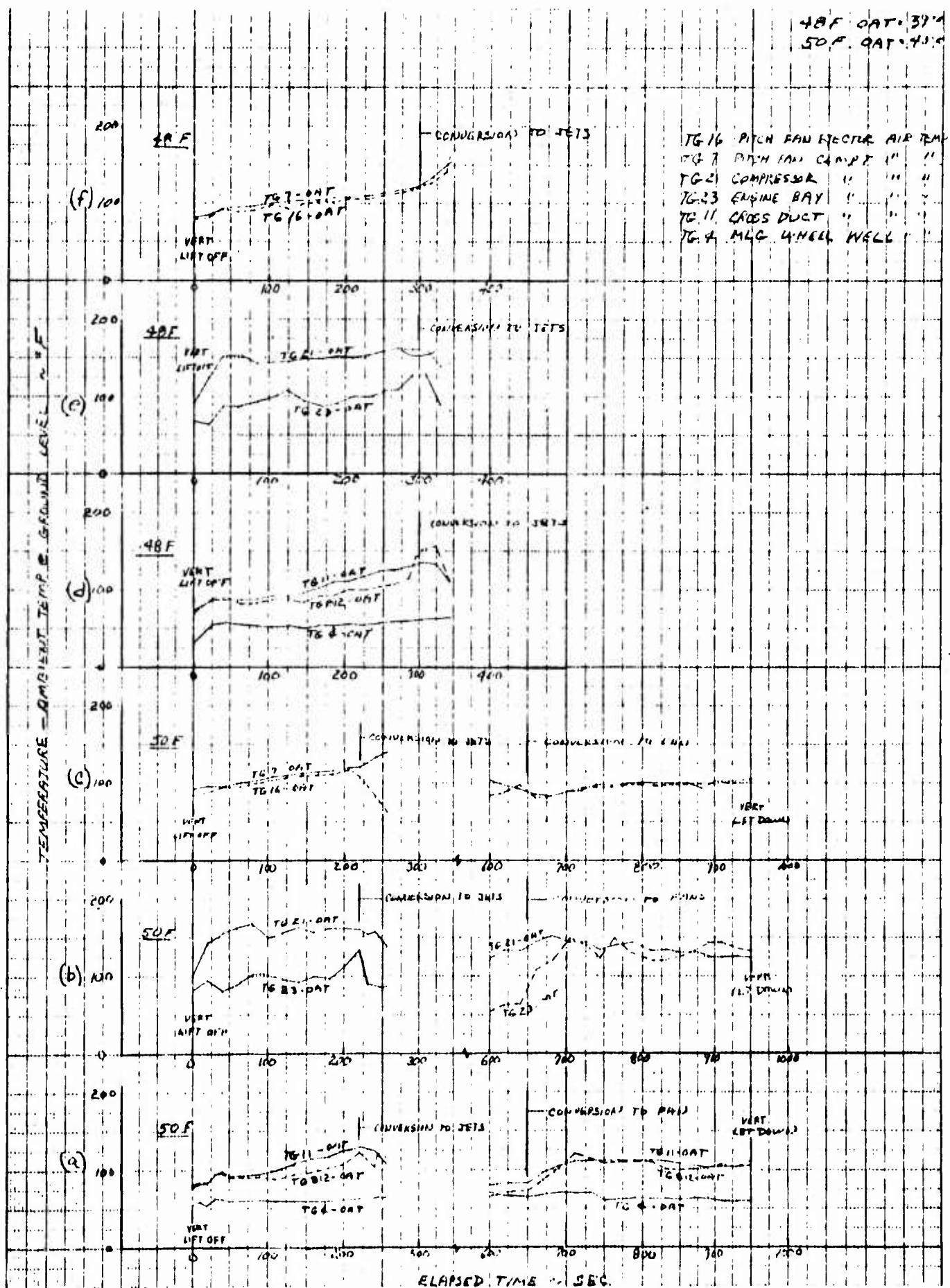


Figure 6.153 Typical Cooling System Temperature Differences for a Series of Vertical Take Off, Transition and Landing Maneuvers

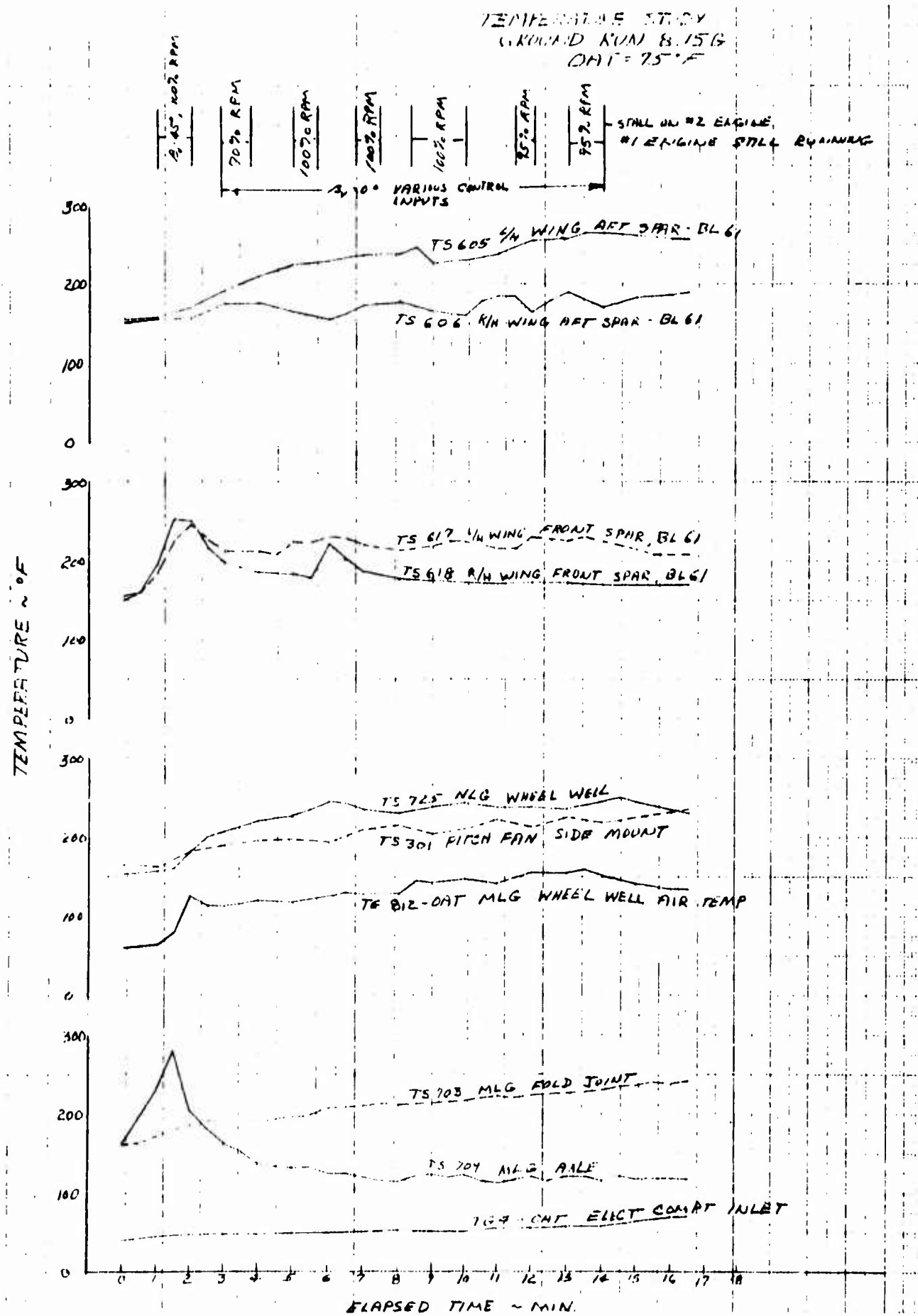


Figure 6.154 Representative Structural Temperatures for Fan Mode Operation in Ground Effect

7.0 CONVENTIONAL FLIGHT TEST RESULTS

7.1 PERFORMANCE

7.1.1 Stalls

Qualitative evaluation of the stall characteristics in various configurations was obtained during tests 5F, 6F and 7F with aircraft serial number 62-4506. Comparison of conventional flight stall speeds with estimated maximum fan mode flight speeds was of primary importance at this time. Pilot familiarization with the aircraft near and at stall speeds was a prerequisite to any attempt to convert from either fan mode flight to conventional flight or conventional flight to fan mode flight. During these early tests the landing gear was fixed in the down position.

For power-on stalls with flaps up (CR configuration with gear extended) the pilot reported that light aft stick pressure was required to keep the nose up all the way to the stall. Pre-stall buffet occurred at approximately two degrees indicated angle of attack prior to stall. Classical stall resulted with nose falling straight through and with no significant wing dropping tendency. Relaxing of aft stick at stall resulted in immediate stall recovery. Stalls were approached with a speed decay of one knot per second or less. Pitch control was good at all times. Power-off stalls with flaps up (G configuration with gear extended) were similar to power-on except for a slight increase in aft stick pressure required to keep the nose up during stall approach.

Power-on stalls were performed with flap deflections of 15, 30, and 45 degrees (P. A. configuration with various flap deflections). The pilot noted a definite decrease in aft stick pressure required to enter the stall with increased flap deflection. Stall break was mild but did produce a definite nose drop. Release of aft stick pressure in all cases resulted in stall recovery.

Stalls conducted in the preconversion mode both power-on and power-off were similar to those with full flap deflection except that there was no tendency for the nose to fall through when aft stick pressure was released. This indicates a neutral stick free stability at the stall. Upon application of forward stick, the nose seemed to drop through more abruptly than in conventional mode stall recoveries.

Pilot familiarization with stall characteristics of aircraft serial number 62-4505 was obtained during test 4F. This aircraft had an operational landing gear at the time of the test. Power-on and power-off stalls were performed in the clean configuration (CR and G, note; landing gear retracted). The pilot indicated a definite reversal in the stick force gradient as he approached the stall. At stall, the aircraft exhibited a neutral stick free stability. A definite application of forward stick pressure and movement was required to recover from the stall. Recovery was immediate following corrective action. Prestall buffet was generally felt as aircraft motion rather than control excitation. In the landing and power approach configuration there was essentially no prestall buffet observed. The stall resulted in a sudden right wing drop with a moderate rolling velocity and subsequent nose drop. The rolling could be arrested by application of forward stick pressure and movement.

In comparing the stall characteristics of the two aircraft several important facts should be noted. First, both aircraft stalled at approximately the same indicated angle of attack. Second, aircraft serial number 62-4506 exhibited a stable stall (nose down trim change) in both the flaps up and flaps deflected configuration. Aircraft serial number 62-4505 exhibited a neutral stick free stability in the clean configuration. The basic configuration difference between the two aircraft during flaps retracted stalls was the fixed extended landing gear on aircraft serial number 62-4506. This indicates that the additional drag of the fixed gear was sufficient to produce a nose down pitching moment at stall in the conventional configuration. However, the change in pitching moment characteristics associated with the preconversion configuration is sufficient to cancel this small static margin resulting in neutral stick free stability in the preconversion mode at stall. Third, the wing dropping tendency of aircraft serial number 62-4505 at stall with flaps deflected could be attributed to a mis-rigged flap or aileron condition since it did not occur with the flaps fully retracted.

Table 7.1 presents a summation of data available on stalls performed. Indicated angle of attack data is presented as the position error of the angle of attack indicator is unknown. Figure 7.1 presents estimated stall speeds for power on and power off conditions. Power off conditions assume zero thrust. Several flight test points have been plotted on this figure. Velocity was obtained from either the pilot callout recorded on the radio log or from the PCM and corrected for instrument and position error based on the best data available. Power setting for these points was idle.

Figure 7.7 presents a typical time history of a stall approach and resulting stall for aircraft serial number 62-4506.

TABLE 7.1
XV-5A SUMMATION OF DATA ON STALL PERFORMANCE

Information Obtained From Radio Log										PCM Data	
Flight No.	A/C Configuration	Gross Weight - Pounds	C. G. Position P. S.	XV-5A			Chase A/C		Comments	XV-5A	
				KIAS	Indicated Altitude - Feet	Indicated Angle of Attack at Stall - Degrees	KIAS	Indicated Altitude - Feet		KIAS	Indicated Angle of Attack at Stall - Degrees
Aircraft Serial Number 62-4505											
4. OF	L	11,209	242.9	106	12,000			11,800			
	L	10,980	242.4			25					
	L	9,900	240.3		11,500	25	97		Buffet at $\alpha_{ind} = 22^\circ$		
	P. A.	10,200	240.6		9,700	25/27	81.5	9,580	PLF @ 125 KIAS		
	P. A.	10,080	240.3			25	83		PLF @ 125 KIAS		
	G	10,780	243.0		11,000	24/25	100		Buffet at $\alpha_{ind} = 23^\circ$		
	G	10,650	242.7		12,100	25			Buffet at $\alpha_{ind} = 23^\circ$		
	G	9,760	240.3		10,800	27	95.5		Buffet at $\alpha_{ind} = 22^\circ$		
	CR	10,540	242.3		8,100	25/27	97		PLF @ 125 KIAS Buffet at $\alpha_{ind} = 22^\circ$		
4. OF	CR	10,400	242.0		9,700			9,550	PLF @ 125 KIAS Buffet at $\alpha_{ind} = 22^\circ$		
Aircraft Serial Number 62-4506											
5. OF	CR (Gear Extended)	9,772	240.9		15,000	25	92		PLF @ 118 KIAS Buffet at $\alpha_{ind} = 22.5^\circ$ (106 KIAS)	105.2	25.3
5. OF	G (Gear Extended)	9,772	240.8		15,000	25			Buffet at $\alpha_{ind} = 24^\circ$	103.6	4.8
6. OF	P. A. (Flaps 15°)	10,022	239.6		14,000	25			PLF @ 127 KIAS Buffet at $\alpha_{ind} = 22^\circ/23^\circ$	95.7	24.4
6. OF	P. A. (Flaps 10°)	9,937	239.4			25/26			PLF @ 122 KIAS Buffet at $\alpha_{ind} = 25^\circ$	93.0	25.3
6. OF	P. A. (Flaps 45°)	9,772	240.0			26			PLF @ 110 KIAS	90.4	24.8
7. OF	L (Flaps 45°)	10,242	239.7		15,000	26			Buffet at $\alpha_{ind} = 24^\circ$	90.4	24.8
7. OF	Preconversion mode (90% RPM _{CG})	9,992	239.4			24	78		Buffet and Nose Drop	86.7	23.9
7. OF	Preconversion mode (90% RPM _{CG})	9,992	239.4			24	78		Buffet and Nose Drop at $\alpha_{ind} = 24^\circ$	86.7	23.9
7. OF	Preconversion mode (Power off)	9,892	239.8			26			Buffet at $\alpha_{ind} = 25^\circ$	91.4	24.8

7. 1. 2 Climb

Figures 7.2 and 7.3 present the predicted values of maximum rate-of-climb and velocity for maximum rate-of-climb, respectively. Flight test points are shown on these plots along with the corresponding predicted point at the flight test weight.

The data for these points were obtained on Flight No. 21F of aircraft serial number 62-4505. This flight consisted of acceleration runs at the three noted altitudes. Data used were obtained from the flight test radio log and consisted of airspeed, altitude and fuel weight vs time as well as outside air temperature. On these runs the test aircraft was accompanied by an Air Force T-38 chase aircraft, No. 197.

The data are suspect since proper calibrations on airspeed and altitude systems were never completed. PCM was not fully operational following changeover in the system from flutter test requirements. However, the data appear to be in reasonably good agreement with predicated values.

At a 10,000 foot altitude and a gross weight of 10,400 pounds the rate-of-climb is about 6000 feet per minute. These values represent a nominal operating condition for this aircraft.

7. 1. 3 Flight Envelope

Figures 7.4, 7.5 and 7.6 present the "as flown" flight experience envelopes for various configurations. The first figure presents information pertaining to the clean configuration. The following figures pertain to various flaps down configurations with landing gear extended and one with the flaps up, gear extended. It will be noted that the preconversion configuration is one of the configurations presented.

Figure 7.4 also shows the estimated speed-altitude envelope for the 10,000 pound gross weight aircraft for comparison. The maximum power line, labeled as 102% RPM, was derived from the original engine specifications. The 102% RPM applies to the present re-rated engines as does also the point labeled 98% RPM. The respective power settings for the engine as originally rated are approximately 100% and 96%.

7.2 STABILITY AND CONTROL

7.2.1 Static Longitudinal Stability

7.2.1.1 Cruise Configuration Longitudinal Static Stability

Stick-fixed static longitudinal stability in configuration "CR" is presented in Figure 7.8. These data show "up" elevator (aft stick) is required to slow the aircraft and "down" elevator (forward stick) is required to increase speed. The low speed value of elevator effectiveness ($dC_{m}/d\delta_e$)

from flight data is .0101 as compared to the estimated value of .0106 from Reference 7.1, and the values of the neutral point are 248.7 in. from flight as compared to 252.5 in. estimated.

These data of Figure 7.8 are for the aircraft trimmed at approximately 135 KIAS, and the neutral point was determined for low C_L 's. Pilot comments indicate the aircraft to be more stable when trimmed above 140 KIAS.

Tail Buffet Problem

During Flight 2F of Aircraft 505, moderate frequency low amplitude longitudinal stick vibrations were felt by the pilot at 180 KIAS. (Later empirical investigation showed these vibrations to be 1 to 2 cps). At 192-194 KIAS there was a sharp nose down trim change and increased stick vibration. The pilot reported that he required approximately 10 to 15 pounds of aft stick force to prevent a nose-over tendency. The chase plane at this time reported visual observation of elevator buffet.

As a result, the fuselage, wing, horizontal stabilizer and elevator were tufted for airflow visualization moving pictures in flight (Figures 7.9 and 7.10). The problem appeared to be a result of flow separation at the intersection of the horizontal stabilizer and vertical tail maximum thickness points, as indicated by the chase plane.

For Flight 5F, vortex generators and turning vanes were installed to the vertical and horizontal stabilizer (Figure 7.11). This particular pattern of generators did not appear to effect any change, so the pattern was altered for the next flight. That change only increased the speed at which the trim change and buffet occurred to 215 KIAS.

Investigations were continued for the next two flights, with revised vortex generators and in different aircraft configurations, with no different effects experienced. Before Flight 9F, all vortex generators were removed and an

aft tail fairing was added (Reference W. O. 505-173). Absence of stick shake was noted by the pilot above 160 KIAS and only in a right sideslip condition ($\beta = 3^\circ$ to 5°) at 220 KIAS did a pitch trim change occur. There was no buffet in straight and level flight up to 235 Kn.

Before Flight 12F, vortex generators in the previous optimum pattern were installed, along with tufts on the lower surface of the horizontal stabilizer and both sides of the vertical. This time the buffet occurred at 200 KIAS at 25,000 foot altitude in 1° right sideslip or 2° angle of attack, with nose-over at 210 KIAS. At 10,000 feet, where the problem was encountered originally, no buffet was induced flying straight and level at 200 KIAS, but a 6° left sideslip would start buffet (at 25,000 feet, 215 knots, 3° left sideslip started stick shake).

Then, prior to Flight 13F, the vortex generators were removed from the vertical and the forward tail cone fairing was installed (Reference 7.2.) Buffet inducement could no longer be accomplished after this alteration; the problem was solved. The vehicle has since been flown at 406 KIAS at 8,000 feet (456 Knots TAS) with no buffet.

Aircraft 506 was not tested in this aforementioned buffet speed regime until Flight 43F, at which time stick vibration was noted at 175 KIAS. Aircraft vibration increased at 192 KIAS, but no nose tuck occurred. No more investigations were made with this aircraft, and prior to Flight 78F, the forward and aft tail fairings were added. The aforementioned asymmetry problem of inducing buffet by sideslip in one direction and not the other, was not evident with Aircraft 506. Further discussion of the sideslip trim problem is contained in Paragraph 7.2.5.5.

Due to the malfunctions and uncertainties inherent in the stick force instrumentation, data were not available for determination of the stick-free neutral point.

However, on the basis of pilot comments during and after flight tests, it was determined that the stick-free neutral point was very close to the stick-fixed neutral point, 248.7 inches F.S., cruise configuration.

7.2.1.2 Landing Configuration Longitudinal Static Stability

The data of Figure 7.12 shows the stick-fixed neutral point for configuration "PA" to be at F.S. 254.3 for lift coefficients between 0.5 and 0.8. These same data show the neutral point to be at 241.8 in. for lift coefficients approaching the stall. The aforementioned data was obtained with the aircraft trimmed near 120 KIAS

Pilot comments during stall approaches with the center of gravity near F. S. 241.5 indicate the stick-fixed stability to be neutral to unstable at the stall for all flap deflections tested. The stability becomes more marginal at the stall as the flap deflection is increased.

Nose Wheel Shimmy

On 8 April 1964, during the taxi tests of Aircraft 506, violent nose wheel shimmy began without notice at 40 Kn. The nose wheel dampers were inspected and made ready for another test after consulting the damper manufacturer and re-adjusting dampers. On 25 April 1964, another taxi was made, and the shimmy occurred at 42 Kn, although not as violently as before. As the aircraft was being slowed, the nose gear collapsed at 20 Kn, causing damage to the underside of the nose and breakage of the nose boom. There were no injuries suffered by the pilot.

Following repair of the fuselage and boom, and with modified dampers installed, the aircraft was taxied up to speeds of 95 Kn with no shimmy of the wheel (26 May 1964). For structural details relating to these incidents, see Paragraph 7.4.5. Final accident report is published as Reference 9.2.

7.2.1.3 Pre-Conversion Configuration Static Longitudinal Stability

The variation of horizontal tail trim settings with airspeed shown in Figure 7.13, and pilot comments, indicate the static longitudinal stability in the pre-conversion configuration to have a stick-free neutral point at approximately 241.5 inches F. S. The stick fixed neutral point will be slightly aft of the stick-free. This condition, according to the pilot, agrees with the flaps down data for the aircraft at high lift coefficients with fan louvers and nose fan doors closed.

Pilot comments on stall approaches in the pre-conversion configuration indicate the control to be satisfactory with the stall and stall recovery technique the same as with fan closures closed. A typical stall approach time history is presented in Appendix Figures A-54 and A-55.

In addition, the pilot reports that for the same speed condition, the aircraft in the pre-conversion configurations feels more stable than with fan closures closed.

Trim change incurred in going from fan closures closed to the pre-conversion configuration in the vicinity of 120 KIAS is $\Delta \delta_e = -2.8^\circ$ and the pilot reports small stick forces. It should be pointed out that the airplane is trimmable with full flaps in the pre-conversion configuration where full flaps cannot be trimmed with closures closed.

7.2.2 Static Lateral-Directional Stability

7.2.2.1 Cruise Configuration Lateral-Directional Static Stability

Stick-fixed static lateral-directional stability is positive for all centers of gravity and speeds tested. Representative plots are presented in Figures 7.14 and 7.15. These data, and comments by the pilot, indicate proper relation of aileron, roll attitude and rudder deflection with sideslip angle. Comparison of $d\beta/d\delta_r$ in flight with that estimated (Reference 7.1) is discussed in Paragraph 7.2.5.4. In Configuration "CK" (with fixed gear) the pilot reports a tendency for the down-wind wing to stall at $\beta = 9^\circ$, but this was corrected by releasing the rudder.

7.2.2.2 Landing Configuration Lateral-Directional Static Stability

The stick-fixed lateral-directional static stability in configurations "L" and "PA" are presented on Figures 7.15 and 7.16. Here again, the data, plus pilot comments, indicate positive stability at all times. The flight test and estimated values of $d\beta/d\delta_r$ for these configurations are discussed in Paragraph 7.2.5.4. The zero sideslip trim problems encountered on takeoff during the program is discussed in Paragraph 7.2.5.5.

7.2.2.3 Static Lateral-Directional Stability - Pre-Conversion Configuration

Static lateral-directional stability in the pre-conversion configuration shown in Figure 7.17 indicates $d\beta/d\delta_r$ to be the same as that for the aircraft with fan inlet louvers and nose fan control doors closed.

Pilot comments indicate the control coordination and force characteristics in steady state sideslips to be good at all speeds tested.

7.2.2.4 Stick-Free Static Lateral-Directional Stability

Pilot comments indicate the stick-free stability is positive for all configurations and conditions tested.

7.2.3 Dynamic Longitudinal Stability

7.2.3.1 Cruise Configuration - Dynamic Longitudinal Stability

Typical time histories showing the dynamic longitudinal stability of the XV-5A are presented as Figures A-56 through A-73. These data and pilot comments show positive damping through the speed range with increasing stick force for stick deflection as the speed is increased.

Found in the Appendix are Figures A-56 through A-58 which show existence of a stick-free long period oscillation (phugoid) of some 50 seconds period with essentially neutral damping. Characteristics of short period damping are summarized in Figure 7.18 for several test airspeeds and altitudes. The data indicate a slight increase in period with increasing altitude but heavily damped oscillations for all test conditions with approximately .70 cycles required to half amplitude. Tests conducted between flight speeds of 130 and 150 KIAS at 12,000 feet altitude showed dead-beat damping to 1/2 amplitude in approximately 1.25 seconds.

7.2.3.2 Landing Configuration - Dynamic Longitudinal Stability

Pilot comments indicate positive damping in configurations "PA" and "L" with the oscillations damping practically dead-beat. A time history of stick hits in configuration "PA" at 130 KIAS is presented in Appendix Figure A-74 which illustrates the foregoing statement.

7.2.3.3 Pre-Conversion Configuration - Dynamic Longitudinal Stability

According to the pilot, the dynamic longitudinal stability in the pre-conversion configuration shows positive damping through the speed range tested. In fact, at 116 KIAS the airplane oscillations were dead-beat in the short period mode, with the pilot saying it was difficult to get the airplane to respond to the stick hit impulses. Typical time histories of a stick hit (short period oscillation) at 116 KIAS and a stick release at 100 KIAS are presented on Figures A-75 through A-80. The long period oscillation damps after some time due to the static stability being marginal according to the pilot, but the data of Figures A-77 through A-80 shows good damping.

7.2.4 Dynamic Lateral-Directional Stability

7.2.4.1 Cruise Configuration Dynamic Lateral-Directional Stability

Aileron-rudder "S" turns of Figures A-81 through A-84 show that the coordination of controls for these maneuvers are in the right direction with control forces, from pilot comments, being nominal with "feel" in the proper sense. The adverse yaw in the aileron turns is indicated to be small by the pilot.

Dynamic lateral-directional stability plots are presented in Figures A-85 through A-109 for control releases from developed steady state sideslips and in Figures A-110 through A-131 for aileron and rudder control impulses.

These data, and pilot comments, indicate positive damping of the short period oscillation through the speed range for the rudder-fixed condition. The rudder-free dynamic stability for the original rudder configuration was marginal to unstable above 300 knots with a low amplitude residual oscillation. A "T" strip was added to the rudder and rudder tab trailing edge as illustrated in Figure 7.19. This modification made the aircraft stable rudder-free to the highest speed tested (406 KIAS).

Characteristics of the lateral-directional short period oscillation are shown in Figure 7.20. No significant effect of altitude on the period is indicated while the period is shown to decrease with increasing flight speed. Damping to half amplitude occurs in 1.25 cycles or less for all test conditions except for rudder-free with the original rudder configuration. Addition of the rudder "T" improves the rudder-free stability to the level of rudder-fixed stability.

Short period damping is shown in Figure 7.21 with relation to the rolling parameter based on indicated airspeed. The ratio of roll to sideslip, ϕ/β , was difficult to determine accurately due to low amplitudes and random data scatter, but satisfactory damping is indicated except for the rudder-free condition. Again, the rudder "T" is shown to provide satisfactory rudder-free stability.

Rate of roll, as measured in the bank-to-bank rolls, has a satisfactory variation with speed and the pilot indicates the stick forces to be within specification limits. Time histories of typical roll maneuvers at 150 KIAS in Configuration "CR" are presented on Figures A-132 through A-139 for rudder locked and coordinated. These data show good response to control deflection, with the adverse yaw buildup within allowable limits and an estimated peak rate of roll of 90 deg./sec.

7.2.4.2 Landing Configuration Dynamic Lateral-Directional Stability

A time history at 130 KIAS of a sideslip with rudder release in Configuration "L" is presented on Figures 7.22 through 7.25 and Figures 7.26 and 7.27 present the same maneuver in Configuration "PA". The data indicate 1-1/2 to 2 cycles to completely damp in Configuration "L" and practically dead-beat in Configuration "PA". The pilot's comments during these flights were that the directional oscillations were highly damped with some nose down trim change as the sideslip angle was increased.

Roll maneuvers at 130 KIAS in Configuration "PA" are presented in Figures 7.28 through 7.35 for both a locked and coordinated rudder. These data indicate a favorable yaw angle of 10° for rudder locked with

a peak roll rate of about 30 deg./sec. The coordinated maneuver halves the favorable yaw but doubles the peak roll rate.

7.2.4.3 Pre-Conversion - Dynamic Lateral-Directional Stability

Representative plots showing the dynamic lateral-directional stability in the preconversion configuration are shown in Figures 7.36 through 7.39. These data indicate the short period oscillation damps to half amplitude in 1 to 1-1/4 cycles, when lateral and directional control force impulses are applied. The pilot reports the airplane has good damping. The pilot also estimated cycles to damp that agree with the data.

Bank-to-bank rolls (15° to 15°) with 3/4-stick throw at 100 KIAS in the pre-conversion mode are presented in Figures 7.40 and 7.41 and show an average peak roll rate of 32 deg./sec. and an adverse sideslip angle buildup of 10° . The response of the airplane to the control input is very good. The roll attitude instrumentation was unreliable for this flight. Pilot comment in regard to the aforementioned rolls was that adverse yaw was small.

7.2.5 Control Effectiveness

7.2.5.1 Taxi Control

Taxi control information consists only of pilot comments both during and after flights. In general, the pilot reported excellent stability during both high and low speed taxi runs. The stiff nose wheel damping gave good longitudinal stability and the pilot reported no divergent directional oscillatory motions.

There was no nose wheel steering and the aircraft used more than average amount of differential braking for maneuverability. Caution had to be exercised in using the brakes, as excessive braking caused brake overheating and fade.

This fade and overheat problem was primarily due to the residual thrust produced by the engines at idle power acting against the brakes. There was enough residual thrust in the idle power position to propel the vehicle at ground speeds up to 50 knots in a no-wind situation. Brake effectiveness was considered marginal but satisfactory in terms of the uses that were intended for the aircraft, i. e., a VTOL flight research vehicle.

Thrust spoiler utilization to aid in decelerating the vehicle after landing or high speed taxi was initiated about half-way through the test program on Aircraft 506. The pilot reported excellent results, the airplane was easier to slow, and the brakes remained much cooler. The spoilers have to be used on any long or high speed taxi runs, to avoid rapid deterioration of the brakes, with the optimum procedure reported to be intermittent modulation of the spoilers to control desired maneuvering speed, with the brakes applied only as necessary.

Both aircraft used thrust diversion for braking, although the spoilers were never used while either vehicle was airborne.

Cross-wind taxi control was reported satisfactory, but with a downwind (unstable) weather-cocking tendency present in the aircraft at speeds less than 20K. This tendency was more severe with the landing gear in the VTOL position, but was not uncontrollable, even in a 20 knot cross-wind. Relatively on-course taxi was accomplished in a cross-wind through the intermittent application of brakes and the use of rudder controls. Rudder deflection alone was sufficient to maintain directional control at speed as low as 20 knots in near still air conditions.

7.2.5.2 Longitudinal Control

Longitudinal control throughout a conventional takeoff was more than adequate and the pilot reported light stick forces. Figures A-140 to A-143 show time histories of a takeoff and indicate the nose wheel lift-off speed is approximately 100 KIAS with -5° stabilizer and -13° elevator and appears to be independent of flap deflection. Pilot indicated with full flaps at most forward C.G., nose wheel lift-off speed is increased 10 knots. Longitudinal control in gusts during takeoff is considered good by the pilot.

The time history of a typical landing with 15° flaps deflection, (Figures A-144 through A-147, indicates the longitudinal control in the presence of the ground to be satisfactory. The pilot reports no control problems in still or gusty air, with light stick forces required during the landing maneuver for all flap deflections tested.

During the flight program, it became evident that the nose-up trim required for full flaps (45°) was more than the stabilizer could handle and 25° flaps was chosen as the landing flap setting.

7.2.5.3 Longitudinal Trim

High speed trim to 400 KIAS is shown in Figure 7.42 and indicates no trim problem was encountered to the maximum speed attained with the aircraft. The elevator angle shown on the subject figure is the free floating angle of the surface. The pilot made the comment that trim to zero stick force is difficult due to the high effectiveness of the surface and the high rate of horizontal tail actuation. Another cause of trim difficulty might be actuator overrun. The trim sensitivity problem can be solved by slowing the horizontal tail surface actuation rate and decreasing the actuator overrun.

The effect of airplane configuration changes on trim are shown in the following table. The figure noted in the aforementioned table presents the transients that occur during the time change. The effect of gear can be obtained from pilot comments only.

<u>TRIM CONDITION</u>	<u>CHANGE</u>	<u>HOLD</u>	<u>REMARKS</u>	<u>FIGURE</u>
Flaps 30° , $V = 140$ KIAS	Flaps to 0°	R/C	$\Delta \delta_e = 5.0^\circ$	A-148
Flaps 45° , Level Flight Power	Max. Power	$H_i = \text{Constant}$	$\Delta \delta_e = 4.5^\circ$	A-149
Flaps 45° , Level Flight Power	Power to Idle	$V_i = \text{Constant}$	$\Delta \delta_e = 2.0^\circ$	A-150
Flaps 0° , $H_i = 10,000$ Ft.	Flaps to 45°	$H_i = \text{Constant}$	$\Delta \delta_e = 5.0^\circ$	A-151
Gear Up, $v = 120$ KIAS	Gear Down	$H_i = \text{Constant}$	Slight Nose Down Trim Change	
Gear Down, $v = 130$ KIAS	Gear Up	$H_i = \text{Constant}$	Slight Nose Up Trim Change	

The stick forces associated with the aforementioned trim changes were reported by the pilot as "not excessive". The only other comment concerning trim was the fact that there was insufficient stabilizer angle to trim out the flaps 45° condition.

7.2.5.4 Lateral-Directional Control

Figures 7.43 and 7.44 present $d\beta/d\delta_r$ for both the clean and landing configurations. For the clean configuration, Figure 7.43 shows the aircraft to be 25% better than the estimate from Reference 7.1. Flight data for this condition was derived from both "CR" and "G" configurations, with the assumption that power effects were negligible.

Figure 7.44 shows that the landing configuration of the actual flight article is 30-35% above the estimate. The aforementioned negligible power effect assumption was applied to flight data here also, since both "PA." and "L" configuration data were used to determine $d\beta/d\delta_r$.

The pilot reports that landings where cross-winds were up to 20 knots at 90° to the flight path were encountered, the aircraft heading could be maintained easily with the rudder alone. Further discussion of cross-wind control is contained in Section 7.2.5.1.

7.2.5.5 Zero Sideslip Trim Problem

Early in the flight test program, the pilot reported that during the early portion of Flight 4F in Aircraft 506, it was necessary to incorporate directional trim to eliminate a positive rolling moment indication, and that the aircraft assumed a slight left sideslip with zero directional trim.

This characteristic continued to exist and during Flight 25F, in the same aircraft, lateral-directional out-of-trim conditions were reported during climb-out, with a tendency for the craft to roll to the left. Yaw and roll indicators were centered prior to the flight and although initially a large amount of right roll trim was used, it did not appear to solve the problem. Then two to three degrees of right rudder were trimmed in, which eliminated the left roll.

During climb-out at the start of Flight 27F, a right roll tendency was again reported, with two degrees of left rudder trim required to correct the condition.

On the next flight, 28F, it was determined that the left wing appeared to produce more lift than the right as the aircraft required full left aileron

trim and two degrees of left rudder trim to fly balanced at 120 knots with full flaps. Slightly less aileron trim was reported required at the same speed, flaps up. The roll characteristic was thus attributed to the differential wing lift condition.

Later flights at higher speeds, 78F, revealed the right wing down out of trim condition tended to increase slightly as airspeed increased.

Several factors, it must be concluded, could be attributing to this out-of-trim condition. Already mentioned, the slightly higher lift on the left wing could cause the roll; mis-alignment of the vertical tail in manufacture might be a contributor. The problem was not satisfactorily resolved during the test program due to urgency of other matters. The problem was not considered serious enough to warrant special investigations.

7.2.6 Control Power

7.2.6.1 Longitudinal Control Power

Although no specific tests were made to investigate in detail the area of longitudinal control power, pilot comments indicate no problems in this area. In some cases, the stick forces were said to be somewhat excessive, but they were well within the margins termed necessary for safety reasons, so that no barriers were constructed against completion of the flight test program.

7.2.6.2 Directional Control Power

During this flight test program, specific tests to evaluate directional control power were not conducted. However, the pilot reports and PCM data generated during the execution of various directional maneuvers revealed no objectionable control power conditions in conventional operation.

7.2.6.3 Lateral Control Power

Maneuvers requiring lateral control power were performed during the program, but no specific flights were made for the express purpose of lateral control power evaluation. Pilot comments and data derived from rudder S-turns, bank-to-bank rolls, spiral turns, etc., indicated no objectionable areas in that flight regime. Thus it appears that lateral control power conventionally is more than adequate.

7.2.7 Miscellaneous

7.2.7.1 Dynamic Response

Aircraft response to control inputs is covered in Paragraphs 7.2.3 and 7.2.4, and will not be discussed here. The dynamic response of the control system itself was dead-beat in all cases, with the exception of the rudder, throughout the program. In the case of the rudder, a low amplitude residual oscillation was encountered during testing in high speed conventional flight. Further investigation fixed upon the addition of a "T" strip on the rudder as the solution to the problem, and thereafter rudder response was also dead-beat.

7.2.7.2 Control Dynamics

Data available on longitudinal stability is very meager due to instrumentation malfunctions. The data available is presented as time histories on Figures A-152 through A-166 for configuration "CR" at about 220 KIAS and in configuration "L" and "PA" at about 130 KIAS and shows $d\delta_e/dg$ to be positive. Pilot comments indicate that the stick force per g increases with speed and becomes excessive for an operational aircraft but is considered satisfactory for a load limited research aircraft.

7.2.7.3 Control Harmony

Control harmony was not an area in which specified quantitative testing was conducted for evaluation. However, through discussion with the pilot during and after such maneuvers as S-turns and spiral turns, it was concluded that control in all areas was satisfactory for a research vehicle.

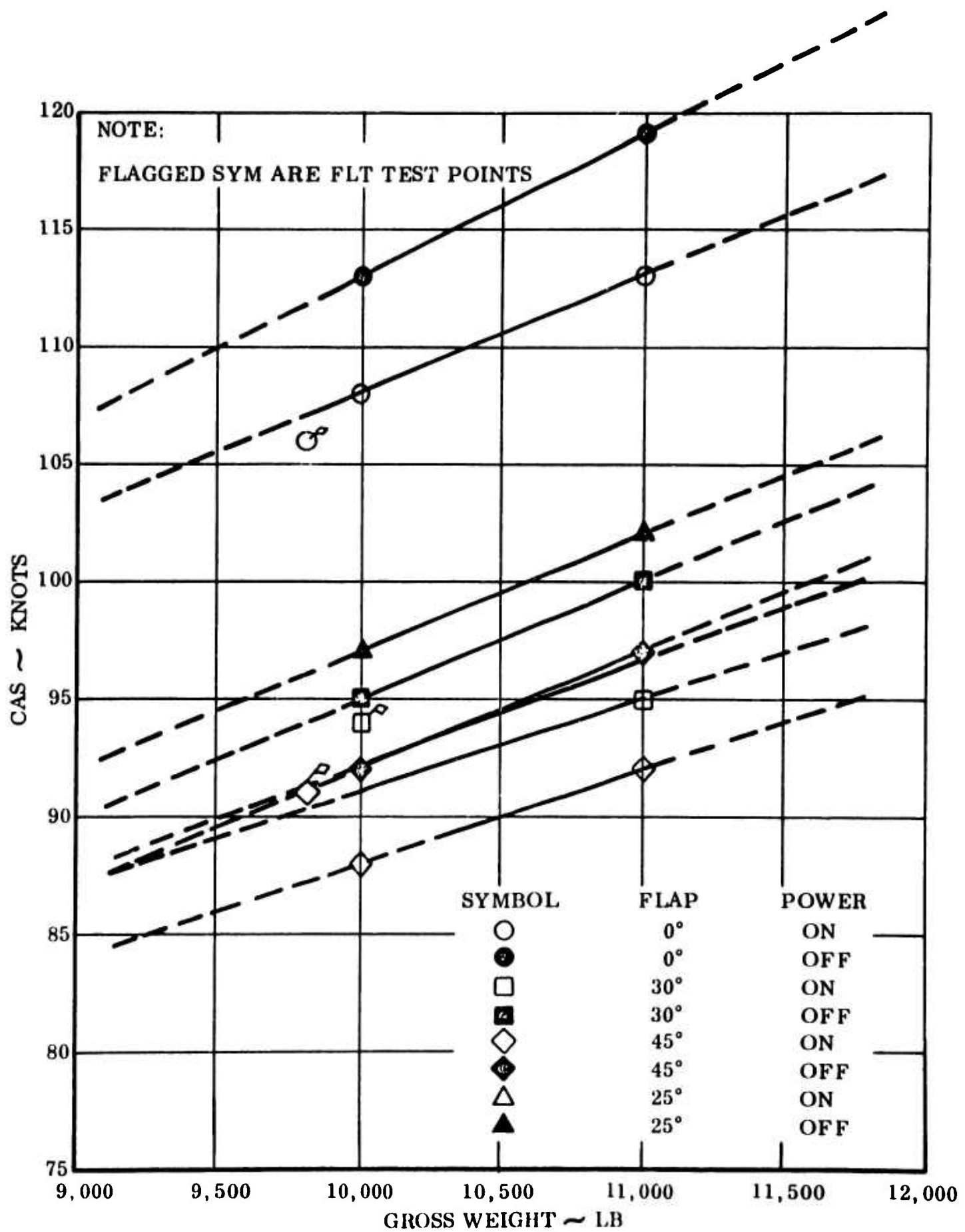


Figure 7.1 Estimated Stall Speeds for Power-on and Power-off

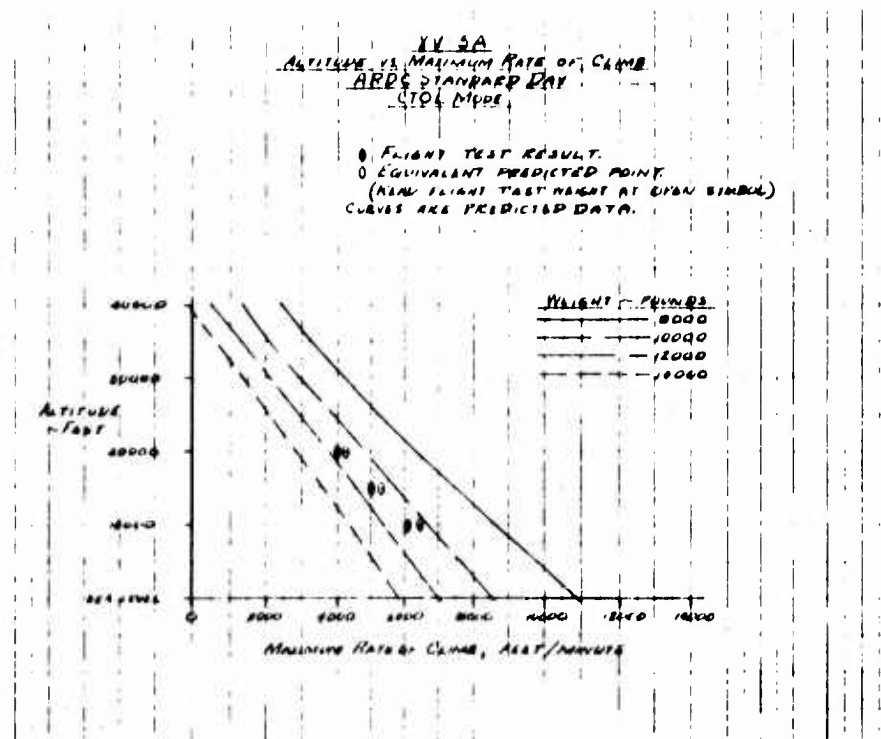


Figure 7.2 Altitude vs Maximum Rate of Climb

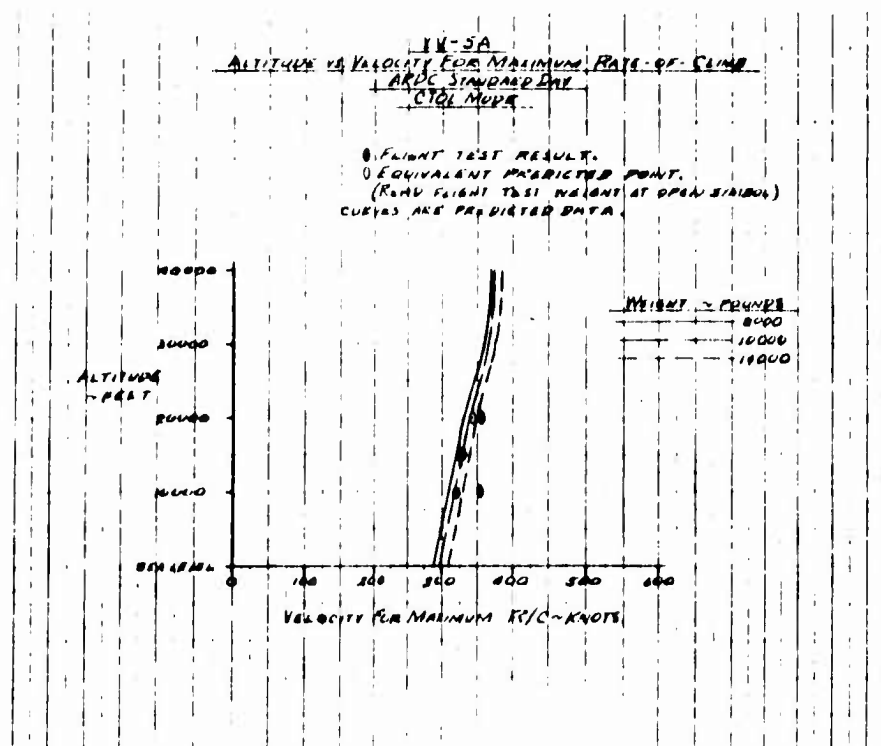


Figure 7.3 Altitude vs Velocity for Maximum Rate of Climb

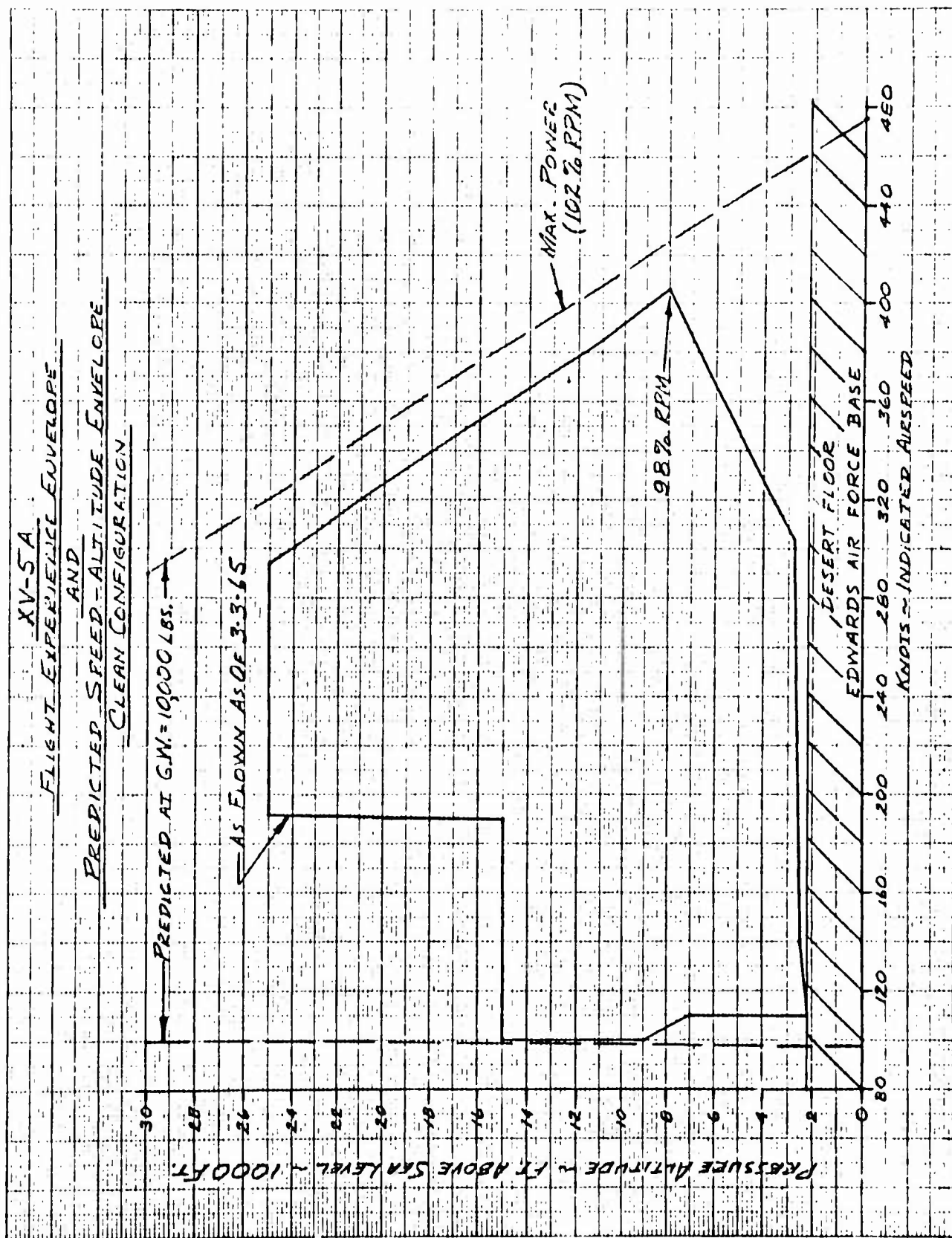


Figure 7.4 Flight Experience Envelope and Predicted Speed-Altitude Envelope

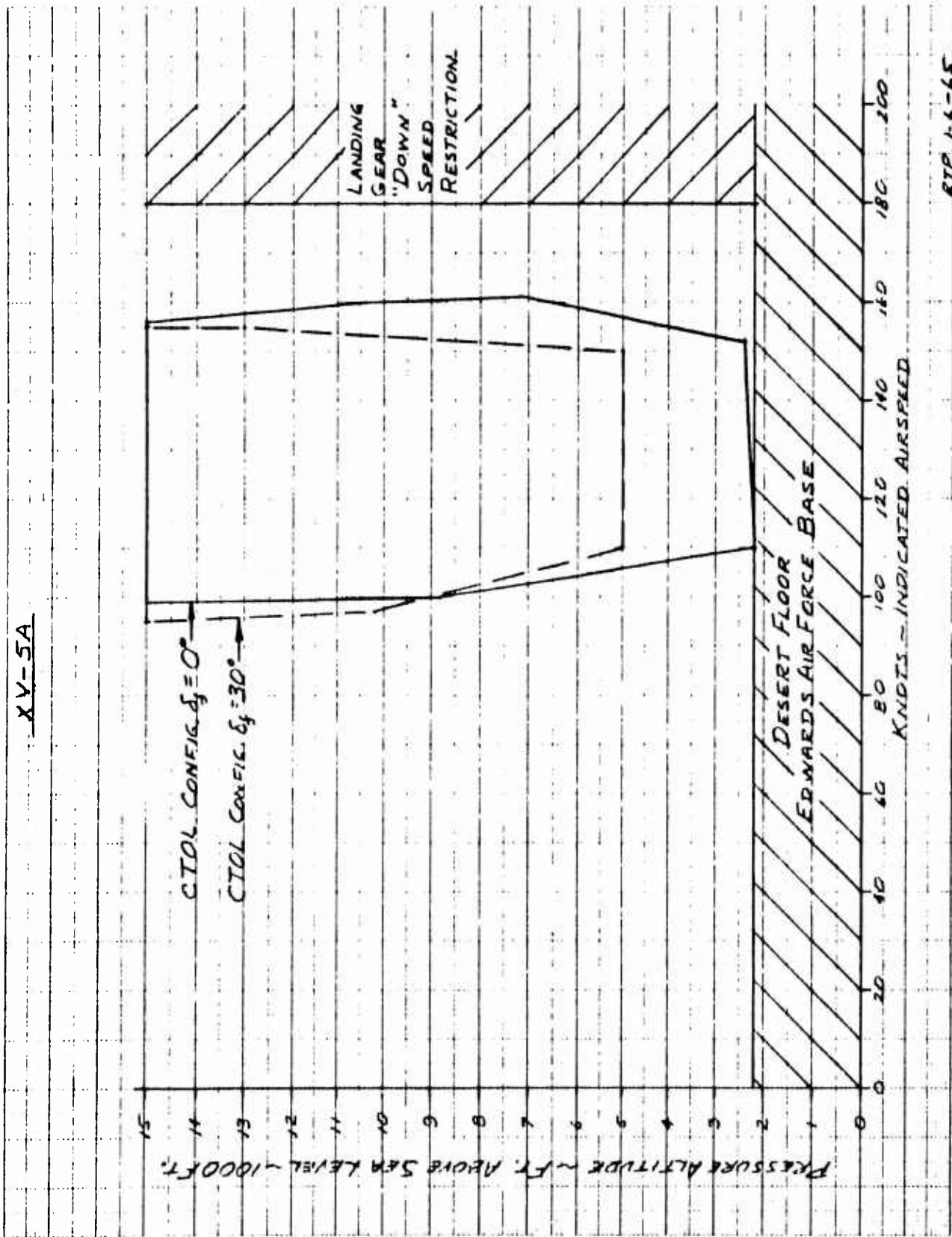


Figure 7.5 As-Flown Flight Envelope

XV-5A
"AS FLOWN" FLIGHT ENVELOPE

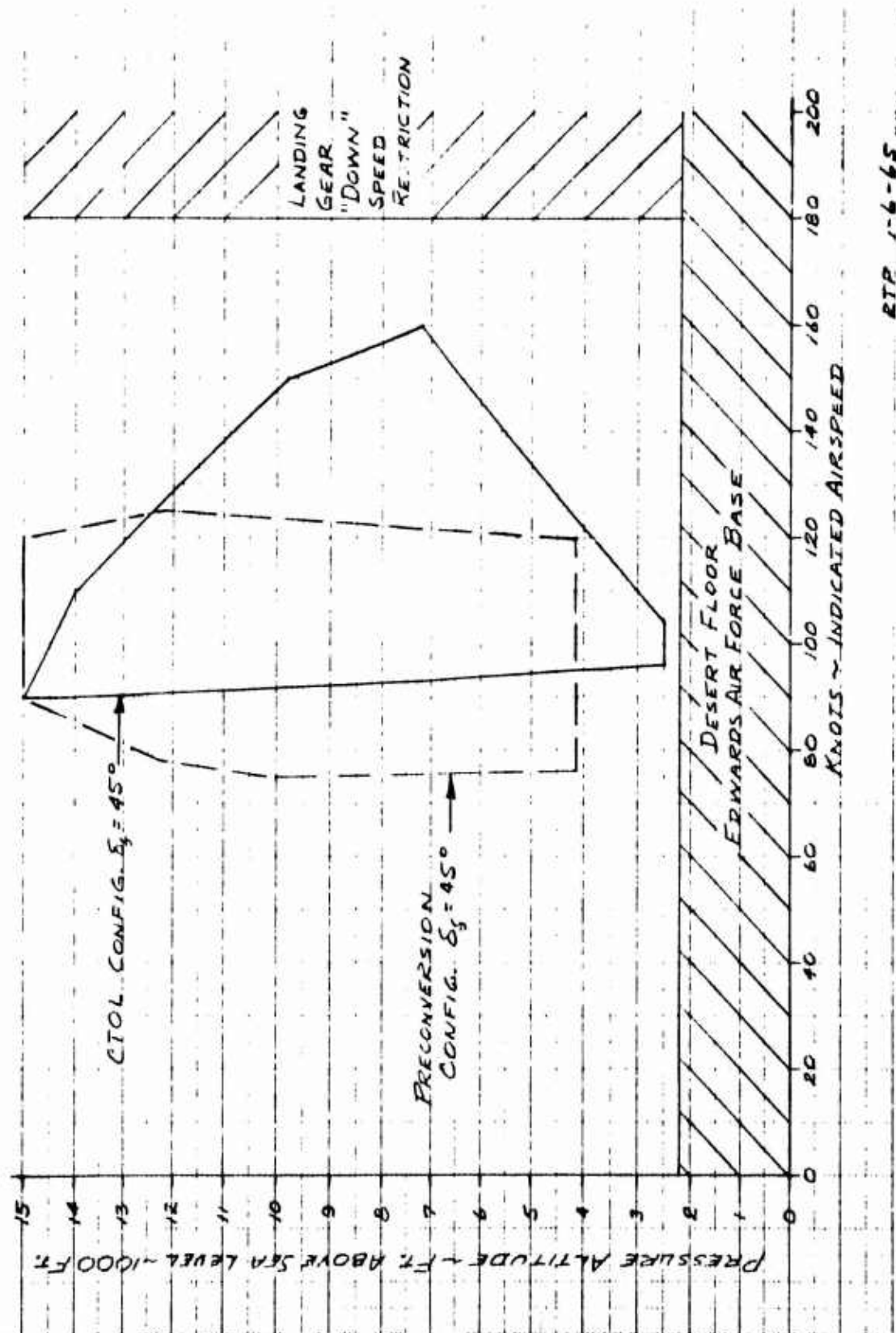


Figure 7.6 As-Flown Flight Envelope

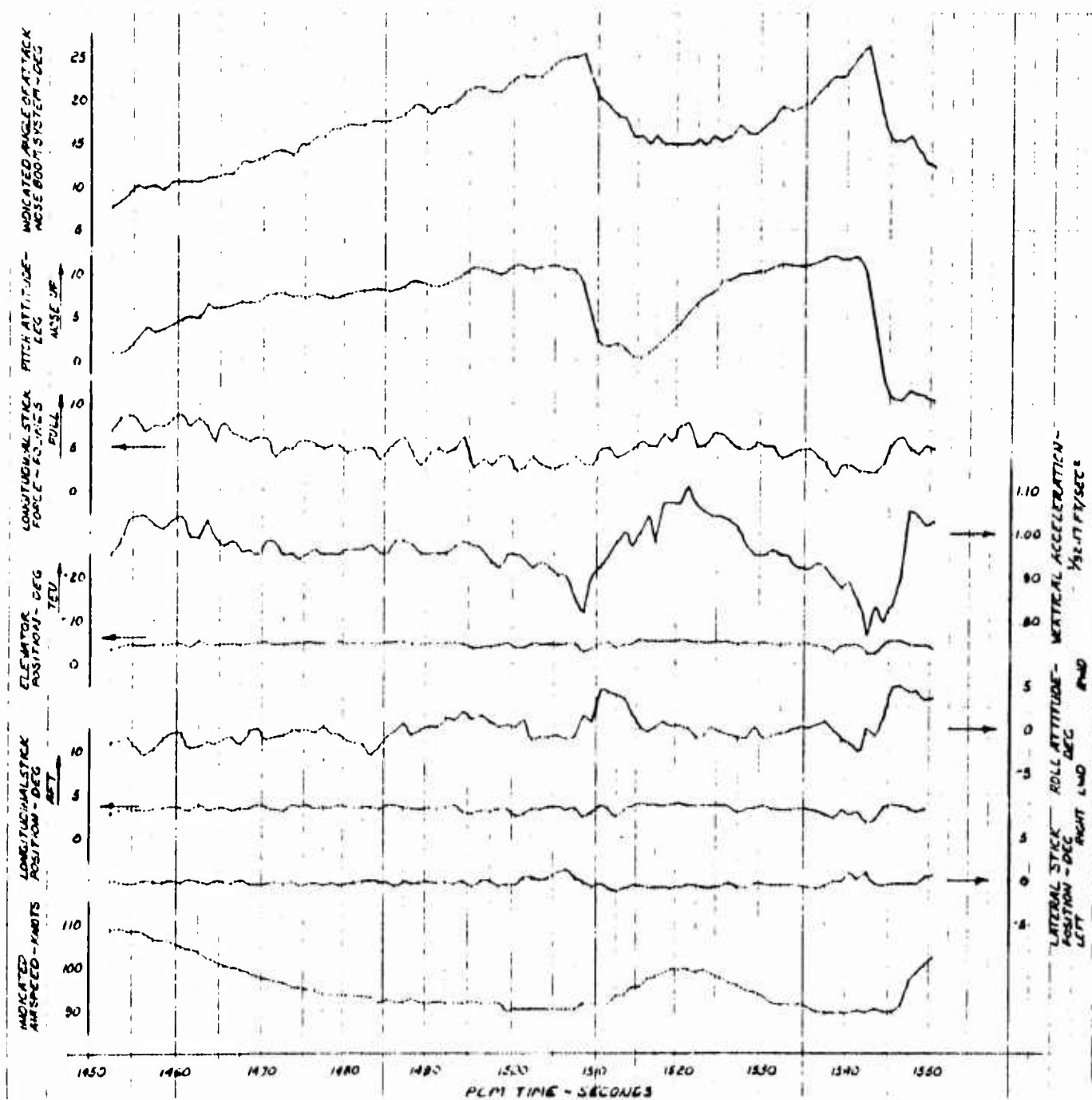


Figure 7.7 Time History - Stall Approach and Stall

RYAN XV-5A
STATIC LONGITUDINAL STABILITY
 CONFIGURATION "CR"

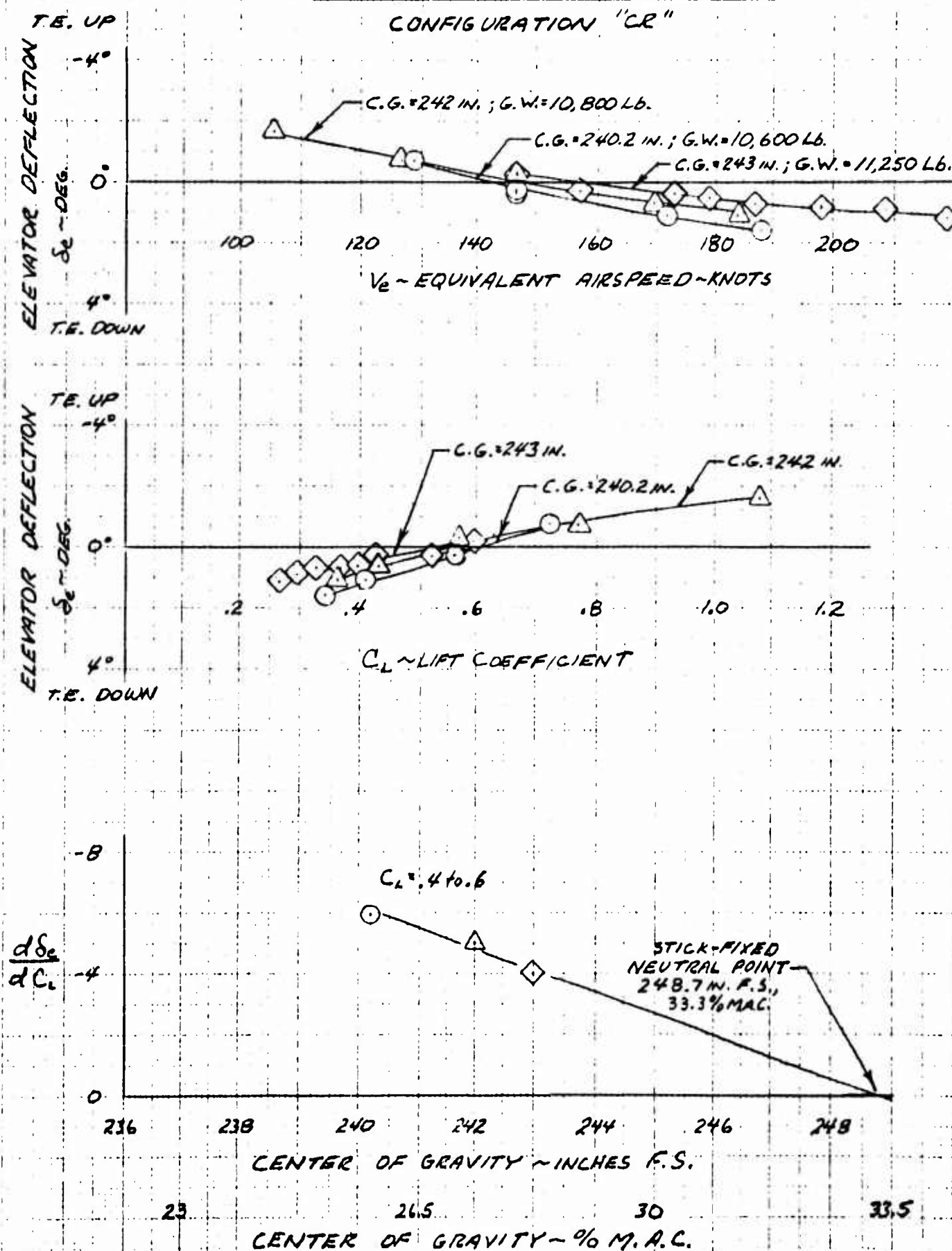


Figure 7.8 Static Longitudinal Stability - Configuration CR



Figure 7.9 Photograph of Tufted XV-5A



Figure 7.10 Photograph of Tufted XV-5A

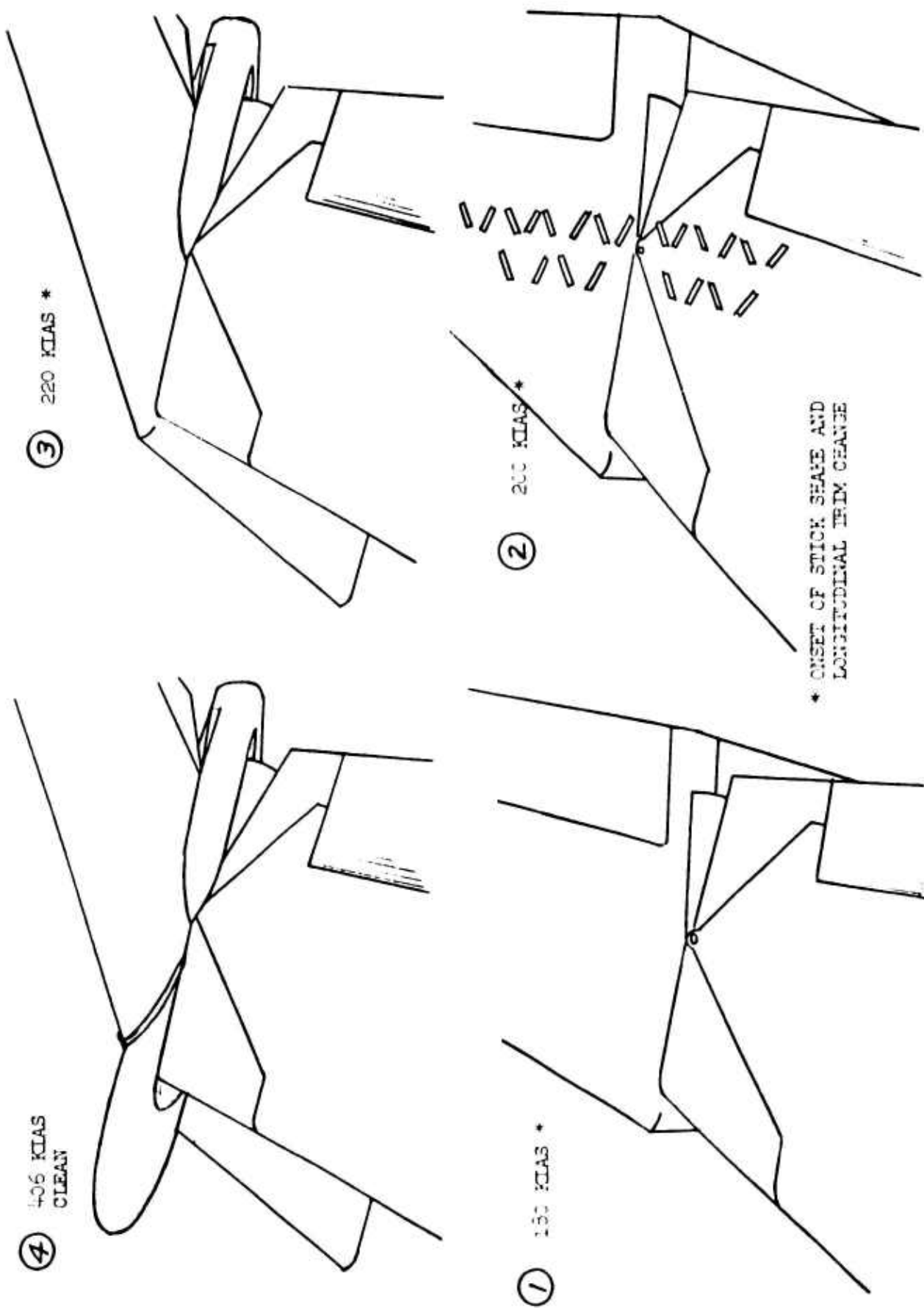


Figure 7.11 Tail Buffet Problem

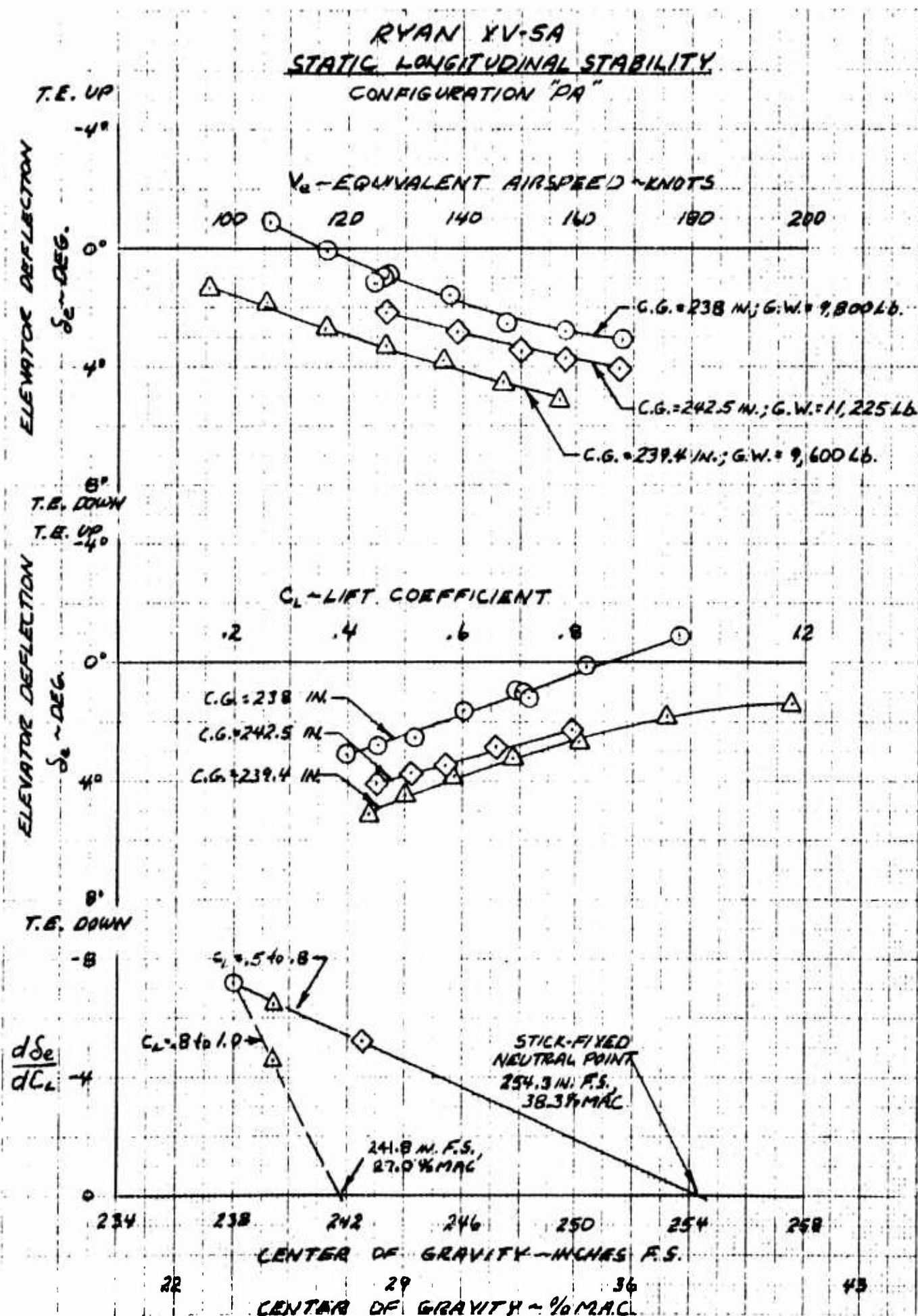


Figure 7.12 Static Longitudinal Stability - Configuration PA

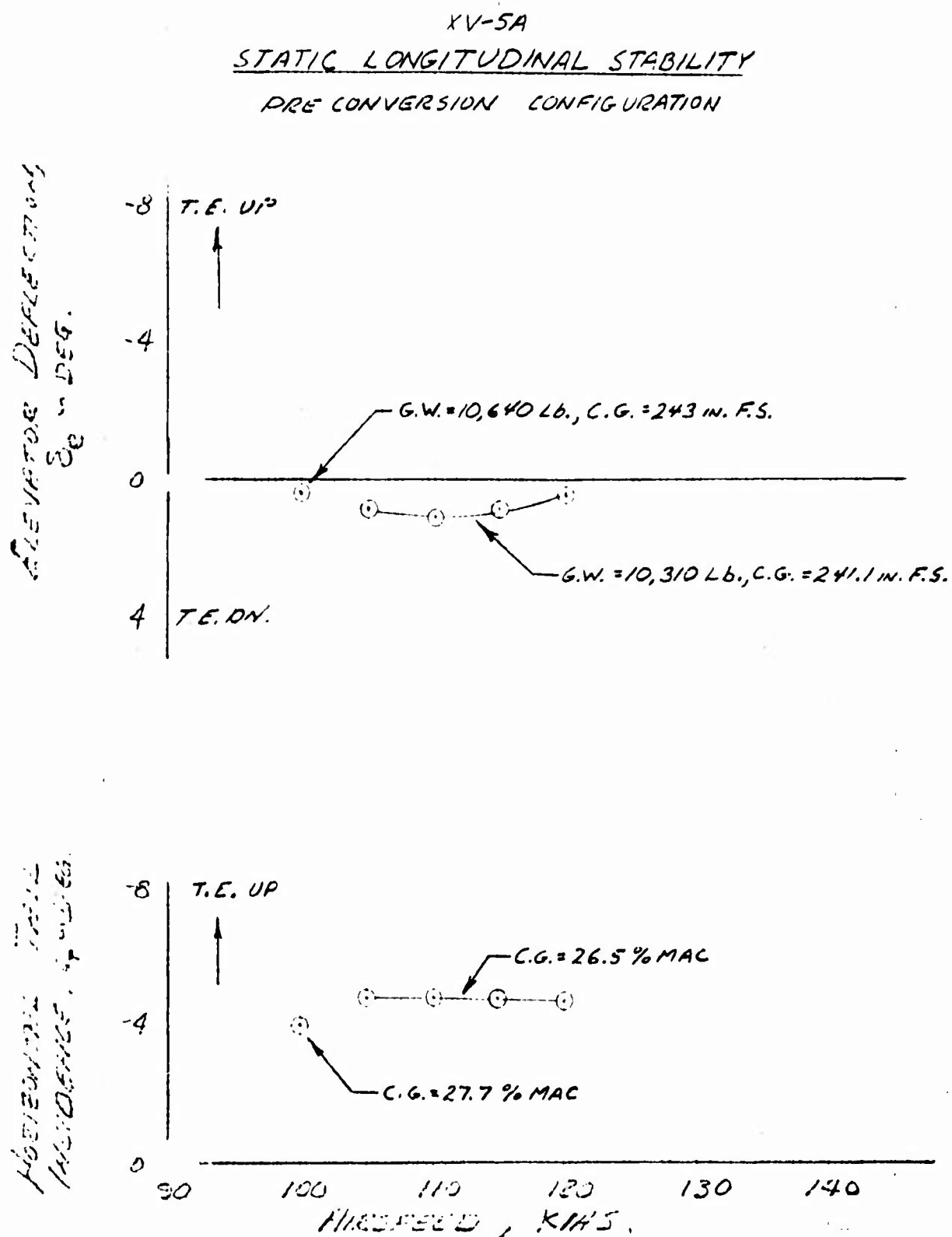


Figure 7.13 Static Longitudinal Stability - Preconversion Configuration

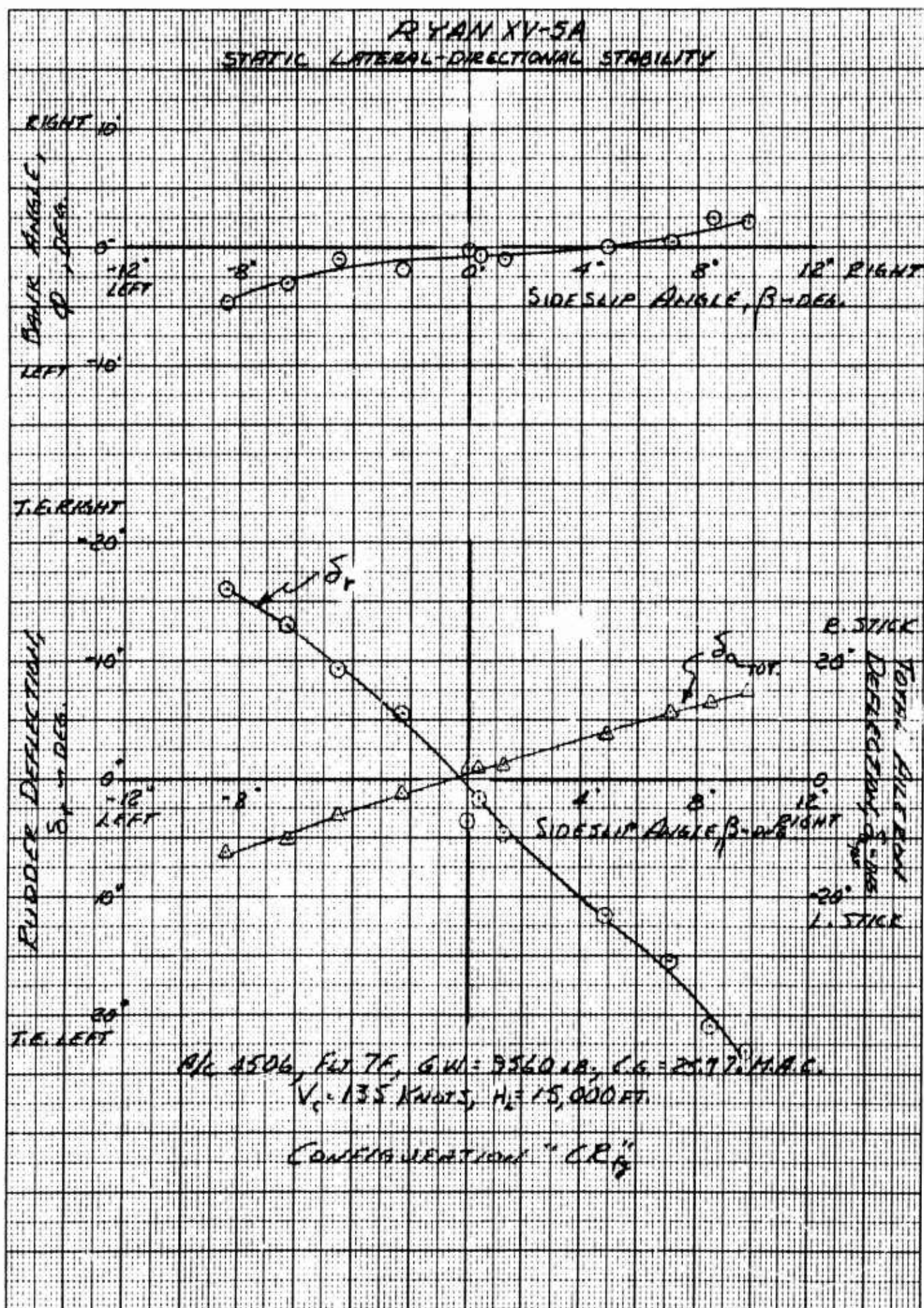


Figure 7.14 Static Lateral-Directional Stability

RYAN XV-5A
STATIC LATERAL-DIRECTIONAL STABILITY
 AVERAGE GROSS WEIGHT = 10,750 LB. ALTITUDE = 12,000 FT.

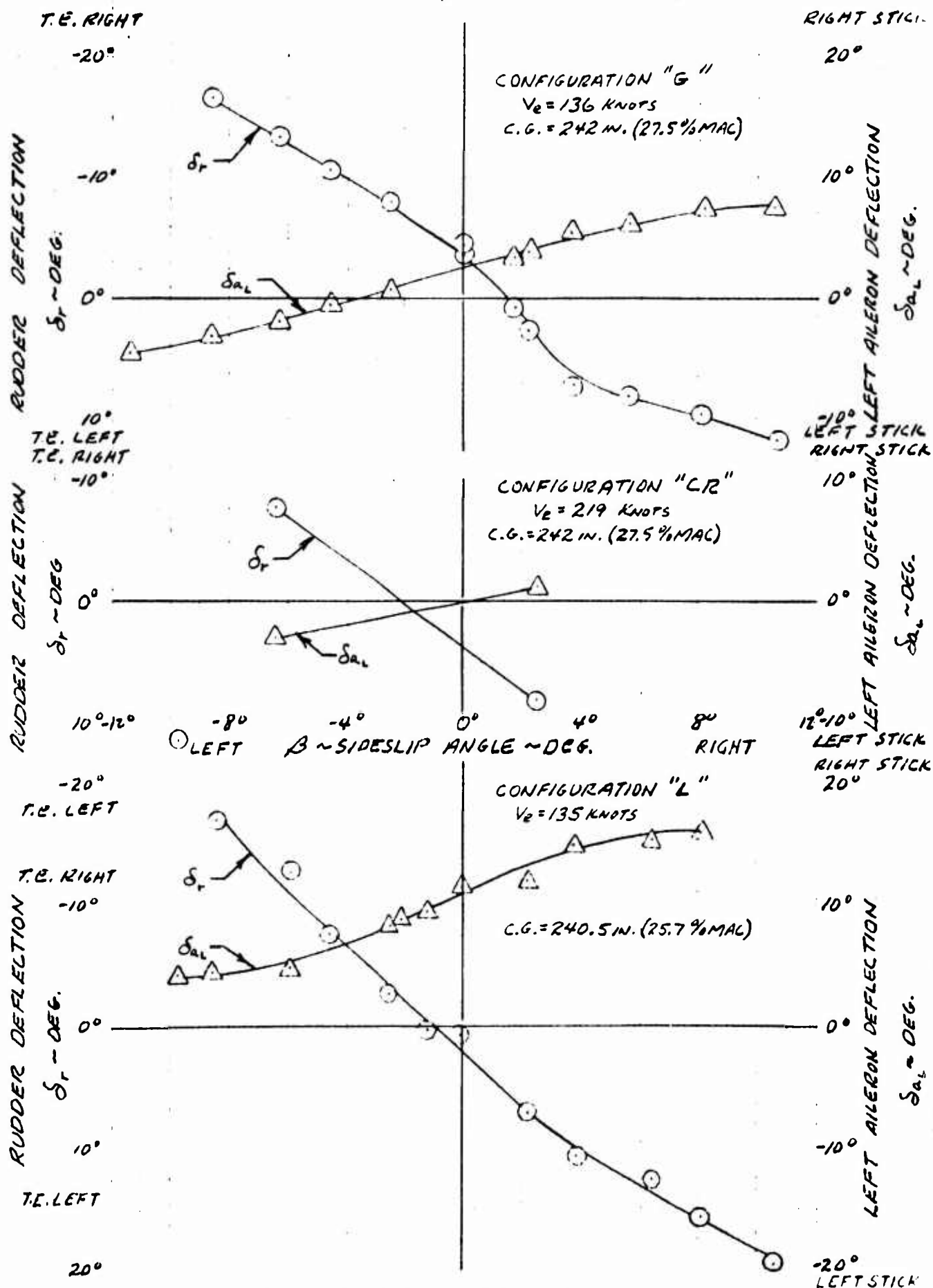
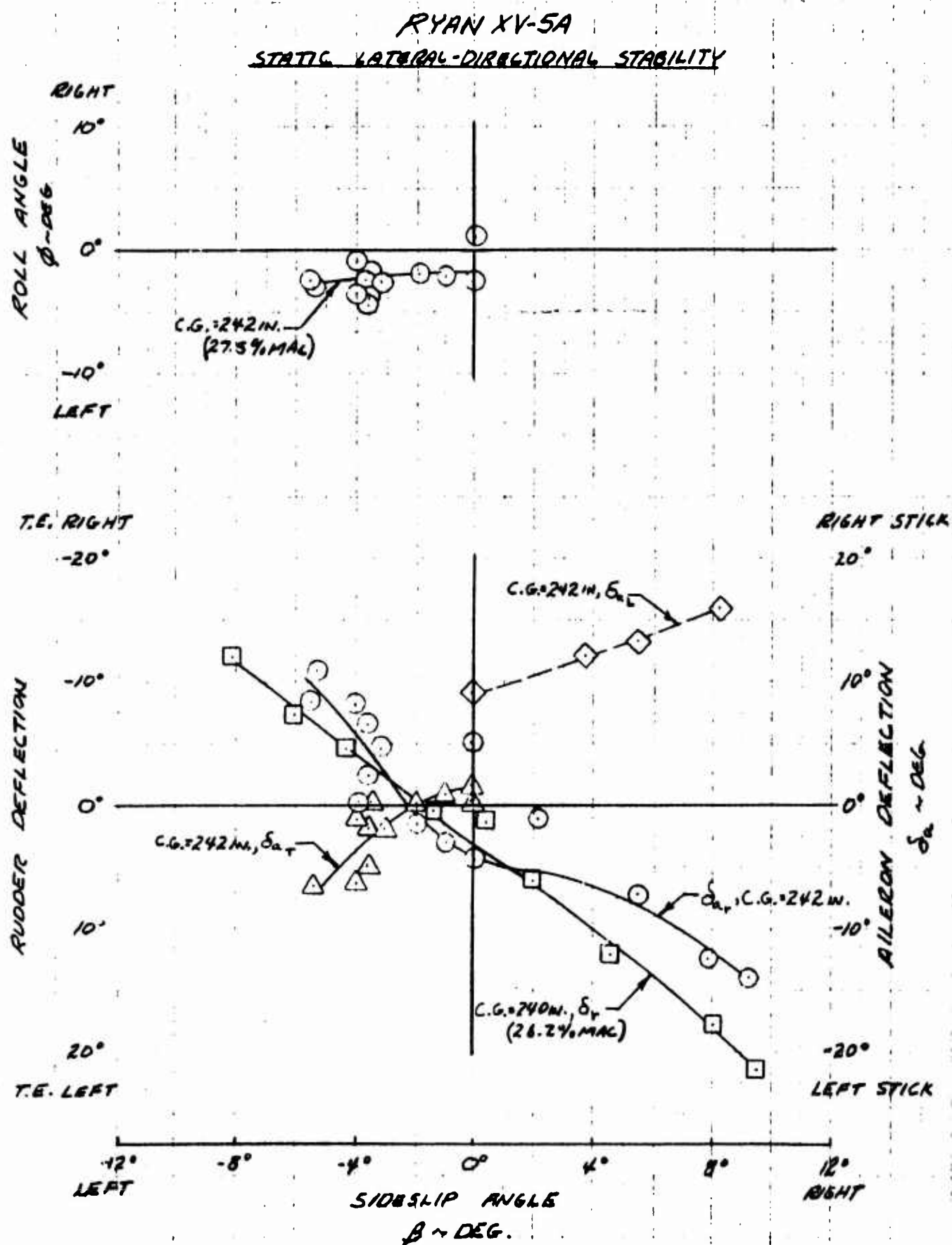


Figure 7.15 Static Lateral-Directional Stability



AVERAGE GROSS WEIGHT = 10,450 LB. VELOCITY = 133 KNOTS (EAS)
CONFIGURATION "PA"

Figure 7.16 Static Lateral-Directional Stability

RYAN XV-5A
STATIC LATERAL-DIRECTIONAL STABILITY
PRECONVERSION CONFIGURATION

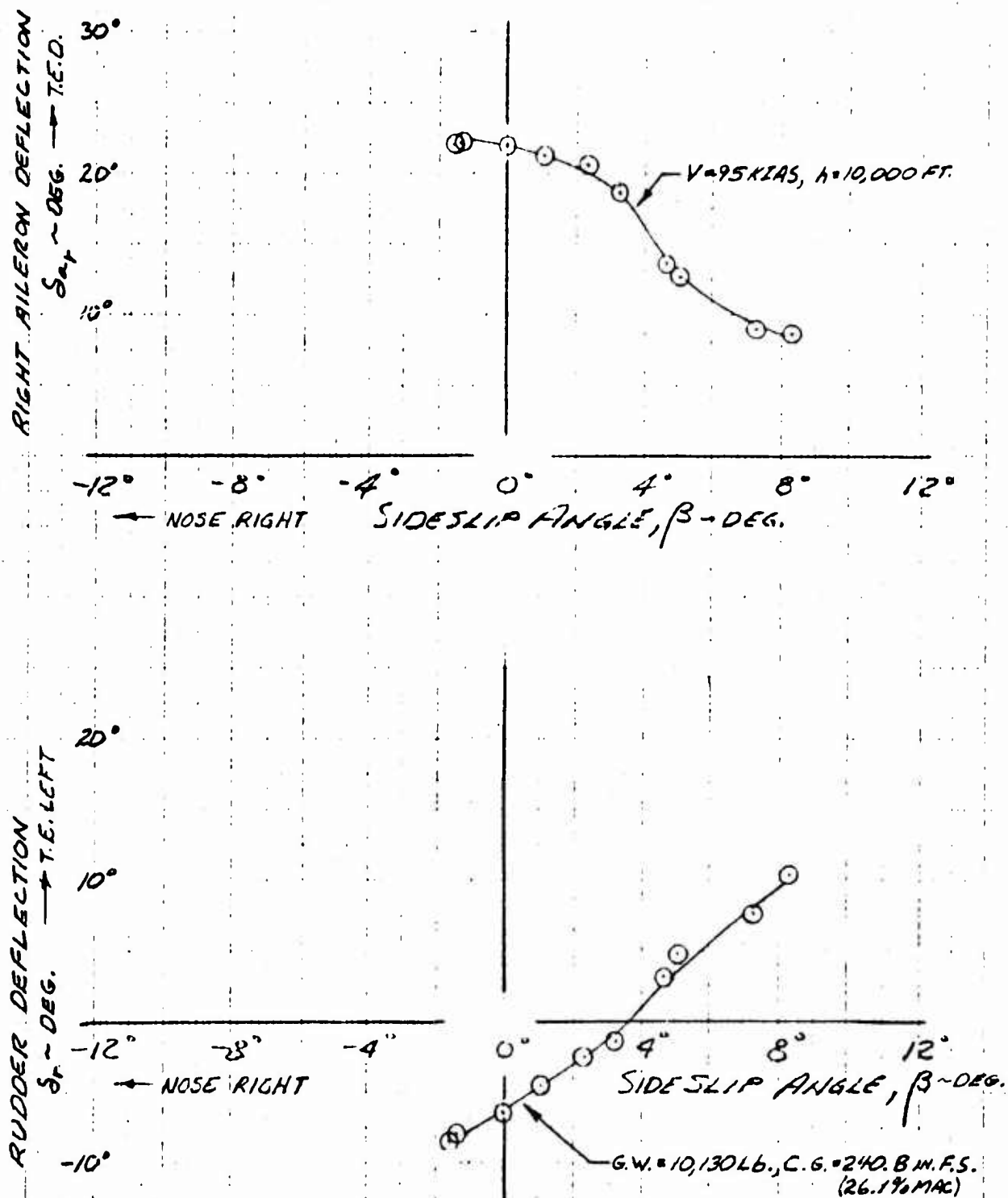
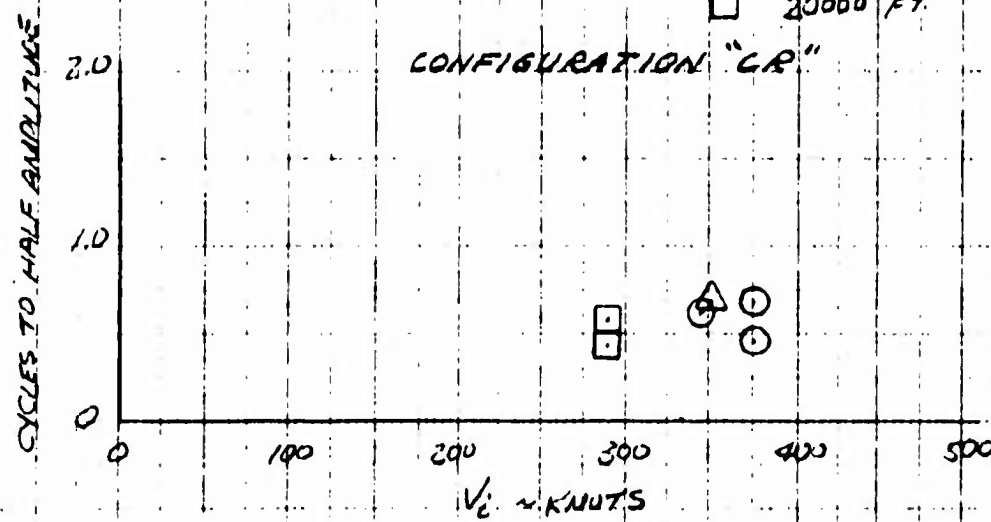
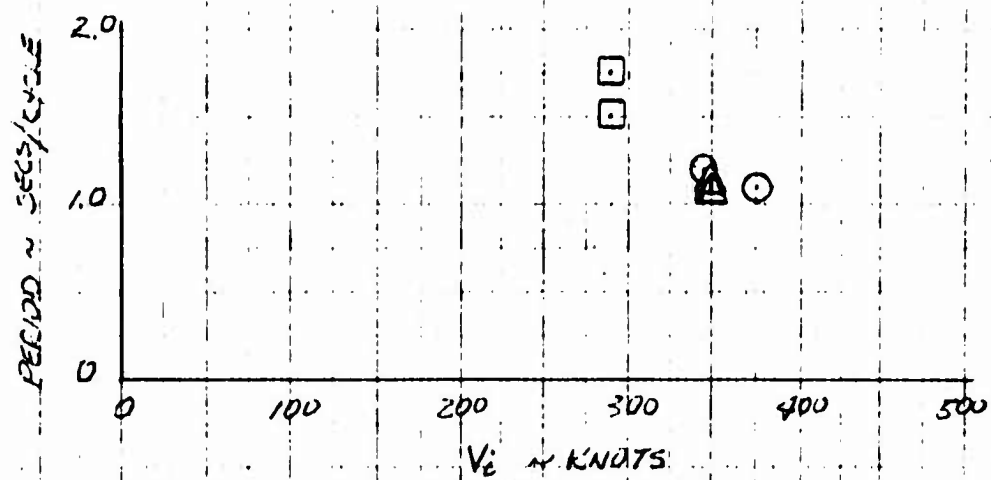


Figure 7.17 Static Lateral-Directional Stability



LONGITUDINAL DYNAMIC STABILITY
SHORT PERIOD DAMPING CHARACTERISTICS

Figure 7.18 Longitudinal Dynamic Stability - Short Period Characteristics

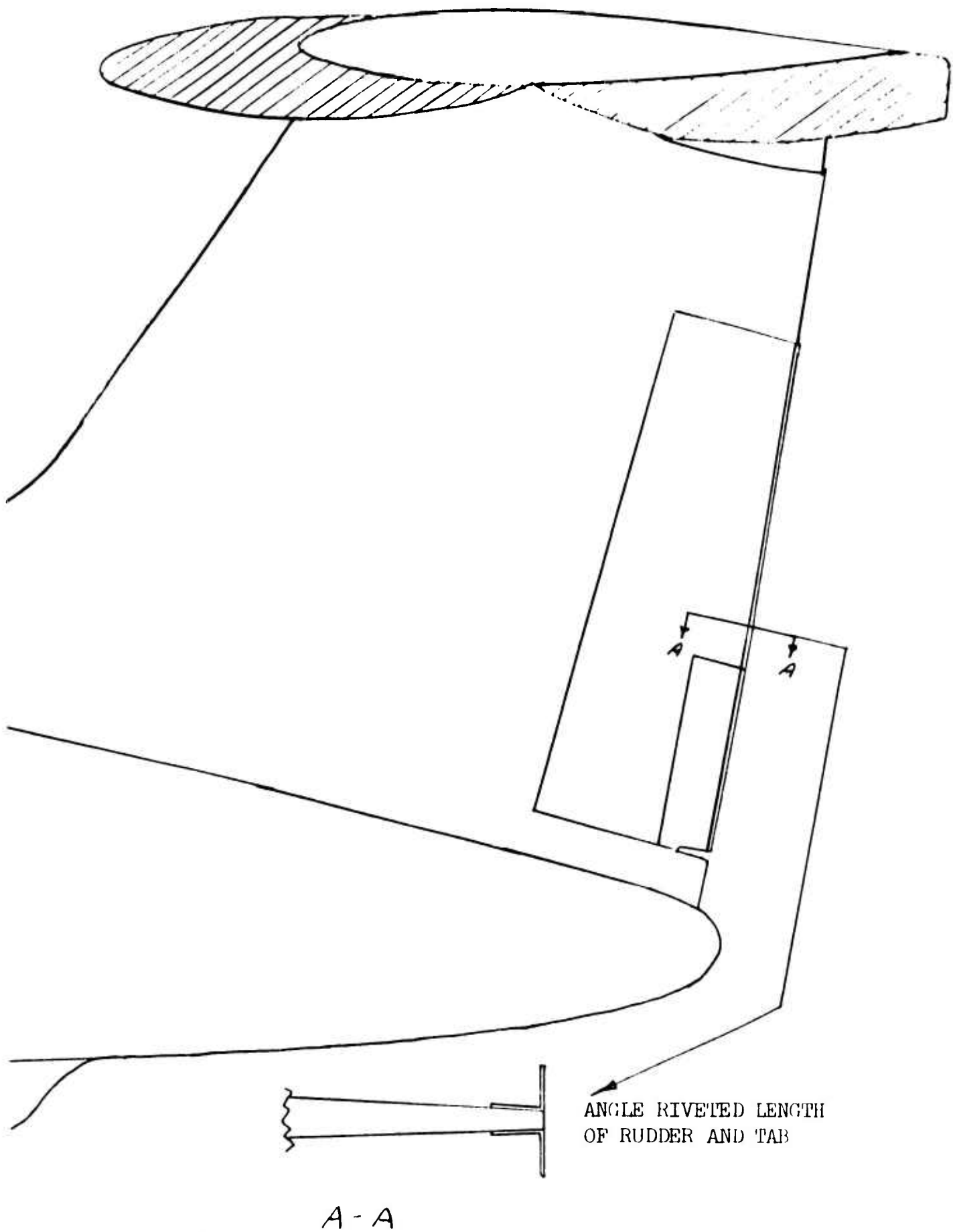


Figure 7.19 T-Section Installation on Rudder and Trim Tab Trailing Edge

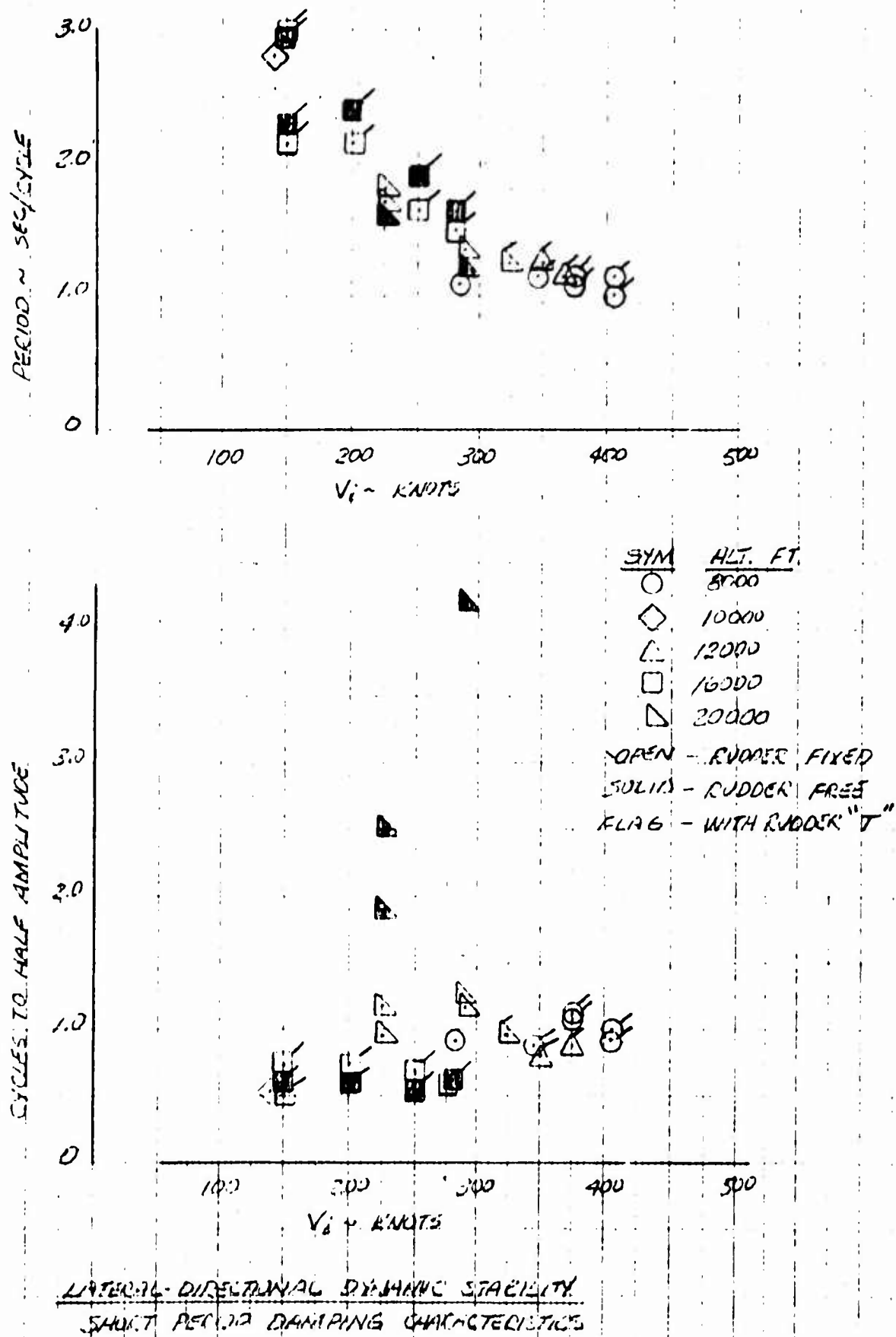


Figure 7.20 Lateral-Directional Dynamic Stability

LATERAL-DIRECTIONAL DYNAMIC STABILITY

SHORT PERIOD CYCLES TO HALF AMPLITUDE
WITH RESPECT TO ROLLING PARAMETER

SYM	ALT. FT.
□	16000
△	20000

OPEN - RUDDER FIXED
SOLID - RUDDER FREE
FLAG - WITH RUDDER "T"

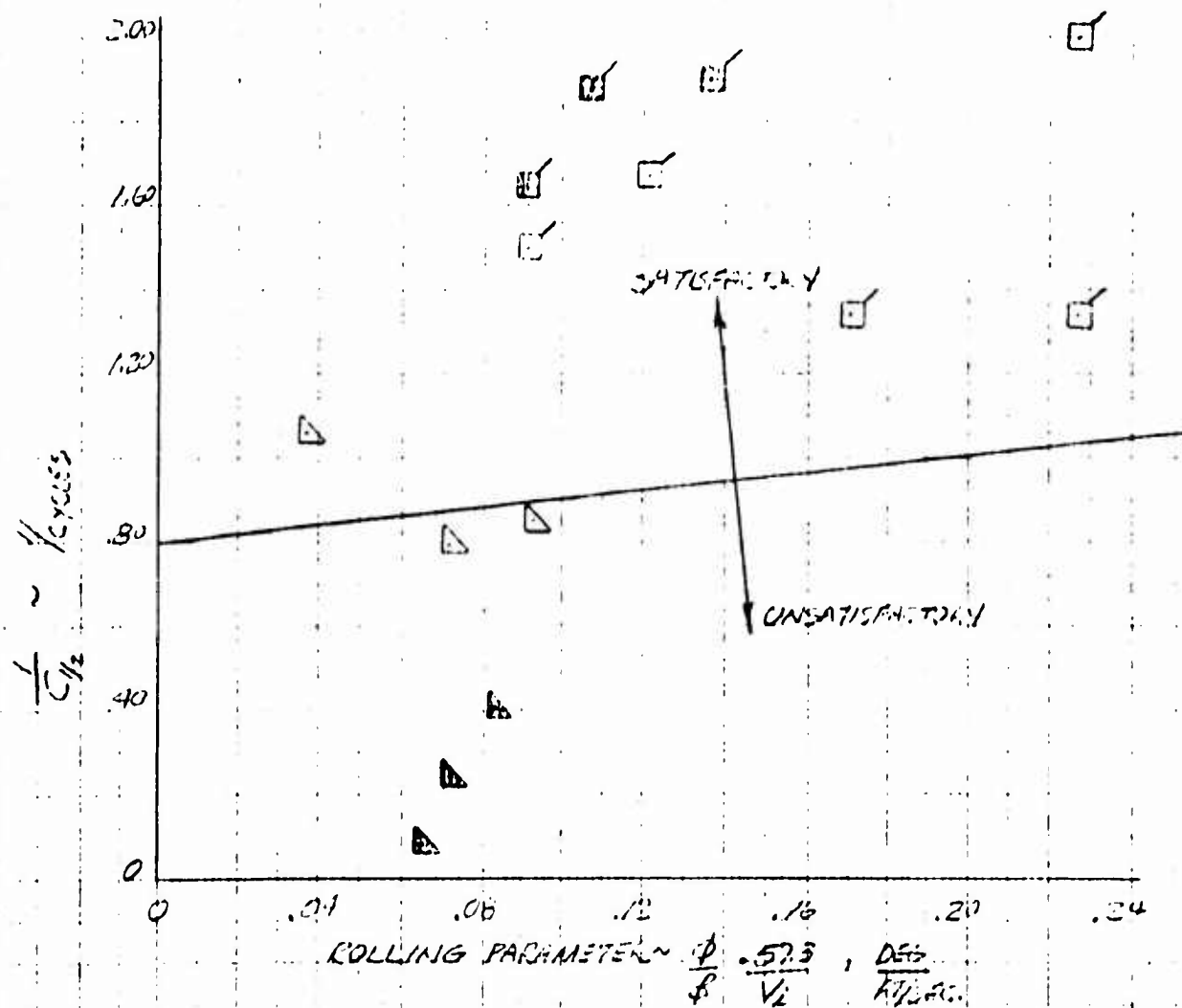
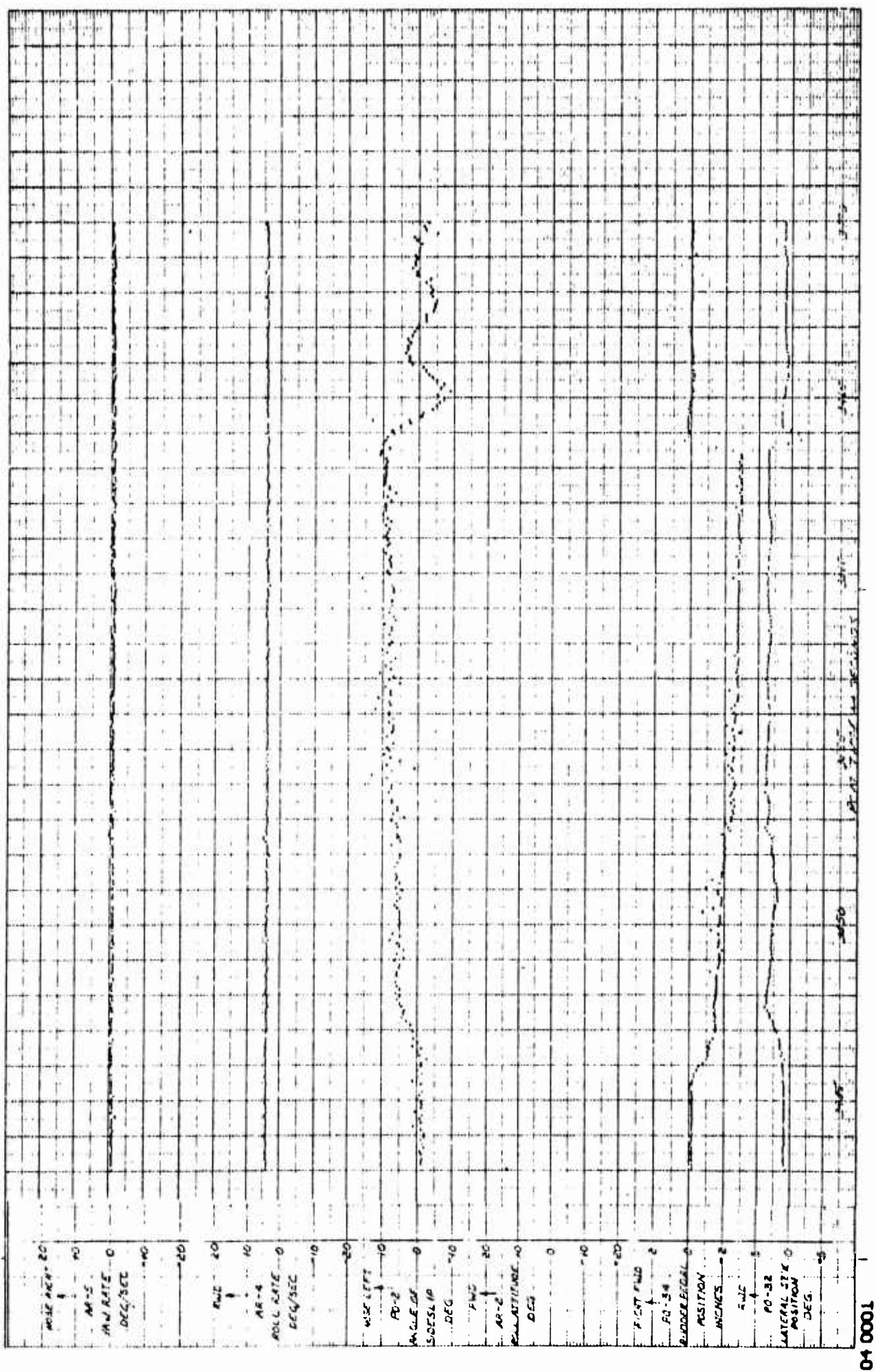


Figure 7.21 Lateral-Directional Dynamic Stability



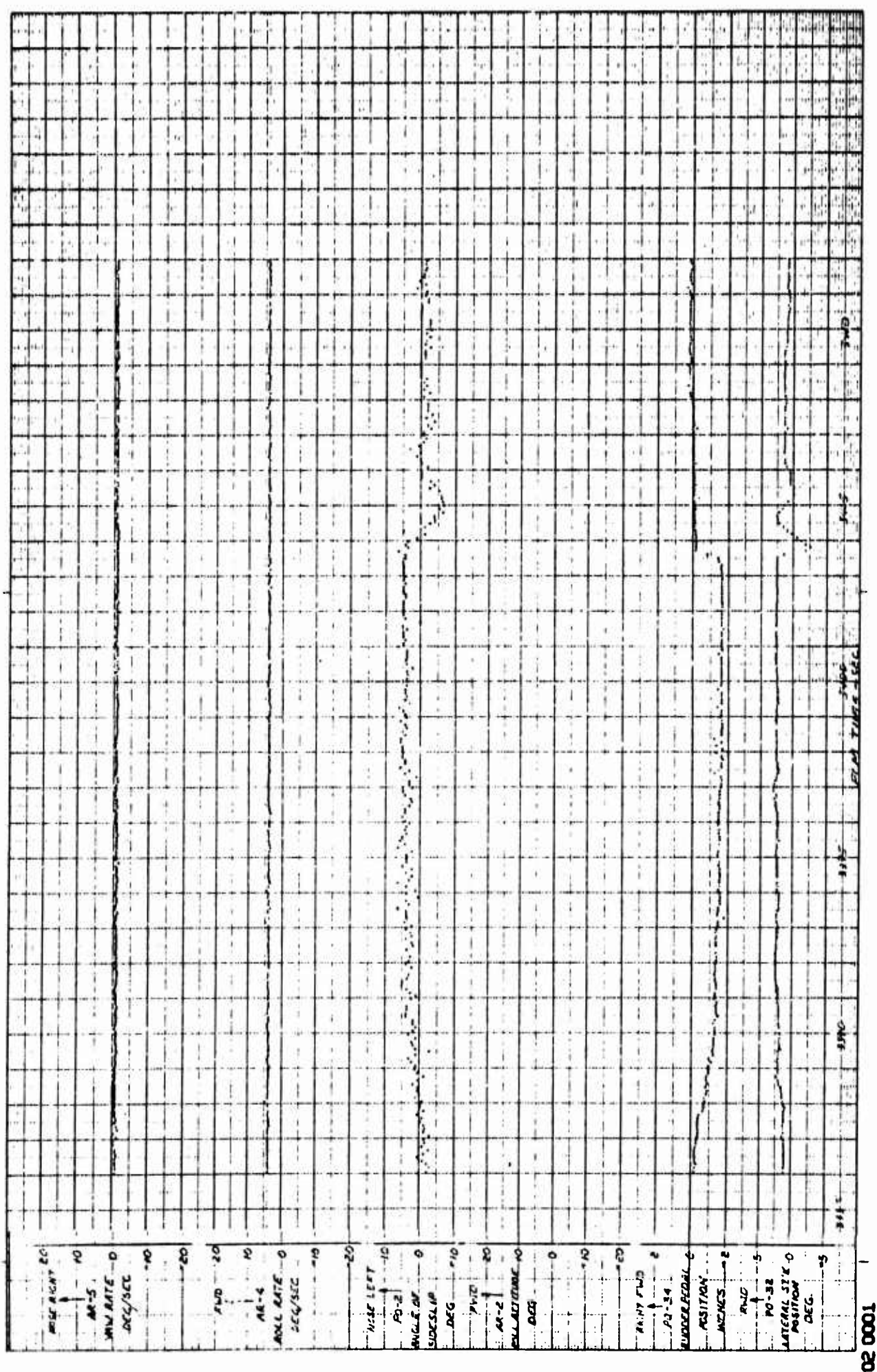


Figure 7.24 Time History of Sideslip with Rudder Release - Configuration L

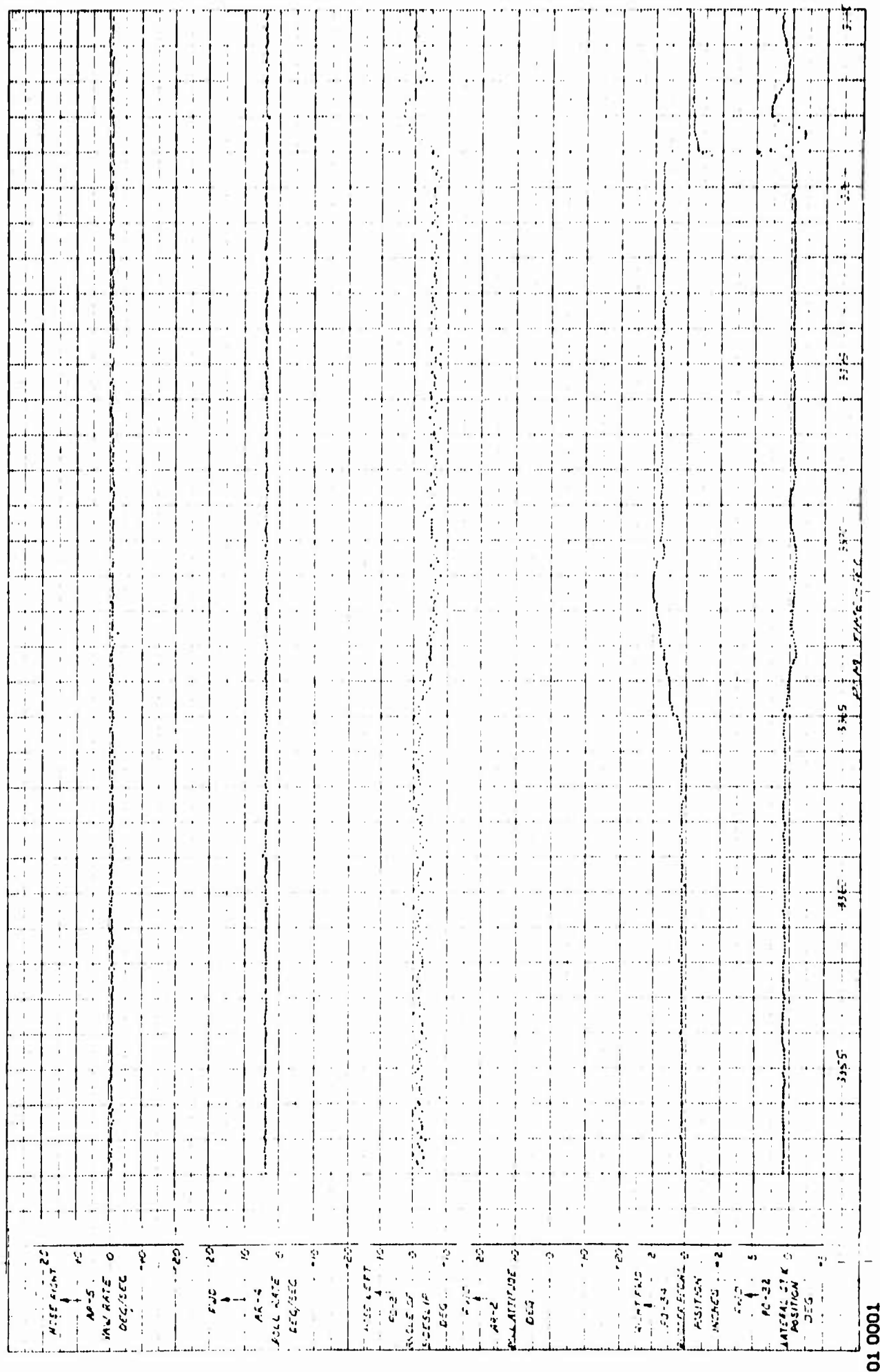
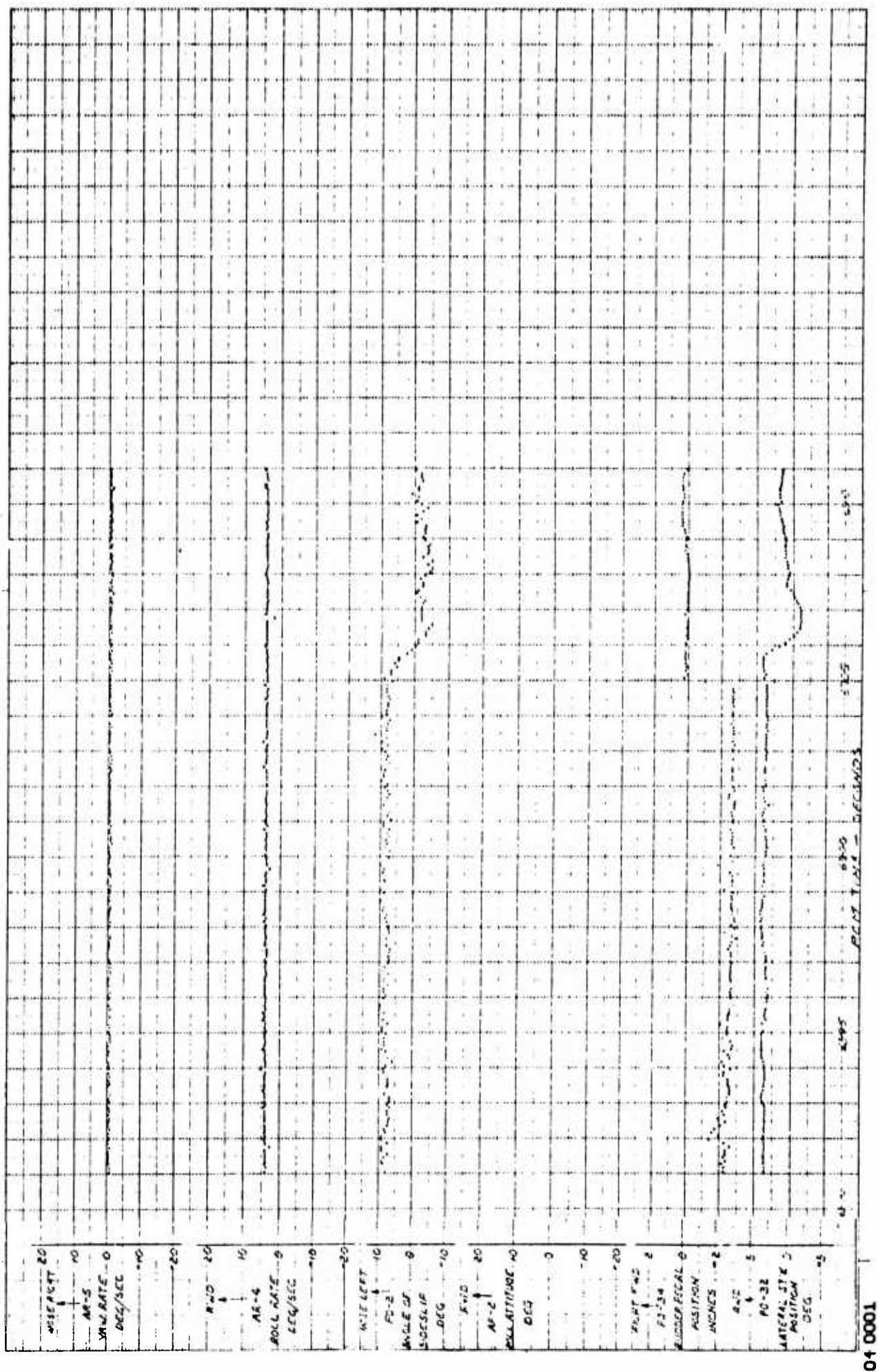


Figure 7.25 Time History of Sideslip with Rudder Release - Configuration L

Figure 7.26 Time History of Sideslip with Rudder Release - Configuration PA



04 0001

Figure 7.27 Time History of Sideslip with Rudder Release - Configuration PA

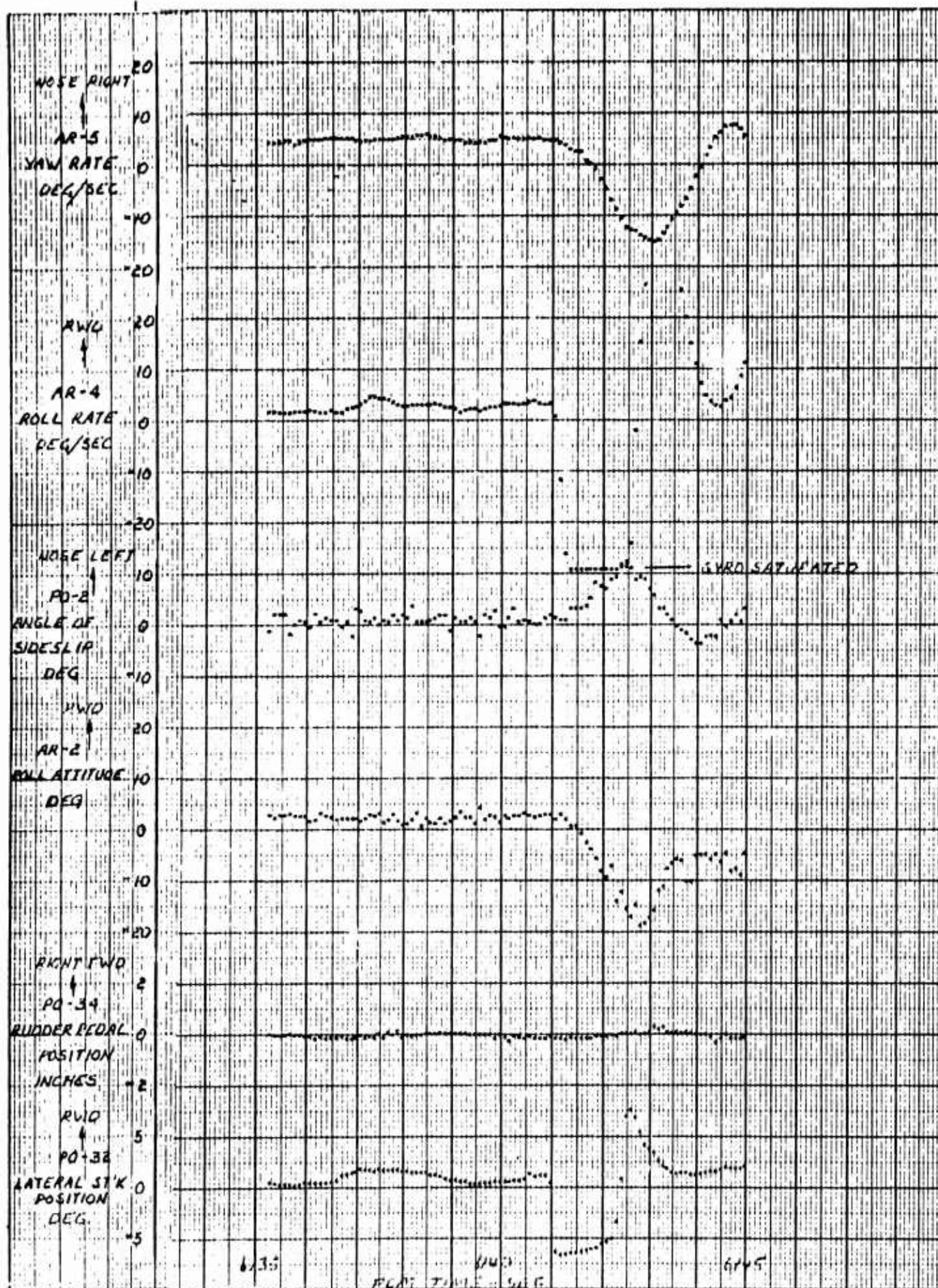


Figure 7.28 Time History of Roll Maneuvers - Configuration PA

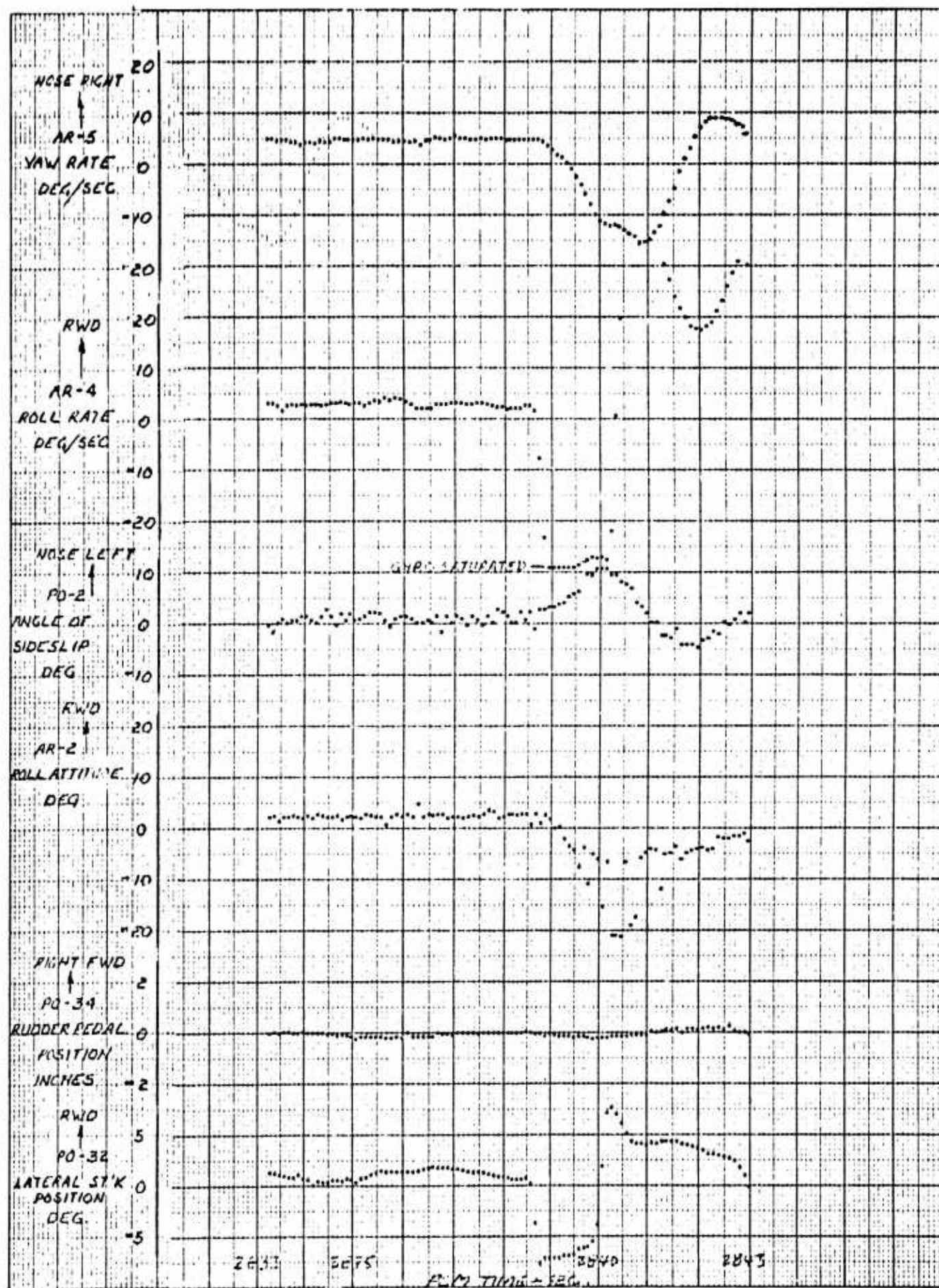


Figure 7.29 Time History of Roll Maneuvers - Configuration PA



Figure 7.30 Time History of Roll Manuevers - Configuration PA

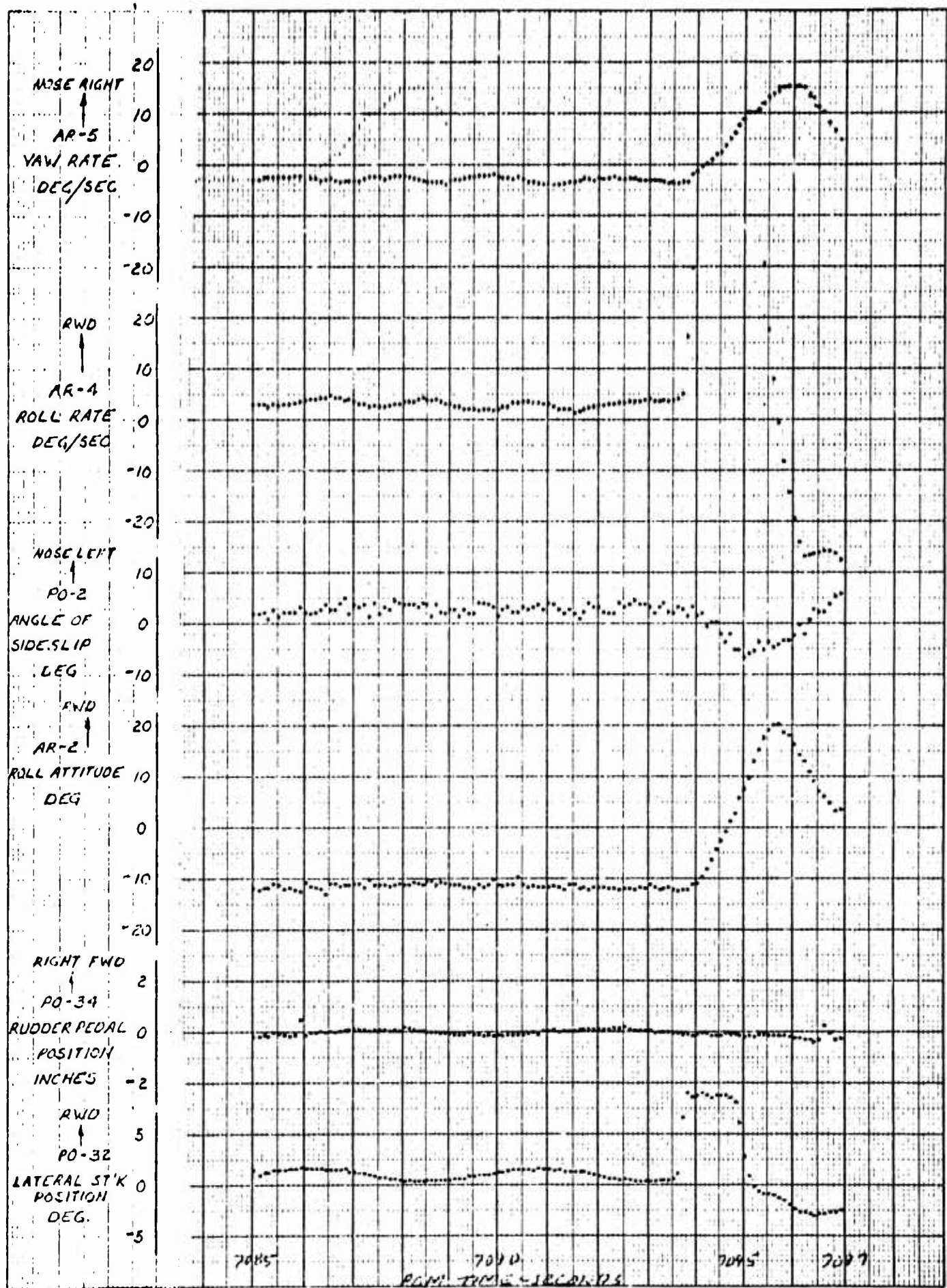


Figure 7.31 Time History of Roll Maneuvers - Configuration PA

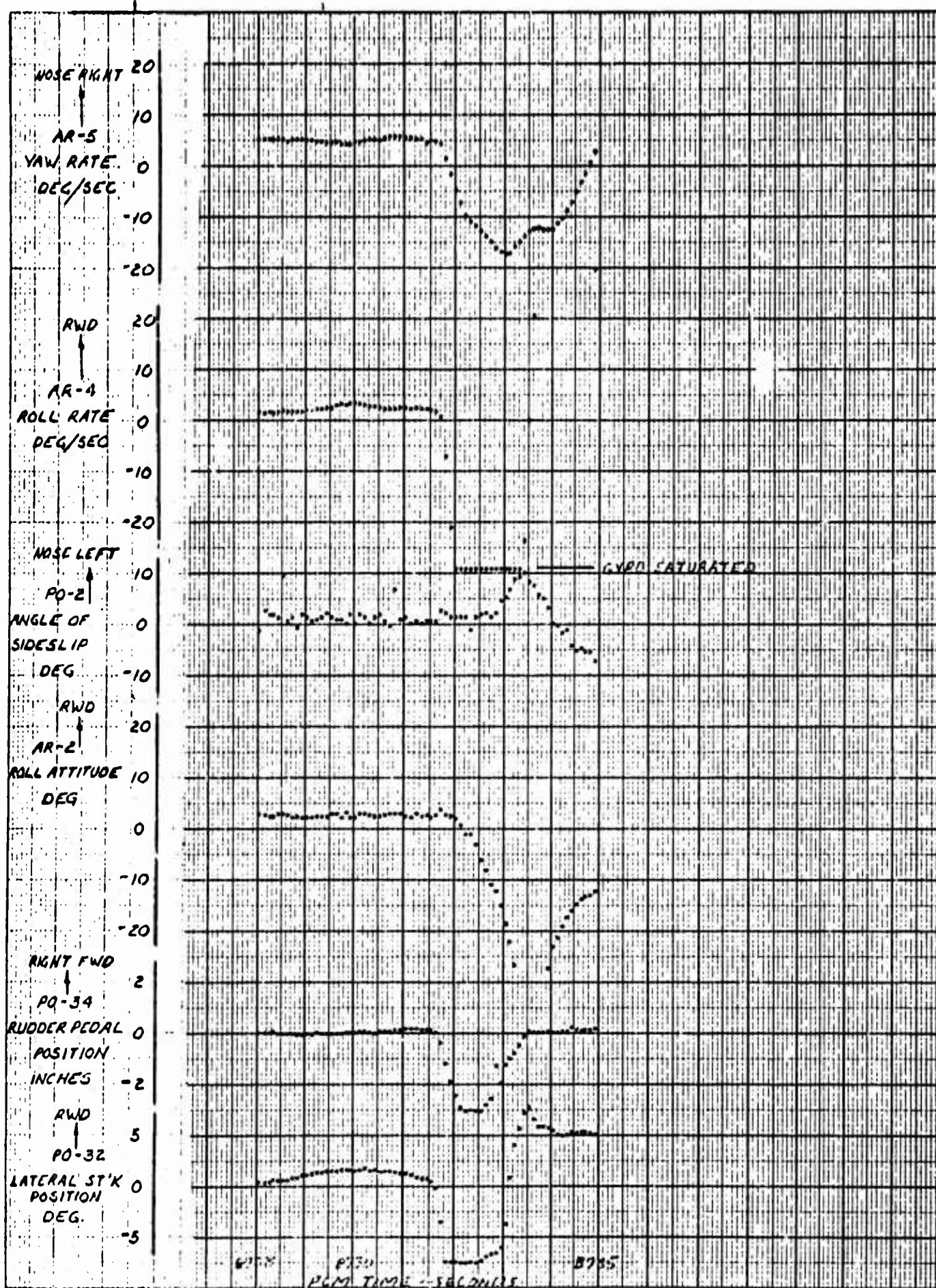


Figure 7.32 Time History of Roll Maneuvers - Configuration PA

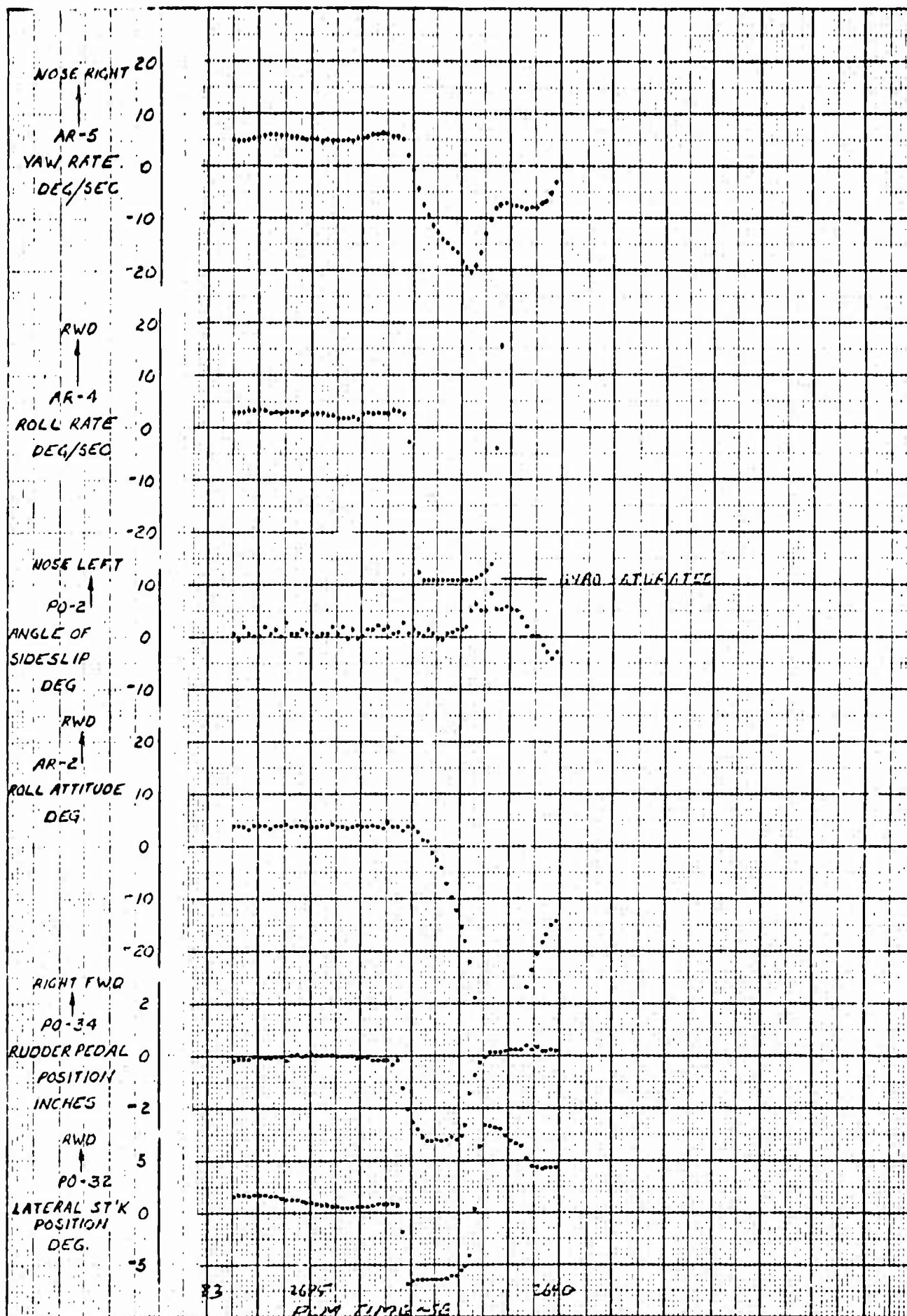


Figure 7.33 Time History of Roll Maneuvers - Configuration PA

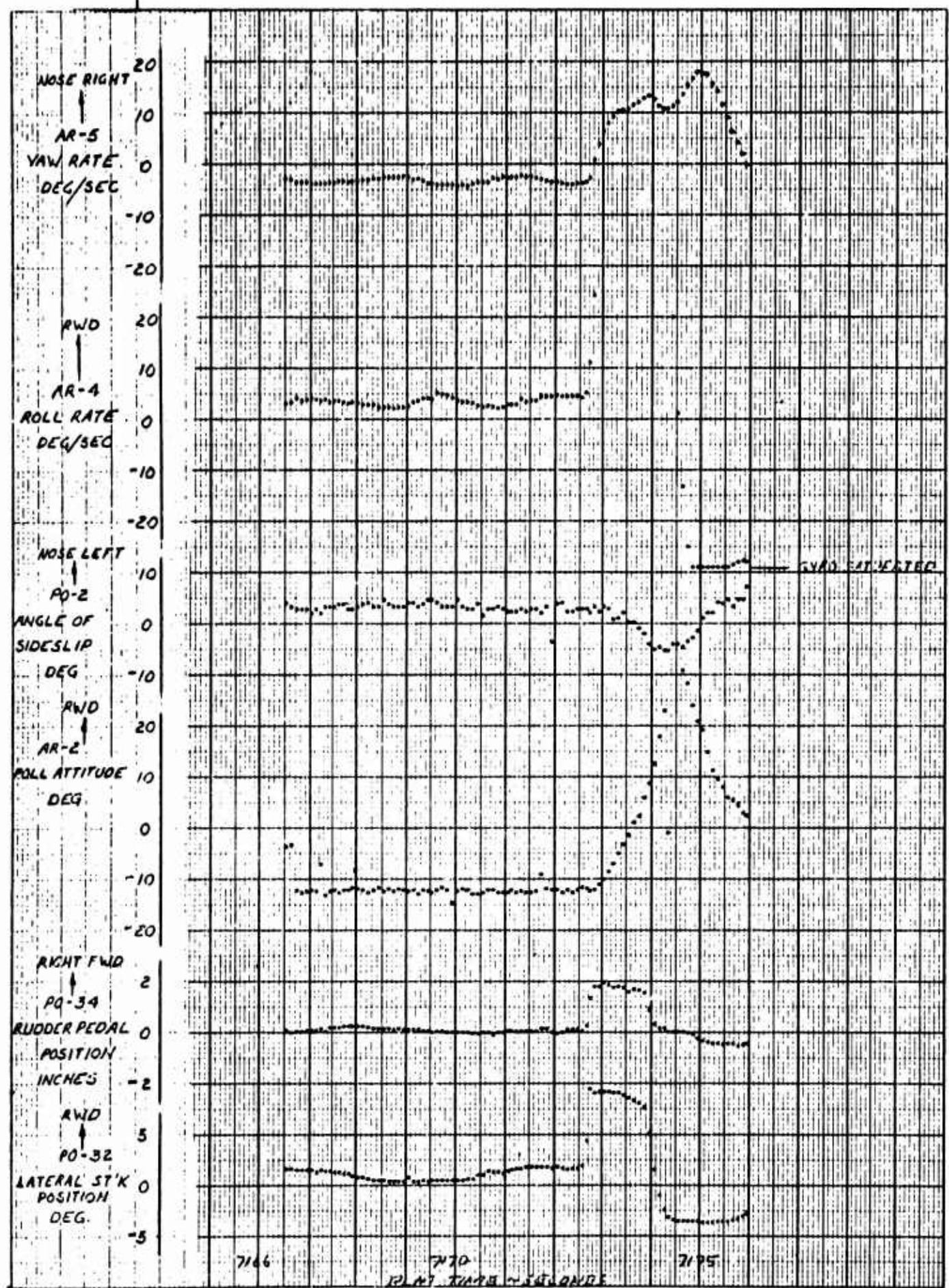


Figure 7.34 Time History of Roll Maneuvers - Configuration PA

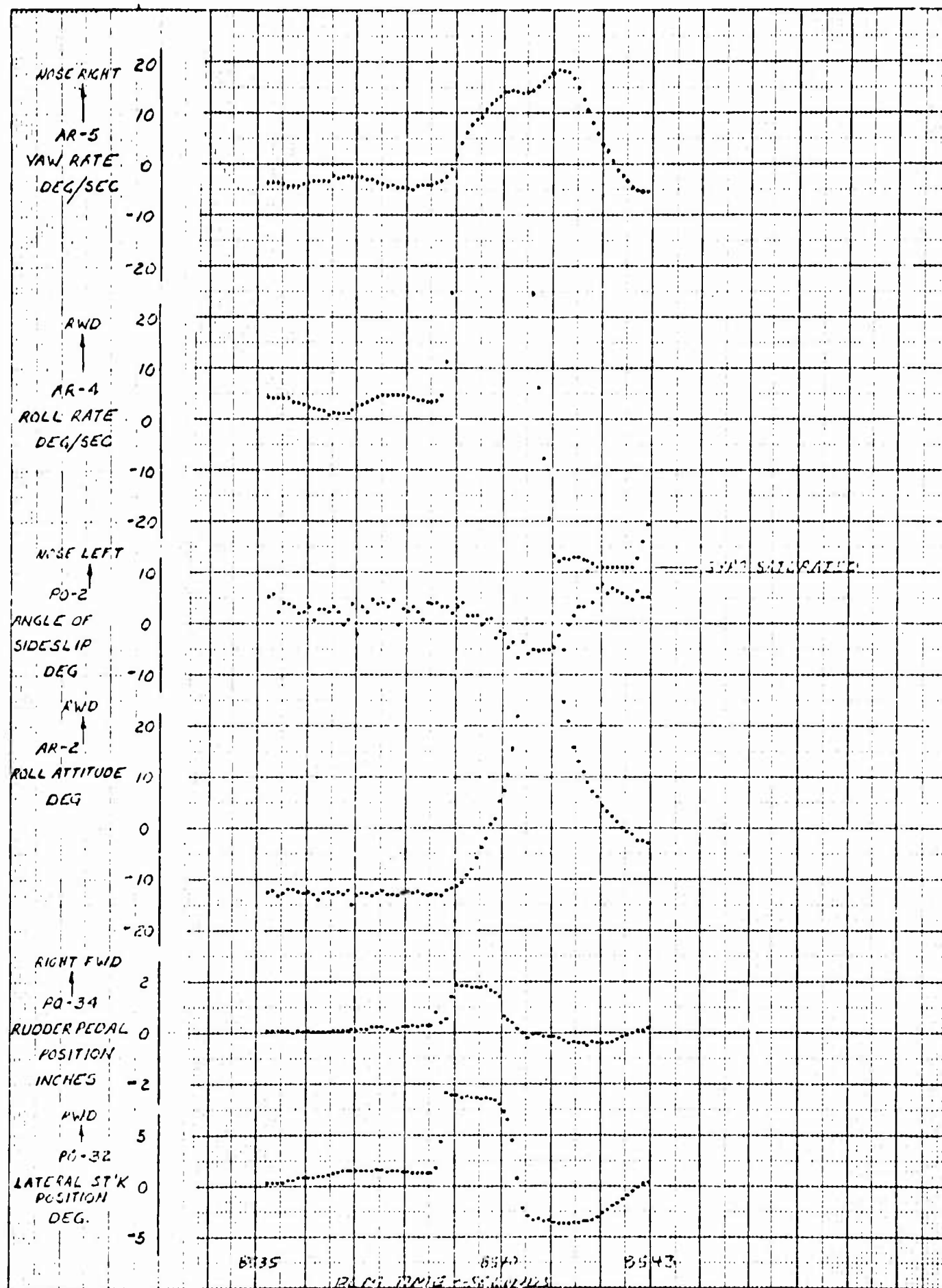


Figure 7.35 Time History of Roll Maneuvers - Configuration PA

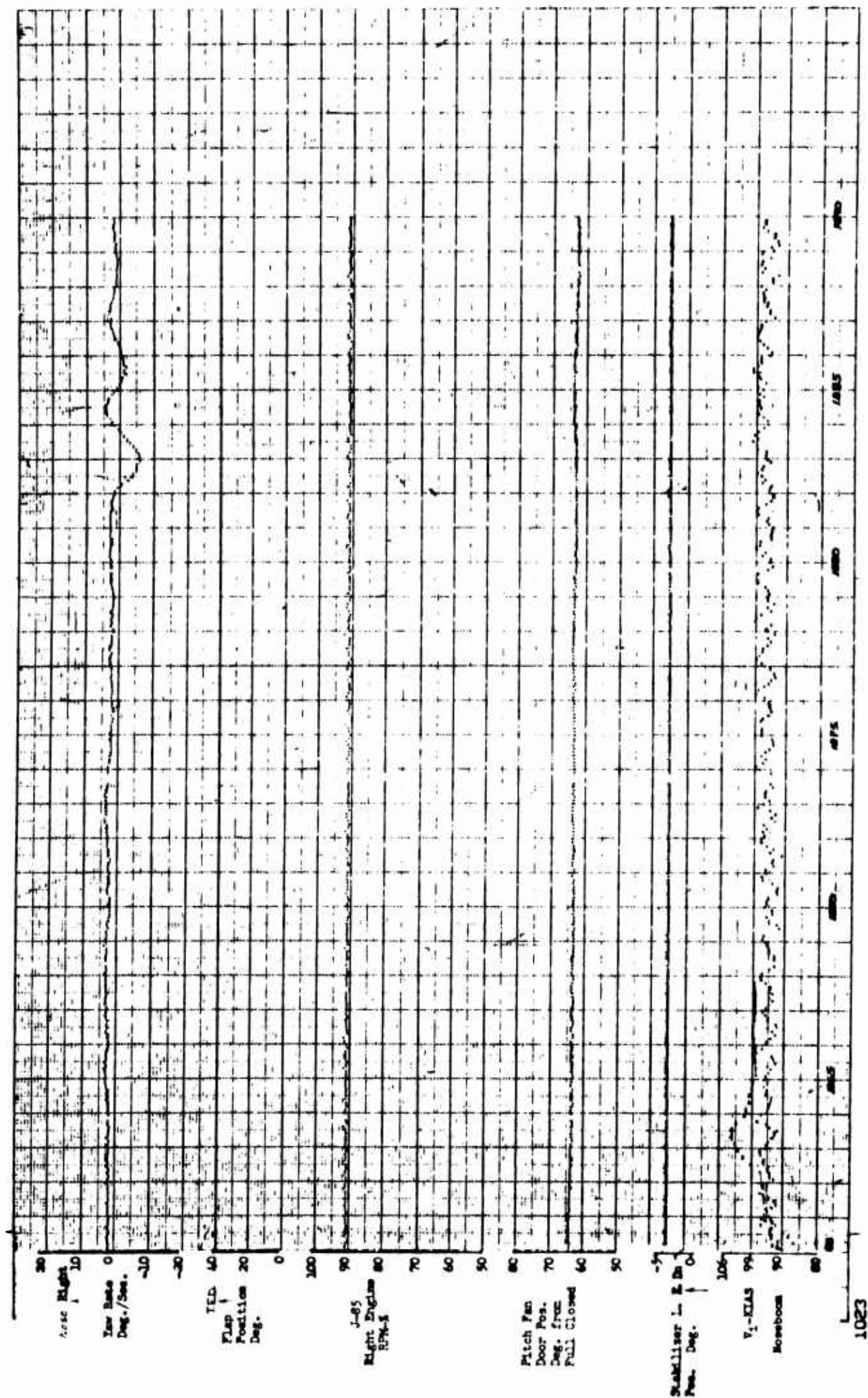


Figure 7.36 Dynamic Lateral-Directional Stability - Preconversion Configuration

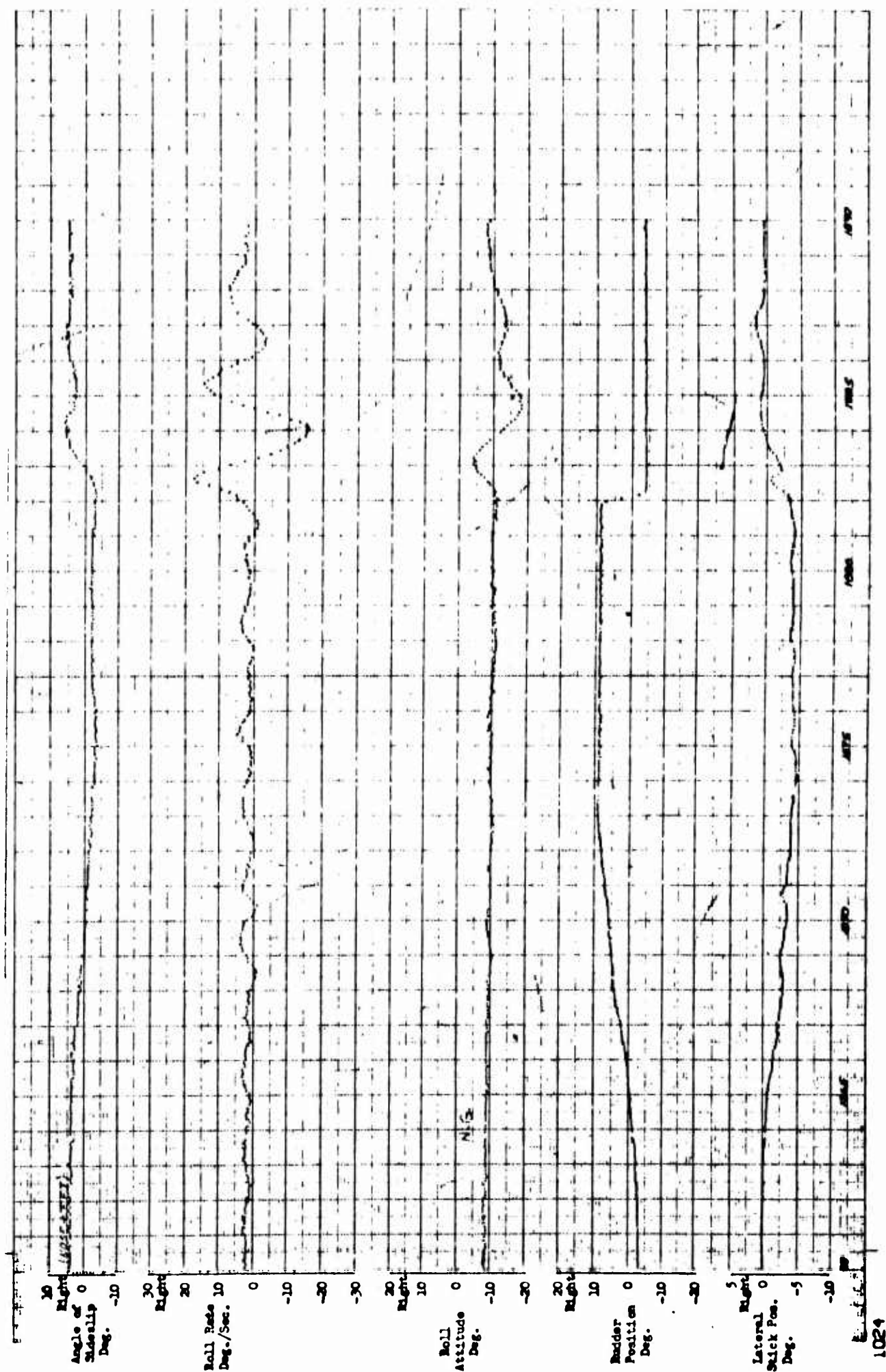


Figure 7.37 Dynamic Lateral-Directional Stability - Preconversion Configuration

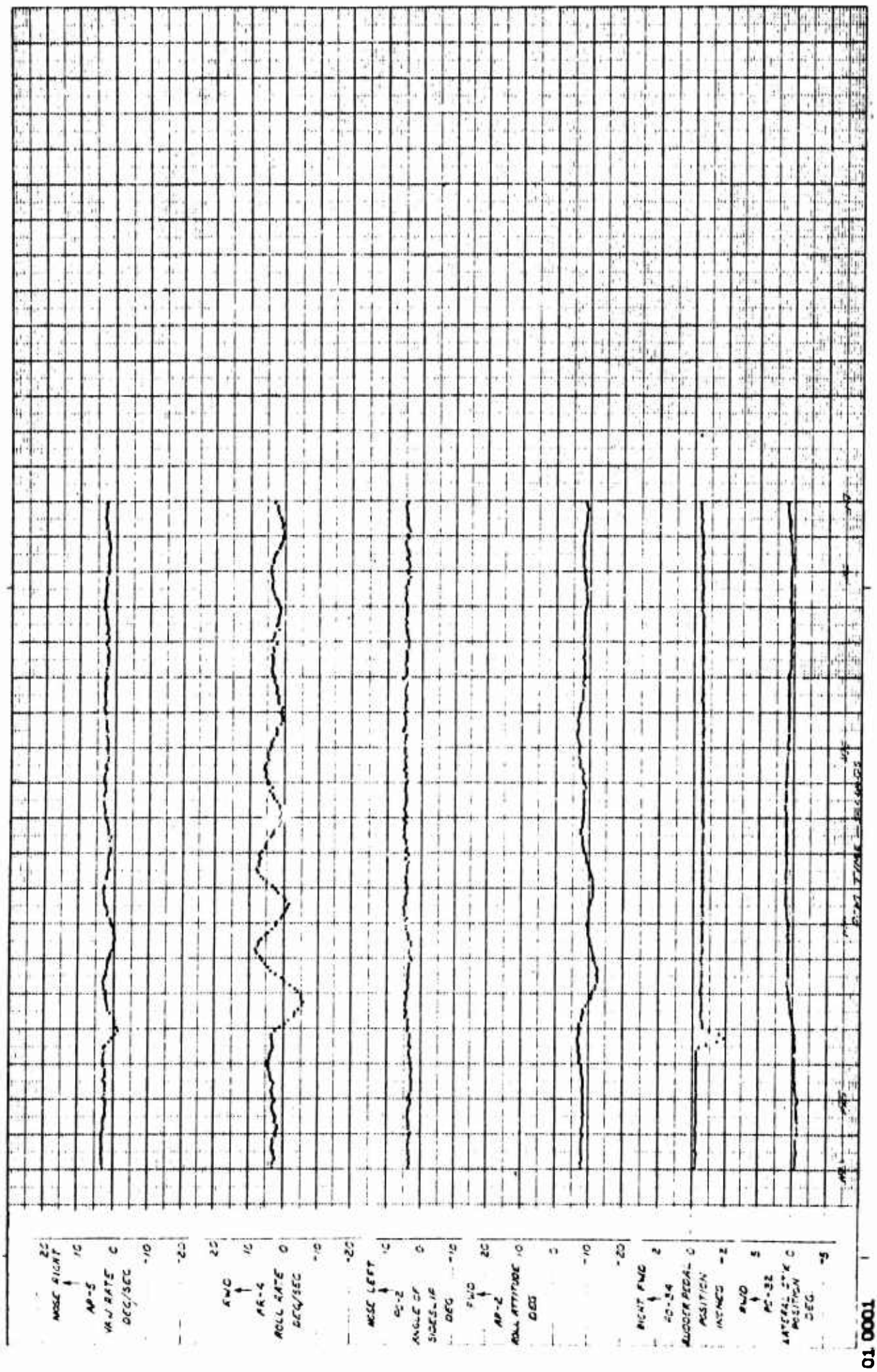


Figure 7.38 Dynamic Lateral-Directional Stability - Preconversion Configuration

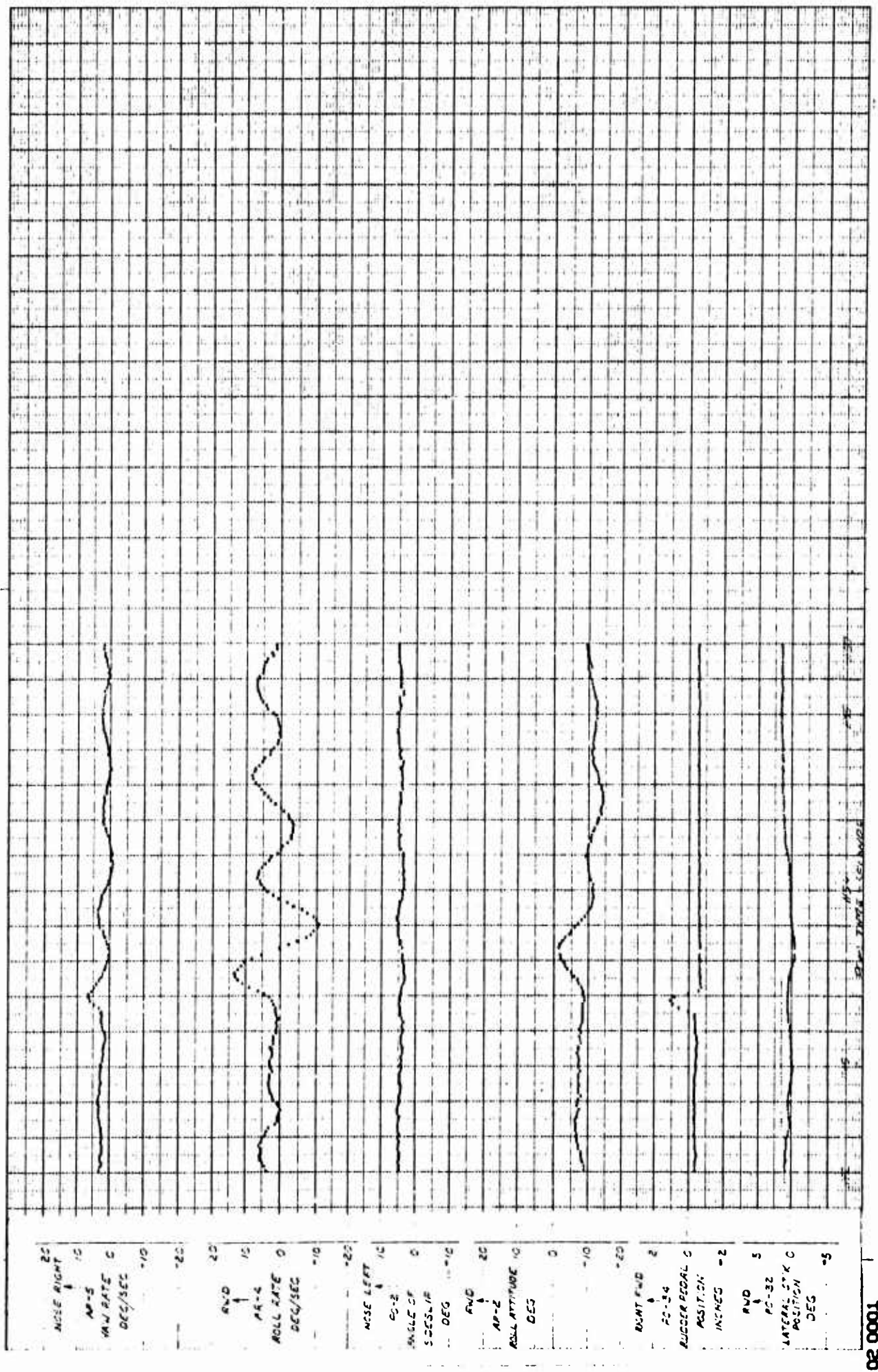


Figure 7.39 Dynamic Lateral-Directional Stability - Preconversion Configuration

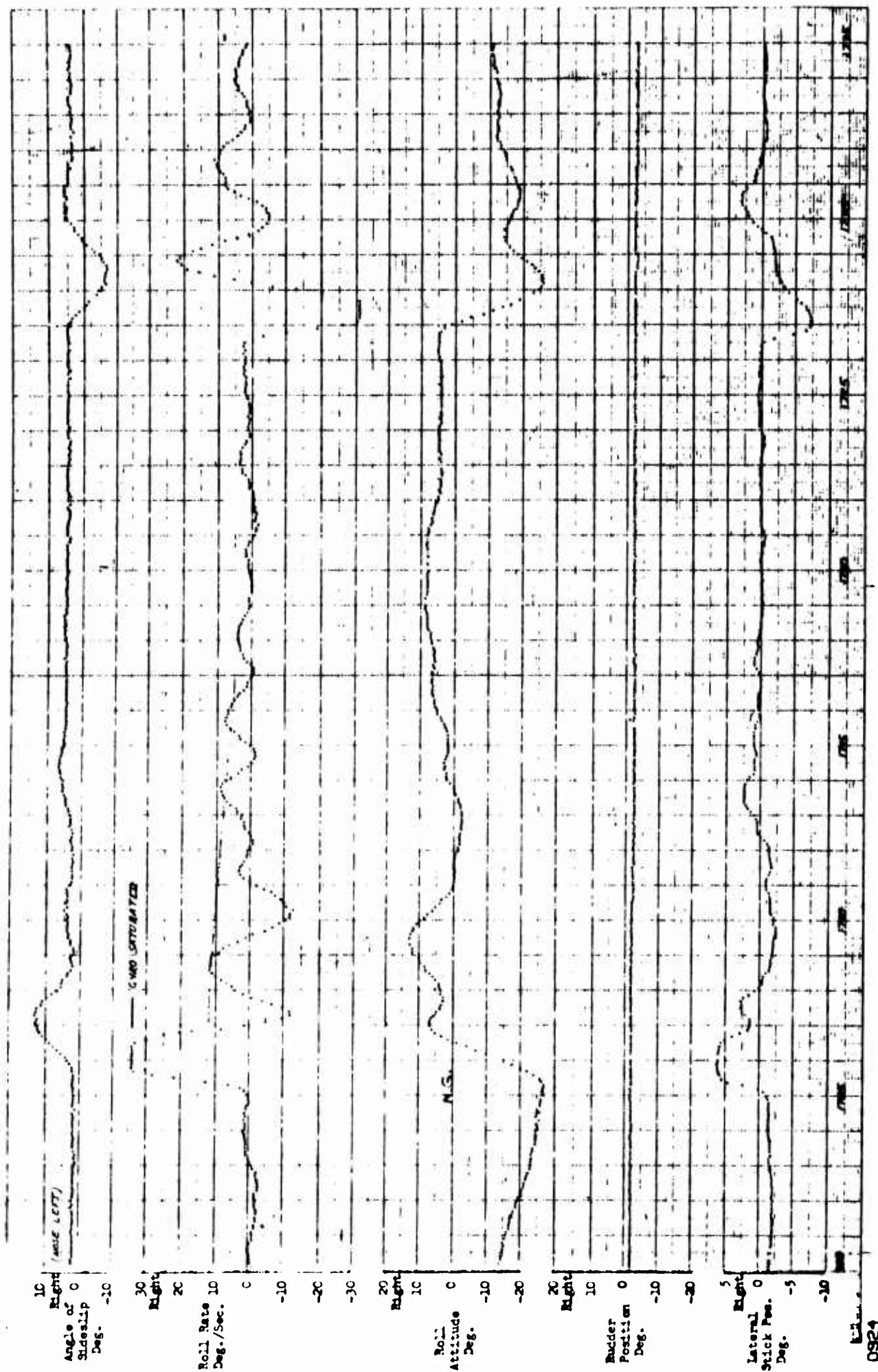


Figure 7.40 Bank-to-Bank Rolls - Preconversion Mode

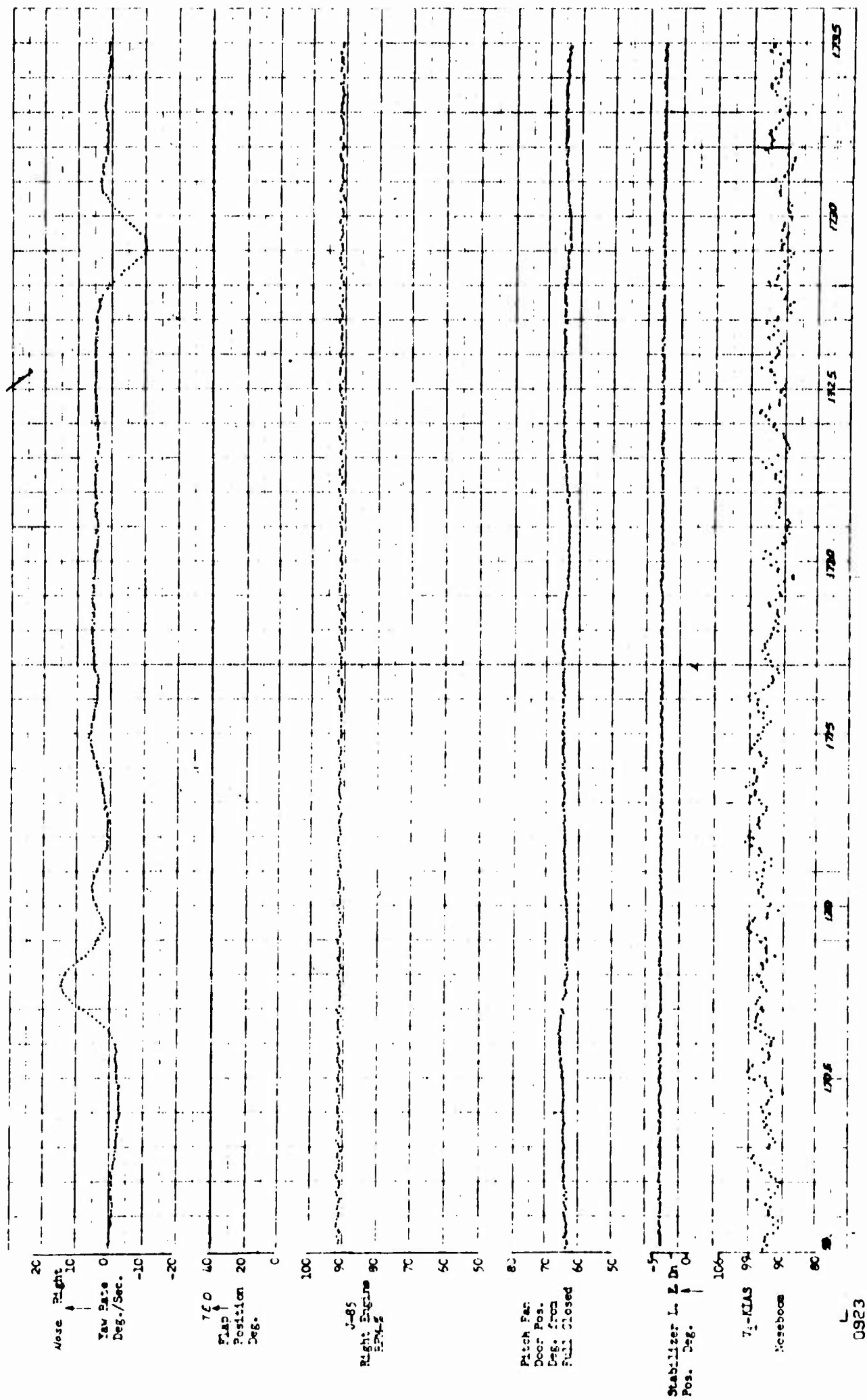


Figure 7.41 Bank-to-Bank Rolls - Preconversion Mode

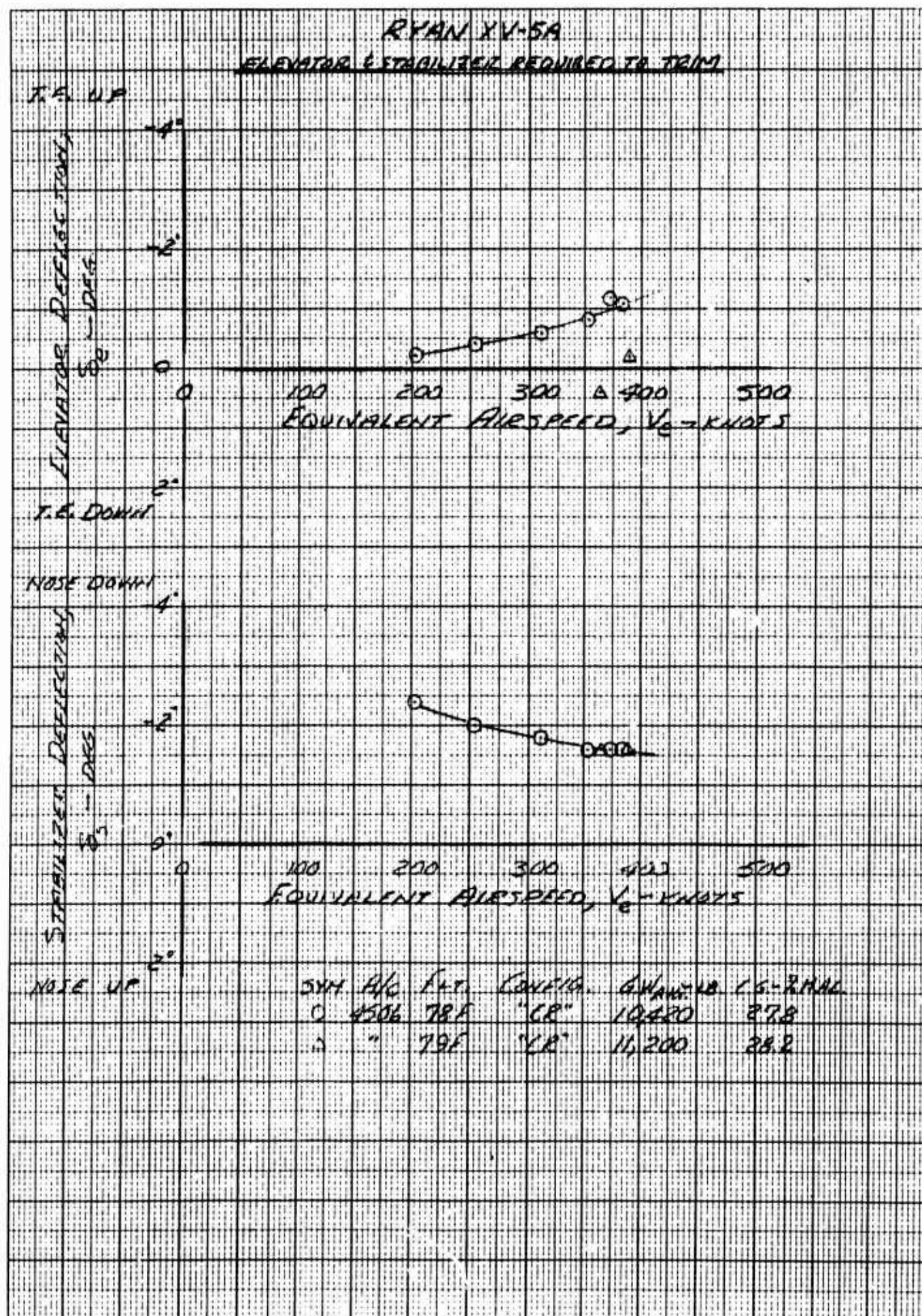


Figure 7.42 Elevator and Stabilizer Required to Trim

RYAN XV-5A
RUDDER EFFECTIVENESS

CLEAN CONFIGURATION

AVERAGE GROSS WEIGHT = 10,750 LB. ALTITUDE = 12,000 FT.

C.G. = 242 IN. (27.5% MAC)

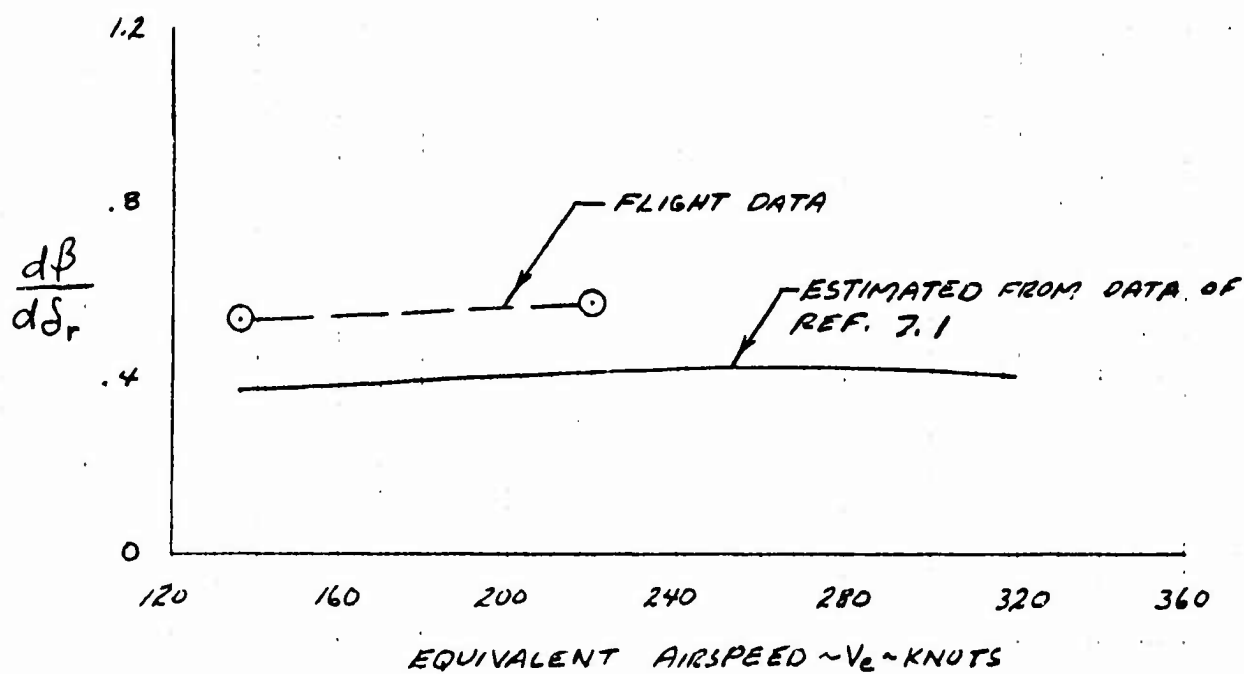


Figure 7.43 Rudder Effectiveness - Clean Configuration

RYAN XV-5A
RUDDER EFFECTIVENESS

LANDING CONFIGURATION

AVERAGE GROSS WEIGHT = 10,500 LB. CG. = 241 IN. (27% MAC)

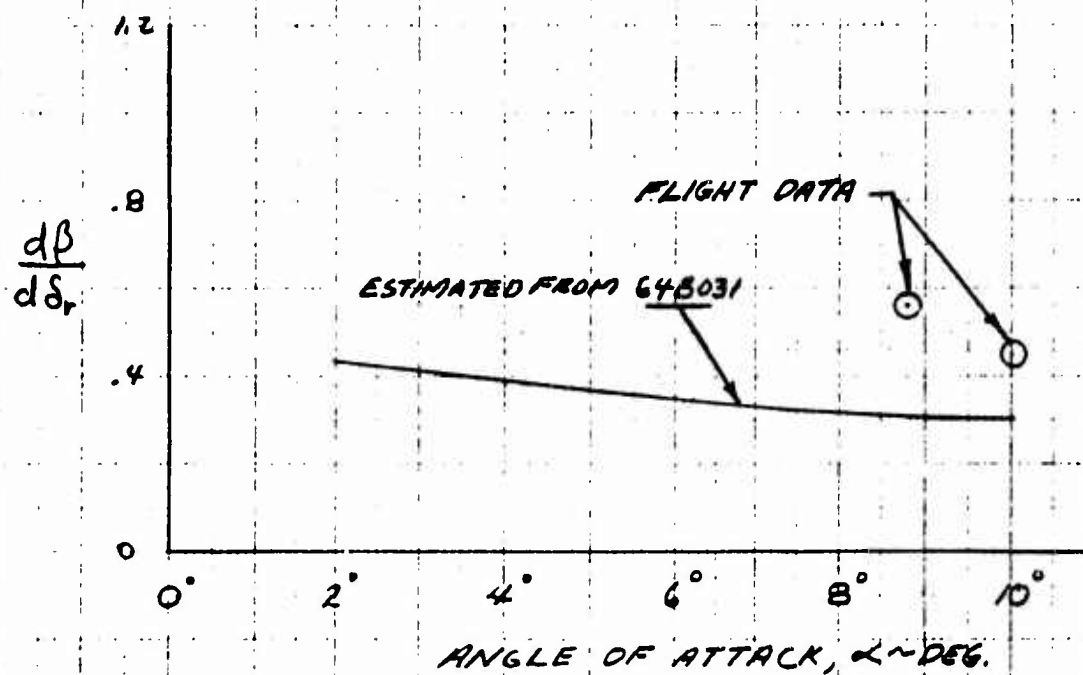


Figure 7.44 Rudder Effectiveness - Landing Configuration

7.3 THERMODYNAMICS

7.3.1 Engine Performance

During XV-5A fan mode flights 143-2-10F and 12F, compressor stalls were experienced by the R/H engine. These stalls generated a major exploratory effort to determine their cause, and to establish measures for preventing their reoccurrence. The urgency for getting on with the flight test program eliminated systematic investigation of possible influencing factors and dictated adoption of several modifications which directionally were believed to relieve the stall problem. These modifications are summarized below:

1. Compressor blade tip cooling by perforating engine air inlet and supplying relatively cool air from the top of the nacelle.
2. Compressor compartment ventilation by an engine bleed air driven ejector.
3. T_{t2} sensor duct relocation and system adjustment to operate approximately 20°F above actual engine inlet air temperature.
4. Interstage bleed valve rescheduling and adjustment to provide a minimum 5% open at maximum power.
5. Maximum allowable rpm increased from 100% to 102%.

A series of engine calibration tests were made in the G.E. engine test stand at EAFB to determine the performance loss resulting from stall-free modifications. Results from these tests are summarized in Figure 7.45 based on data reported in G.E. Datem, References 5 and 6. Curve A-A represents a standard engine as tested; curve D-D is an adjustment of this engine performance values which would represent the engine if tested at EGT values of 680°C at 1% physical speed. Comparing performance curves D-D and B-B representing respective before and after stall free modifications at a corresponding corrected gas generator speed, (compare 100% on curve D-D with 102% on curve B-B of Figure 7.45) shows zero performance losses. The performance loss increases with ambient temperature as shown on Figure 7.47. Also presented are representative installed turbojet mode thrust data for one and two engine operation. Comparisons of the results with engine specification performance (Curve C-C) and estimated installed propulsion system performance are possible with the data included. Measured installed thrust data are equal or better than one might expect, considering the reduction in performance due to stall-free modification. This is due largely to the increase of allowable % rpm to 102%. Turbojet flight performance should show degradations corresponding to the measured static performance degradations corresponding to the measured static performance degradations.

Above 95% corrected rpm, the measured fuel flow rate corrected for ambient conditions corresponds closely to specification 112 data when rpm is increased by an increment of 2% as shown in Figure 7. 46.

7. 3. 2 Compartment Cooling

The XV-5A aircraft heating is much less severe in turbojet mode, therefore only the few representative compartment air temperatures of Figures 7. 48 and 7. 49 are presented. The former is for relatively low speed flight and the latter is for near maximum speed flight.

Two critical regions exist for which adequate data coverage do not exist. These are fan cavities and the aft fuselage. Fan cavities have a tendency to exceed the 250° F and 300° F temperature limits during turbojet operation in the clean configuration because of diverter valve leakage. Generally, it is the right hand, forward quadrant which is heated, a phenomenon which can be traced to ducting, geometry and diverter valve seal problem interrelationships. Using the preconversion configuration or reducing power as during climb, has been shown to be an effective means of reducing fan cavity temperatures.

The aft fuselage heating occurs only during thrust spoiler actuation during taxi operation or during engine idle conditions whereby hot gases drift along the fuselage skins. Resulting temperatures are not too high structurally, but they appear to cause some heating problems in the battery compartment which also houses the inverters. This is a suspected problem area which needs further evaluation, as is the case of the fan cavity heating problem.

ENGINE THRUST PERFORMANCE SUMMARY

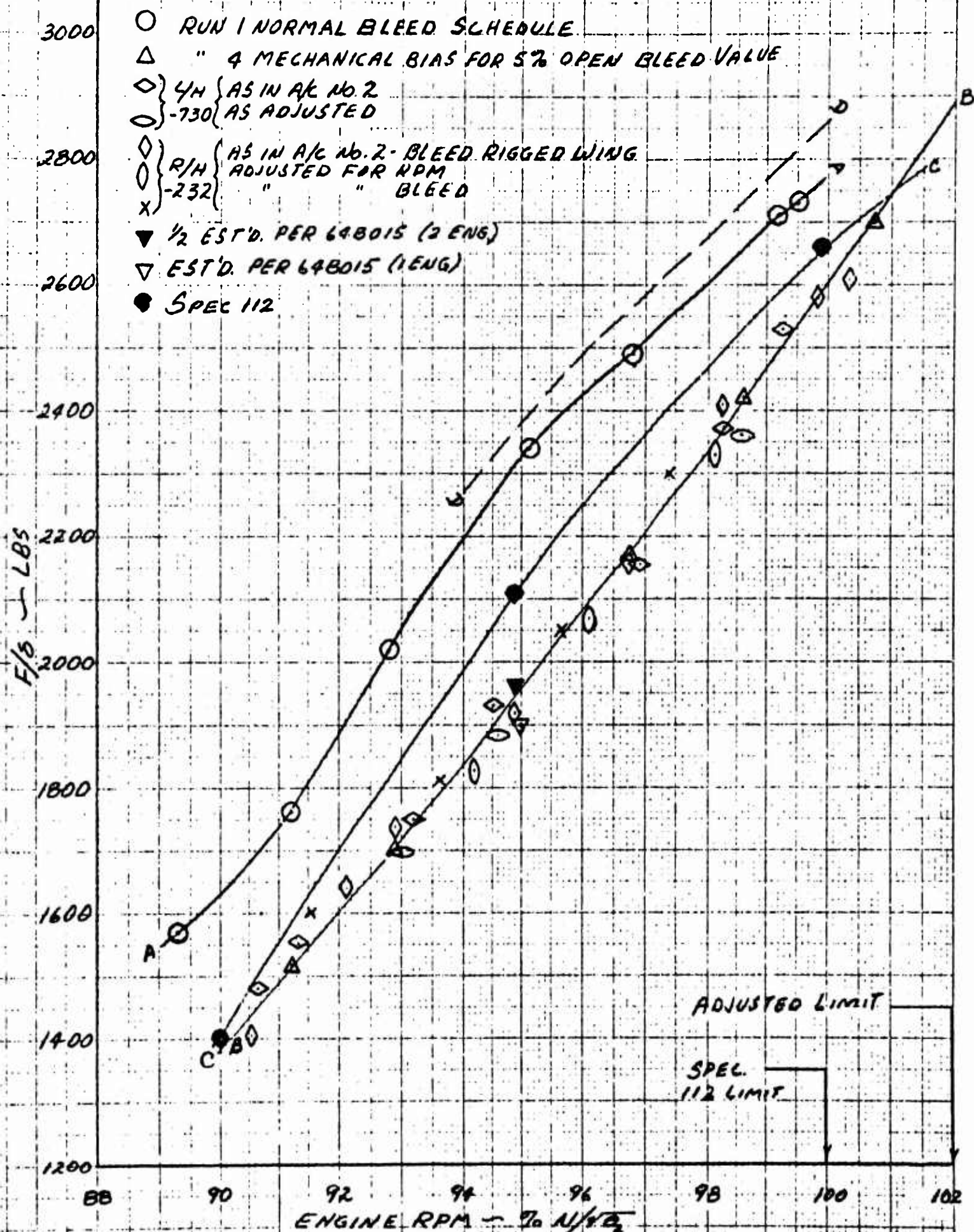


Figure 7.45 Engine Thrust Performance Summary

XV-5A
A/C NO 624576
FUEL FLOW VS % GAS GENERATOR RPM

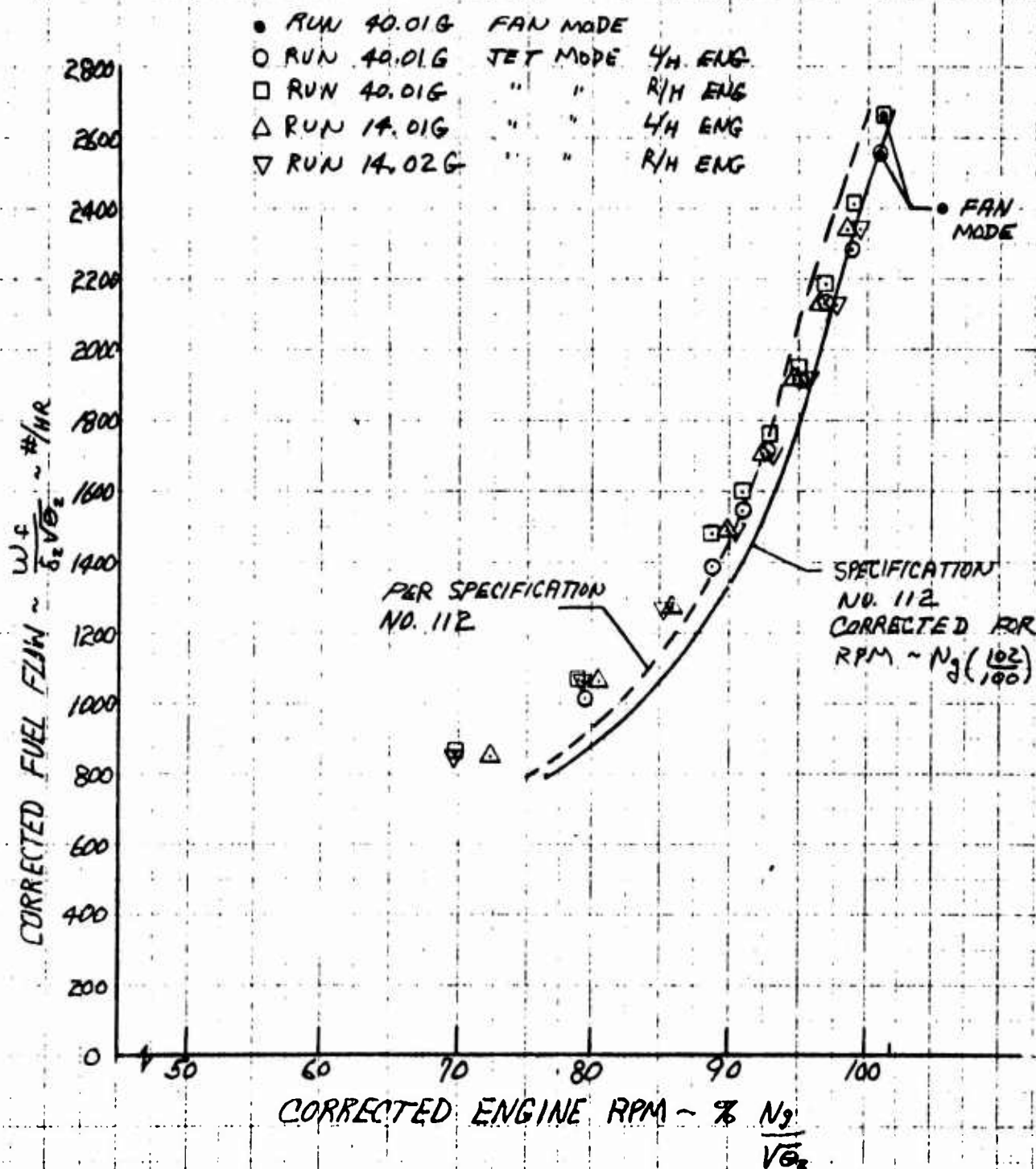


Figure 7.46 Fuel Flow vs Engine RPM

THRUST LOSS DUE TO STALL FREE OPERATION MODIFICATIONS

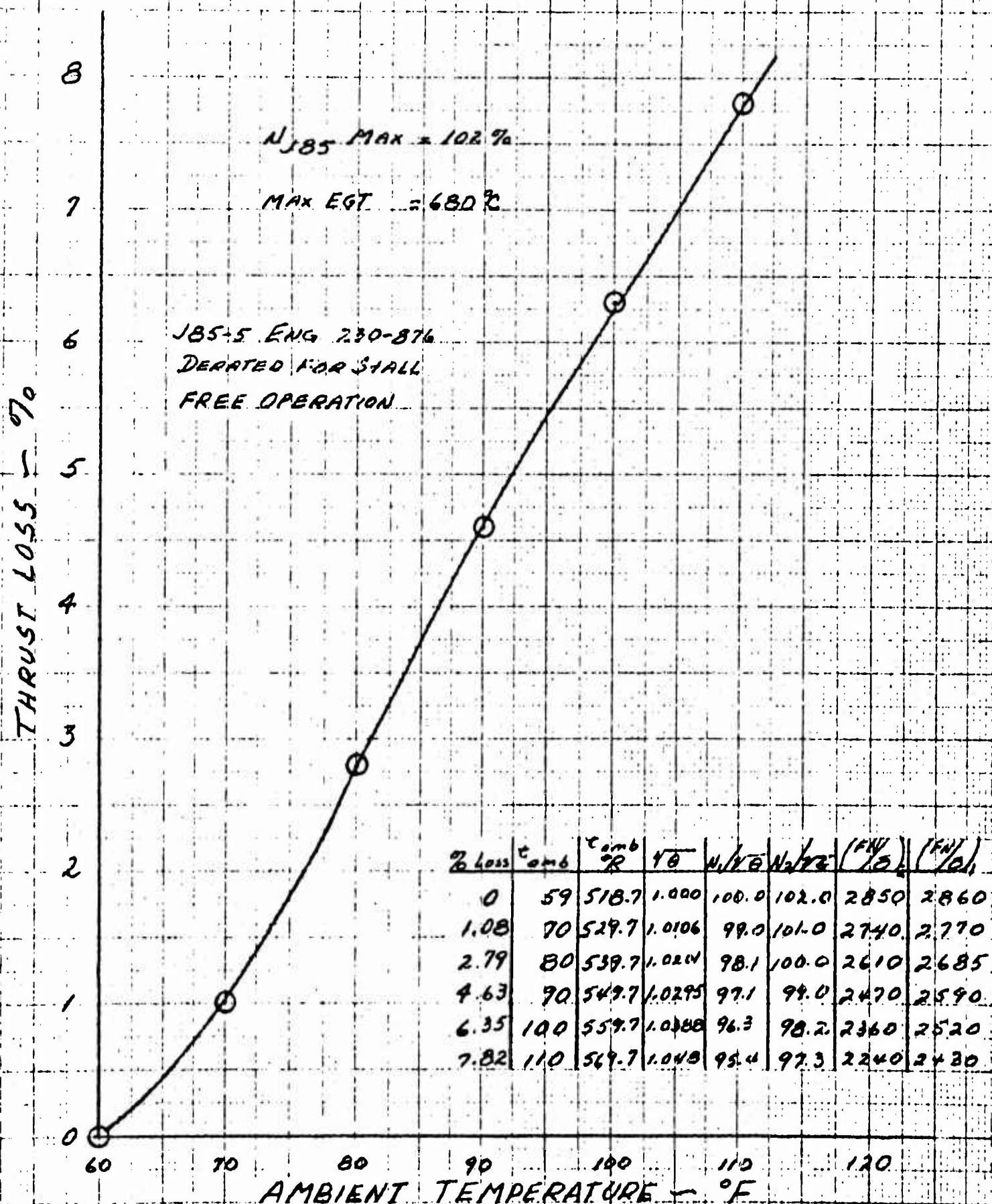


Figure 7.47 Thrust Loss due to Stall Free Operation Modifications

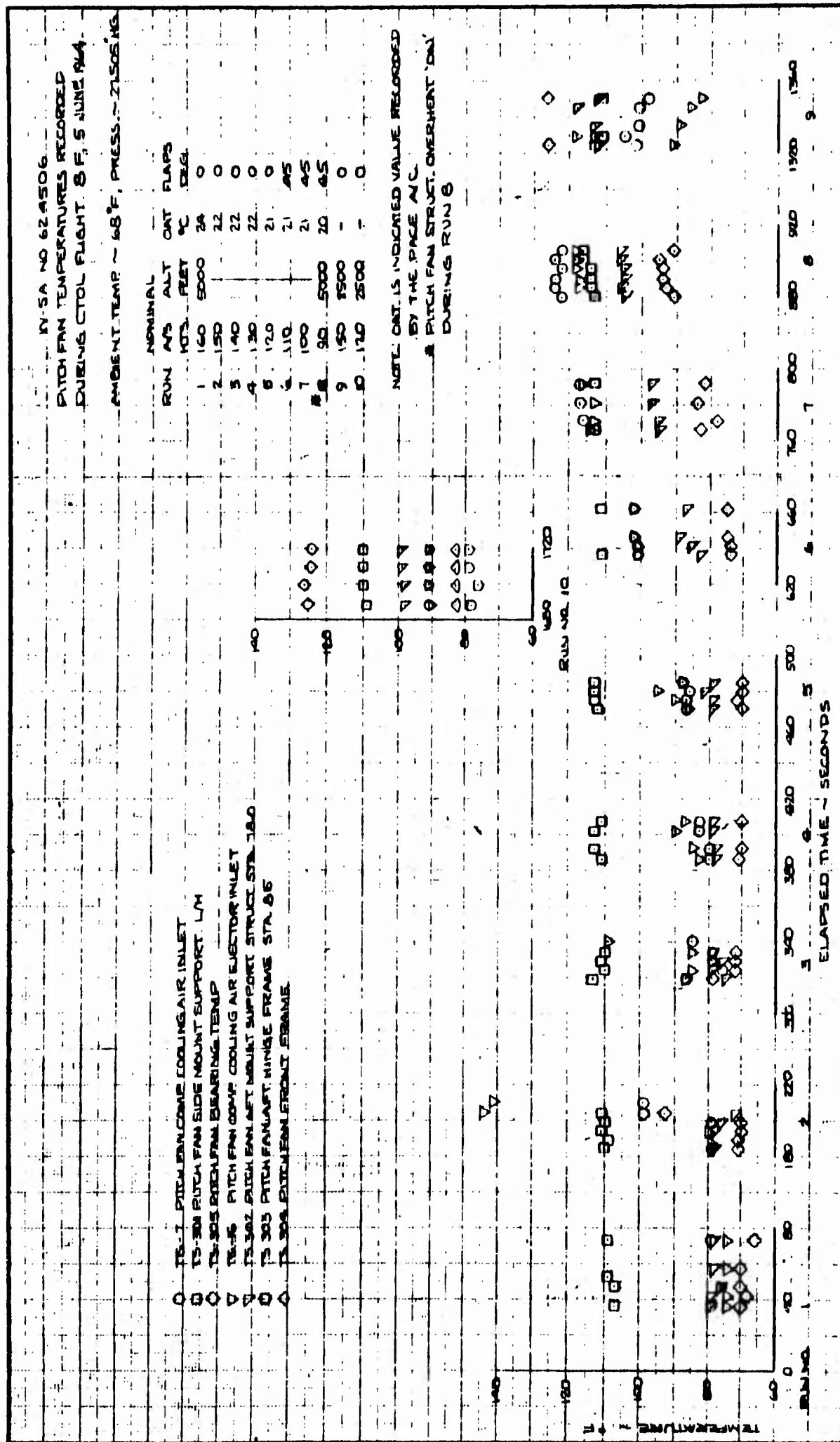


Figure 7.48 Pitch Fan Temperatures for Conventional Flight

XV-5A
A/C NO 624506
TEMPERATURE STUDY
JET MODE

TG 4 ELECTRIC COMP INLET AIR TEMPERATURE
TG 7 FRESH AIR COMP INLET " "
TG 21 ENGINE COMPRESSOR SECTION " "
TG 23 ENGINE TURBINE SECTION " "
TG 27 WING FAN AFT EJECTOR " "
TG 25 ENGINE TAILPIPE EJECTOR " "
TL 1 L/H ENGINE OIL TEMPERATURE
TL 2 R/H ENGINE OIL TEMPERATURE

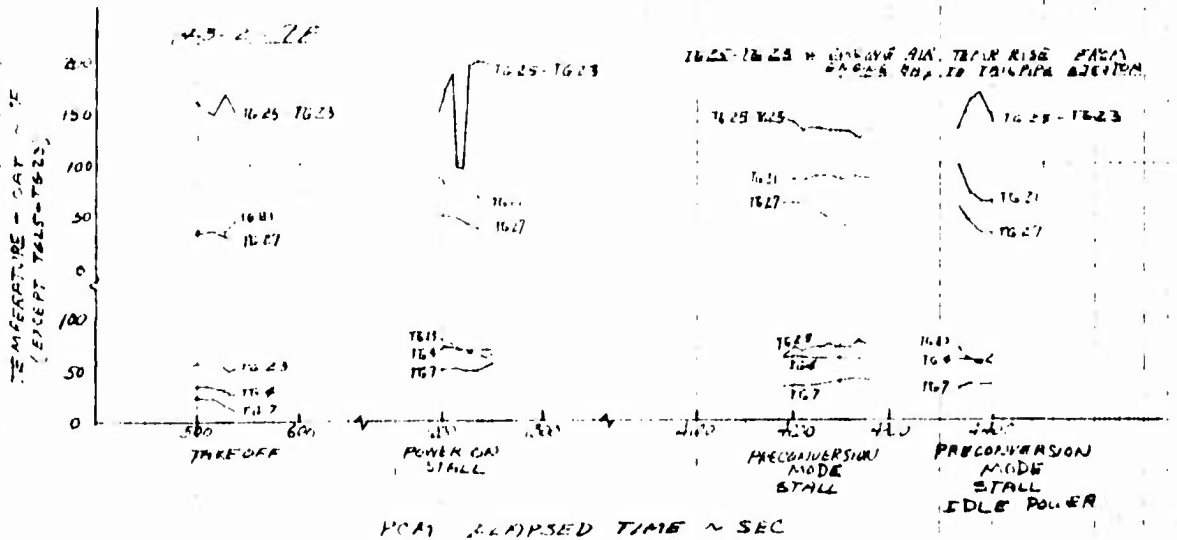
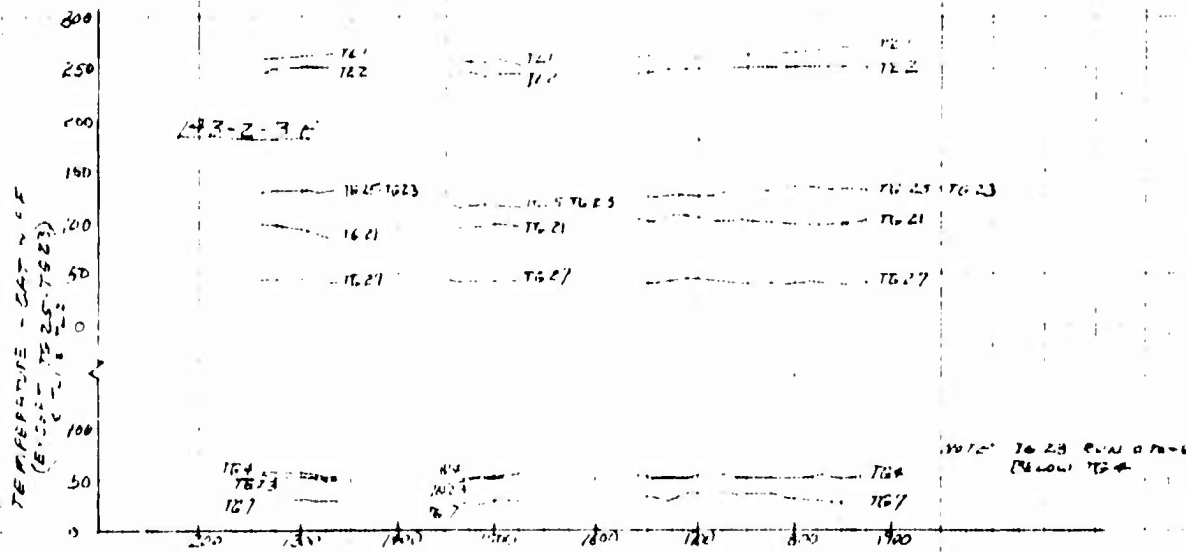


Figure 7.49 Temperature Study - Turbojet Mode

BLANK PAGE

8.0 AIRCRAFT SYSTEMS

8.1 HYDRAULIC

8.1.1 Hydraulic System History

When the flight test program was started on aircraft S/N 62-4506, the horizontal stabilizer actuator, SCD H0008, was not yet qualified. The vendor was unable to demonstrate performance compliance to specification requirements. As a result, the aircraft was restricted from conversion flights until an alternate design had been completed, manufactured and fully qualified.

Due to delays in the flight test program brought about by the exit louver actuator problems (discussed below), and the nose gear shimmy problem, the newly designed actuator was installed prior to the first flight of the aircraft.

During the first hovering liftoff attempts, ground runs .06G and .07G, it became apparent that directional and lateral control power were inadequate. Subsequent tiedown engine runs demonstrated that the louver servos were stalling under louver loads in the staggered condition. Load links were installed to determine actual louver loads throughout the control range, and new servo actuators were designed to meet the performance requirements under these loads.

These servo actuators were fabricated, qualified and installed in the aircraft prior to the first successful hovering attempt.

For historical information on the mechanical control system, refer to Section 6.2.7.

8.1.2 Hydraulic System Performance

The in-flight instrumentation of hydraulic system performance consisted of left hand and right hand reservoir fluid temperatures and the left hand diverter valve actuator temperature during Flights 2F through 80F and System No. 1 and System No. 2 pressures during Flights 2F, 3F, 4F, 8F, 9F, 10F, 13F, 14F and 17F.

Reservoir temperature is considered to be a good indication of overall system temperature with temperatures of approximately 10° F higher anticipated in the pump pressure lines. (This was confirmed during simulator tests.)

The diverter valve actuator is considered to be the hottest spot within the hydraulic system due to its close proximity to the diverter valve body.

The instrumentation for hydraulic system pressures apparently was malfunctioning during the majority of the flights. During Flights 11F and 17F, however, the data appears to be valid and shows very little pressure fluctuation during nominal maneuvering. (Flight 11F involved moderate pilot inputs for fore and aft maneuvering, sideslips and yaws; Flight 17F involved investigation of transients during switching from Primary to Standby S. A. S.) Pressure fluctuation during both flights was less than 60 PSI which is in agreement with flight simulator performance during nominal maneuvering.

The left hand diverter valve actuator temperature, in general, is considerably higher in the VTOL mode than in the conventional mode, although still well within the 275° F limits for a Type II Hydraulic System.

In the VTOL flight mode, it stabilized at 258° F after 6-1/2 minutes, 1,000 feet altitude, 70-90 KIAS, Flight 36F, and at 245° F after 7-1/2 minutes, 2,000 feet altitude, 90 KIAS, Flight 34F. In the latter flight, at approximately 8 minutes, the aircraft was converted to CTOL mode and the diverter valve actuator immediately started cooling and stabilized at 155° F after approximately 4-1/2 minutes.

The reservoir oil temperature is also higher in the VTOL mode than in the conventional mode, which is to be expected since all VTOL controls are hydraulically operated and only the ailerons in the conventional controls are hydraulically operated.

The left hand reservoir oil temperature tends to run somewhat higher than the right hand during fan mode flight. The left hand reservoir oil temperature stabilized at 155-160° F after approximately 5 minutes during Flight 34F, STOL takeoff, fan mode flight at 90 KIAS, 2,000 feet altitude. The right hand temperature stabilized at 135-140° F. Both systems cooled down to 120-125° F after converting to CTOL flight mode. During Flight 15F, fan flight out-of-ground effect, the left hand reservoir oil temperature stabilized at 171° F after approximately 6 minutes and during Flight 17F, fan flight investigating S. A. S. switching transients, it stabilized at 143° F after approximately 5-1/2 minutes. The right hand reservoir oil temperature stabilized 15° F cooler during this flight.

In general, these temperatures are extremely low for a Type II Hydraulic System, and should result in long life for all hydraulic system components.

The instrumentation for hydraulic system pressures was malfunctioning during all of the conventional flights. However, system demand during conventional flight is very small (only the ailerons and horizontal tail trim are hydraulically operated), and system pressure should hold very close to pump cut-off pressure (3000-3050 PSI). This has been confirmed on the flight control simulator.

The left hand diverter valve actuator temperature is considerably lower in the conventional flight mode than in the VTOL flight mode. It stabilized at 125-130° F after 10 minutes at 12,000-14,000 feet altitude, Flight 25F, and at 148° F after four minutes at 2000 feet altitude, 120 KIAS, Flight 33F.

The reservoir oil temperature is also lower in the conventional flight mode than in the VTOL flight mode. Both reservoir oil temperatures stabilized at 105-110° F after approximately 10 minutes, during Flight 25F, 14,000 feet altitude, and at 115-120° F after approximately 14 minutes during Flight 33F, 2000 feet altitude, 120 KIAS.

8.2 ELECTRICAL

8.2.1 Electrical System Chronology

Prior to rollout for functional testing, preliminary electrical control systems tests were made in the hangar. These were performed with an auxiliary power unit and in conjunction with the ground vibration tests made on Aircraft S/N 506. All control surfaces and electrical support systems including the conversions control system received a complete operational check. The same check was performed on Aircraft S/N 505 although no vibration testing was performed on this aircraft at this time. Results were:

- a. Total power required did not exceed 1.5 KW.
- b. The flaps down signal properly operated the preconversion mode, however a flaps up signal improperly caused a reversal of the preconversion sequence.

The load analysis prediction of 3.3 KW maximum power requirement included an allowance of approximately 1.5 KW for flight test instrumentation. Since this equipment was not operating, power requirements were satisfactory.

The improper preconversion operation was researched and attributed to a voltage spike caused by a flaps actuator contactor inductive surge which triggered a sensitive relay in the control system. A zener suppressor was installed, after which the airplane operated satisfactorily.

Engine powered functional tests for both aircraft started 11 December 1963 and were concluded 11 March 1964. It is estimated that each aircraft experienced an electrical "power on" condition of approximately 100 hours. During this time an estimated 50 hours of systems operation was performed. Within this 50 hours, Aircraft No. 506 experienced approximately 8 hours of engine run time and Aircraft No. 505 had 5 hours time in which engines were running and the aircraft were operating on ships' generator power. In addition, Aircraft No. 505 was tested under electrical power for 27 hours at the Ames test facility; ships' generators were not used during this time.

Data taken from early runs in the test enabled the adjustment of generators voltage (required only on Aircraft No. 506) to assure proper bus voltage and generator equalization. All subsequent runs demonstrated steady state bus voltages within specification. Load sharing and equalization met specifications. Steady state power requirements did not exceed 3.0 KW (includes test instrumentation requirements). Since system capability is 9.0 KW, adequate circuit fault clearing was and is assured.

During the functional test the following modifications were made:

- a. The flaps switch was changed and relocated.
- b. The VTOL operation of the horizontal stabilizer was changed.
- c. The horizontal stabilizer emergency trim circuits were changed.
- d. The structure overheat warning sensitivity was changed.
- e. Abort command provisions were installed to enable rapid reconversions.

These changes are described more fully below.

Flaps control was obtained by mechanically operating a lever on the throttle quadrant which articulated concealed plunger actuated switches. As a matter of pilot convenience, this control was removed and a toggle switch was installed in the instrument panel in proximity to the louver switch.

In the VTOL mode, the horizontal stabilizer received a programmed trim signal as a function of longitudinal stick displacement. As a result of simulator studies, this function was removed and changes in the electrical mixer and controls interlock system were made to provide for an automatic stabilizer full up command as a function of louver angle $\leq \beta_v 40^\circ$. (This angle was later changed during flight test.)

One of the functions of the electrical mixer box was to provide for emergency horizontal stabilizer trim. Reliability studies prompted the change so that separate isolating relays and circuitry were installed to provide an alternate shunt path around the electrical mixer and controls interlock system for trimming the stabilizer.

During test runs frequent structures overheat warnings were obtained. Comparisons were made with thermal data taken by instrumentation. Localized heating was evident. Because the warning system utilizes "continuous loop" sensing, the data variables were compared with the optimizing parameters. A careful change was made in the system biasing resistor with safe reservation for a future change which was in fact made later (during flight test).

Because of a programmed time delay between the horizontal stabilizer motion and the diverter valves command during a VTOL mode change, the pilot was unable to rapidly reconvert to VTOL mode. New circuits were added to the existing stabilizer actuator position switches. Later (during flight test) these circuits were removed and new separate stabilizer position switches and circuits were installed to improve systems reliability.

At the conclusion of the functional test program Airplane No. 506 was shipped to Edwards AFB. While there and prior to entering into flight test, the electrical system was modified as follows:

- a. A fan cavity overheat warning system was installed.
- b. A horizontal stabilizer motion indication system was installed.

Evidence of excessive diverter valve leakage in the CTOL mode during functional testing warranted the installation of thermocouples, lead circuitry, and appropriate cockpit instruments to permit the pilot to monitor the fans cavities temperatures.

Simulator studies decided the need for early warning of a possible runaway horizontal stabilizer. Accordingly, a system was installed utilizing stabilizer motion transponder switches, a cockpit signal light, and an

audible warning signal generator to provide an alerting tone in the pilot's headset at any time stabilizer motion occurred.

At Edwards AFB test operations, several minor changes were made prior to the first hover operations (Flight No. 9). They were:

- a. Fan bearing temperature warnings were removed from the pilot's annunciator system.
- b. The fuel systems control panel was modified.

Instrumentation circuitry installed for data recording and telemetering of the fans bearings temperatures caused spurious warnings on the annunciator system. Accordingly, the warning circuitry was removed from the sensitive relays in the ships' systems. These were later restored at the completion of Phase I operations and filters were installed to damp out stray pickup on the thermocouple leads.

The direction and sense of rotation of the fuel systems management switches were changed as a matter of pilot convenience. On-off flag indicators were installed to display the actual condition of the fuel control valves. Additional wiring and relays were added to permit display of a fuel low level condition on the annunciator panel. Fuel low level condition is now displayed on both the fuel management panel and the annunciator system.

Thermal problems were encountered in the nacelles, therefore prior to Flight No. 13 the following changes were made:

- a. Fire warning sensitivity was changed.
- b. A blinker system was installed for fire warning.

Investigation showed that the effects of engine compressor compartment temperatures (associated with engine stall characteristics) and radiant and infrared heating in the combustion chamber areas of the nacelles caused premature fire warnings. Accordingly, the "temperature sensing loop detectors" were rerouted and a new biasing resistor was installed in each nacelle warning circuit.

Blinker relay timers were installed to each fire warning system to provide early warning of a nacelles overheat condition. The blinker signal now precedes the "steady on" fire warning. No spurious fire warnings have occurred since this change although there have been a few instances where the blinker warning has been received and was correlated with a known in-flight high temperature condition.

Between Flights 21 and 26 thermal problems due to wing fans scroll temperatures made the following changes in the structures overheat warning system necessary:

- a. Insulation was applied to the "thermal sensing loop".
- b. The structures overheat warning sensitivity was changed.

In the wing and fuselage space frame areas adjacent to the fans scrolls, such sections of the "temperature sensing loop" that might be affected by direct radiant heat were insulated with a metallic tape to reduce the "rise time". This was done only after a thorough assessment by the Thermal Group. Along with this change, the resistor bias for the warning system was again changed (reference change made during functional test). No spurious warnings have been experienced since this final rework, however valid warnings have been received that correlate with known structures overheat conditions.

Flights were made with takeoffs in the STOL configuration up to and including Flight No. 33. During this period it was determined that the airplane flew best (on fans) at an indicated louver angle of $\beta_V 45^\circ$. The conversion controls interlock system was devised such that conversions were to be made at an indicated louver angle of $\beta_V 50^\circ$. Accordingly, the following temporary changes were made prior to the first conversion VTOL to CTOL (Flight No. 34):

- a. Adjusted louver interlock switches to $\beta_V 45^\circ$.
- b. Adjusted louver/fans trim interlock switches to $\beta_V 35^\circ$.

The conversion control interlock switches in the wing fans exit louver actuator SCD E0045-1 were adjusted to permit conversion to CTOL mode at/or before $\beta_V 45^\circ$ indicated angle (set point is $\beta_V 43^\circ$). The ability for the pilot to control louver angle to $\beta_V 50^\circ$ however was still maintained.

Those switches whose signal caused the pilot's trim functions to change over from CTOL trim to VTOL trim at $\beta_V 40^\circ$ were changed to affect the changeover to $\beta_V 35^\circ$. This is the same point at which the horizontal stabilizer receives a programmed "full up" signal.

Conversion flights were made including Flight No. 38 which involved full transition, after which final adjustment of louver actuator switches was made to achieve the optimum louver interlock angles. These adjustments now provide for:

- a. Open louvers in preconversion to $\beta_v 45^\circ$, was $\beta_v 50^\circ$.
- b. Convert to VTOL interlocks at $\beta_v 45^\circ$, was $\beta_v 50^\circ$.
- c. Close louvers in VTOL to $\beta_v 45^\circ$, was $\beta_v 50^\circ$.
- d. Convert to CTOL interlocks at $\beta_v 45^\circ$, was $\beta_v 50^\circ$.
- e. Changeover trim from CTOL to VTOL at $\beta_v 30^\circ$, was $\beta_v 35^\circ$; was $\beta_v 40^\circ$. At this angle the horizontal stabilizer now receives a programmed "full up" command from the vector actuator.

At this same time, the diverter valve delay when converting from CTOL to VTOL mode was changed from 0.30 seconds to 0.15 seconds to reduce transients about the longitudinal axis.

The diverter valves had undergone progressive increase in tightening in an effort to reduce gas leakage. After the conclusion of Flight No. 40, during hangar inspections, it was determined that the diverter valve seals were acting as springs. Their stored energy caused the diverter to move out of mode position when electrical power was temporarily removed during systems changeover. Accordingly, the following changes were made to the controls interlock systems:

- a. Bipolar relays (magnetic latching) were installed as slave relays to the diverters hydraulic valves signal control.
- b. Additional diverter valve position switches were installed in each mode position and wired to provide a final motion position signal to the interlock system. These switches now serve a redundant function, providing for mode latching.

The final change made to the electrical control system was made at the conclusion of Flight No. 64. Studies showed a reliability improvement could be made if separate switches were installed to replace the Abort Command signal function obtained from switches in the horizontal stabilizer actuator. Accordingly, the new installation was made.

No further changes were required and the electrical system continued to function to specifications to Flight No. 80, the conclusion of Phase I testing for Aircraft No. 506. Aircraft No. 505 was returned from the Ames test facility, all electrical changes incorporated and also made 29 successful flights to conclude the testing program.

8.2.2 Electrical System Performance

There is no significant difference in steady state power requirements in either VTOL or CTOL mode. The electrical systems function well, and per specification in either mode, including mode change. Changes made to the electrical systems throughout the flight test program Phase I were, in general, not significant to the successful operation of the aircraft in any one mode (see chronology and details given in preceding section).

8.3 PROPULSION SYSTEM HISTORY

The propulsion system components, whose difficulties or modifications were of significance, are listed below. The major components are separate and listed by the first flight on which the modification or repair was flown. Airplane S/N 505 was modified prior to its first flight to incorporate improvements required by Airplane No. 506 experience.

AIRCRAFT S/N 505

<u>Flight</u>	<u>Date</u>	<u>L. H.</u>	<u>R. H.</u>
---------------	-------------	--------------	--------------

Engines J-85-5B

1F	10-26-64	S/N 230-876	S/N 230-875	These engines were installed prior to first flight and operated throughout Phase I without incident.
----	----------	-------------	-------------	--

Diverter Valves L. H. P/N 4012001-937 and R. H. P/N 4012001-938

IF	10-26-64	S/N 007	S/N 008	
13	12-16-64	S/N 007	S/N 008	Reworked seal segments of aft door of both valves to improve sealing.
24	1-13-65	S/N 007	S/N 008	Tack welded all door heat shield hold down tabs.
25	1-20-65	S/N 007	S/N 008	Replaced diverter valve micro switches P/N 12HR12RB.

<u>Flight</u>	<u>Date</u>	<u>L. H.</u>	<u>R. H.</u>
---------------	-------------	--------------	--------------

Pitch Fan P/N 4012001-940

1			S/N 002	Installed prior to first flight and operated throughout Phase I
---	--	--	---------	---

Wing Fans L. H. P/N 4012001-941 and R. H. P/N 4012001-942

1	10-26-64	S/N 005	S/N 006	
7	11-19-64	S/N 005	S/N 006	Aluminum exit louvers P/N 4012153-749G1 through G21 (21) and P/N 4012153-748G1 through G 21 (21 installed.
24	1-13-65	S/N 005	S/N 006	Installed steel circular vanes P/N 4012001-405.

Miscellaneous Components

5	11-16-64	SCDP0021-1	Shaft - Accessory Drive	Replaced shaft due to vibration.
---	----------	------------	-------------------------------	----------------------------------

AIRCRAFT S/N 506

Engines J-85-5

1 F	5-25-64	S/N 230-730	S/N 230-729	
12 F	7-23-64	S/N 230-730	S/N 230-233	S/N 230-729 removed after stall and flameout.
13 F		S/N 230-730	S/N 230-233	Repair fuel flow Transmitter Elec. Harness. Rescheduled fuel control.
15 F		S/N 230-730	S/N 231-232	S/N 230-233 removed after an overtemp.

<u>Flight</u>	<u>Date</u>	<u>L. H.</u>	<u>R. H.</u>
---------------	-------------	--------------	--------------

Engines J-85-5 (Continued)

41F	10-28-64	S/N 230-730	S/N 231-232	Engines removed for inspection and diverter valve repair after S/N 231-232 flameout due to diverter valve door failure.
-----	----------	-------------	-------------	---

Diverter Valve L. H. P/N 4012001-937 and R. H. P/N 4012001-938

9F	7-16-64	S/N 005	S/N 006	Aft Door - R. H. Div. Valve cracked 4 places pivot point weld. Fwd Door - R. H. Div. Valve cracks in pivot point welds. Aft door and fwd door L. H. Div. Valve cracks in pivot point weld. Aft trunnion frozen in ball.
22F	9-10-64	S/N 005	S/N 006	S/N 006 Aft door removed for rework of seal segments; repaired doors of valves.
38F	10-9-64	S/N 005	S/N 006	S/N 005 - Repair weld weld around L. H. lower trunnion mount and actuator support bracket.
41F	10-28-64	S/N 005	S/N 006	S/N 005 - Doors removed for inspection and repair. S/N 006 - Valve door failed causing flameout. Installed secondary switches. Replaced doors of S/N 006.
51F	11-18-64	S/N 005	S/N 006	S/N 005 - Repaired cracks in both doors by welding. S/N 006 - Repaired cracks in both doors.

<u>Flight</u>	<u>Date</u>	<u>L. H.</u>	<u>R. H.</u>
---------------	-------------	--------------	--------------

Diverter Valves (Continued)

61F	12-7-64	S/N 005	S/N 006	Hydraulic actuator leaking excessively - "O" rings replaced.
67F	12-18-64	S/N 005	S/N 006	2 small cracks repaired. Welded in aft door of each diverter valve.
78F	1-14-65	S/N 005	S/N 006	Both valves - tack welded all heat shield hold down tabs both doors - one tab missing S/N 006

Pitch Fan P/N 4012001-940

1F	5-25-64	S/N 003		
13	8-15-64	S/N 001		S/N 003 Sustained F. O. D. removed.
41F	10-28-64	S/N 001		Replaced instrumentation slip rings.
71F	12-29-64	S/N 001		Minor F. O. D. to pitch fan bucket carrier, P/N 4012001-173, and bucket shroud lip - no repair required.

Wing Fans L. H. P/N 4012001-941 and R/H. P/N 4012001-942

9	7-16-64	S/N 007	S/N 004	R. H. fan air seals cracked, worn and broken. Circular inlet vanes installed. P/N 4012001-318 modified to fit. Repaired cracks in 2 turbine exit louvers, 1 from each fan. Installed new louvers and actuators, push rods and reworked rear frame.
---	---------	---------	---------	--

<u>Flight</u>	<u>Date</u>	<u>L. H.</u>	<u>R. H.</u>	
<u>Wing Fans (Continued)</u>				
22	9-10-64	S/N 007	S/N 004	Replace circular inlet vanes with new type P/N 4012284-446.
26	9-23-64	S/N 007	S/N 004	S/N 007 replaced loose bolt fwd quarter outbd circular vane.
31	9-26-64	S/N 007	S/N 004	S/N 004 - Rotor blade platform P/N 4012001-164R-G1 S/N 69 removed cracked trailing edge and bottom tab not replaced.
38F	10-9-64	S/N 007	S/N 004	S/N 007 - Turbine exit louver P/N 4012001-760G1 W/N 003L.
51F	11-18-64	S/N 007	S/N 004	S/N 007 - Blade Platform P/N 4012001-159G1 cracked loose at fwd end - removed.
59F	11-25-64	S/N 007	S/N 004	S/N 007 (2) Blade platform position 6 and 23 cracked loose causing slight damage to rear frame. S/N 004 R. H. outbd fwd quadrant Mod. III aluminum circular vane removed and replaced with instrumented steel vane P/N 4012001-405G2 for Flight 59F only.
63F	12-9-64	S/N 007	S/N 004	S/N 004 - Blade platform P/N 4012001-164 pos. 13 cracked and removed.
64F	12-14-64	S/N 007	S/N 004	S/N 007-6 - Blade platforms P/N 4012001-159 pos. 19, 13, 28, 7, 26, and 33 cracked and removed.

<u>Flight</u>	<u>Date</u>	<u>L. H.</u>	<u>R. H.</u>	
<u>Wing Fans (Continued)</u>				
66	12-15-64	S/N 007	S/N 004	S/N 007 (2) blade platforms pos. 12 and 17 cracked - removed.
67 F	12-18-64	S/N 007	S/N 004	S/N 007 (3) blade platforms removed after Zyglo showed 14 platforms cracked on S/N 007 and 18 on S/N 004.
78 F	1-14-65	S/N 007	S/N 004	New modified blade platforms installed.

Miscellaneous Components

1 F	5-25-65	SCDP0043-1	Fire Ex- tinguisher bottle	Insulated bottle to prevent loss of fluid due to over-heating after shutdown.
2 F	5-27-65	143P006	Engine Air Inlet	Ram Air flapper hinge re-paired.
13 F	8-15-64	143P094	Pitch Fan Inlet	Reinforced lower lip. In- stall compressor Comp. ejectors - both engines.
		143P006		Eng. air inlet ducts per- forated to increase engine stall margin. Modified T2 sensor inlets.
41 F	10-28-64	143P011	Starting System	Starter ducting modified to locate inlet fwd of wing.
		143P010	Pitch Fan Inlet	Installed close tol. pins, heavier rods, stops and new load limiting actuators.
52 F	11-19-64	SCDP0021-1	Shaft Ac- cessory Drive	Removed, cleaned, and re- lubricated shaft - vibrating.

Flight Date

Miscellaneous Components (Continued)

61F	12-7-64	SCDP0012-1	Valve-Start- er Check	Cleared interference by grinding after valve stuck open.
76F	12-31-64	143 P015	Thrust Spoiler Instl.	Repair welded cracked hinge bracket.
78F	1-14-65	143 P015	Thrust Spoiler Instl.	Repair welded cracked hinge bracket and rigged correctly.
79F	1-26-65	143 P006	Engine Air Inlet	Repaired hinge cooling air inlet flapper.

8.4 XV-5A LANDING GEAR

During the early phases of taxi testing, problems were encountered involving dynamic oscillation of the nose wheel (see Paragraph 7.2.1.3). A complete dynamic analysis led to the following design changes:

Increased fork stiffness

Increased torque linkage stiffness

Positive axle retention

Enlarged capacity shimmy damper, using higher viscosity damping fluid

Increased rigidity of Shimmy Damper mounting

The effectiveness of these changes was demonstrated by a shimmy test program conducted at the Lockheed/California shimmy test facility prior to installation on the aircraft.

Early in the engine ground test runs it became apparent that thermal insulation was required to protect the main gear and main gear well during extended fan mode operations in ground effect (see Paragraph 6.3.2). Heat shields were developed for the main gear members. A fixed closure was developed to replace the folding main gear doors.

Extensive fan mode testing in a fixed gear configuration with these devices installed, provided basic data leading to the design of external thermal blankets for the retractable door configuration.

After installation of the door heat blankets and refinement of the gear heat shielding, the aircraft performed its specified transition missions, in the retractable gear configuration without overheating problems.

Early in the high speed flight testing with gear retracted, a problem was encountered with intermittent unsafe gear cockpit indications. This was traced to mis-rigging of the forward and aft door closed lock linkages permitting marginal actuation of the DOORS "CLOSED AND LOCKED" switch. Refinement of rigging technique eliminated this problem.

Brake overheating problems were encountered during the test program. These were traced to excessive pilot use of brakes to limit taxiing speed over the long distance taxi runs required by some operations at Edwards AFB. Use by pilots of the engine thrust spoilers during taxiing largely eliminated the problem. The following design changes were also made and introduced with new orders of brake spares:

- a. Material of brake anvil casting changed from magnesium to aluminum.
- b. Thickness of brake disc increased from .343 to .468 with corresponding increase in K. E. capacity.
- c. Revised assembly technique developed to maintain adequate pad to disc running clearance.

No flight discrepancies attributable to the landing gear hydraulic system were noted during the Flight Test Program.

No situation arose during the Flight Test Program requiring emergency gear extension and no problems with the system were encountered during routine hangar checkouts. The only change to the emergency system involved relocation of the system pressure gauge and provision of an additional charging valve at the rear end of the wheel bay. This change facilitated ground maintenance with the gear in the fixed configuration.

No problem was encountered during the flight test program attributable to the landing gear cockpit indication and warning system.

8.5 AIRSPPEED SYSTEM

8.5.1 General Description and History

The original airspeed systems consisted of a low airspeed indicator and a high airspeed indicator/Mach meter mounted in the pilot's instrument panel and connected to the wing boom pitot static system. In addition, an airspeed transducer for the PCM was connected to the nose boom pitot static system. During Phase I of the Flight Test Program, a number of changes were initiated in both the pilot's airspeed system and the PCM airspeed system in an attempt to improve the accuracy of the two systems, especially for fan mode flight. Figures 8.1 through 8.14 present a chronological history of the airspeed systems in aircraft S/N 62-4505 and 62-4506.

The histories have been documented based on Flight Test Engineering Work Orders, Instrumentation Calibrations, and Flight Summary Reports. Exact configuration during some periods is unknown due to insufficient data. Applicable instrument correction curves (ΔV_{ic}) and position error correction curves (ΔV_{pc}) are listed for the individual systems.

The wing boom pitot static system proved unacceptable for the pilot's low airspeed indicator during fan flight mode. Consequently the pilot's low airspeed indicator was connected to the nose boom pitot static system in parallel with the PCM transducer. This was accomplished prior to Test 24.01G on aircraft S/N 506 and prior to 27 F on aircraft S/N 505. The small I. D. tubing installed in the nose boom pitot static system for the PCM instrumentation proved to be too small for the dual systems producing a lag in the airspeed readings under dynamic conditions. Figure 8.15 illustrates this lag by comparing the wing boom indicated airspeed as called out by the pilot and corrected for instrumentation error with the nose boom indicated airspeed as recorded on the PCM. Large I. D. tubing was installed in the system to eliminate this problem prior to Test 41.0F on aircraft S/N 506 and prior to the first flight with aircraft S/N 505.

Prior to Test 5 on aircraft S/N 505 and prior to Test 78 on aircraft S/N 506, the wing boom pitot static head was rotated 180 degrees so that the static ports would be located on the bottom side of the probe. This was accomplished to increase the accuracy of the pilot's high airspeed indicator system in the conventional flight mode.

Aircraft S/N 506 originally had a valve installed between the low airspeed indicator and the wing boom pitot static pressure line to protect the low airspeed indicator at high airspeeds. This valve was actuated by a solenoid

and triggered by the mode selector switch. The valve closed off the pitot static pressure line and permitted the pressure to the indicator to bleed off at a given leakage rate designed into the system. Problems with this system early in the program resulted in replumbing the low airspeed indicator system, by-passing the shut-off valve, and restricting the maximum airspeed of the aircraft to the maximum reading on the low airspeed indicator. Prior to Test 78, the low airspeed cut-off valve was again installed in preparation for high speed flight. The leakage rate introduced into the nose boom pitot static system by this valve installation resulted in a large error in the PCM airspeed as illustrated by Figures 8.16 and 8.17. Details of the installation on aircraft S/N 505 are unknown, since no drawings are available on the low airspeed cut-off valve. The first indication of a low airspeed indicator being used is prior to Test 23.01G (reference W/O 505-200, 1-5-65).

From Test 24.01G through 77.0F aircraft S/N 506 had two low airspeed indicators mounted in the cockpit for the pilot. One was connected to the wing boom pitot static system and the other to the nose boom pitot static system. During this period the high airspeed indicator/Mach meter was removed from the aircraft. This was done in an attempt to determine the effectiveness of the wing boom probe in fan flight. At times it was impossible to determine from the radio logs which airspeed system the pilot was reading.

In order to obtain better resolution on the PCM low airspeed data, the 0 to 1.0 psid transducer was replaced with a ± 0.3 psid transducer prior to Test 22.0F on aircraft S/N 506 and prior to hover flight (Test 25.0F) on aircraft S/N 505. Intermittent electrical noise proved to be a constant problem with the PCM airspeed system.

8.5.2 Calibrations and Data Accuracy

Figures 8.18 through 8.20 present the pitot static boom correction curves for the wing boom in the CTOL mode only and the nose boom in both the CTOL and VTOL modes. The appropriate correction curves are designated by numbers 1, 2, and 3 in the chronological histories of the airspeed systems. The instrument correction curves for both the cockpit indicators and the PCM transducers are listed by their appropriate calibration number. (Example, PG-3-002-1, PG-3 low airspeed, -002 second calibration, -1 PCM transducer.)

Only the nose boom system should be used in correlating flight data with airspeed in the fan flight mode.

The wing boom position error correction was calculated from data obtained after the pitot static probe had been inverted so that the static ports were located on the bottom of the probe. When using this correction on flights prior to inverting the probe (Test 5.0F, aircraft S/N 505, Test 78.0F, aircraft S/N 506) a small error is expected, however, it should be small.

PCM and low airspeed indicator data are suspect for Tests 24.0F through 29.0F, aircraft S/N 505 and Tests 78.0F through 80.0F, aircraft S/N 506. During this period modifications were being made to the nose boom pitot static system in an effort to get the low airspeed shut-off valve operating correctly. No airspeed indicator lag correction ($\Delta V_{ic\ell}$) has been determined, therefore only steady state data should be considered.

8.5.3 Calculations

Calibrated airspeed is obtainable from the following equation:

$$V_c = V_i + \Delta V_{ic} + \Delta V_{pc}$$

V_i is defined as the indicated airspeed and applies to both the cockpit instrument and as recorded by the PCM system. ΔV_{ic} is defined as the airspeed indicator instrument correction. In the case of the PCM system it applies to the transducer calibration curve and the corrections required due to the limitations of the data reduction system. ΔV_{pc} is defined as the airspeed indicator position error correction and applies to both the cockpit instrument and the PCM system since it is a function of the location of the pitot static probe. During most of the Phase I Flight Test Program V_i was recorded by the PCM system in PSID. This differential pressure may be easily converted to knots by use of standard tables (see ANA Bulletin No. 418, 21 November 1952).

Step 1 - Obtain indicated airspeed (V_i) from either pilot callouts as entered in the radio log, from PCM tab data, or plotted PCM data.

Step 2 - Airspeed indicator instrument correction (ΔV_{ic}) is obtained from the appropriate curve as listed in Figures 8.1 through 8.14. The ΔV_{ic} curves are filed in the Instrumentation Calibration Book under their corresponding calibration number. If the last digit of the calibration number is a 1, the curve applies to the PCM transducer airspeed indicator. If the last digit is a 4, the curve applies to the pilot's airspeed indicator.

Step 3 - Indicated airspeed corrected for instrument error (V_{ic}) is equal to $V_i + \Delta V_{ic}$.

Step 4 - The airspeed indicator position error correction (ΔV_{pc}) is obtained from Figures 8.18 through 8.20 as listed in the chronological histories of the airspeed system (Figures 8.1 through 8.14).

Step 5 - Calibrated airspeed (V_c), or indicated airspeed corrected for instrument error and position error is equal to $V_{ic} + \Delta V_{pc}$. No airspeed indicator lag correction (ΔV_{icl}) has been determined, therefore only steady state data should be considered.

8.6 XV-5A FUEL SYSTEM

The fuel system and supporting systems have operated satisfactorily throughout the flight testing. No specific fuel system flight tests have been accomplished. To date only minor discrepancies have been reported, such as: the failure of the booster pump solenoid control valve to reopen due to high air pressures during high powers at low attitude. In the design phase it was decided that the lighter valve would be adequate inasmuch as normally there would be no purpose in closing the normally open valves, much less at high powers at low altitude. Higher capacity valves are presently being procured to replace the existing valves to avoid incident during training and testing.

There have been some fuel shut-off valves replaced due to teflon seat warpage, apparently due to excessive ambient temperature.

Most other discrepancies have been traced to accidental damage during maintenance.

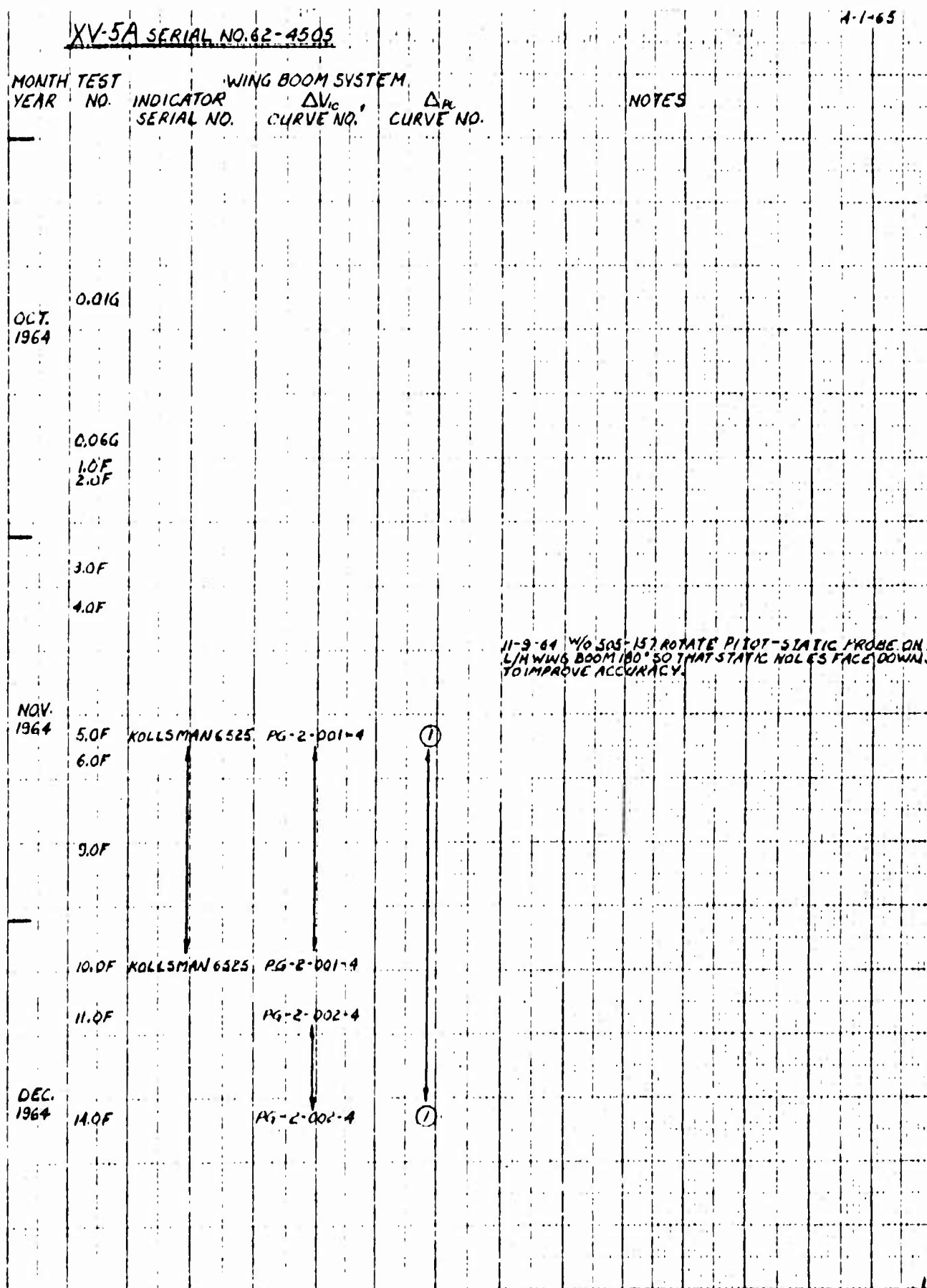


Figure 8.1 Airspeed Measurement System History

XV-5A SERIAL NO. 62-1505					4-1-65
MONTH YEAR	TEST NO.	INDICATOR SERIAL NO.	ΔV_L CURVE NO.	ΔV_H CURVE NO.	NOTES
DEC. 1964	23.0F				
	23.916				1-5-65 W/O 305-200 CONNECT LOW AIRSPEED INDICATOR IN COCKPIT IN PARALLEL WITH NOSE BOOM AIRSPEED SYSTEM TO PCM. DISCONNECT LOW AIRSPEED FROM WING BOOM. CONFIRM INSTALLATION OF LOW AIRSPEED SYSTEM CUT-OFF AT HIGH AIRSPEEDS FUNCTIONALLY. COCKPIT INSTALLATION SHOULD INCLUDE: A-ONE LOW AIRSPEED INDICATOR CONNECTED TO NOSE BOOM. B-ONE HIGH AIRSPEED INDICATOR (MACH METER) CONNECTED TO WING BOOM.
JAN. 1965					
	29.0F				
NOTE: 1- AIRSPEED INDICATOR INSTRUMENT CORRECTION CURVES ARE FILED IN THE INSTRUMENTATION CALIBRATION BOOK.					

Figure 8.2 Airspeed Measurement System History

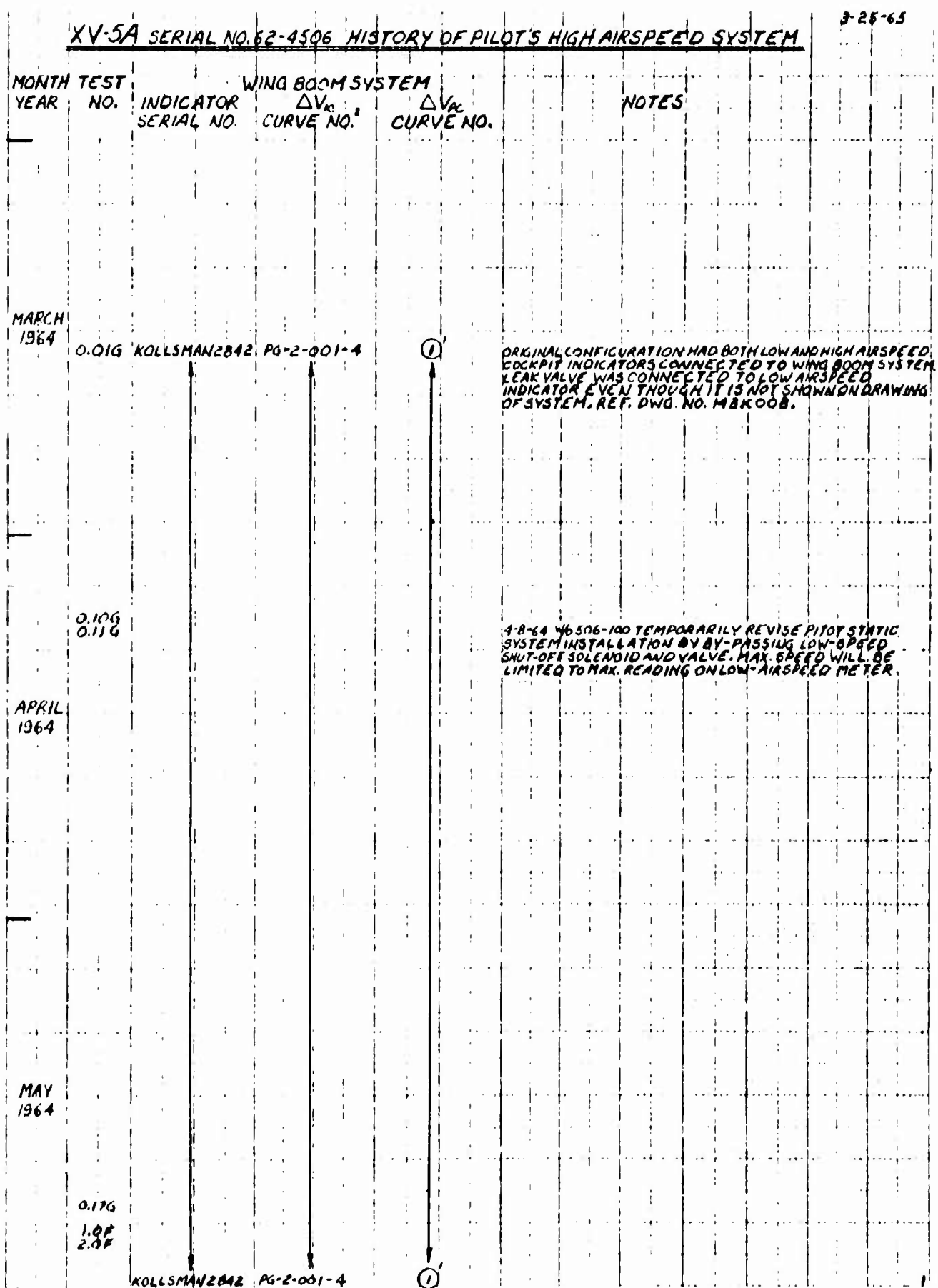


Figure 8.5 Airspeed Measurement System History

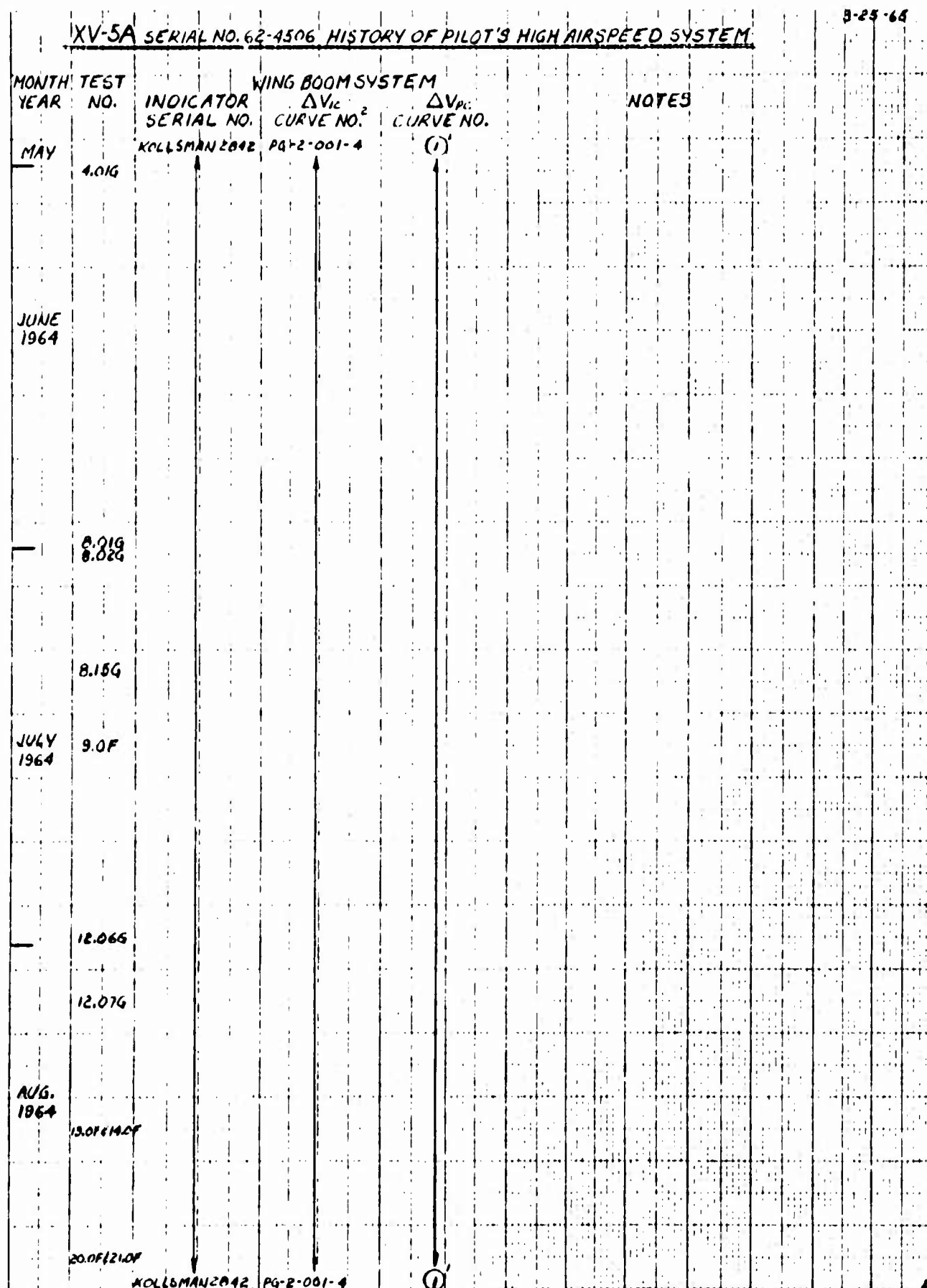


Figure 8.6 Airspeed Measurement System History

XV-5A SERIAL NO. 62-4506 HISTORY OF PILOT'S HIGH AIRSPEED SYSTEM					3-11-65
MONTH YEAR	TEST NO.	INDICATOR SERIAL NO.	WING BOOM SYSTEM ΔV_{IC} CURVE NO.	ΔV_{IC} CURVE NO.	NOTES
AUG. 1964		KOLLSMAN 2842	PG-2-001-A	(1)	
	21.01G				
	21.05G	KOLLSMAN 2842	PG-2-001-A	(1)	
	22.0F				
SEPT. 1964					9-10-64 40506-367 REMOVE THE TWO AIRSPEED INDICATORS FROM THE PILOT'S COCKPIT AND INSTALL TWO 0-160 K INDICATORS, CONNECT ONE TO THE NOSE BOOM PITOT STATIC SYSTEM AND ONE TO THE WING BOOM PITOT STATIC SYSTEM.
	31.0F				
	32.0F				
OCT. 1964					
	43.0F			(1)	
	44.0F/45.0F				REMOVED COCKPIT LOW AIRSPEED INDICATORS AND INSTALLED HIGH AIRSPEED INDICATORS PRIOR TO TEST 43.0F, FLIGHT SUMMARY REPORT EIL-5A-12-43F, NO W/O TO VERIFY REPLACEMENT.
	46.0F/47.0F				INSTALLED LOW AIRSPEED INDICATORS IN COCKPIT INSTRUMENT PANEL PRIOR TO TEST 44.0F, FLIGHT SUMMARY REPORT EIL-5A-12-44F, NO W/O TO VERIFY REPLACEMENT.
NOV. 1964					
	57.0F				
	59.0F				

Figure 8.7 Airspeed Measurement System History

XV-5A SERIAL NO. 62-4505 HISTORY OF PILOT'S HIGH AIRSPEED SYSTEM					8-24-65
MONTH YEAR	TEST NO.	INDICATOR SERIAL NO.	WING BOOM SYSTEM ΔV_{ic} CURVE NO.	ΔV_{pc} CURVE NO.	NOTES
NOV. 1964	60.0F				
DEC. 1964	76.0F, 77.0F				
JAN. 1964	78.0F	FF08309	PG-2-001-4 1/2	(1)	
	79.0F, 80.0F	FF08309	PG-2-001-4 1/2	(1)	
1-3-65 4/5 5/4-485 CONNECT COCKPIT LOW AIRSPEED INDICATOR TO NOSE BOOM SYSTEM. CONNECT HIGH AIRSPEED INDICATOR/ MACH METER TO WING BOOM SYSTEM. ACTIVATE LOW AIR- SPEED SYSTEM CUT-OFF VALVE AND FUNCTIONAL CHECK- OUT SAME. ROTATE WING BOOM PITOT-STATIC HEAD 180°.					
NOTES: 1-FROM TEST 0.016 THROUGH 77.0F THE WING BOOM PITOT TUBE STATIC PORTS WERE LOCATED ON THE TOP SIDE OF THE BOOM. 2-AIRSPEED INDICATOR INSTRUMENT CORRECTION CURVES ARE FILED IN THE INSTRUMENTATION CALIBRATION BOOKS.					

Figure 8.8 Airspeed Measurement System History

[illegible]

Figure 8.10 Airspeed Measurement System History

Figure 8.12 Airspeed Measurement System History

Figure 8.14 Airspeed Measurement System History

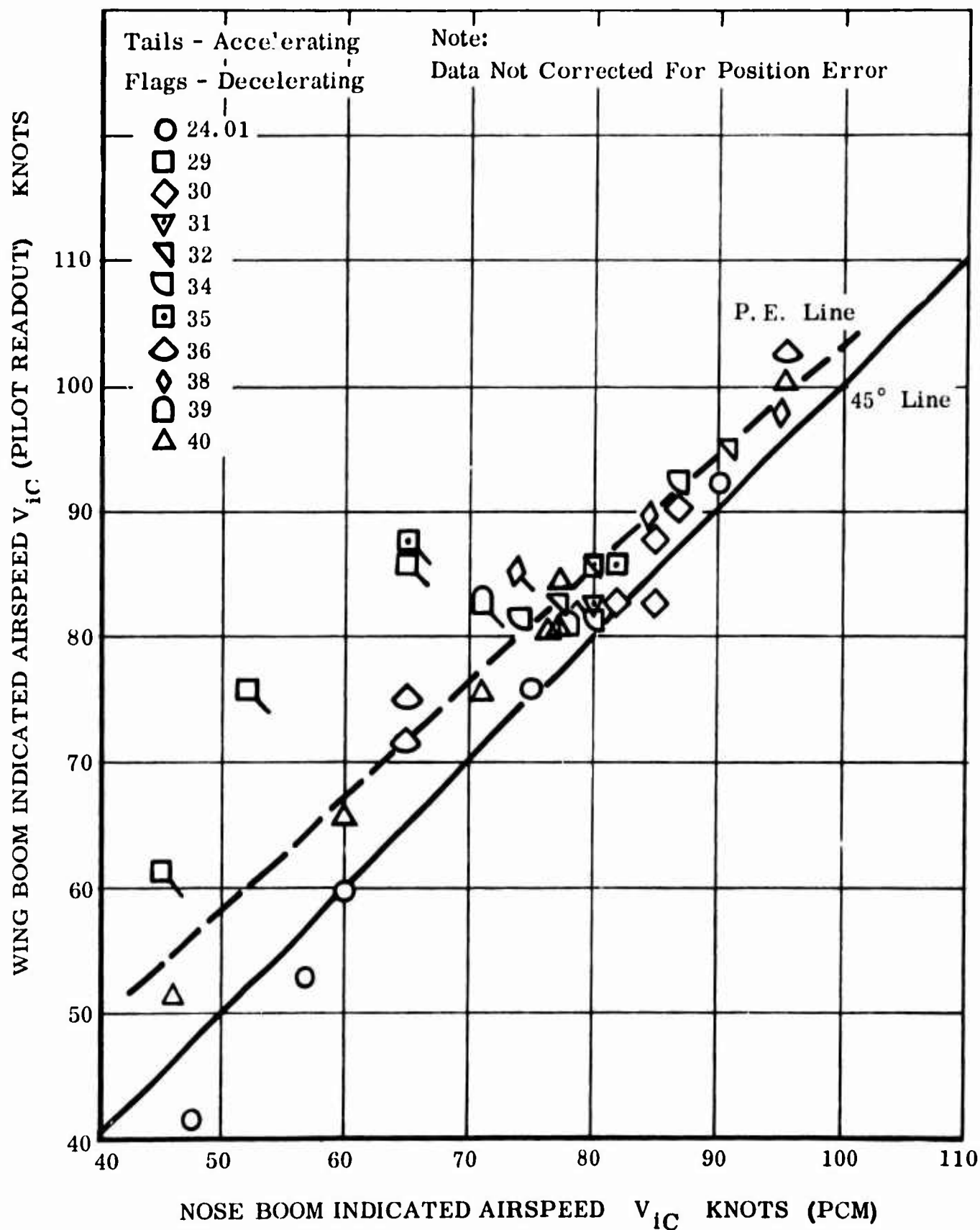


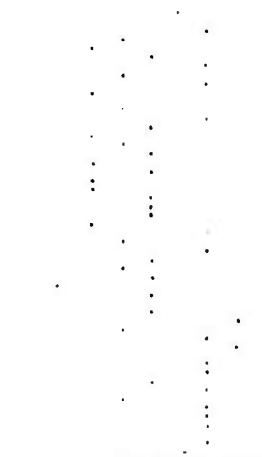
Figure 8.15 Comparison of Nose and Wing Pitot Static Readouts

XV-5A SERIAL NO. 62-4528
NOSE BOOM SYSTEM ~ PCM

$V_C = 233 K = 1.359 PSID$ (CHASE)
 $V_A = 227 K = 1.350 PSID$

(2)

1.30
1.20

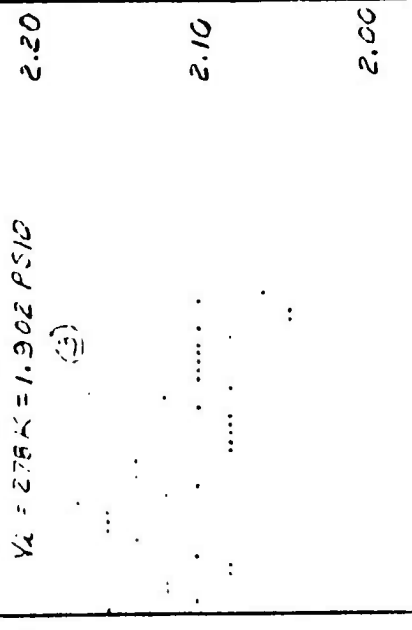


$V_C = 213 K = 2.440 PSID$ (CHASE)

$V_A = 275 K = 1.902 PSID$

(3)

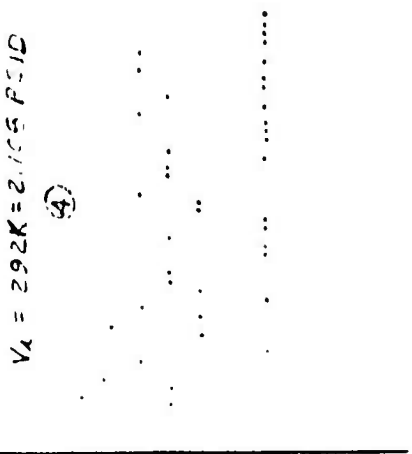
2.00
1.90
1.80



$V_A = 292 K = 2.105 PSID$

(4)

2.20
2.10
2.00



1280

1260

1240

1190

1160

1140

1050

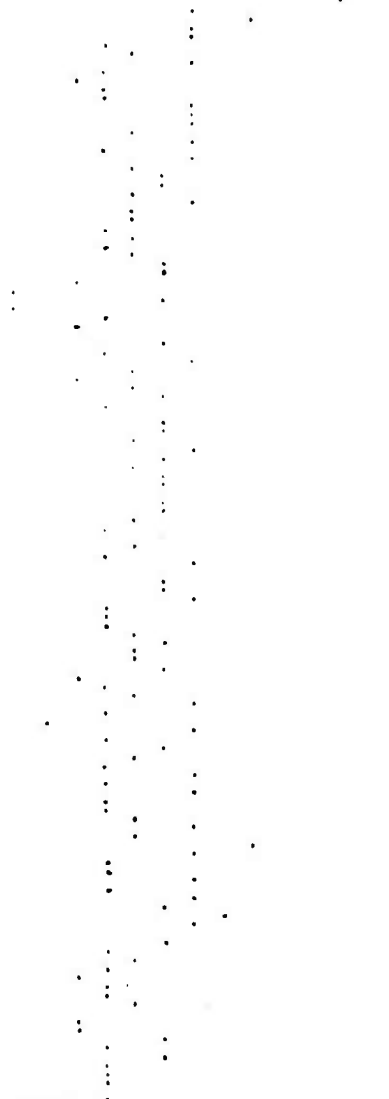
1030

1010

990

PCM TIME - SECONDS

.80
.70
.60



$V_C = 203 K = .994 PSID$ (CHASE)

$V_A = 176 K = .743 PSID$

(1)

980

960

940

920

900

880

860

840

820

800

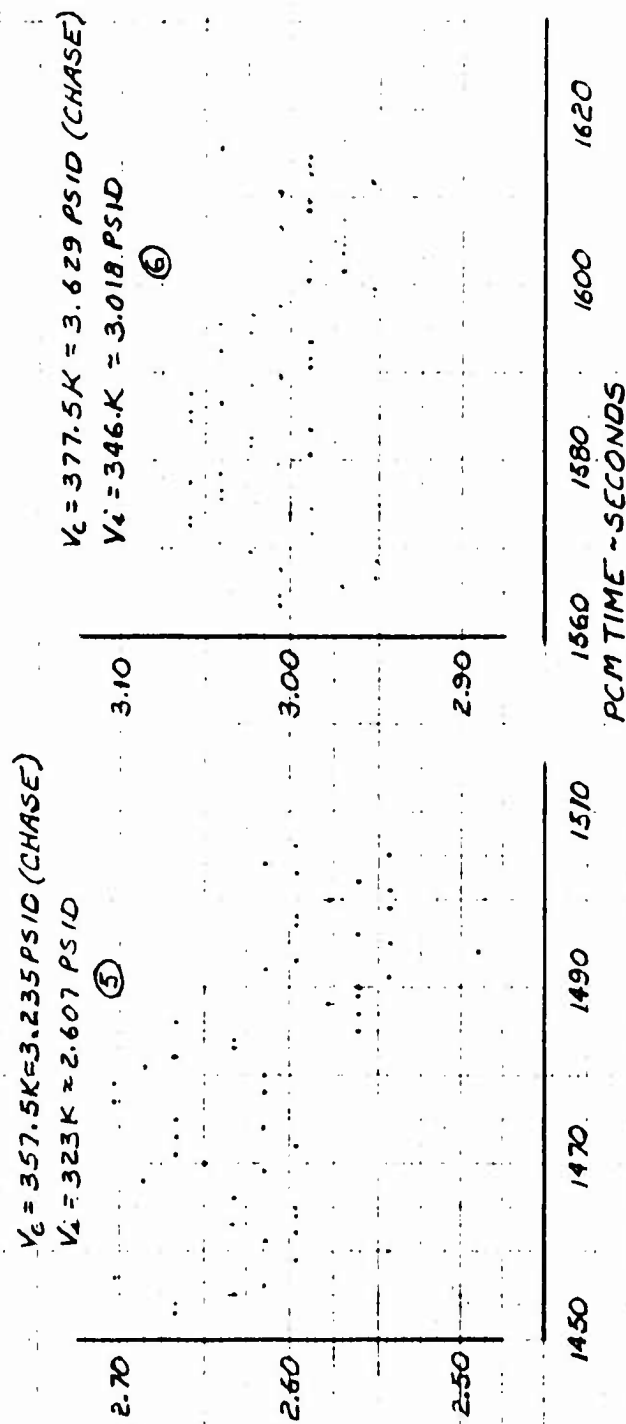
PCM TIME - SECONDS

NOTE: PCM CALIBRATED WITH A LEAKAGE OF 5 KNOTS/MIN. @ 500 KNOTS. (CGC ± 5 PSID X DUCT)

3-19-65 JZ

Figure 8.16 Effect of Airspeed System Leakage

XV-5A SERIAL NO. 62-4506
NOSE BOOM SYSTEM ~ PCM



NOTE: PCM CALIBRATED WITH A LEAKAGE RATE OF 5A NOTS/MIN. @ 500KNOTS. (CEC ± 5 PSID X DUCKER)

3-19-65 DOS

Figure 8.17 Effect of Airspeed System Leakage

XV-5A

① AIRSPEED POSITION ERROR CORRECTION

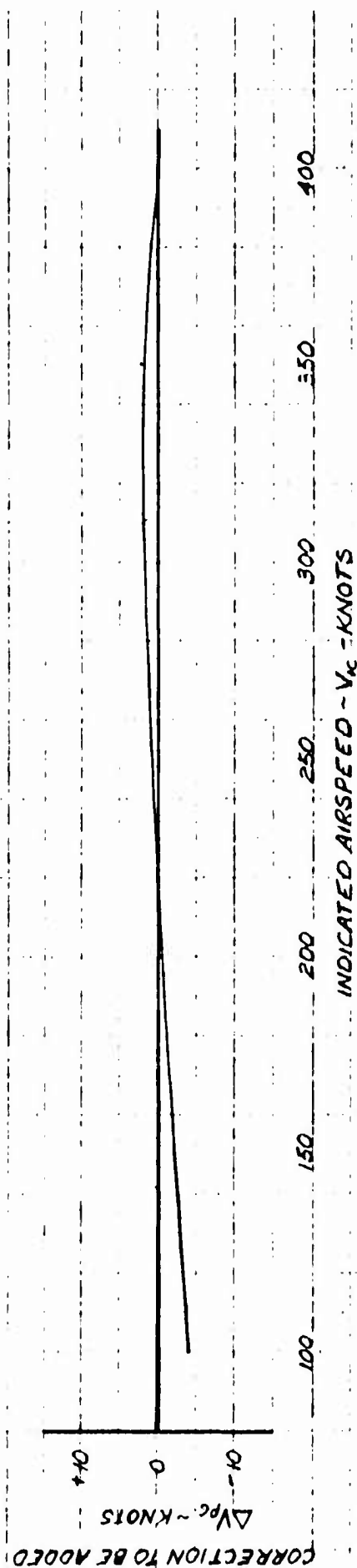
WING BOOM SYSTEM

CTOL MODE

NOTES:

1- PITOT TUBE STATIC PORTS LOCATED ON BOTTOM SIDE OF BOOM

2- FLAP DEFLECTION 0° TO 45°



REF. XV-5A-153 D. WILLIAMS 12-31-64 AC SERIAL NO. 62-4505

TEST 78.0F, 1-M-65 AC SERIAL NO. 62-4506

3-24-65

Figure 8.18 Airspeed Position Error Correction - Wing Boom System

XV-5A

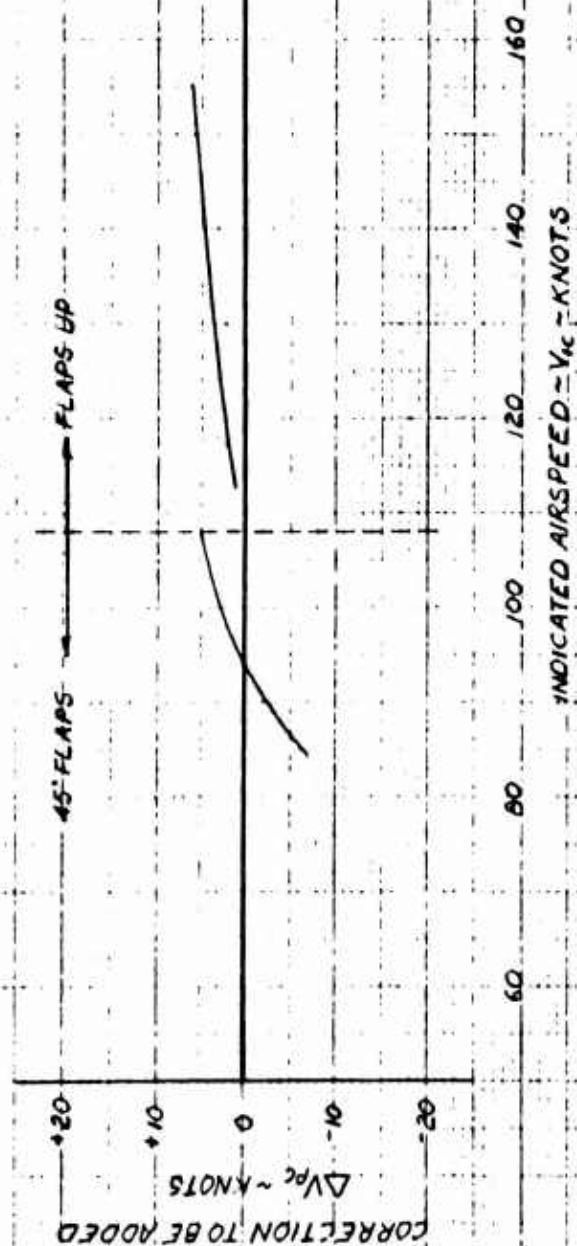
② AIRSPEED POSITION ERROR CORRECTION

NOSE BOOM SYSTEM

CTOL MODE

NOTES:

1- DATA OBTAINED WITH GEAR DOWN IN CTOL POSITION



REF. D. WILLIAMS, C-4-64, 1st SERIAL NO. 62-4506

3-24-65

Figure 8.19 Airspeed Position Error Correction - Nose Boom System

XV-5A

③ AIRSPEED POSITION ERROR CORRECTION

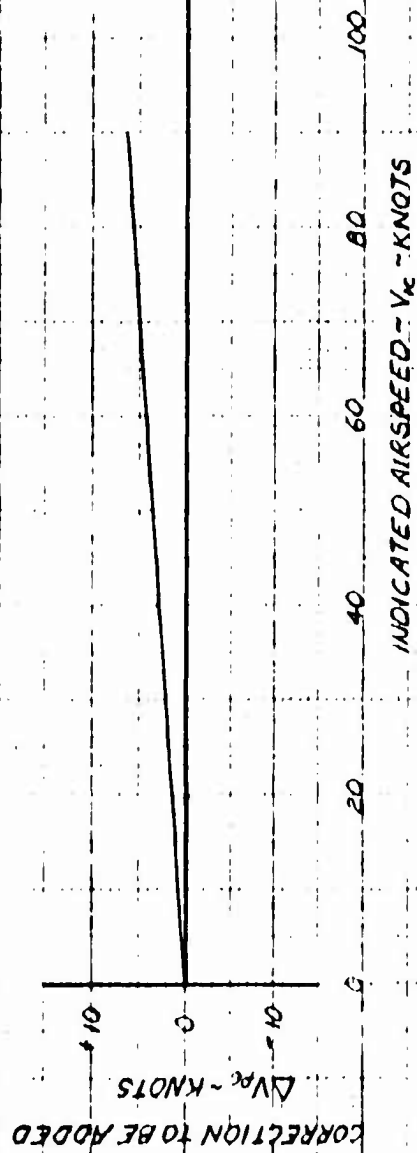
NOSE BOOM SYSTEM

VTOL MODE

NOTES:

1- DATA OBTAINED WITH GEAR DOWN IN CTOL POSITION.

2- ZERO ANGLE OF ATTACK ± 2 DEG.



REF. DA MIL-1 JAMS, 10-29-64, 5% SERIAL NO. 62-4506

3-24-65

Figure 8.20 Airspeed Position Error Correction - Nose Boom System

9.0 STRUCTURES AND LOADS

9.1 STRUCTURES

9.1.1 Strain Gage Evaluation

A total of 13 strain gages were installed in the airframe of S/N 506 airplane: 9 of these were in the center fuselage or space frame, 3 were in the wing, and 1 was on the horizontal tail actuator. Five gages were installed in No. 1 airplane, all in the center fuselage or space frame.

These strain gages were monitored during certain flights with the intent of collecting data from which stresses in primary structural members could be evaluated in the event of unusually severe flight loads which approached or exceeded design limits. This data would have been used possibly in the assessment of load magnitude or any resulting structural damage. Since no such conditions occurred either in fan or conventional flight, the data was not subjected to any detailed reduction. Spot checks of the data, however, indicated low stress changes.

During early ground engine runs, strain gages were placed on certain engine mount members to determine the order of magnitude of dynamic stress, to see whether there may be a potential fatigue problem in the 18 NiCoMo maraging steel used in the engine mounts and space frame. The oscillograph trace exhibited very low fluctuation of stress, indicating that no objectionable engine vibration was present. This observation, in view of the relatively high dynamic stress (5000 psi) used in earlier spectrum-loading tests on fatigue specimens of this material, is further evidence that the fatigue life of engine mounts and space frame should equal or exceed the 250 hour life of the airplane.

9.1.2 Structural Modifications

The results of Phase I ground and flight tests (including wind-tunnel tests) indicated that certain structural modifications were necessary. Summaries of the more significant of these modifications, both for conventional and fan flight, are given in Table 9.1.

9.1.3 Normal Load Factors Demonstrated in Flight

The XV-5A Program did not provide for any structural flight test or flight

load survey; however, operational limits beyond those required for normal mission performance were specified, and these limits, including envelopes for speed-altitude and speed-load factor (V-n), were approached during Phase I flight testing without any structural, or other, difficulty.

A few of the more noteworthy speed-load factor points were taken from flight test data and superimposed on the maneuvering envelope - gust diagram (Figure 9.1). As may be noted, the maximum normal load factor experienced in Phase I was approximately 80% of the 4.0 maximum design limit load factor, based on 9200 pounds basic design gross weight. This point and the others (particularly those close to the more critical upper part of the operational or desired envelope) are added evidence of airframe airworthiness.

TABLE 9.1

SIGNIFICANT STRUCTURAL MODIFICATIONS ARISING FROM
PHASE I CONVENTIONAL AND FAN FLIGHT

<u>Incident or Difficulty</u>		<u>Summary of Difficulty and Action Taken, Including Structural Modification</u>		<u>Ref.</u>
<u>Description</u>	<u>Date</u>	<u>A/C No.</u>		
Excessive Flexibility of Pitch Fan Louver System	3-64	1	<p><u>Difficulty:</u> During ground engine runs the pitch fan louver system was found to be too flexible; also, the louvers themselves came unbonded at the ends.</p> <p><u>Action Taken:</u> The pitch fan louver system was stress analyzed and deflections were calculated, confirming the observed excessive deflection. The louvers were then strengthened by adding closing ribs at the ends, and the entire system was readjusted. These changes resulted in satisfactory operation for the initial tests. As a final fix, however, (on 10-26-64) the installation in each of the aircraft was revised to include closer tolerance pins, heavier rods, centerline stops, and new load limiting actuators. No further difficulty was experienced.</p>	9.1
Nose Ldg. Gear Shimmy	4-15-64		<p><u>Difficulty:</u> Nose wheel shimmy occurred during taxi at 40 k. Wheel came off and gear collapsed.</p> <p><u>Action Taken:</u> Shimmy tests were conducted at Lockheed's Rye Canyon facility. After these and dynamics analysis were done, recommendations for redesign were made to H. W. Loud Machine Works, Inc., the manufacturer. Stiffness of fork and torque links was increased. Shimmy damper was redesigned. New installation proved satisfactory in shimmy tests. Fuselage repaired. New gears installed on both aircraft and proved satisfactory in high-speed taxi, takeoff, and landing.</p>	9.2 9.3 9.4

TABLE 9.1 (Continued)

<u>Incident or Difficulty</u> <u>Description</u>	<u>Date</u>	<u>A/C No.</u>	<u>Summary of Difficulty and Action Taken, Including Structural Modification</u>	<u>Ref.</u>
Fan-Flight Roll Power Deficiency	4-64	2	<p><u>Difficulty:</u> During hover tests the roll power was found to be inadequate</p> <p><u>Action Taken:</u> The wing fan louver dual actuator power was increased from 3300 lb. limit to 9600 lb. limit, which resulted in redesign of the wing fan strut, control links and push rods, actuators, and actuator support brackets. These newly designed components were analyzed for full actuator power acting in stop positions. The rebuilt system, including new steel actuator brackets, was tested satisfactorily up to full actuator power, both in a separate wing fan instal. and later in the airplane. After successful demonstration of required function and strength, both aircraft were revised according to the new design.</p>	9.5
Horiz. Stab. Spring Rate Increase	5-64		<p><u>Difficulty:</u> Flutter analysis revealed that the spring rate of the horizontal stabilizer needed increasing.</p> <p><u>Action Taken:</u> A deflection analysis of detail elements of the "spring" was made, which resulted in the following changes to both A/C: Change from alum. to steel of actuator body tube and horiz. stab. fitting; added doublers to local webs in both horiz. and vertical stab. The calculated increase in stiffness exceeded the minimum requirement by a substantial margin.</p>	9.6
Failure of Wing Fan Inlet Vanes	During Wind Tunnel Tests	1	<p><u>Difficulty:</u> After about 4 hours of wind tunnel testing up to 80 k, the forward inboard quadrant of the inlet guide vane on the L. H. wing fan ruptured and deflected into the wing rotor.</p> <p><u>Action Taken:</u> Considerable study and testing were conducted. The first</p>	

TABLE 9.1 (Continued)

<u>Incident or Difficulty</u> <u>Description</u>	<u>Date</u>	<u>A/C No.</u>	<u>Summary of Difficulty and Action Taken, Including Structural Modification</u>	<u>Ref.</u>
(Continued)				
			<p>mods. consisted primarily of improving the heat treat of the aluminum vanes, adding rivets along the circular vane trailing edge, and adding doublers over spot weld joints. In tests that followed, however, cracks developed again. An extensive mod (Mod II) was then made to the alum. vanes, the most significant changes being an improved mounting system and more efficient joints. The mod. worked well during flight tests. The alum. vanes were replaced later with steel vanes similarly mounted, and these vanes have performed since without difficulty in both aircraft.</p>	
Panel Vibration of Lower Access Fairing (Canoe)	During Wind Tunnel Tests	1	<p><u>Difficulty:</u> During wind tunnel tests, cracks due to panel vibration developed in the .016 gage titanium of the lower access fairing (canoe), in the location adjacent to the wing fans. High local temperature contributed to the problem.</p> <p><u>Action Taken:</u> In order to complete wind tunnel tests, temporary doublers were added in the area affected. Later a design change was made which consisted of local increase of skin gage and the addition of longitudinal stiffeners. These changes were made on both aircraft, and no further difficulty has been observed.</p>	9.7
Failure of Upper Wing Fairing	During Wind Tunnel Tests	1	<p><u>Difficulty:</u> 143W041 Upper Forward Wing Fairing, which serves also as a wing cooling ejector duct, failed during fan powered wind tunnel tests.</p> <p><u>Action Taken:</u> Temporary repairs consisted of clips and doublers which were not successful. A stress analysis was conducted for a net pressure based upon 125 k forward velocity and a fan overspeed cond. of 103^{°C} max.</p>	9.8

TABLE 9.1 (Continued)

<u>Incident or Difficulty</u> <u>Description</u>	<u>Date</u>	<u>A/C No.</u>	<u>Summary of Difficulty and Action Taken, Including Structural Modification</u>	<u>Ref.</u>
(Continued)				
			R. P. M. This analysis showed that the following redesign would be satisfactory: increase side panel gage from .032 to .050 (alum.); add edge stiffener angle as an integral part of the new attach.; add new clip attach to the fan strut. New parts were made accordingly and installed on the two aircraft and have given no further trouble.	
Yielding of Horiz. Stab. Pivot Bushings	6-9-64 8-6-64	2 1	<u>Difficulty:</u> Slight yielding of the horizontal tail pivot bushing resulted in undesirable free play. <u>Action Taken:</u> The bushing holes were line reamed and the bolts were chrome plated to make a tight fit.	9.9
Brake Failures	6-1-64 9-17-64 10-2-64	2	<u>Difficulty:</u> The L. H. brake faded on 1 June 1964 during a high-speed taxi run following failure of chute to deploy. During a fan taxi and lift-off mission on 17 Sept. 1964 the L. H. brake faded and caught fire; the brake anvil ruptured. Following a conventional landing on 2 Oct. 1964 a failure occurred similar to the one previous. <u>Action Taken:</u> Following each of the first two incidents inspections were made and parts replaced as required. Following the third difficulty the brake instal. was changed to provide additional built-in operating clearance between disc and pads; in addition, use of the thrust spoilers was adopted as standard procedure during extended taxi. Since then, no further brake difficulty has occurred. From a design standpoint, a detailed study was made, which included a stress analysis of anvil and disc. The main design changes which re-	9.10

TABLE 9. 1(Continued)

<u>Incident or Difficulty</u> <u>Description</u>	<u>Date</u>	<u>A/C No.</u>	<u>Summary of Difficulty and Action Taken, Including Structural Modification</u>	<u>Ref.</u>
(Continued)				
Addition of Empennage & Fairings	11-64 & 12-64	1	<p>sulted were a material change for the anvil casting (from mag. to alum. for more rigidity) and an increase in the disc thickness. Future parts will be in accordance with these design changes.</p> <p><u>Difficulty:</u> As a result of aerodynamic requirements, which are described in the foregoing, the 143V113 Aft Empennage Fairing was installed on A/C No. 1. Later, 143T112 Fwd Bullet Fairing and 143T113 Fwd Wiper Surface Fairing were added to the empennage.</p> <p><u>Action Taken:</u> Insofar as the structural aspects of the fairings are concerned, they were stress analyzed for loadings corresponding to V_{Limit} flight ($q = 850$ psf) with 5 degrees sideslip or angle of attack. The analysis showed that the fairings and attachments are good for unrestricted flight. The fairings were installed on both A/C.</p>	9.11
Inadvertent Spin Chute Deployment	12-9-64	2	<p><u>Difficulty:</u> During Flight 63F while converting from VTOL to CTOL for landing, the spin chute inadvertently deployed then failed to release.</p> <p><u>Action Taken:</u> Ground tests were conducted, and with tail cone (or chute cover) properly installed, it could not be disengaged by applying reasonable external forces. It was concluded then that if the chute is packed properly (keeping chute spring load against the cover to a minimum) and the cover itself is properly installed, that the chute should not deploy inadvertently. Regarding the failure to release, inspection showed that the hook surface</p>	9.12

TABLE 9. 1 (Continued)

<u>Incident or Difficulty</u> <u>Description</u>	<u>Date</u>	<u>A/C No.</u>	<u>Summary of Difficulty and Action Taken, Including Structural Modification</u>	<u>Ref.</u>
(Continued)				
Failure of Wing Fan Door Edge Seals	1-8-65		<p>which engages the spool was not machined to the proper angle. The angle was increased 7 degrees. Ground tests then indicated that the chute releases satisfactorily. The change was made on both aircraft.</p> <p><u>Difficulty:</u> The .008 gage stainless steel springs which encompass a conventional flight seal around the wing fan doors cracked during high-speed flight.</p> <p><u>Action Taken:</u> The springs were redesigned. The material was changed from stainless steel to 6A1-4V titanium. The thickness of the springs was increased, varying from .025 for forward locations down to .016 for aft locations. New seals were made and installed on both A/C. Since that time there has been no further difficulty.</p>	9.13
Failure of Flap Hinge Ftg. Fairing	1-14-65		<p><u>Difficulty:</u> The Fiberglas fairing which covers the flap hinge fitting failed during high-speed flight.</p> <p><u>Action Taken:</u> The old fairings on both aircraft were replaced with new ones made of thicker Fiberglas. No further difficulty has been reported.</p>	9.14

Weight and balance records were maintained for most flights. A plot of center of gravity versus weight as fuel was consumed is included in these records, affording center of gravity location for analysis at any time during the flight.

Extreme effort was extended to keep weight growth to a minimum, however increases due to nose wheel shimmy correction, fan exit louver stiffening, etc. were mandatory for safety of flight. The aircraft increased approximately 350 pounds since start of Phase I testing.

Insuring the center of gravity would be within the limits established was accomplished by installing lead ballast on structure provided for this purpose. Aft center of gravity extremes were no problem. Whenever excessive items of instrumentation were installed in the cockpit it was necessary to add ballast at the location provided at Fuselage Station 481.

At no time did problems of weight or balance interrupt the flight program.

10.0 REFERENCE

REFERENCE NUMBER

- 2.1 Harding, W.E., and J.E. Moroney
 XV-5A Detailed Flight Test Program
 Ryan Report Number 63B, February 1964
- 4.1 DiBartola, P.E. and D.G. Schattschneider
 Test Results Edwards Air Force Base AFFTC
 VTOL Thrust Stand XV-5A, Aircraft Number
 2 Serial Number 62-4506, 8 July to
 10 July 1965.
 EIL-5A-119, 14 September 1964
- 4.2 Final Report XV-5A Cross-Wind VTOL
 Landing Incident Flight 21F on 25 August 1964
 Ryan Report Number 64B122, 15 September
 1964.
- 4.3 Krupnick, M.
 Flight Flutter Test U.S. Army XV-5A
 Lift - Fan Research Aircraft
 Ryan Report Number 65B035 (Unpublished)
- 6.1 Ela, B.W.
 Calculated Installed Power Plant
 Performance for U.S. Army XV-5A Lift
 Fan Research Aircraft.
- 6.2 DiBartola, P.E. and D.G. Schattschneider
 Test Results NASA Ames Ramp Test XV-5A
 Ship Number 1, Serial Number 62-4505,
 April 28 to 18 May 1964.
 EIL-tA-106, 28 July 1964
- 6.3 Robinett, D.V.
 Acceptance Test Performance, Lift Fan 004,
 Pitch Fan 002.
 G. E. DM Number 63-98 Class II,
 23 March 1963.

**REFERENCE
NUMBER**

- 6.4 General Electric Company
 X353-5B Propulsion System Specification.
 Specification Number 112, 15 January 1962.
- 6.5 General Electric Company
 X376 Pitch Fan Specification
 Specification Number 113, 1 March 1962.
- 6.6 Davis, W. B.
 XV-5A Flying Qualities Specification.
 Ryan Report Number 62B062,
 15 December 1962
- 6.7 Parks, W. C. , and D. G. Schattschneider
 Wind Tunnel Test Report, One - Sixth
 Scale Powered Lift-Fan Model, U. S. Army
 XV-5A Lift-Fan Research Aircraft.
 Ryan Report Number 63B092, 11
 11 September 1963.
- 6.8 DeManuel, G.
 Model 143 (XV-5A) Control Systems Rigging
 Procedures.
 Ryan Number 14359-5, 10 September 1963
- 6.9 Ryan Drwg Number 143T111
 Boom Installation, Horizontal Stabilizer
 Model XV-5A.
- 6.10 Ryan Drwg Number 1437110
 Slat Installation - Horizontal Stabilizer -
 Fixed.
- 6.11 Ela, B. W.
 Calculated Heat Transfer and Cooling System
 Performance, U. S. Army XV-5A Lift Fan
 Research Aircraft.
 Ryan Report Number 64B017, 15 February 1965

REFERENCE
NUMBER

- 7.1 XV-5A Stability and Control Group Estimated Static, Stability and Control Characteristics of the U.S. Army XV-5A Lift Fan Research Aircraft.
Ryan Report Number 64B031, 6 March 1964.
- 7.2 Ryan Drwg. Number 1437112
Fairing - Bullet Forward
- 9.1 LeBaron, A. D.
Structural Analysis of Engine Air Inlet, Thrust Spoiler Installation, and Pitch Fan Louver Installation of the U.S. Army XV-5A Lift Fan Research Aircraft.
Ryan Report Number 64B140, 15 October 1964.
- 9.2 Starkey, H. B. ,
Final Accident Report, XV-5A Nose Landing Gear Collapse, Run 0.15G - 15 April 1964.
(No Report Number Assigned) 18 August 1964.
- 9.3 H. W. Loud Machine Works, Incorporated
Shimmy Damper Qualification Testing.
Report Number 1511L TR-Z, July 1964.
- 9.4 H. W. Loud Machine Works, Incorporated
Drwg Number 1511L100
Shock Strut - Nose Gear.
- 9.5 Ryan Drwg. Number 143W013
Bracket - Aft Actuator Support, Fan Louvers

Ryan Drwg. Number 143W014
Bracket - Forward Actuator Support Wing
Fan Louvers
- 9.6 Ryan Drwg. Number 143T002
Stabilizer Assembly Horizontal

Ryan Drwg. Number 143T005
Forward Spar and Bulkhead Installation
Vertical Stabilizer.

**REFERENCE
NUMBER**

- 9.6
(Cont.) Ryan Drwg. Number 143T064
Spar - Horizontal Stabilizer Forward.
- Ryan Drwg. Number 143T065
Fitting Assembly - Horizontal Stabilizer -
Actuator.
- Ryan Drwg. Number 143T069
Rib Installation - Horizontal Stabilizer BL 3.26.
- 9.7 Ryan Drwg. Number 143F076
Fairing Lower Access Sta. 214-275.87
- 9.8 Ryan Drwg. Number 143W041
Fairing - Installation and Assembly BL 61.0
Wing - Upper.
- 9.9 Ryan Drwg. Number 143T001
Empennage Assembly
- 9.10 Ryan Drwg. Number SCDL0003
Lightweight Wheel and Brake Assembly
Main Landing Gear.
- 9.11 Ryan Drwg. Number 143T113
Fairing - Wiper Surface Installation
- Ryan Drwg. Number 143V113
Installation - Empennage Fairing Aft Section
(Test)
(Miscellaneous Details Empennage Fairing,
Sheet 2 of 2).
- 9.12 Ryan Drwg. Number 143Q003
Hook Assembly - Anti-Spin Chute Release
Mechanism.
- 9.13 Ryan Drwg. Number 143W052
Edge Seals Wing Fan Inlet Doors.
- 9.14 Ryan Drwg. Number 143W090
Fairings - Trailing Edge Root.

G.E. XV-5A
DATEM REFERENCE
NUMBER

- 1 Smith, E.G.
 Estimated Stagger Effectiveness - Stiffened
 Exit Louver System.
 XV-5A Datem Number 1 (G.E.) 27 August 1964
- 2 Przedpelski, Z.J.
 Experimental Results Propulsion System
 Power Output.
 XV-5A Datem Number 2 (G.E.) 27 August 1964
- 3 Clark, D.E.
 Summary of Total Aircraft Weight in Hover
 (Flights 9F-21F).
 XV-5A Datem Number 3 (G.E.) 28 August 1964
- 4 Smith, E.G.
 Some Comments on Reingestion - Ames Wind
 Tunnel Results.
 XV-5A Datem Number 4 (G.E.) 1 September 1964
- 5 Przedpelski, Z.J.
 Comparison of J85 Engine Performance with
 and without Stall Free Modifications.
 XV-5A Datem Number 5 (G.E.) 28 August 1964
- 6 Przedpelski, Z.J.
 J85 Calibration Runs
 XV-5A Datem Number 6 (G.E.) 1 September 1964
- 7 Przedpelski, Z.J.
 Test Plan for Engine Ground Checkout in
 Aircraft Number 2.
 XV-5A Datem Number 7 (G.E.) 1 September 1964
- 8 Przedpelski, Z.J.
 Yaw Inputs from the Pitch Fan.
 XV-5A Datem Number 8 (G.E.) 10 September 1964

**G.E. XV-5A
DATEM REFERENCE
NUMBER**

- 9 Clark, D.E.
Ames Wind Tunnel Results. Problem Areas
in Operation, Control, and Stability in
Transition.
XV-5A Datem Number 9 (G.E.) 11 September 1964
- 10 Clark, D.E.
Estimated Absolute Ceiling and Rate of Climb
Using Ames Wind Tunnel Data.
XV-5A Datem Number 10 (G.E.)
16 September 1964
- Przedpelski, Z.J.
Hi-Speed Fan Powered Flight (Supersedes
Datem Number 10).
XV-5A Datem Number 10a (G.E.)
25 September 1964
- 11 True, H.C.
High Fan Powered Flight.
XV-5A Datem Number 11 (G.E.)
25 September 1964
- 12 Przedpelski, Z.J.
Rate of Climb and Descent vs. Altitude.
XV-5A Datem Number 12 (G.E.)
8 October 1964
- 13 Przedpelski, Z.J.
Fan and Engine Transients during Fan to
Jet Conversion (Flight 34).
XV-5A Datem Number 13 (G.E.) 8 October 1964
- 14 Przedpelski, Z.J.
Estimated Maximum Sustainable Altitude in
Fan Mode.
XV-5A Datem Number 14 (G.E.) 9 October 1964
- Przedpelski, Z.J.
Addition to Datem Number 14.
XV-5A Datem Number 14a (G.E.) 12 October 1964

G.E. XV-5A
DATEM REFERENCE
NUMBER

- 15 Przedpelski, Z.J.
Hover Performance after Engine Adjustments.
XV-5A Datem Number 15 (G.E.) 9 October 1964
- 16 Przedpelski, Z.J.
Hover Performance of the XV-5A System
(Flight 22-40) Supersedes Datem Number 15.
XV-5A Datem Number 15a (G.E.) 26 October 1964
- 16 Smith, E. G.
Longitudinal Trim during Transition.
XV-5A Datem Number 16 (G.E.)
14 October 1964
- 17 Clark, D. E.
Transition Evaluations:
(a) Stick Position - Tail Off
(b) Stick Position Change - One Engine Out.
XV-5A Datem Number 17 (G.E.)
21 October 1964
- 18 Przedpelski, Z.J.
Single Engine Reingestion Results.
XV-5A Datem Number 18 (G.E.)
4 November 1964.
- 19 Clark, D. E.
Comparision of Flight and Wind Tunnel Lift
and Drag - Flight 40F.
XV-5A Datem Number 19 (G.E.)
6 November 1964
- 20 Przedpelski, Z.J.
Reingestion during Low Altitude Transitions.
XV-5A Datem Number 20 (G.E.)
10 November 1964
- 21 Przedpelski, Z.J.
One Engine Fan Mode Performance.
XV-5A Datem Number 21 (G.E.)
16 November 1964

**G.E. XV-5A
DATEM REFERENCE
NUMBER**

- 22 Smith, E.G.
XV-5A Transition Characteristics Based on
Flight 58F.
XV-5A Datem Number 22 (G. E.)
7 December 1964
- 23 Smith, E.G.
Composite Performance and Control Effective-
ness in Transitional Flight.
XV-5A Datem Number 23 (G. E.)
16 December 1964
- 24 Smith, E.G.
Estimated System Performance for a Range
of Angle of Attack and Sideslip.
XV-5A Datem Number 24 (G. E.)
17 December 1964
- 25 Smith, E.G.
Comparison of Longitudinal Stick for Hover
Between Aircraft Number 1 and Aircraft
Number 2.
XV-5A Datem Number 25 (G. E.)
21 January 1965
- 26 Smith, E.G.
Some Conclusions Concerning Hover and
Lo-Speed Performance of Aircraft Number 1
Flight Number 26F.
XV-5A Datem Number 26 (G. E.)
22 January 1965
- 27 Smith, E.G.
Procedures for Determining Engine Power
During XV-5A Flight Test.
XV-5A Datem Number 27 (G. E.)
5 February 1965
- Smith, E.G.
Procedures for Determining Engine Power
During XV-5A Flight Tests - Added Curves.
XV-5A Datem Number 27a (G. E.) 24 February 1965.

**G. E. XV-5A
DATEM REFERENCE
NUMBER**

- 28 Smith, E. G.
Check-out Run J-85-5A, Serial Number
231-233.
XV-5A Datem Number 28 (G. E.)
5 February 1965
- 29 Smith, E. G.
Procedures for Performing Engine Fan Runs
for Determination of Gas Generator Power
Capability.
XV-5A Datem Number 29 (G. E.)
12 February 1965
- 30 Smith, E. G.
Procedures for Determining Engine Gas Horse-
power using Static Runs of the XV-5A.
XV-5A Datem Number 30 (G. E.)
16 February 1965
- Scherr, W. P.
Revision to Figure 1 of Datem Number 30.
XV-5A Datem Number 30a (G. E.)
3 March 1965
- 31 Smith, E. G.
Rate of Climb in Fan Mode.
XV-5A Datem Number 31 (G. E.)
17 February 1965
- 32 Smith, E. G.
Methods of Presenting Standardized XV-5A
Performance
XV-5A Datem Number 32 (G. E.)
18 February 1965
- Smith, E. G.
Correction to Datem Number 32
XV-5A Datem Number 32a (G. E.)
4 March 1965

**G. E. XV-5A
DATEM REFERENCE
NUMBER**

- 33 Smith, E. G.
Effects of Certain Variables on XV-5A Fan
Mode Flight Performance.
XV-5A Datem Number 33 (G. E.)
18 February 1965
- 34 Smith, E. G.
Engine Calibration Runs of XV-5A
Number 62-4505 on 25 February 1965.
XV-5A Datem Number 34 (G. E.) 5 March 1965
- 35 Scherr, W. P.
Static Thrust Performance of the XV-5A
Exhaust System in the Jet Mode.
XV-5A Datem Number 35 (G. E.) 16 March 1965
- 36 Smith, E. G.
Engine Calibration Runs of XV-5A
Number 62-4506 on 8 March 1965
XV-5A Datem Number 36 (G. E) 16 March 1965
- 37 Scherr, W. P.
Procedure for Determining Engine Thrust in
the Jet Mode During XV-5A Flight Tests.
XV-5A Datem Number 37 (G. E.) 22 March 1965

11.0 CONCLUSIONS

Specific conclusions resulting from the 8-month test program which ended 28 January, 1965 are categorized below according to flight regime.

HOVERING

1. Propulsion system hover lift performance for the "stall-free" engine configuration equaled predicted values based on original system specifications.
2. Flying qualities in steady hover and translations were appraised as satisfactory. Although yaw control power was less than predicted, control solely derived from the lift fan system provided satisfactory control characteristics.
3. The partial authority stability augmentation system functioned as predicted permitting hovering flight with ease. Investigations at reduced system gains showed the necessity for operation of pitch and roll channels, while use of yaw channel was considered optional.
4. Operation in proximity to the ground increased levels of disturbance and fan exhaust gas reingestion into engines and fans. Effects noticeable to the pilot diminished above 3 feet gear height and basically disappeared at 10 feet. Level of reingestion of exhaust gases into engine inlet at very low ground heights was largely dependent on control positions.
5. High levels of translation speed stability predominated in forward, sidewise translations; a characteristic regarded as highly desirable.

TRANSITION

1. Engine power and longitudinal trim requirements generally matched expectations. Excess power margin and fan overspeed limit climb, maximum speed, and acceleration capabilities of present configuration in EAFB hot-day operations.
2. Negative speed stability characteristic, occurring above speed for maximum nose down trim, was not considered detrimental to evaluations of the capabilities of the aircraft.

3. Positive dihedral effect existed at all forward speeds; directional static stability was negative at low speeds and became positive at indicated airspeeds above 35 knots.
4. Phasing of authority of fan controls as a function of vector angle appeared to be satisfactorily coordinated with flight speed and conventional aerodynamic control effectiveness, although vectoring at low speeds without increase in flight speed produced noticeable reduction in control effectiveness.
5. During a series of Army envelope expansion tests before the completion of the flight test program, steady state flight between approximately minus 5 and plus 8 degrees angle of attack over the transition speed regime was demonstrated.
6. Short period responses to disturbances were well damped for both longitudinal and lateral directional modes. Records indicate a period of approximately 3 seconds for the longitudinal mode. Approximately the same frequency is shown for the lateral - directional mode although some departure from this mean takes place below 60 knots where uncoupled roll and yaw motions occur.

CONVENTIONAL FLIGHT

1. Conventional flight performance closely matches predicted performance based on climb and level flight capability demonstrations. Engine static performance in the "stall-free" configurations exceeded predicted values based on the propulsion system specifications.
2. Flutter tests (not reported herein) were conducted to 406 knots calibrated airspeed ($M=.7$) and both aircraft were flown to this speed in acceptance demonstrations.
3. Nose wheel lift-off speeds were lower than predicted but still higher than that required to meet conventional flying qualities specifications. This characteristic for future versions may be corrected with more forward positioning of the main landing gear.
4. Stall with and without flaps was characterized by prestall buffet which was indicated approximately 2 degrees angle of attack before reaching conditions for maximum lift coefficient.

5. Conventional roll control was considered to be quite sensitive and to have low lateral stick forces. Rudder control was effective in maintaining heading during taxi above 20 knots. Although elevator control power was high, stick force per g increased to moderately high levels at increasing speeds. Due to decreasing stability margins at higher angles of attack, only slight aft stick force was required to trim full 45 degrees flap conditions at more critical forward cg condition.
6. The dynamic longitudinal short period mode was heavily damped at all test conditions. Damping of the phugoid was neutral in cruise configuration. Typical of wind tunnel model indications, flap deflection produced reductions in longitudinal static stability at higher angles of attack as stall was approached.
7. Control induced dutch-roll oscillations were well damped at all speeds. Mild adverse yaw was encountered during bank-to-bank rolling maneuvers in cruise and preconversion configurations, while favorable yaw was shown in rolling maneuvers in landing configurations.

CONVERSION

1. Fan to turbojet mode conversions were conducted with ease over a range of calibrated airspeeds at 86 to 109 knots and required no pilot corrections.
2. Turbojet to fan mode conversions performed over a speed range from 90 to 115 knots CAS were somewhat more difficult requiring the development of a technique involving throttle advance coordinated with conversion initiation. Thrust spoilers were not used. Simulator derived diverter valve time delay following start of horizontal test programming was determined detrimental to smoothly performing the maneuver.

* * *

Certain minor modifications were required to complete the planned flight test program, but none indicated any concept deficiency. The wing fan exit louver actuators required increased power to motivate the louvers in the high load areas of maximum stagger and the louvers themselves required structural strengthening to eliminate bending under load. A nose wheel shimmy problem encountered during initial high speed taxi tests required structural strengthening of the nose wheel fork and a revised shimmy dampener.

An engine compressor stall problem brought about by reingested hot gases during hover operations in close proximity to the ground was eliminated by increasing engine "stall margin". This was effected by making both engine installation and engine control changes. Maximum J-85 engine speed was increased to 102 percent as a part of this stall alleviation program.

Various local minor structural heating problems, often created because of research mission test requirements, were solved by additional insulation in the appropriate areas.

In high speed conventional flights, a local aerodynamic flow separation of the empennage intersection causing "stick shake" and longitudinal trim changes was eliminated by the addition of a "bullet" fairing in the area. An aircraft directional oscillation remaining after "rudder-kick" maneuvers was eliminated by the addition of 3/8" T-section along the trailing edge of the rudder.

On the basis of tests completed during the contractor flight test program, the XV-5A is considered flightworthy for evaluation flight testing by the U.S. Army. While aircraft performance closely matches predictions, significant improvements can be gained through modification. It is recommended that a program for evaluation of possible improvement measures be initiated at the earliest possible date.